BLOOD MICROENVIRONMENT OF VASCULAR DISEASES AND DEVICES

By

Tia Casandra Lynn Kohs

A DISSERTATION

Presented to the Department of Biomedical Engineering

Of the Oregon Health & Science University

School of Medicine

In partial fulfillment of the requirements for the degree of

Doctor of Philosophy

In Biomedical Engineering

March 2023

OREGON HEALTH & SCIENCE UNIVERSITY

SCHOOL OF MEDICINE – DEPARTMENT OF BIOMEDICAL ENGINEERING

CERTIFICATE OF APPROVAL

This is to certify that the Ph.D. Dissertation of

Tia Casandra Lynn Kohs

"Blood Microenvironment of Vascular Diseases and Devices"

has been approved

_____

Mentor: Owen J.T. McCarty, Ph.D.
Professor and Chair
Department of Biomedical Engineering

_____

Member/Chair: Yali Jia, Ph.D.
Professor
Ophthalmology and Biomedical Engineering

_____

Member: Fikadu G. Tafesse, Ph.D.
Associate Professor
Molecular Microbiology and Immunology

_____

Member: Jonathan W. Nelson, Ph.D.
Instructor of Medicine
Division of Nephrology and Hypertension

_____

Member: Philip F. Copenhaver, Ph.D.

Professor
Cell, Developmental and Cancer Biology

In dedication to…

David Lyle Kohs, my father and role model, who taught me to always trust the man upstairs and to keep it simple stupid. Although his was cut short here on Earth, his lessons will never be forgotten.

Table of Contents

List of Figures

CHAPTER 1

CHAPTER 2

CHAPTER 3

CHAPTER 4

CHAPTER 5

CHAPTER 6

CHAPTER 7

CHAPTER 8

CHAPTER 9

List of Tables

CHAPTER 3

CHAPTER 7

CHAPTER 8

List of Abbreviations

ACT	Activated clotting time
ADP	Adenosine diphosphate
ALKP	Alkaline phosphatase
ALT	Alanine transaminase
APC	Activated protein C
aPTT	Activated partial thromboplastin time
AST	Aspartate aminotransferase
AT	Antithrombin
BBB	Blood brain barrier
BK	Bradykinin
BMI	Body mass index
BMX	Bone marrow tyrosine kinase gene in chromosome X
BSA	Bovine serum albumin
BT	Bleeding time
BTK	Bruton’s tyrosine kinase
BUN	Blood urea nitrogen
CAS	Contact activation system
CBC	Complete blood count
CDI	Cumulative disease index
cDNA	Complementary DNA
CEU	Contrast-enhanced ultrasound

CFT	Clot formation time
CFH	Complement factor H
CI	Confidence interval
CNS	Central nervous system
COVID-19	Coronavirus disease 2019
CRP-XL	Cross-linked collagen-related peptide
CT	Clotting time
CVD	Cardiovascular disease
EAE	Experimental autoimmune encephalomyelitis
ECs	Endothelial cells
ECMO	Extracorporeal membrane oxygenation
ECOS	Extracorporeal organ support
EGF	Epidermal growth factor
ELSO	Extracorporeal Life Support Organization
ETC	Endocrine Technologies Core
EV	Extracellular vesicle
F	Factor
GCT	Glucose challenge test
GPCR	G-protein coupled receptor
GPIbα	Glycoprotein-Ibα
GPVI	Glycoprotein VI
HAEC	Human aortic endothelial cell
h1A6	Humanized 1A6

HGFA	Hepatocyte growth factor activator
HK	High molecular weight kininogen
ICAM-1	Intercellular adhesion molecule 1
IgG	Immunoglobulin G
IL	Interleukin
IP	Intraperitoneal
ITAM	Immunotyrosine activation motif
mAb	Monoclonal antibody
MCF	Maximum clot firmness
MMP	Matrix metalloproteinase
MOG	Myelin oligodendrocyte glycoprotein, peptides 35–55
MPO	Myeloperoxidase
NATEM	Non-activated thromboelastometry
NHP	Nonhuman primate
ONPRC	Oregon National Primate Research Center
OPC	Oligodendrocyte progenitor cell
OR	Odds ratio
PAR	Proteinase-activated receptor
PCR	Polymerase chain reaction
PK	Prekallikrein
polyP	Polyphosphate
PPP	Platelet poor plasma
PRP	Platelet rich plasma

PS	Phosphatidylserine
PT	Prothrombin time
PTX	Pertussis toxin
RFU	Relative fluorescent units
RT	Room temperature
STAT3	Signal transducer and activator of transcription 3
sVCAM-1	Soluble vascular cell adhesion molecule 1
TAT	Thrombin-antithrombin complex
TEC	Tyrosine kinase expressed in hepatocellular carcinoma
TFKs	TEC family kinases
TFPI	Tissue factor pathway inhibitor
TNF	Tumor necrosis factor
TNFR	Tumor necrosis factor receptor
TRAP-6	Thrombin receptor activator peptide 6
UFH	Unfractionated heparin
VA	Veno-arterial
VAD	Ventricular assist device
VCAM-1	Vascular cell adhesion molecule 1
VE-cadherin	Vascular endothelial-cadherin
VEGF	Vascular endothelial growth factor
VEGFR	Vascular endothelial growth factor receptor
vWF	von Willebrand factor
VV	Veno-venous

Acknowledgements

First and foremost, I would like to express my gratitude for my Ph.D. advisor, Dr. Owen McCarty. From sitting in the microscopy suite tinkering to long brainstorming sessions in his office, his support as a mentor is nothing short of remarkable. Perhaps some of the most memorable experiences with Owen come from times where he is fully embracing his role as 'theplateletwalker'. Those of you that know Owen know that the only thing that rivals his love of science is his love of long-distance hiking. Whether it be calling me with patchy cell signal in the midst of his infamous thru-hiking trips or chatting animatedly with a full entourage jogging to keep pace with his stride, there has never been a boring moment working for him. His impeccable ability to see the larger picture and knack for providing just the right amount of structure are truly admirable.

I would also like to thank my Dissertation Advisory Committee. Dr. Yali Jia, serving as the Chair of my committee, has been a phenomenal role model as a fellow woman in science and has helped refine my data analysis skills. Dr. Fikadu Tafesse has been a visionary and inspiration, pioneering novel research endeavors to study the SARS-CoV-2 variants. Dr. Jonathan Nelson has gone above and beyond, taking the time to meet with me before each committee meeting to chat about not only science, but also about personal development throughout the graduate school process. Last but not least, Dr. Philip Copenhaver graciously agreed to serve as my last committee member.

I am grateful for Drs. Florea Lupu, Ravi Keshari, and Robert Silasi (Oklahoma Medical Research Foundation) for the continued collaboration and for generating data that helped define the contact pathway activity. I thank Dr. David Gailani (Vanderbilt University) as well as Drs.

Erik Tucker, Michael Wallisch, Christina Lorentz, Norah Verbout, and Brandon Markaway (Aronora Inc.) for the illuminating discussions surrounding FXI and continued project support. I thank Dr. João Seixas (Targtex), Dr. Gonçalo Bernardes (University of Cambridge), and Bárbara Sousa (Universidade de Lisboa), for teaching me about drug development and testing. I thank Dr. Mark Larson (Augustana University) for teaching me the ways of platelet aggregation and building my confidence with wet lab skills.

The opportunity to conduct studies at the Oregon National Primate Research Center would not have been possible without: Drs. Monica Hinds, Jonathan Lindner, David Erickson, Paul Kievit, and Michelle Pounder. Technical support from Jennifer Johnson, Carrie McArthur, Melissa Kirigiti, Aris Xie, James Hodovan, Matthew Muller was greatly appreciated.

A special thank you to the Department of Biomedical Engineering, especially the members of the McCarty group who welcomed me and made the lab feel like a second home: Drs. Cristina Puy, Joseph Aslan, Anh Ngo, Stephanie Reitsma, Hari Lakshmanan, Tony Zheng, Ivan Parra-Izquierdo, Si Han Wang, and Chih Jen Yang. I thank Meghan Fallon for all the of long chats and fun calendar invites over the years. I thank Alexander Melrose for showing me the ropes in the lab and for running increasingly long races with me. I thank Gavin Young and Benjamin Weeder for rescuing me when R was being fickle. I thank Victoria Duke and Sami Moellmer for never failing to make me laugh and for being the sisters I never had. Jiaqing Pang, Nhu Nguyen, Helen Vu, and Kelley Jordan also contributed greatly with their technical support. Last but not least, Angelyn Kimball, Caitlin Currie, and Catherine Hogan played key roles in supporting the McCarty group.

It has also been a pleasure to work with the clinicians: Drs. Sven Olson, Patricia Liu, Vikram Raghunathan, Michael Pfeffer, Luke Masha, Malinda West, Bishoy Zakhary, and David Zonies. A special thanks to Dr. Joseph Shatzel and his extensive mentorship during my time in the program.

I would also like to express my gratitude for my parents, Carrie and Matthew Knight, for always believing in me and encouraging me to keep going. After this defense, you will no longer need the binder with my publications. A huge thanks to my second family, the Bodenhamer's—our crazy 'cow ideas' make for the best stories. The unwavering support from my fiancé, Andrew Obst, has also been instrumental in my success. I look forward to starting our life together in Washington D.C.

Abstract

Blood Microenvironment of Vascular Devices and Disease

Tia C.L. Kohs

Department of Biomedical Engineering

School of Medicine

Oregon Health & Science University

March 2023

Dissertation Advisor: Owen J.T. McCarty, Ph.D.

The blood microenvironment is a dynamic system consisting of a diverse range of cells and plasma proteins that function together to maintain homeostasis. In my dissertation, I explored the intricate interplay amongst the different components of the blood microenvironment (e.g. endothelial cells, platelets, and coagulation factors) in studies ranging from *in vitro* experiments, to *in vivo* studies with nonhuman primates (NHPs), and clinical studies. My objective was to leverage knowledge of complex blood microenvironment interactions to develop tools targeting the intracellular and extracellular pathways that contribute to the manifestation of vascular diseases and responses to vascular devices.

My dissertation began by examining the role of Tec family kinases (TFKs) and coagulation factor (F) XI in the thromboinflammatory milieu associated with diet-induced hyperlipidemia. In our *in vitro* studies, we showed that VEGF-A induced endothelial activation dependent on the TFK, bone marrow tyrosine kinase on chromosome X (Bmx). In a pilot study using a nonhuman primate (NHP) model of diet-induced hyperlipidemia, we observed a reduction in platelet deposition and endothelial cell activation following treatment with the TFK inhibitor, ibrutinib. These data suggest that TFKs may be complicit in the pathologies underlying thromboinflammatory diseases, such as atherosclerosis, making them a promising therapeutic target.

As an alternative mechanism, we investigated the role of FXI in maintaining the thromboinflammatory phenotype observed in chronic hyperlipidemia. NHPs from the diet-induced hyperlipidemic cohort were treated with the anti-FXI monoclonal antibody, humanized 1A6 (h1A6). This blocked FXIIa-mediated activation of FXI, as well as FXIa-mediated activation of FIX and FV. Following treatment with h1A6, we observed: 1) a reduction in the inflammatory biomarker, C-reactive protein; 2) decreased platelet reactivity to activation by GPVI and PAR-1 agonists; and 3) endothelial cell activation as measured by VCAM-1 levels. These findings imply that therapeutic agents targeting FXI may extend beyond anticoagulation to include both antiplatelet and anti-inflammatory benefits.

The next set of studies evaluated if the benefits of pharmacologically targeting FXI could extend to the murine model of multiple sclerosis (MS), experimental autoimmune encephalomyelitis (EAE). As such, EAE mice were treated with the monoclonal

antibody, 14E11. Note, this antibody selectively inhibits FXIIa-mediated activation of FXI and the reciprocal FXIa-mediated activation of FXII *in vitro*.[1,2] We found that treatment with 14E11 reduced disease severity, immune cell migration, axonal damage, and BBB disruption in mice with EAE. Based on these findings, therapeutic agents against FXI and/or FXII may be used to treat autoimmune and neurologic disorders.

We then performed a series of functional assays to characterize select anti-FXII antibodies developed by our group. From our preliminary analysis, we selected 1B2 for additional screening in a baboon model of vascular device-initiated thrombosis. Following treatment with 1B2, we observed a reduction in platelet deposition and fibrin formation. These results provide the rationale for targeting coagulation factors to reduce or prevent vascular-device associated thrombosis in a variety of clinical settings, including extracorporeal membrane oxygenators (ECMO).

In the concluding chapters of my dissertation, multivariate logistic regression models were used to identify predictors of clinically relevant outcomes for patients on ECMO, including thrombotic and hemorrhagic events. The first retrospective cohort analysis was a single-center study investigating the incidence, predictors, and clinical consequences of severe thrombocytopenia in ECMO patients. It was determined that severe thrombocytopenia was predictive of thrombosis in adult ECMO patients. In a subsequent retrospective cohort study, we queried the Extracorporeal Life Support Organization (ELSO) Registry from 2015 to 2019. We found that patients with ECMO runs that exceeded 14 days and higher pump flow rates were at an increased thrombotic risk. Moreover, our multivariate regression indicated that thrombosis increased the likelihood

of in-hospital mortality. Although it remains difficult to ascertain associations between clinical factors and thrombosis, this work was hypothesis-generating.

Overall, the studies included in my dissertation provided new insights regarding the contribution of TEC family kinases and blood proteins, specifically coagulation factors (F) XI and XII, to our understanding of vascular diseases and devices. Findings from this work may be used to create novel biochemical tools and inform directional changes in thrombosis research.

Chapter 1. Introduction to the Interactions of the Blood Microenvironment with Vascular Diseases and Devices

1.1 Overview

The blood microenvironment is a complex milieu of cells and plasma proteins that work in concert to maintain homeostasis. Under physiological conditions, the vascular endothelium serves as a selective and dynamic regulator of membrane permeability and vascular tone.[3-5] Meanwhile, platelets quiescently circulate in blood, patrolling for vascular leaks.[6] In the event of vascular damage or injury, the blood vessel vasoconstricts and endothelium becomes activated. This in turn exposes blood cells and coagulation factors to the extracellular matrix (ECM) proteins and tissue factor (TF) expressing cells that comprise the extravascular space. When circulating platelets detect that the endothelial barrier has been compromised, they begin repairing the vasculature through a process known as hemostasis.[6] Initially, platelets tether to the exposed ECM proteins and activate through a series of intercellular signaling processes that facilitate the formation of a temporary platelet plug. In concert, the coagulation cascade is initiated upon exposure to tissue factor, ultimately leading to thrombin generation. Thrombin acts as a potent platelet agonist, thus amplifying the platelet activity; it also is the main serine protease that cleaves fibrinogen into fibrin, which facilitates the formation of a stable fibrin clot.[7,8]

In the following chapters, I will describe the interplay between endothelial cells, platelets, and coagulation in the blood microenvironment. I will narrate how these interactions impact both physiological processes (e.g. endothelial barrier function, hemostasis) and

pathological processes (e.g. chronic inflammation, autoimmune disease, vascular device-related thrombosis) (**Figure 1.1.**).

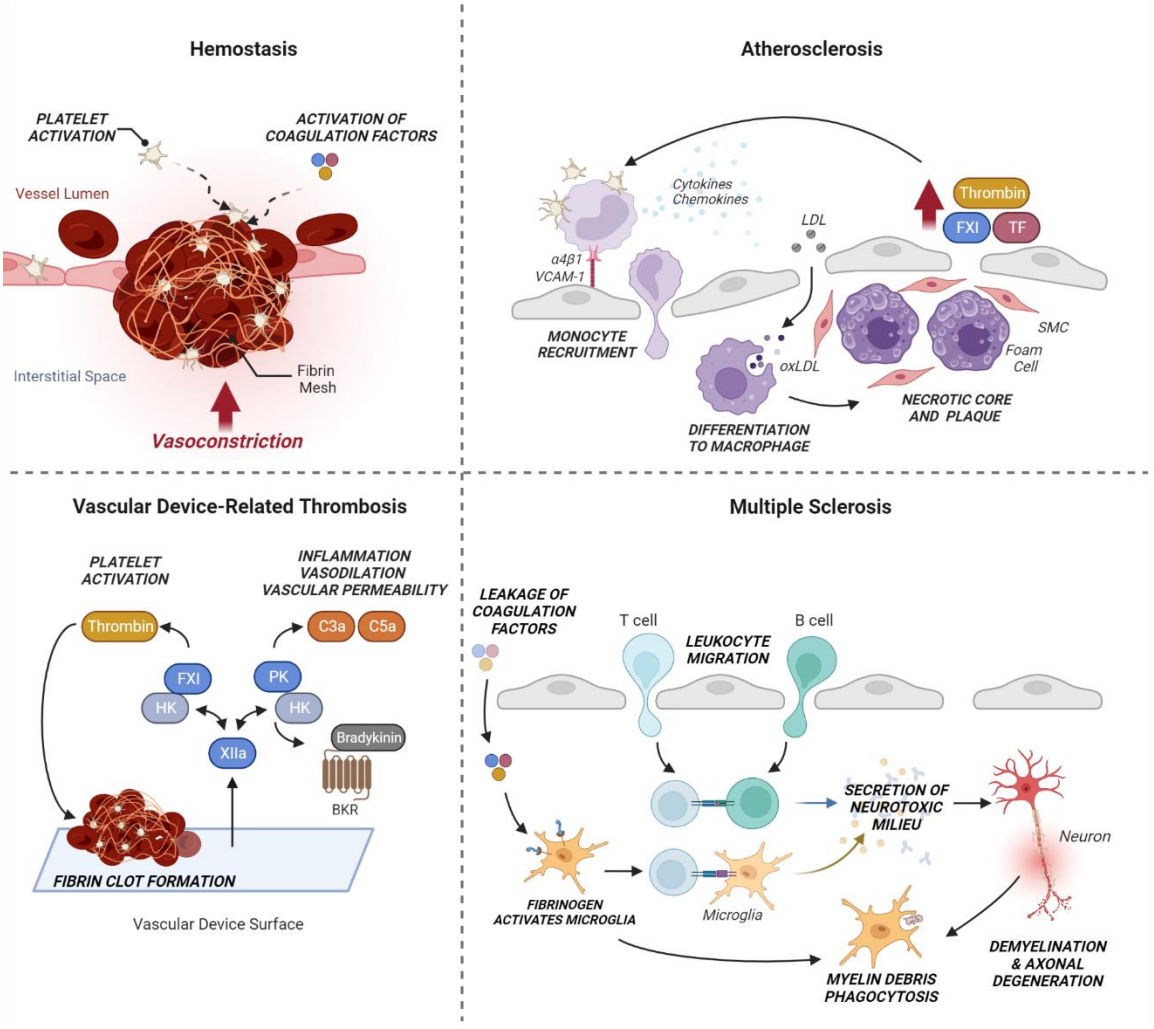

Figure 1.1 Role of endothelial cells, platelets, and coagulation factors in vascular devices and disease. The blood microenvironment is a dynamic system comprised of various cells and plasma proteins that together regulate maintain homeostasis. In the coming chapters, I outline my studies: 1) examining the intricate interplay of endothelial cells, platelets, and coagulation factors in hemostasis; and 2) investigating how these interactions impact the development of vascular diseases like atherosclerosis and multiple sclerosis, as well as responses to vascular device-related thrombosis. My work aims to create effective tools targeting intracellular and extracellular pathways within the blood microenvironment, while identifying key factors that predict adverse clinical outcomes to enhance patient care. Figure created with BioRender.com by Tia C.L. Kohs.

1.2 Vascular Endothelium

The vascular endothelium is a monolayer of cells that line the interior of blood vessels, serving as a barrier between circulating blood in the lumen and the surrounding tissues. It is comprised of cobble-stone shaped endothelial cells (ECs) anchored to an 80 nm thick basal lamina (BL). While EC morphology varies widely based on its position in the vascular tree, ECs typically measure 10–30μm in width, 30–50μm in length, and 0.1–10μm in thickness.[9] The luminal surface is directly exposed to circulating blood components and cells, whereas the basolateral surface is anchored to a glycoprotein basement membrane. To mitigate the shear stress exerted by the flowing blood, the ECs orientate themselves along the axis of the vessel walls.[9] While initially thought to be an inert and hemocompatible barrier, the utility of the vascular endothelium extends to other processes that dynamically regulate vascular permeability and vascular tone.[4,9] In the following sections, I will describe the integral role of the endothelium in the vascular microenvironment.

1.2.1 *Barrier Function and Vascular Permeability*

Endothelial barrier function and vascular permeability are modulated by intercellular junctions (e.g. gap, adherens, or tight junctions) that form a selective barrier against the egress of plasma and macromolecules from the circulation (**Figure 1.2**).[3,4] These junctions also play key roles in other cellular functions, including cell differentiation, proliferation, migration, signal transduction, and gene expression.[10] Herein, I will summarize the molecular underpinnings that regulate these junctions.

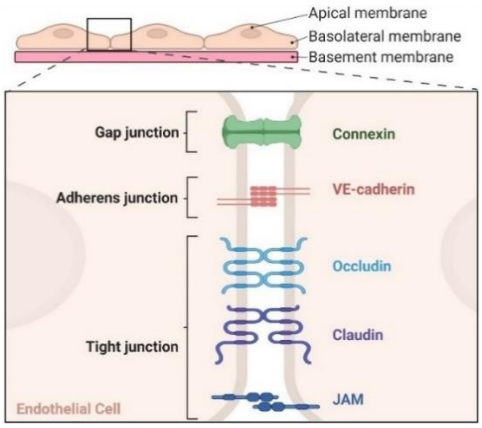

Figure 1.2 Intercellular junctions regulate endothelial cell barrier function and vascular permeability. Endothelial cells use intercellular junctions as mediators of endothelial cell barrier function and vascular permeability. These junctions include: gap junctions (e.g. connexins), adherens junctions (e.g. VE-cadherin), and tight junctions (e.g. occludin, claudin, JAM). VE, vascular endothelial. JAM, junctional adhesion molecule. Figure created with BioRender.com by Tia C.L. Kohs.

1.2.1.1 Gap Junctions

Gap junction (GJ) channels are intercellular communication structures that provide a passageway for solutes with low molecular weights.[11] These channels are comprised of connexins (Cxs). In the human genome, there are 21 different connexin genes that encode Cx proteins. Each of these Cx proteins have molecular weights ranging from 20-62 kDa and share the same protein topology, including: four transmembrane domains, two extracellular loops, a cytoplasmic loop, and N- and C-terminal domains.[12,13] They are synthesized in the endoplasmic reticulum (ER), oligomerized into hexameric connexons in the endoplasmic reticulum or the Golgi apparatus, and shuttled along microtubules by vesicles to the plasma membrane. When hemichannels from adjacent ECs dock, they form GJ channels that can facilitate ion and small metabolite exchange.[12] Although GJs are traditionally understood to regulate membrane permselectivity and conductivity, it is

important to note that emerging evidence indicates that connexins also play a role in endothelial barrier function through crosstalk with other junction proteins.[14,15]

Vascular ECs predominantly express the following connexins: Cx37, Cx40, Cx43, and Cx45.[12,13,15] However, the expression of GJs in vascular endothelium differ based on their location and the type vessel. For example, Cx37 and Cx40 are highly co-expressed in the straight regions of healthy ECs in arteries where they are exposed to high shear stress from laminar blood flow, and downregulated at bifurcations due to turbulent blood flow. In this setting, Cx37, Cx40, and Cx43 are typically located between the ECs, whereas Cx43 and Cx45 are located between smooth muscle cells. Conversely, Cx43 expression is induced at these arterial branchpoints. With respect to ECs on venous valves, Cx43 is expressed on the upstream side, whereas Cx37 is expressed on the downstream side.[12] Note, both Cx expression and gap junction function in ECs is influenced by pro-inflammatory stimuli and closely correlated with activation of ECs.

1.2.1.2 Adherens Junctions

Adherens junctions (AJs) provide ECs with mechanical anchorage by regulating actin polymerization and actomyosin contraction.[12,16] When the ECs are quiescent, junctional actin filaments either run parallel or perpendicular to the cell surface, with AJs indirectly anchoring actomyosin stress fibers to the membrane.[16] AJs are transmembrane adhesion proteins belonging to the cadherin family that form multimeric complexes in the peripheral regions of cells. In the case of ECs, vascular endothelial (VE)-cadherin is strongly localized to the AJs.[11] VE-cadherin binds directly to β- or γ-catenin (plakoglobin) or catenin p120, and indirectly to α-catenin via β- or γ-catenin.[3,16] When

dimeric α-catenin binds to actin filaments, Arp2/3 activity is inhibited and formin is activated, resulting in suppressed actin branching and the formation of linear actin cables, respectively. Concomitantly, β-catenin regulates actin polymerization and actomyosin contractility through Rho family GTPases, Rac and Rho. Note, increased contractility of myosin can compromise barrier function in the EC allow free passage of cells and molecules; however, it has been demonstrated that inhibition of Rho activity can spare EC junctional stability. Taken together, the dynamic reorganization local of AJs can create functional units that allow ECs to withstand the stress of hemodynamic changes and junctional remodeling in the setting of inflammation, transmigration of leukocytes, and angiogenic responses.[16] Of note, neural cadherin (N-cadherin) and placental cadherin (P-cadherin) are also present in EC; however, these cadherins are dispersed on the cell surface.[17]

1.2.1.3 Tight Junctions

The endothelial barrier is principally regulated by tight junctions (TJs) sealing the transcellular space.[12] These junctions support the structural integrity of both endothelial and epithelial tissues and form highly polarized barriers that are selectively permeable to solutes and various cells.[18] Tight junctions consist of proteins such as occludin, claudins, and junctional adhesion molecules. Each of these TJs will be detailed below.

Occludin: Occludin is a 65 kDa tetraspan protein found localizing to epithelial and endothelial TJs by Furuse et al. in 1993,[19] making it the first integral membrane TJ protein to be identified. It is comprised of four transmembrane domains, a short intracellular turn, two extracellular loops, and a long carboxy- and a short amino-terminal

cytoplasmic domain.[20] The N-terminal extracellular region contributes to the adhesive function of occludin. Meanwhile, at the C-terminal, serine/threonine and tyrosine residues are phosphorylated by multiple kinases and SH3 and PDZ-containing zonula occluden (ZO) proteins are recruited, thereby anchoring occluding to actin fibrils.[10] Thus, the reversible phosphorylation of these residues is functionally a switch that regulates the assembly and maintenance of TJ. Nonetheless, while early studies led people to believe that occluding was the core transmembrane protein of TJ, later investigations demonstrate that occluding is actually dispensable in TJ strand formation.[20]

Claudins: Claudins are the largest family of tight junction proteins, with at least 24 claudins present in the human genome. They are comprised of four transmembrane proteins and, with the exception of claudin-12, include a PDZ-binding domain at the C-terminal that binds to scaffold proteins.[10] The role of claudins in regulating barrier function and intercellular interactions in endothelia or epithelia is mediated by claudins dimerizing through homophilic- and heterophilic-*trans*/*cis* interactions. It has been hypothesized that the larger first extracellular loop is critical for regulating paracellular tightness and selective ion permeability, whereas the second extracellular loop is shorter and may reduce the size of the paracellular cleft and hold opposing cell membranes together.[21] These interactions appear to be calcium-independent, unlike those regulated by cadherins.[10] Based on the degree of sequence homology and the sequence-structure function relationships, claudins are classified as either classic claudins (1–10, 14, 15, 17, 19) or non-classic claudins (11–13, 16, 18, 20–24).[21]

Junctional Adhesion Molecules: Junctional adhesion molecules (JAMs) are members of the immunoglobin (Ig) superfamily and are comprised of: two extracellular Ig-like domain, one transmembrane domain, and a short cytoplasmic domain.[22] Within the cytoplasmic domain is the PDZ domain that serves as a scaffold to bind to proteins (e.g. ZO-1, AF-6, MUPP1, PAR-3) that allow JAMs to mediate barrier function and regulate interactions between ECs, platelets, and leukocytes (**Figure 1.3**).[10,23] JAMs are not only expressed endothelial cells, but also in leukocytes and platelets, and support a number of homophilic and heterophilic interactions.[24]

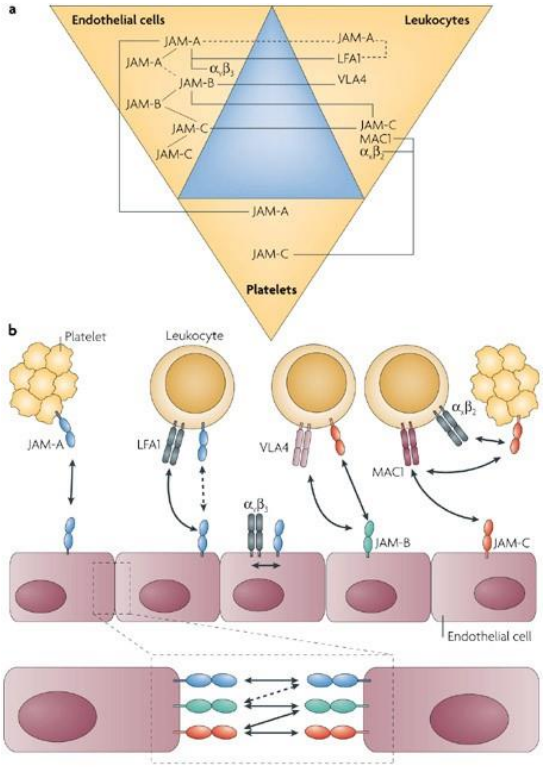

Figure 1.3 Junctional adhesion molecule facilitate interactions between ECs, platelets, and leukocytes. (a) Interactions published in the literature are designated with solid lines and interactions predicted are designated with dashed lines. (b) Homophilic and heterophilic interactions between JAMs and/or integrins support binding of leukocytes to the endothelium, platelet adhesion to leukocytes and the endothelium, and intercellular EC connections. JAM, junctional adhesion molecule. LFA1, lymphocyte function-associated antigen 1. VLA4, very late antigen 4. Figure reprinted with permission from Weber et al., *Nat Rev Immunol*, 2007 June;7:467-477.[24]

1.2.2 *Regulation of Vascular Tone*

The endothelium regulates vascular tone by maintaining a balance of vasoactive factors. In the subsequent subsections, I will outline key vasodilators and vasoconstrictors.[5]

1.2.2.1 Nitric Oxide

Nitric oxide (NO) is a key vasodilator that is formed when the enzyme nitric oxide synthase (NOS) converts the amino acid $_{L}$-arginine to NO. NO potentiators (e.g. bradykinin, acetylcholine, ATP, ADP, thrombin) influence eNOS activation and release of Ca^{2+} from the endoplasmic reticulum. Alternatively, eNOS can be activated by protein kinases, shear stress resulting from increased blood flow, or blood-borne agonists signaling through EC receptors to increase intracellular Ca^{2+} levels. Once synthesized, NO diffuses across the EC into the adjacent smooth muscle, which leads to a downstream decrease in smooth muscle tension.[5]

1.2.2.2 Prostacyclin and Thromboxane A_2

Prostacyclin (PGI_2) and thromboxane A2 (TXA_2) belong to a family of lipid mediators known as prostanoids and are generated through cyclooxygenase (COX) activity. In a healthy vessel, PGI_2 and TXA_2 are concomitantly regulated to mediate vessel tone. On one hand, PGI_2 functions as a vasodilator by binding to prostacyclin receptors (IP) on vascular smooth muscle cells. When PGI_2 binds to smooth muscle cell IP receptors, it activates adenylate cyclase, leading to the synthesis of cyclic adenosine monophosphate (cAMP). cAMP then activates protein kinase A, causing relaxation of the smooth muscle. Note, PGI_2 can also bind IP receptors on the surface of platelets, thereby inhibiting platelet aggregation. Conversely, TxA_2 functions as a vasoconstrictor by binding to

thromboxane-prostanoid (TP) receptors on smooth muscle cells. Upon binding to smooth muscle cell TP receptors, intracellular Ca^{2+} levels are increased, resulting in the constriction of the smooth muscle. When TxA_2 binds to TP receptors on the surface of platelets, platelet aggregation is induced. Taken together, both PGI_2 and TXA_2 are important mediators of vessel tone.[5]

1.2.2.3 Endothelin-1

Endothelin-1 (ET-1) is a vasoconstrictor that is both produced and released in response to inflammatory signals (e.g. interleukins and TNF-α). ET-1 induces vasoconstriction by binding to ET-1 receptors on ECs ($ET\text{-}_{B1}$) and smooth muscle cells (ET_A and $ET\text{-}_{B2}$). Upon binding these receptors, the endothelium releases NO and PGI_2 and smooth muscle cells open their Ca^{2+} channels to allow for an influx of extracellular Ca^{2+}.[5]

1.2.2.4 Endothelium-Derived Hyperpolarizing Factor

Endothelium-derived hyperpolarizing factor (EDHF) describes vasodilator substances that signal through pathways that alter the membrane potential of smooth muscle cells.[5] For example, EDHF-mediated signaling leads to increased intracellular Ca^{2+} levels in the endothelium, which subsequently causes an efflux of K^+, and EC hyperpolarization.[25]

1.3 Platelets

Platelets are anuclear, discoid cells that circulate in blood at concentrations of 150 to 400 million per milliliter for approximately 10 days. They are derived from megakaryocytes that originate in the bone marrow.[6] Under physiological conditions, quiescent platelets circulate in the bloodstream and patrol the vasculature for sites of damage. At sites of vessel wall damage, platelets play a pivotal role in repairing the vasculature through a

process known as hemostasis. This process is achieved through the adhesion and activation of platelets, as well as the coagulation cascade.[6] In this section, I will summate the contribution of platelet adhesion, activation, and aggregation in bleeding cessation at the site of injury.

1.3.1 *Platelet Adhesion to Extracellular Matrix Proteins*

When the vasculature becomes damaged, platelets are exposed the extracellular matrix (ECM) proteins.[6] These proteins can either be synthesized by vascular wall cells (e.g. von Willebrand Factor [vWF], collagen, laminin, fibulin, thrombospondin) or become immobilized onto the ECM upon injury (e.g. fibrinogen, fibrin, vitronectin).[26] Below I have highlighted some key ECM proteins that interact with platelets.

1.3.1.1 von Willebrand Factor

von Willebrand factor (vWF) is multimeric glycoprotein synthesized by ECs and megakaryocytes. It is stored in: 1) EC Weibel-Palade bodies and platelet α-granules, 2) in a soluble form in plasma, or 3) in the subendothelial matrix.[27] Structurally, mature vWF contains identical subunits of 2050 amino acid residues and up to 22 carbohydrate side chains that are joined by disulfide-bonds to make ~500 kDa dimers. These dimers are then joined by additional disulfide-bonds to form multimers up to 20 MDa.[28]

The domains of vWF are responsible for different functionalities of the protein. Indeed, the D′-D3 domains bind to the procoagulant factor, FVIII; the A1 domain contains the only binding site for platelet receptor glycoprotein (GP) Ibα of the GPIb-IX-V complex; the A2 domain is cleaved by the plasma metalloprotease, a disintegrin and metalloprotease with thrombospondin type motifs 13 (ADAMST13), which inactivates

vWF; the A3 domain binds to collagen, the C1 domain that contains the RGD sequence recognized by platelet αIIbβ3 and αvβ3 integrins.[6,28,29]

1.3.1.2 Collagen

Collagen is the most abundant fibrous protein in the extracellular matrix.[30] There are 28 members in the collagen superfamily, each with three α chains forming a triple helix. While there is great functional diversity of collagens, we will focus on fibrillar collagens as they not only play key roles in regulating the structural and mechanical properties of tissues, they also serve as potent triggers for thrombosis.[31] It is important to note that these fibrillar collagens are differentially expressed in the ECM. For example, fibrillar collagens localized to the deeper layers of the ECM (e.g. type I, III, and V) are not exposed following superficial injuries. Conversely, fibrillar collagens type IV, VIII, and XVIII are closer to the endothelial layer and expressed in the basement membrane. When the endothelium is damaged, platelets are captured by GPIb-vWF interactions and roll along deposited vWF (see Section 1.3.1.2). This allows collagen-specific platelet receptors, platelet glycoprotein VI (GPVI) or integrin $\alpha_2\beta_1$, to bind to the exposed collagen and induce platelet activation.[27]

1.3.1.3 Fibrin(ogen)

Fibrinogen is a 340-kDa homodimeric glycoprotein that is predominantly synthesized in hepatocytes. It is comprised of 2Aα, 2Bβ, and 2γ polypeptide chains linked by 29 disulfide bridges.[32] Under physiological conditions, fibrinogen circulates in plasma at relatively high concentrations (2–5 mg/mL); in the setting of acute inflammation, however, levels of fibrinogen can exceed 7 mg/mL.[33] In the event of vascular injury,

fibrinogen binds to the platelet surface receptor, αIIbβ3 (also known as glycoprotein GPIIb/IIIa), to facilitate stable platelet adhesion and platelet-platelet interactions that are necessary for thrombus formation.[26,34]

Fibrin, the cross-linked insoluble polymer of fibrinogen, is generated when fibrinogen is proteolytically cleaved by the serine protease, thrombin, during coagulation. This in turn provides a meshwork of fibrin that helps in stabilizing the emerging blood clot.[33] Fibrin can also facilitate platelet adhesion by synergizing with immobilized vWF.[35]

1.3.2 *Platelet Signaling During Activation*

Platelet activation is driven by a myriad of intracellular signaling events that are mediated through the binding of platelets to adhesive proteins in the ECM, as well as soluble agents that signal through platelet surface receptors (**Figure 1.4**).

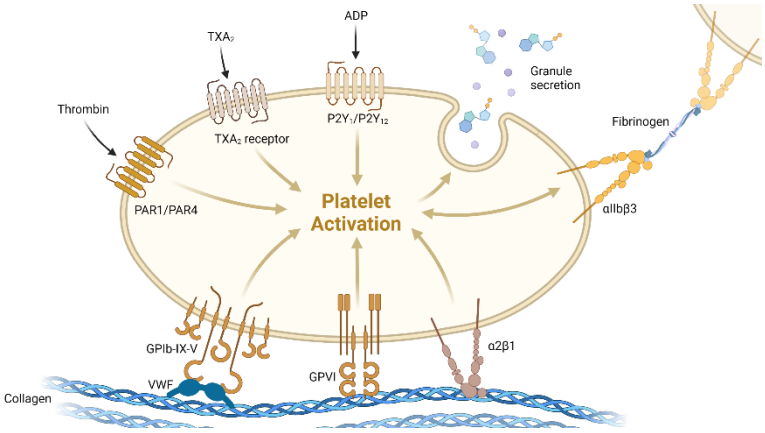

Figure 1.4 Key receptors and ligands that contribute to the activation of platelets. Platelet activation is triggered by specific receptors on the platelet surface, including glycoprotein Ib/IX/V (GPIb/IX/V), glycoprotein VI (GPVI), integrin α2β1, protease-activated receptors (PARs), thromboxane A2 (TXA_2) receptors, P2Y receptors, and integrin αIIbβ3. These receptors bind to ligands such as von Willebrand factor (vWF), collagen, thrombin, adenosine diphosphate (ADP), and fibrinogen, ultimately leading to platelet activation. Reprinted from "Platelet Activation", by BioRender.com (2023). Retrieved from https://app.biorender.com/biorender-templates.

1.3.2.1 Adhesion Receptor-Mediated Signaling

During the initial stages of hemostasis, activated platelets are recruited to the damaged endothelium where various platelet surface receptors facilitate adhesive interactions. These receptors include the platelet GPIb-IX-V receptor complex that binds vWF and the platelet GPVI receptor that binds to collagen.[6]

GPIb-IX-V: GPIb-IX-V is a receptor complex found on the surface of platelets, which plays a critical role in platelet function and regulation. The GPIb-IX-V complex consists of four subunits: GPIbα, GPIbβ, GPIX, and GPV. These subunits are classified as type I transmembrane proteins and consist of a large N-terminal extracellular domain with a leucine-rich repeat (LRR) domain that varies in length, a single-pass transmembrane helix and a short cytoplasmic tail.[36]

The primary function of the GPIb-IX-V complex is to mediate platelet adhesion to the subendothelial matrix following vascular injury under conditions of high shear stress. In this setting, platelets initially adhere transiently to the endothelium by forming 'catch bonds' or 'flex bonds' via the interaction between GPIbα and the A1 domain of vWF.[37] Indeed, the cytoplasmic domain of GPIbα interacts with the Src family kinases (SFK) Lyn, phosphoinositide 3-kinase (PI3K), and Akt, which leads to elevated levels of Ca^{2+} and activation of platelet integrins downstream.[37]

GPVI: Glycoprotein VI (GPVI) belongs to the Ig superfamily of receptors and is exclusively expressed in megakaryocytes and platelets, with 3,000–4,000 copies per human platelet. It contains two Ig domains (D1, D2), a mucin-like stalk, and a cytoplasmic tail containing calmodulin- and Src kinase–binding sites. Note, both the

expression and signaling of GPVI require GPVI to be bound to a dimeric Fc receptor γ-chain (FcRγ) that contains an immunoreceptor tyrosine–based activation motif (ITAM) signaling motif.[38]

When collagen binds to platelet GPVI, the Src family kinases (SFK), Fyn and Lyn, induce tyrosine phosphorylation of the FcR γ-chain ITAM. This results in downstream activation of Syk, which in turn phosphorylates a number of substrates bound to the transmembrane adapter, linker for activation of T cells (LAT) signalosome. The LAT signalosome includes Bruton's tyrosine kinase (BTK), Tec family kinases, phosphoinositide 3-kinase (PI3K), and phospholipase C γ2 (PLCγ2).[38] Together, these kinases signal downstream to activate protein kinase C (PKC) and release intracellular Ca^{2+} stores. This leads to secretion of intracellular α-granules and dense granules, as well as activation of 'inside-out' activation platelet integrins, which culminates in platelet aggregation.[39]

1.3.2.2 Soluble Agonist-Mediated Signaling Through G-Protein Coupled Receptors

G-protein coupled receptors (GPCRs) represent the largest family of proteins in the human genome and consist of seven transmembrane-spanning domains, with an extracellular N-terminus and an intracellular C-terminus.[40,41] They are aptly named as GPCRs signal through heterotrimeric G proteins that are bound to the intracellular loop. The G protein has three subunits (α, β, and γ) and can be further classified based on the α subunits ($G_{12/13}$, G_q, G_i, and G_s).[37] Following the activation of the receptor, the α subunit is converted from a GDP-bound form to the active GTP-bound form. This allows

the active Gα and the Gβγ subunits to dissociate from the receptor and interact with downstream targets in the GPCR signaling pathway.

At the site of a new vessel injury, platelet activation of nearby platelets will be amplified via feedback activation pathways mediated by GPCRs to further the formation of a hemostatic plug.[6] Indeed, soluble factors that are released when platelets are activated (e.g. such as adenosine diphosphate [ADP] and thromboxane [TXA_2]), as well as thrombin from the coagulation cascade, are key components that signal through GPCRs to amplify platelet activation and recruitment.[37] Note, these cell-signaling pathways lead to platelet cytoskeleton remodeling, granule secretion, and integrin activation (**Figure 1.5**).[6] In the following subsections, I will detail select GPCRs that amplify platelet activation or mediate inhibition.

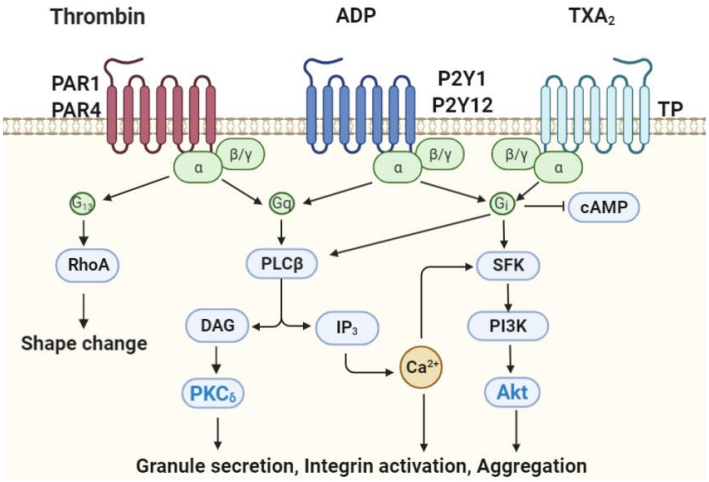

Figure 1.5 Platelet signaling through G-protein coupled receptors. At the site of a vascular injury, feedback activation of platelets mediates aggregation and propagation to form a hemostatic plug. GPCRs bind to soluble factors released from activated platelets themselves (e.g. adenosine diphosphate [ADP], thromboxane A_2 [TxA_2]) or thrombin generated during coagulation processes. Downstream GPCR signaling initiates platelet shape change, granule secretion, integrin activation, and aggregation. Figure created in BioRender.com by Dr. Stephanie E. Reitsma.

Protease Activated Receptors 1 and 4: Thrombin is a serine protease that serves as the main effector in the blood coagulation system and is generated cellular surfaces, including the surface of activated platelets.[40] Thrombin potently activates platelets through protease activated receptors (PAR) 1 and 4 coupled directly to G_{13}, G_q and possibly G_i. Signaling through G_{13} results in activation of the RhoA/Rho-kinase pathway, which ultimately induces platelet shape change.[40] In the G_q-mediated signaling pathway, phospholipase C (PLC) is activated, which then hydrolyzes phosphatidylinositol 4,5-bisphosphate (PIP2) to release inositol trisphosphate (IP_3) and diacyglycerol (DAG).[34] This allows protein kinase C (PKC) to be activated downstream and intracellular Ca^{2+} to be released, thus contributing to platelet activation and aggregation.

$P2Y_1$ and $P2Y_{12}$: ADP is stored in platelet dense granules at high concentrations and is released when platelets are activated.[40] Released ADP binds to the G_q-coupled receptor, $P2Y_1$, and the G_i-coupled receptor, $P2Y_{12}$.[6] Signaling through $P2Y_1$ activates phospholipase C (PLC), which produces diacylglycerol (DAG) and inositol tris-phosphate (IP_3). This in turn leads to the downstream activation of protein kinase C (PKC) and release of intracellular Ca^{2+}. Concomitantly, the $P2Y_{12}$-mediated signaling results in the activation of phosphoinositide 3-kinase (PI3K)-dependent pathways and inhibition of cyclic adenosine monophosphate (cAMP).[41] Although the signaling pathways for $P2Y_1$ and $P2Y_{12}$ differ, they both play a role in platelet activation and aggregation.

Thromboxane: Thromboxane (TXA_2), like ADP, plays an important role in the positive-feedback mediator during platelet activation. It is produced through the metabolism of

arachidonic acid mediated by cyclooxygenase-1 (COX-1) and thromboxane synthase.[41] The resulting thromboxane binds to thromboxane receptors, TPα and TPβ; however, it is important to note that TPα is the predominant isoform in human platelets, which is coupled to G_{13} and G_q.[27,40] Consequently, TXA_2-mediated signaling will activate the RhoA/Rho-kinase pathway and PLC-mediated signaling events that induce platelet shape change as well as platelet activation and aggregation.

1.3.2.3 Convergence of Platelet Signaling Pathways

As outlined in the previous sections, platelets can signal through a multitude of receptors, each triggering unique mechanisms; however, platelet signaling converges on common events (e.g. granule secretion and integrin activation).

Granule Secretion: When platelets are activated, they secrete over 300 bioactive substances from intracellular granules that amplify platelet activation and recruitment of other platelets to form a stable.[42] There are at least three distinct types of granules housed in platelets, including: alpha (α) granules, dense (δ) granules, and lysosomes.[42,43] α-granules are the most abundant, with approximately 50–80 α-granules per platelet. α-granule-derived mediators play a pertinent role in hemostasis, as well as in the innate immune system (e.g. platelet adhesion receptor expression, cytokine release that affects leukocyte function).[44] The contents of α-granules include: adhesive glycoproteins (e.g. P-selectin, fibrinogen, vWF); coagulation and fibrinolytic factors; cytokines and chemokines; mitogenic factors; and angiogenic factors (e.g. vascular endothelial growth factor [VEGF]).[34,42,44] Dense granules also contribute to coagulation, with an additional role in cancer metastasis. They are comprised of hemostatically active, non-protein

molecules including: nucleotides (e.g. ADP, ATP, GTP); catecholamines (e.g. serotonin, histamine); divalent cations (e.g. Ca^{2+}) pyrophosphates; and polyphosphates.[34,44] Unlike α-granules and dense granules, lysosomes demonstrate bactericidal activity through their proteolytic enzymes (e.g. glycosidases, acid proteases, and cations).[44]

Integrin Signalling:

There are five platelet integrins expressed at the surface: αIIbβ3 (fibrinogen receptor), α5β3 (vitronectin and collagen receptor), α2β1 (collagen receptor), α5β1 (fibronectin receptor) and α6β1 (laminin receptor).[34,45] Of these different types of integrins, αIIbβ3 is the most abundant.[34] Indeed, there are 50,000–100,000 copies of αIIbβ3 located on the surface of unstimulated platelet surfaces alone, with even more stored in intracellular α-granule membranes.[46]

When platelets are activated, αIIbβ3 transitions from a resting low-affinity state into an activated high-affinity state. This conformational change is facilitated through a process referred to as "inside-out" signalling, and ultimately results in active αIIbβ3 binding to the Arg-Gly-Asp (RGD) sequence of its ligands, which include fibrinogen, fibronectin, von Willebrand factor, and vitronectin (**Figure 1.6A**).[47] Once bound by its respective ligand, αIIbβ3 triggers a number of cellular processes (e.g. cytoskeletal reorganization, granule secretion, stable adhesion) via "outside-in" signaling (**Figure 1.6B**).[34,47]

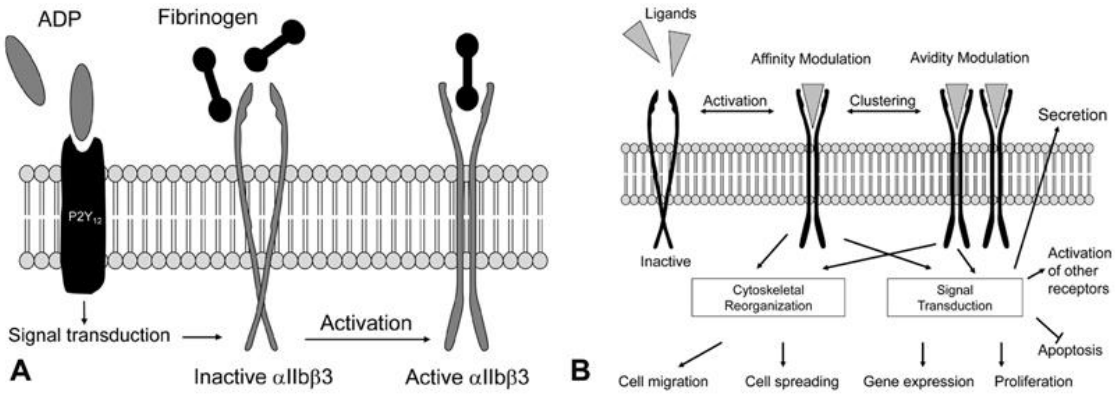

Figure 1.6 Platelet integrin αIIbβ3 signals through "inside-out" and "outside-in" pathways. (A) The platelet integrin, $\alpha_{IIb}\beta_3$, transitions from a low- to high-affinity state when platelets are activated, either through adhesion to the extracellular matrix or via soluble agonists (e.g. ADP, thrombin, etc.). This process is referred to as "inside-out" signalling since information is being passed from within the cell to the extracellular domain of αIIbβ3. (B) A number of cellular processes are initiated by way of "outside-in" signalling when the integrin αIIbβ3 receptor is occupied by its respective ligand. Figure reprinted from Joo, *Korean Circ J*, 2012 May;42(5):295-301.[47] Permission is not required by the publisher for this type of use.

1.3.3 *Platelet Aggregation*

Platelet aggregation is a multi-step process by which platelet-platelet interactions facilitate the formation of a hemostatic plug. Following platelet adhesion to the site of vascular injury, platelets are activated by various agonists (**Section 1.3.2**), which ultimately increases the concentration of intracytoplasmic calcium ions and facilitates adhesion receptor-ligand interactions.[27] With respect to the increased levels of intracellular calcium, this induces platelet shape change, a process during which platelets transition from a discoid shape to a sphere with a spiny appearance.[27] Concomitantly, the adhesion receptor-ligand interactions result in aggregate formation. In the traditional understanding of platelet aggregation, this process is driven by the homodimeric adhesive protein, fibrinogen, forming a noncovalent bridge between the platelet integrin αIIbβ3

(also known as GPIIb/IIIa) on adjacent platelets.[48] However, it has now been shown that von Willebrand factor (vWF) and fibronectin bind to αIIbβ3 in place of fibrinogen under high shear conditions (e.g. in cases of rapid blood flow where wall shear rates exceed 1000 s^{-1}) to facilitate the initial tethering of platelets. Nonetheless, the fibrin(ogen)-integrin αIIbβ3 interaction remains imperative for the formation of stable aggregates.[27,48]

1.4 Coagulation

In the cell-based model of hemostasis, the coagulation cascade can be divided into three distinct, yet overlapping phases.[8] During the initiation phase, active coagulant factors are generated in low amounts via the extrinsic pathway on TF-bearing cells. In the amplification phase, the level of activated coagulation factors increases through a positive feedback of thrombin on platelets. During the propagation phase, thrombin is generated on a larger scale when activated coagulation factors bind the procoagulant surface activated platelets via the intrinsic pathway.[7,8]

1.4.1 *Extrinsic Pathway of Coagulation*

The initiation phase begins when a blood vessel is injured, triggering the extrinsic pathway of coagulation. In this setting, plasma FVIIa forms a complex with tissue factor (TF), a membrane protein that is constitutively expressed by cells underlying blood vessel endothelium. The resulting complex proteolytically cleaves both FIX and FX, resulting in FIXa and FXa, respectively. Subsequently, FXa forms a prothrombinase complex on TF-expressing cells through an association with FVa, thus resulting in prothrombin (FII) being converted to thrombin.[7] This activity is limited, however, by fibrin and platelets accumulating at the site of vessel injury and by endogenous inhibitors

including tissue factor pathway inhibitor (TFPI) and antithrombin (AT).[49] During the amplification phase, trace amounts of thrombin from the initiation phase induce a higher level of procoagulant activity by further activating platelets adhered to the injury site. Concomitantly, thrombin activates the cofactors FV and FVIII on the platelet surface, thus amplifying prothrombinase activity and supporting generation of FXa, respectively.[7]

1.4.2 *Intrinsic Pathway of Coagulation*

During the propagation phase, thrombin generation occurs in large bursts on surfaces containing procoagulant phospholipids (e.g. activated platelets) to facilitate the formation of a fibrin clot via the intrinsic pathway.[8] The intrinsic pathway, also known as the contact activation system, consists of: coagulation factor (F) XII, prekallikerin (PK), FXI, and high-molecular-weight kininogen (HK). It is triggered when a primary complex forms on exposed collagen during endothelial damage. When this occurs, activated FXII (FXIIa) activates FXI, subsequently activating FIX and feeding into the common pathway. This sequence of reactions ultimately leads to thrombin generation and fibrin formation.

Concomitantly, FXIIa can cleave PK to generate active plasma kallikrein, which catalyzes the activation of FXII into FXIIa and cleaves high molecular weight kininogen (HK) to liberate bradykinin (BK), a pro-inflammatory molecule.[50] This promotes systemic inflammation and vascular permeability. Recent evidence suggests that FXI also plays a role in activating FXII and PK, *in vivo.*[2] This bidirectional relationship provides a mechanism by which the intrinsic pathway extends beyond thrombin generation and

fibrin deposition to include regulation of inflammatory pathways, such as the kallikrein-kinin system.

1.4.2.1 Coagulation Factor XII

FXII (Hageman factor) is the 80-kDa zymogen precursor of serine protease, FXIIa. FXII comprised of seven structural domains: a fibronectin domain type II, two epidermal growth factor (EGF) domains, a fibronectin domain type I, a kringle domain, a proline-rich region, and a protease (catalytic) domain.[51] Activation of FXII is facilitated through interactions with kallikrein, FXIa, or through auto-activation in the presence of negatively charged surfaces and HK.[52] During infections, such charged surfaces may include: pathogen surfaces and bacterial wall products, bacterial or platelet polyphosphate, subendothelial collagen, misfolded proteins, neutrophils, glycosaminoglycans and nucleic acids released from dying cells or from neutrophil extracellular traps.[53]

Upon activation, FXII is cleaved resulting a 353-residue heavy chain (α-FXIIa) connected to a 243-residue light chain (β-FXIIa) via a disulfide bond (**Figure 1.7**).[51,54] The resulting FXIIa protease is positioned at the nexus of the kinin-kallikrein,

complement, coagulation and fibrinolytic pathways. With respect to the kallikrein-kinin and complement systems, α-FXIIa can activate prekallikrein to α-kallikrein, which can then convert FXII to α-FXIIa in a reciprocal feedback mechanism. Moreover, α-FXIIa can activate the complement cascade via activation of the C1qrs complex,[55] while kallikrein has been shown to activate factor B, C3 and C5.[56] Additionally, α-FXIIa plays a role in coagulation by activating FXI to FXIa, which accelerates production of thrombin that drives platelet activation, fibrin formation, and exerts effects on a variety of cells.[51,57] When α-FXIIa is cleaved after Arg334, the resulting β-FXIIa can generate kallikrein, which cleaves HK to release bradykinin, a systemic vasoregulatory and inflammatory mediator.[58,59] β-FXIIa is unable to activate FXI and thus does not participate in the coagulation system.[51]

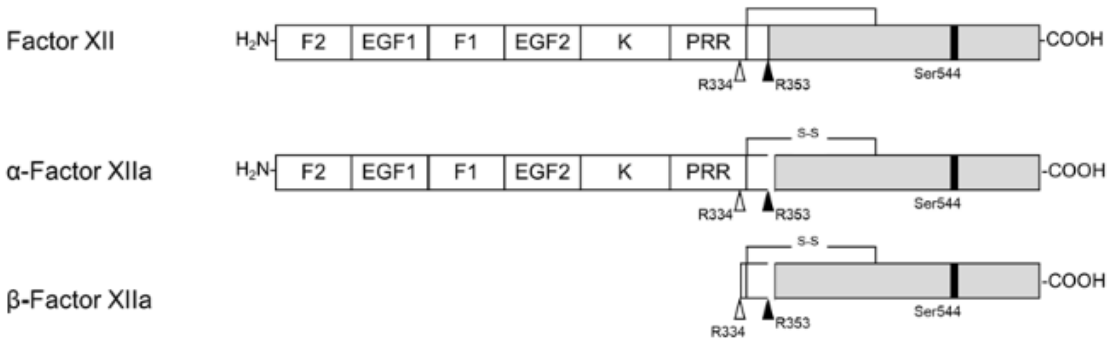

Figure 1.7 The structure of coagulation FXII(a). When factor XII is activated, cleavage of a disulfide bond results in two separate fragments- a heavy chain (α-FXIIa) and a light chain (β-FXIIa). Figure adapted from Kohs et al., *Cell Mol Bioeng*, 2020 Oct 13;14(2):161-175.[60] Reprinted with permission.

1.4.2.2 Coagulation Factor XI

Section 1.4.2.2 is adapted from a work originally published by Thieme Medical Publishers.

Lira AL, **Kohs TCL**, Moellmer SA, Shatzel JJ, Mccarty OJT, Puy C. Substrates, Cofactors, and Cellular Targets of Coagulation Factor XIa. *Seminars in Thrombosis and Hemostasis*, 2023: In Press.

Reprinted with permission

Regarding structure, FXI and PK are both comprised of four apple domains (A1 to A4) and a trypsin-like protease domain.[15] Uniquely, FXI is a homodimer with two identical 80 kDa subunits covalently linked by a disulfide bond connecting the A4 domains, whereas PK is a monomeric protein.[16–18] In 2006, Papagrigoriou *et al.* were the first to report that each FXI apple domain consists of seven β-strands that form an antiparallel sheet that supports a single α-helix with three internal disulfide bonds that compel the domains.[15] The apple domains form a planar structure, proximally 60 Å wide, with the N-terminal of the A1 domain linking to the A4 domain. They are inclined to each other, assuming an inverted "V" form, while the protease domain is configured in a 'cup and saucer' adjustment on the apple domains.[17,18]

The apple domains are essential for FXI activation and activity. FXIIa, FXIa, and thrombin generate FXIa by cleaving the Arg369-Ile370 bond located in the protease domain of FXI.[19,20] The activation of FXI to FXIa induces a conformational change, which exposes an exosite located at the A3 domain of FXIa that is specific for FIX interaction, thereby allowing for FXIa to activate FIX (**Figure 1.8**).[16,18]

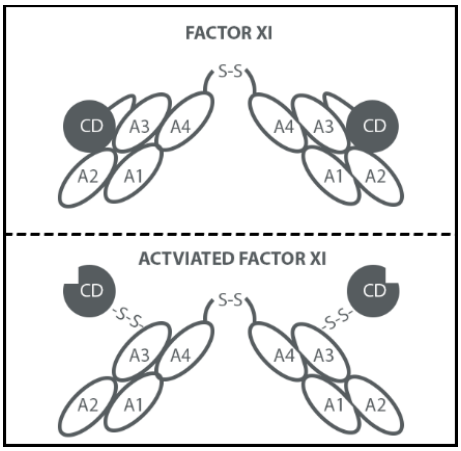

Figure 1.8 The structure of coagulation FXI(a). FXI(a) consists of two identical 80 kDa subunits, each comprised of four apple domains (A1 to A4) and a trypsin-like protease domain, also known as the catalytic domain (CD). These subunits are covalently joined by a disulfide bond between the A4 domains to form a homodimer. FXIa is generated when the Arg369-Ile370 bond in the protease domain of FXI is cleaved, thus inducing a conformational change. Figure adapted from Mohammed et al., *Thromb Res*, 2018 Jan;161:94-105.[61] Reprinted with permission.

At present, the FXI binding sites for thrombin and FXIIa remain uncertain. Nonetheless, studies suggest that thrombin binds residues in the A1 domain near the activation loop containing the cleavage site,[8,21] whereas FXIIa likely binds to the A4 domain.[22] The A2 domain also appears to be the binding site for FXIIa, as an anti-FXI A2 antibody blocks FXIIa-mediated activation of FXI.[23]

1.4.3 *Common Pathway*

The intrinsic and extrinsic pathways of coagulation converge on the common pathway. This pathway involves the activation of FX to FXa. FXa in the presence of its cofactor, FV, as well as tissue phospholipids, platelet phospholipids and calcium ions form the prothrombinase complex that converts of prothrombin (FII) to thrombin (FIIa). The resulting thrombin cleaves circulating fibrinogen to insoluble fibrin and concomitantly

activates factor XIII, thereby forming a mesh-like structure of crosslinked fibrin polymers around platelets and red blood cells.[62] The resulting hemostatic plug stops the bleeding and allows for tissue repair and healing to occur.

1.5 Coagulation and Endothelial Cell Interactions

Serine proteases regulate endothelial cell (EC) signaling pathways responsible for physiologic processes (*e.g.* maintenance of vessel barrier function).[76] In the setting of hemostasis, the endothelium can limit thrombin generation and platelet activation both directly as well as indirectly, thereby preserving physiologic blood flow while preventing vessel occlusion.[77,78] Meanwhile, and relevant to the contact pathway, the physiological processes of vasoconstriction and vasodilation are regulated in part by generation of bradykinin.[79] This proinflammatory peptide is generated by the assembly of the serine proteases, FXIIa and plasma kallikrein, on the endothelial cell surfaces by the urokinase receptor, cytokeratin 1, and complement protein C1q receptor (gC1q-R). [80] An understanding the role of FXI in regulating endothelial cell function is just now emerging.

In 1992 Berrettini and colleagues were the first to report that FXI and FXIa interact with ECs. In this study it was shown that HK serves as the primary binding partner mediating FXI-endothelial cell interactions.[81] Follow up studies demonstrated that FXI or FXIa could also bind directly to ECs in the absence of HK,[82] indicating that the endothelium expresses receptors for FXI(a). The binding of FXI to the endothelium appears to be species-dependent. For example, a non-circulating pool of FXI associated with glycosaminoglycans is observed in mice, but not in primates.[83] The ability of FXI and

FXIa to bind to ECs was confirmed in a study by Mahdi *et al*., yet they found that this interaction did not contribute significantly to thrombin generation.[84] Baird *et al.* even claimed that the FXI-EC interaction reported in the literature was due to an artifact of the binding assay and that ECs do not support FIX activation by FXIa.[85,86] In short, the mechanism by which ECs may regulate FXIa activity has remained an open question.

Our group recently confirmed that even though FXIa binds to ECs, this interaction does not support the procoagulant activity of FXIa. Instead, our group found that the endothelium promotes the activation of the kallikrein-kinin system (KKS), yet inhibits FXIa through its interaction with plasminogen activator inhibitor-1 (PAI-1).[87] Indeed, these observations support the concept that the endothelium exhibits an anticoagulant phenotype with PAI-1 playing a major role in inhibiting the enzymatic activity of FXIa. The observation that ECs selectively block FXIa, yet not the KKS, provides a mechanism that reconciles the previously assumed contradictory findings. Still, while the team detected FXIa-PAI-1 complexes in the circulation of nonhuman primates after administration of a lethal dose of *S. aureus*, the significance of PAI-1 inhibition of FXIa *in vivo* is still unknown. Our group is actively pursuing the hypothesis that the internalization and trafficking of EC-PAI-1 complexes regulates endothelial cell biology including barrier function.

Our group observed that the interaction of FXIa with ECs effect the anticoagulant properties and integrity of the endothelium. For example, our group demonstrated that FXIa cleaves the principal inhibitor of the TF/FVIIa complex on endothelial cells, TFPI-β, thereby enhancing the rate of activation of the extrinsic pathway of coagulation.[47] Moreover, Ngo *et al.* recently found that FXIa decreases the expression of VE-cadherin

on ECs *in vitro,* and that the inhibition of FXI preserved the expression of VE-cadherin in aortic sinus lesions of low-density lipoprotein receptor-deficient mice.[88] These results suggest that aberrant activation of FXI in the setting of atherosclerosis and other inflammatory diseases may contribute to vascular damage and loss of EC barrier function. If this tenet proves true, inhibition of FXI activation or activity may serve to preserve EC integrity in the setting of cardiovascular disease.

1.6 Coagulation and Platelet Interactions

Serine proteases regulate blood platelet activation and physiologic to pathological functions, ranging from essential roles in preserving endothelial cell barrier function to sinister roles in thrombotic complications.[63] As an active participant in this process, exposure of phospholipids dominated by phosphatidylserine (PS) on the surface of activated platelet serves as a site of catalysis for the activation of coagulation factors that including prothrombin and FX.[64,65] As a structural outsider looking in, FXI's lack of a Gla domain precludes it from the million-fold increase in enzymatic rate of activation experienced by FX and prothrombin by way of the tenase and prothrombinase complexes, respectively.[66] Still, platelets express receptors that are implicated in binding and perhaps mediating FXI activation, or shielding FXIa from inactivation; [15,19,20] taken together, these interactions increase the overall effective enzymatic activity of FXIa.

Walsh and colleagues were the first to report interactions between FXI and platelets more than 30 years ago.[67] Subsequent studies have found that FXI has approximately 1,500 FXI binding sites per activated platelet.[42] Notably, the A3 domain of FXI interacts with the leucine-rich repeat (LRR) on the NH_2-terminal of GPIbα.[42] Additional receptors

including apolipoprotein E receptor 2 (ApoER2), a member of the low-density lipoprotein (LDL) receptor family, have been found to mediate FXI-platelet interactions. As FXI circulates as a homodimer, it is plausible that FXI concurrently binds to multiple receptors. [68] Still, FXI binding to these two receptors alone seems to still offer an incomplete mechanism describing FXI interactions with platelets, or if these or additional platelet surface receptors serve to catalyze FXI activation.

Historical studies first claimed that platelets, and in particular the platelet receptor GPIbα, facilitated FXI activation by thrombin. However, the amplification of thrombin-mediated activation of FXI in the presence of platelets was not able to be reproduced, resulting in the retraction of these works.[69,70] This topic was revisited by Kossmann *et al*., who showed *in vivo* evidence that platelet-localized FXI induced vascular inflammation and arterial hypertension in a GPIbα -dependent manner.[71] The same group also identified platelet CD36, a receptor that is constitutively expressed on the platelet surface, also amplifies FXI-dependent thrombin generation when the levels of exposed procoagulant phospholipids are limited.[72] It is also possible that polyP, secreted by or retained on the surface of activated platelets, serves as a cofactor for FXI activation by thrombin or FXIIa.[27,28,73]

While these studies report that platelets amplify FXI activation, the exact mechanism by which platelets regulate FXIa-dependent thrombin generation remains unclear. In contrast to FXI, FXIa-platelet interactions appear to be independent of GPIbα, with the platelet receptor for FXIa still unknown.[74,75] Still, despite this lack of knowledge of the receptors involved, our group recently demonstrated that the platelet surface can modify FXIa allosterically by enhancing FXIa-mediated FIX activation and even preventing FXIa

inhibition by inhibitors released from activated platelets themselves.[75] While this protective effect is independent of presence of either polyP or PS on the membrane of activated platelets, it remains to be seen if this is dependent on platelet CD36. This in turn could explain the additional function by which CD36 amplifies the aforementioned feedback activation of FXI by thrombin in the absence of procoagulant phospholipids.[72]

1.7 Coagulation and Inflammation

1.7.1 *Coagulation and the Kallikrein-Kinin System*

In the traditional model of the kallikrein-kinin system (KKS), plasma kallikrein cleaves HK, which leads to the generation of the proinflammatory peptide, bradykinin, a pain mediator and strong vasodilator.[90] Concomitantly, FXIIa activates FXI, which leads to the generation of thrombin.[92] However, this model is being revised to highlight FXI(a) as the central node between the KKS, complement, and coagulation systems.[93] In this updated model, FXIa activates FXII and cleaves HK to generate bradykinin.[94,95] While plasma kallikrein mediates these reactions more efficiently than FXI, FXI predominantly incites the cytokine storm in response to an inflammatory challenge. This is evidenced by the fact that FXI-deficient mice exhibited a blunted cytokine response with reduced consumption of FXII and PK compared to wild type mice in a model of sepsis induced by cecal ligation and puncture.[93]

In subsequent work by our group, we observed that the anti-FXI A2 antibody which blocks activation of FXI by FXIIa also blocked the activation of FXII and PK. Additionally, this antibody prevented the cleavage of HK following a lethal dose of heat-inactivated *S. aureus* injected into baboons.[93] These data suggest that FXIa generation

may occur prior to FXII activation during systemic inflammation; in this case, FXIa may be an activator of the KKS *in vivo*, perhaps by activating FXII.

1.7.2 *Coagulation and the Complement System*

The crosstalk between the complement system and coagulation cascade implicate one another as deficiency or altered function in complement or coagulation proteins lead to thrombotic and inflammatory diseases;[96] yet, the mechanisms behind this are still not fully understood. *In vivo* evidence suggests that the activation of FXII or FXI promotes complement activation during systemic inflammation. Moreover, *in vitro* studies show that FXIIa and plasma kallikrein activate the complement system. FXIIa initiates the classical complement pathway by activating the C1qrs complex, whereas plasma kallikrein supports the alternative complement pathway by activating factor B, C3, and C5.[97,98] Novel interactions of FXIa with components of the complement system have recently emerged as well. Indeed, we have observed that FXIa inhibits complement factor H (CFH), the primary inhibitor of the alternative complement pathway. FXIa cleaves CFH at the Arg341/Arg342 bond, which reduces the cleavage of C3b by factor I and the decay of C3bBb and amplifies the alternative pathway.[99] Another group recently demonstrated that FXI can also bind another regulator of the alternative complement pathway, properdin.[100]

FXIa could also regulate inflammation by cleaving other inflammatory proteins, including beta2-glycoprotein I (β_2GPI) and prochemerin.[101,102] β_2GPI is structurally related to CFH and is the primary antigen recognized by autoantibodies in patients with antiphospholipid syndrome. β_2GPI exhibits anticoagulant properties, including the

inhibition of FXI activation by thrombin.[103] Notably, FXIa can cleave β_2GPI at the C-terminus (Lys317/Thr318) to form cβ_2GPI, which mitigates its anticoagulant effects. Accordingly, elevated levels of cβ_2GPI are found in patients with lupus anticoagulant or disseminated intravascular coagulation;[104,105] indeed, FXIa could even be the major protease responsible for this cleavage. Following this theme of FXIa cleaving inflammatory proteins, Ge *et al*. found that FXIa can cleave prochemerin to generate the chemoattractant and adipokine chem158K in plasma.[102] As the active form of prochemerin, chem158K contributes to: 1) leukocyte recruitment into the thrombus, 2) proliferation of smooth muscle cells and adipocytes, and 3) apoptosis of vascular ECs.[102,106] Thus, the generation of chem158K by FXIa provides yet another link between FXIa activity and inflammation. Indeed, levels of chem163S, the inactive prochemerin, found in the plasma of FXI-deficient patients has been shown to be significantly higher compared to a healthy control group. However, it remains to be seen if pharmacological inhibition of FXIa in ongoing clinical trials reduces these inflammatory markers.

1.8 Atherosclerosis

Thromboinflammation associated with hyperlipidemia and resultant atherosclerosis is an underlying driver in cardiovascular disease (CVD) that contributes to significant morbidity and mortality worldwide. In the United States, CVD accounts for nearly 30% of deaths annually, with estimated direct healthcare cost of $200 billion per year.[63,64]

1.8.1 *Progression of Atherosclerosis*

Chronic vascular inflammatory disease results, in part, from lipoprotein accumulation in the artery walls. In this hyperlipidemic state, vascular inflammation and endothelial cell

dysfunction result in the localized loss of endothelial barrier function.[65-69] The resultant atherogenesis involves the upregulation and secretion of select chemokines and chemoattractants. This in turns promotes the recruitment of monocytes and other leukocytes to the surface of inflamed ECs and eventually into the intima.[65] There, monocytes differentiate into macrophages and internalize modified lipoprotein particles to generate foam cells (the hallmark of the nascent atheroma), which in turn secrete additional inflammatory cytokines and reactive oxygen species, among other mediators.[70] The accumulation of dying macrophages leads to the formation of a necrotic core of the mature plaque. Erosion, and ultimately rupture, of atherosclerotic plaques is highly thrombogenic and is a common cause of myocardial infarction and stroke.[71,72]

Meanwhile, activation of the coagulation cascade culminates in thrombin generation, inciting platelet activation and pathological thrombus formation. Indeed, endothelial dysfunction serves as a basis for inflammation and thrombosis that leads to terminal complications in the setting of atherosclerosis.[73,74] When the endothelium is damaged, blood is exposed to extracellular matrix proteins (e.g. collagen, vWF, tissue factor), which in turn activates platelet adhesion receptors (e.g. GPVI, GPIb, CLEC-2) and allows TF to bind FVII-FVIIa to initiate the extrinsic pathway of coagulation.[75,76] Concomitantly, the inflamed endothelial cells activate platelets and support platelet-platelet binding interactions (e.g. GPIb-IX-V to vWF, GPIIb/IIIa to fibrinogen).[77] Activated platelets release a number of substances that further drive endothelium degradation and activation. These processes have been summarized in **Figure 1.9.**

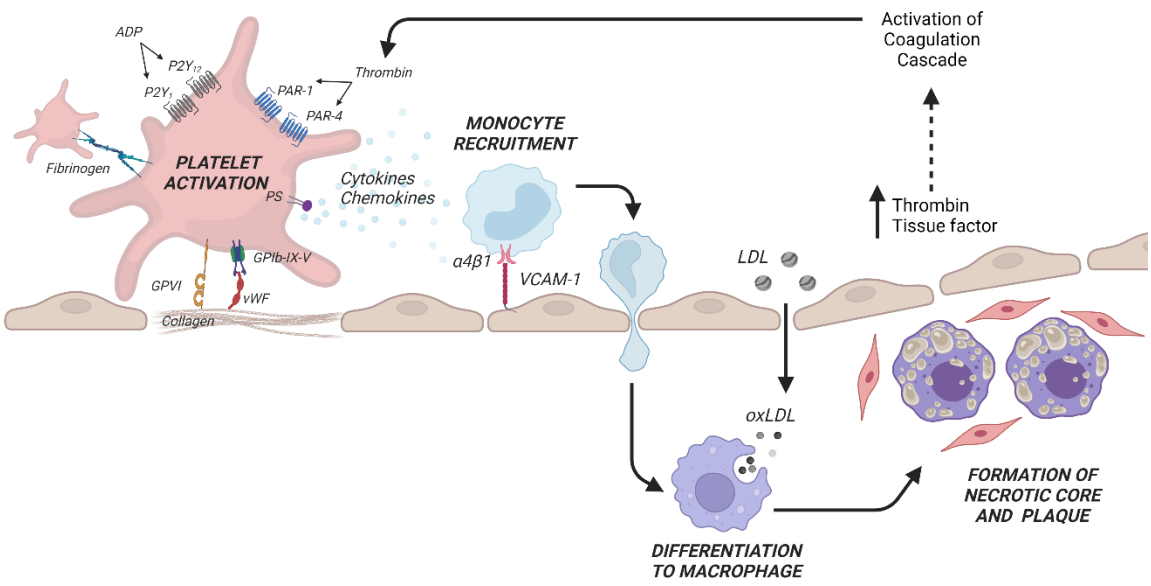

Figure 1.9 Progression of atherosclerosis. Atherosclerosis is a chronic inflammatory disease that is characterized by a hyperlipidemic state and activation of the endothelium, which culminates in atheromatous plaque formation. When the endothelium is damaged, blood is exposed to extracellular matrix proteins, which activates platelet adhesion receptors and facilitates the release of soluble agonists. This, in turn, both amplifies platelet activation and facilitates the recruitment of monocytes and other leukocytes to the inflamed endothelial cell surface. By way of diapedesis, monocytes are translocated into the arterial intima and differentiate into macrophages that internalize modified lipoprotein particles to generate foam cells. This results in the downstream formation of a mature plaque with a necrotic core. In late-stage atherosclerosis, plaque rupture activates the coagulation cascade and leads to pathologic thrombus formation. ADP, adenosine diphosphate. PAR, protease-activated receptor. PS, phosphatidylserine. GPIb/IX/V, glycoprotein Ib/IX/V. GPVI, glycoprotein VI. vWF, von Willebrand factor. VCAM-1, vascular cell adhesion molecule-1. LDL, low-density lipoprotein. oxLDL, oxidized low-density lipoprotein. Figure created with BioRender.com by Tia C.L. Kohs.

1.8.2 *Current Treatment Strategies*

Many current treatment options, such as antiplatelet and anticoagulant therapies, moderately alleviate thrombotic events of atherosclerosis, yet carry a risk for bleeding and hemorrhagic complications.[78-80] Thus, there remains an unmet clinical need to develop effective cardioprotective therapies with reduced bleeding other than aspirin and current antiplatelet therapies for primary and secondary prevention of CVD.[81] Guidelines

currently recommend indefinite aspirin therapy for patients with prior CVD events,[82] with additional antiplatelet agents in combination with aspirin or as monotherapy as needed; however, long-term use of dual antiplatelet therapy is undesirable because its 20% increase in antithrombotic efficacy is eventually outweighed by a larger increase in bleeding. Bleeding rates are cumulative and prohibit aggressive combination antiplatelet therapies. Moreover, the combination of anticoagulation and dual antiplatelet therapy doubles the rate of major bleeding when compared to dual antiplatelet therapy alone.[83,84] Thus, there remains a clear unmet clinical need that warrants further investigations into the molecular underpinnings of hemostasis and thrombosis to develop safer and more effective therapies.

1.9 Multiple Sclerosis

Neurological disorders are the second leading cause of death worldwide, accounting for 16.5% of deaths.[85] The most prevalent neuroinflammatory disorder, multiple sclerosis (MS), affects over 2.2 million individuals worldwide and is the most common disabling neurological disease of young adults.[86] Clinical and experimental evidence suggest that the pathologies associated with MS can be worsened by the involvement of coagulation components.[87,88] For example, plasma FXII levels are elevated in MS patients,[89] whereas FXII deficiency is protective in EAE.[90] However, the exact mechanism of how the intrinsic pathway of coagulation contributes to MS pathologies remains unclear.

1.9.1 *Increased Blood-Brain Barrier Permeability*

One of the key features of the blood-brain barrier (BBB) is its relative impermeability to molecules that do not freely diffuse across membranes to maintain brain homeostasis.[91]

The tightness of the BBB is largely regulated by tight junctions (TJs) and adherens junctions (AJs), and together these junctions create a rate-limiting barrier to the diffusion of solutes between endothelial cells (**Section 1.2.1**).[92,93]

BBB disruption in the setting of MS is often attributed to interactions between activated immunocompetent cells with the cerebral endothelial cells. Once the central nervous system (CNS) is activated in MS, antigen-presenting cells and Th1-type lymphocytes release pro-inflammatory cytokines that alter microvascular endothelial cells, resulting in increased leukocyte adhesion and vascular permeability. This remodeling is largely the result of various cytokines (e.g. IL-1β, TNFα, IFN-γ), chemokines (e.g. CXCL8, CCL2), matrix metalloproteinases (e.g. MMP-2, MMP-9), and adhesion molecules (e.g. ICAM-1).[94] As a result of the increased BBB permeability, hemostatic components can leak into the brain parenchyma.[95] These hemostatic components will then signal through both the extrinsic and intrinsic pathways of coagulation to facilitate fibrin formation, systemic inflammation, and further increase vascular permeability of the BBB.[96]

1.9.2 *Demyelination and Axonal Degeneration*

A hallmark of immune-mediated, neurodegenerative disorders such as MS is the destruction of the myelin sheath that surrounds axons, a process known as demyelination.[97] Remyelination is an endogenous repair mechanism whereby new myelin is produced following the proliferation, recruitment, and differentiation of oligodendrocyte precursor cells (OPCs) into myelin-forming oligodendrocytes.[98] This process is necessary to protect axons from further damage, and to restore saltatory electrical impulse conduction and metabolic/trophic support.[98-100] However, remyelination is limited or fails altogether in the

progressive phase of MS, which is considered to contribute to the axonal damage and loss that correlates to sensory, motor and cognitive decline.[9] Given that there are no approved therapies to drive remyelination in MS, identifying the cellular and molecular drivers of remyelination is key in the development of novel therapeutics.[9]

Remyelination relies upon maturation of oligodendrocyte progenitor cells (OPCs) into myelinating oligodendrocytes. Microglia and astrocytes play key roles in oligodendrocyte development and myelination. Under physiologic conditions, microglia and astrocytes continuously survey their microenvironment for stimuli that might indicate injury or infection, and are ready to respond to this by entering an activated state characterized by cytokine secretion and phagocytosis.[99,101] However, under pathological and demyelinating conditions, reactive astrocytes and activated microglia/macrophages can support both beneficial and deleterious effects, the balance of which appears to be critical for tissue regeneration.[101]

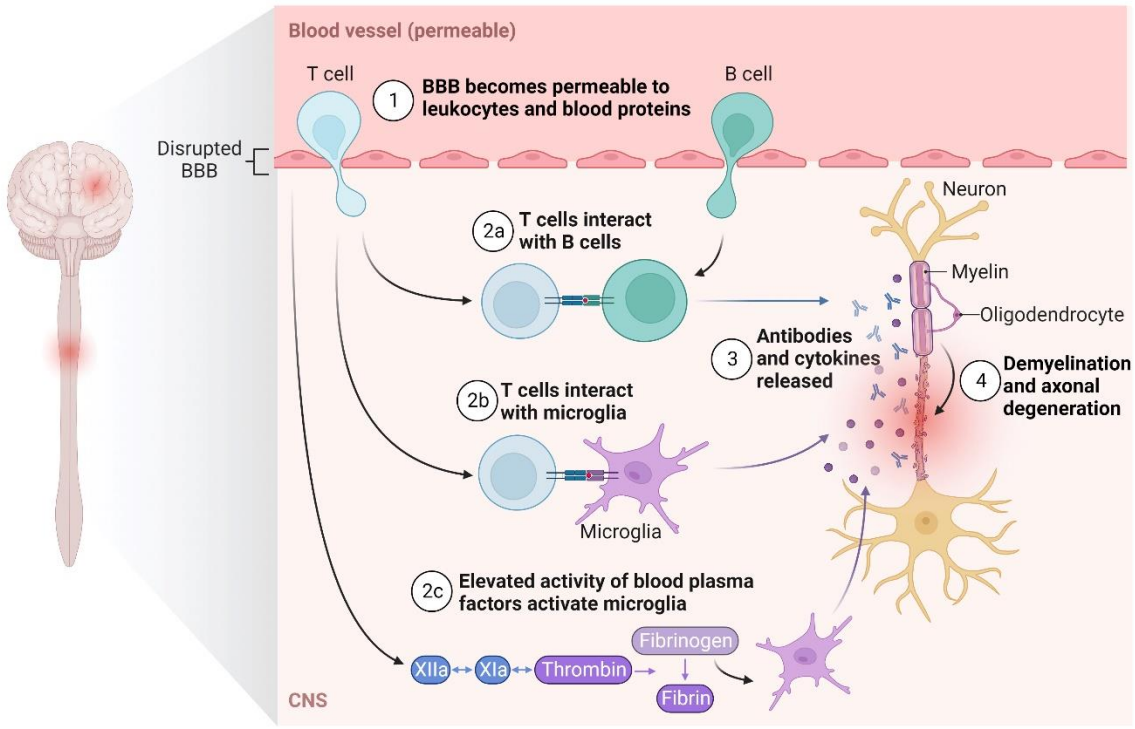

Figure 1.10 Pathologies associated with the progression of multiple sclerosis. A hallmark of multiple sclerosis is increased permeability of the blood-brain barrier (BBB). When the BBB permeability increases, various hemostatic components (e.g. leukocytes, blood proteins) are able to leak into the CNS. There, T-cells can interact with both B-cells and microglia, resulting in the release of antibodies and cytokines. Concomitantly, increased activity of blood plasma factors in the CNS facilitates additional microglial activation, further contributing to the inflammatory milieu. Taken together, this results in the demyelination and degeneration of axons. Figure created with BioRender.com by Tia C.L. Kohs.

1.9.3 *Current Treatment Strategies*

Current treatment strategies for managing acute MS include: 1) steroids to promote BBB integrity, 2) inhibitors of inflammatory mediators such as cytokines, chemokines, or adhesion molecules; 3) small molecules or monoclonal antibodies directed at modulating adaptive immune responses; and 4) agents directed at stabilizing intracellular brain endothelial interactions and/or the signaling molecules involved in remodeling junctional

complexes.[94,99] While these therapies have shown clinical efficacy, relapses still occur during which patients develop new symptoms or old symptoms worsen; moreover, most disease modifying therapies predispose patients to infection, autoimmune conditions, and malignancy.[102] Thus, there remains an unmet need for safe and effective therapies for the treatment and management of MS.

1.10 Extracorporeal Membrane Oxygenation

1.10.1 *Applications of Extracorporeal Membrane Oxygenation Therapy*

Extracorporeal membrane oxygenation (ECMO) is a modified form of cardiopulmonary bypass that can provide adequate oxygen delivery to vital tissues in patients with severe cardiac and/or respiratory failure.[103] This is accomplished by removing the blood from venous circulation, passing it through an artificial lung that adds oxygen while removing carbon dioxide, and then returning the blood to circulation at venous or arterial sites. While there are many configurations, a standard ECMO circuit includes a mechanical blood pump, a membrane oxygenator (gas exchange device), and a heat exchanger all connected with circuit tubing that extends from the access cannula to either an arterial (VA) or venous (VV) infusion cannula (**Figure 1.11**).[104]

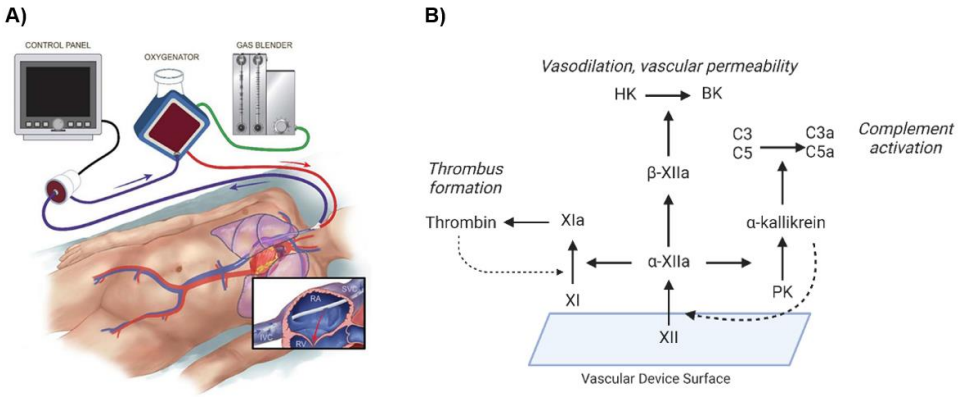

Figure 1.11 Extracorporeal membrane oxygenation. (A) Extracorporeal membrane oxygenation (ECMO) circuits facilitate gas exchange by oxygenating blood and removing carbon dioxide to provide support for patients with severe respiratory or cardiac failure. Although there are numerous ECMO circuit configurations, this figure depicts a venovenous extracorporeal membrane oxygenation circuit. The image has been adapted with permission from *ASAIO Journal* 68(2):133-152.[104] (B) The intrinsic pathway of coagulation is activated following the exposure of blood to the surface of a vascular device. Once activated, coagulation factor (F) XII triggers a series of sequential reactions, leading to downstream thrombosis formation, vasodilation, regulation of vascular permeability, and activation of the complement system.

1.10.2 *Potential Thrombotic and Hemorrhagic Complications*

Despite the potentially lifesaving benefits associated with ECMO treatment,[105,106] ECMO represents an exceptionally complex hemocompatibility problem, encompassing both vascular device-associated thrombus formation and anticoagulation-associated bleeding.[107-109] ECMO is a key adjunctive therapy for cardiogenic shock, acute respiratory distress syndrome (ARDS), as well as some forms of major trauma.[110,111] However, in addition to frequent thrombotic device failures, major bleeding complications associated with ECMO include surgical site bleeding (17%), cannulation site bleeding (14%), and intracranial hemorrhage (11%).[112] Thrombotic events include clots in the circuit (15%) and the oxygenator (12%) as well as hemolysis (10%).[113,114]

These coagulation-related morbidities and mortalities demonstrate the need for agents that effectively inhibit thrombosis without causing bleeding.

1.10.3 *Current Treatment Strategies*

The standard of care requires the administration of anticoagulants to prevent thrombotic occlusions of the oxygenator and the associated tubing in the circuit. Anticoagulant and antiplatelet drugs reduce device-initiated thrombus formation,[115] but, at the relatively low doses administered, remain insufficient since "breakthrough thrombosis" still occurs. However, serious bleeding also remains the dose-limiting toxicity of all current antithrombotic agents,[116] placing limits on the intensity of anticoagulation therapy. Thus, there exists a critical unmet need to discover and develop safer antithrombotic strategies to limit vascular device-initiated clotting without comprising the patient's hemostatic capability. Efforts to address this dilemma have historically focused on pacifying the surface of vascular devices.[117,118] Though it has improved the biocompatibility in numerous devices, systemic anticoagulation is often still necessary in settings such as hemodialysis, cardiopulmonary bypass, ventricular assist devices, or ECMO.[119-122]

A deeper understanding of risk factors in this population may lead to better informed decision-making in hemostasis management. At present, there is a knowledge gap regarding predictors of thrombosis in adult patients on ECMO. Prior studies have been limited by small sample size,[123] have been restricted to pediatric populations[124], or limited to one ECMO modality.[125] Additionally, querying recent data may reflect updates in technologic advances and practice changes, which is crucial in refining treatment strategies and determining risk factors for thrombosis in this population.

1.11 Current and Emerging Therapies for Vascular Diseases and Device-Related Thrombosis

1.11.1 *TEC Family Kinases as Therapeutic Targets*

The TEC family kinases (TFKs) are a subfamily of the non-receptor protein tyrosine kinases (PTKs). This family consists of five distinct members (TEC, BTK, ITK/EMT/TSK, ETK/BMX, and TXK/RLK).[126] TFKs share a common domain organization that consists of a N-terminal pleckstrin homology (PH) domain that mediates membrane association. This is followed by a TEC homology (TH) domain, which contains a BTK motif (BH) that is involved in the binding of GTP to the Gα subunit of the heterotrimeric G protein, and one to two proline-rich (PR) regions that intramolecularly binds SRC homology (SH) 3 domain to affect protein targeting and enzyme activation. The SH3 domain that follows also mediates protein-protein interactions and houses all autophosphorylation sites for the TFKs. Next, there is a SH2 domain that hyperphosphorylates docking proteins and stabilizes PR-SH3 interactions. Finally, there is a carboxy-terminal catalytic kinase domain (SH1).[126-128] Interestingly, the residues in the ATP binding site of the kinase domain share 40–65% identity and 60–80% similarity, which may explain the promiscuity of TFK inhibitors.[129] A schematic representation of these domains is provided in **Figure 1.12.** For my dissertation, I will focus on Bruton's tyrosine kinase (BTK) and bone marrow tyrosine kinase on chromosome X (ETK/BMX).

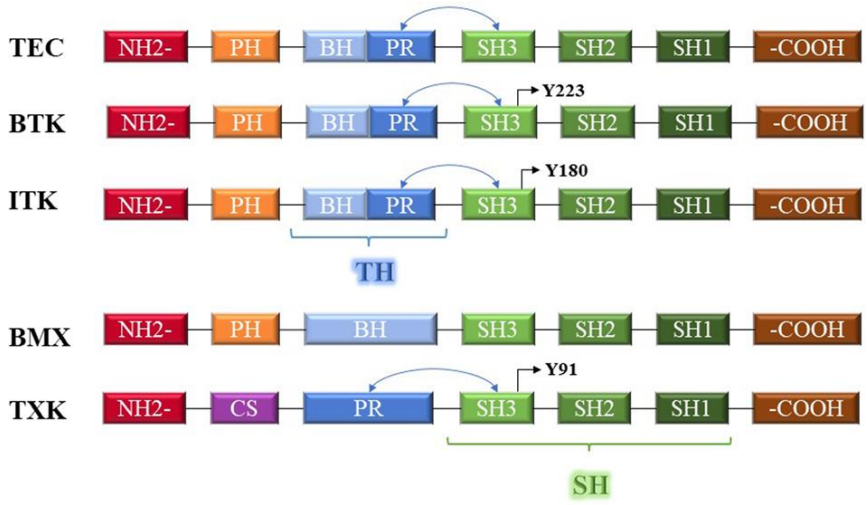

Figure 1.12 TEC family kinases and their domains. There are five distinct members of the TEC family kinases (TFKs): TEC, BTK, ITK/EMT/TSK, ETK/BMX, and TXK/RLK. This family shares a common domain organization, depicted in this schematic representation. BH, Btk homology. PR, proline-rich. SH, SRC homology. TH, TEC homology. CS, cysteine. PH, pleckstrin homology. Reprinted from Yin *et al.* 2022.[126] Permission is not required by the publisher for this type of use.

Bruton's Tyrosine Kinase (BTK): A pediatrician at Walter Reed Army Hospital reported the first case of congenital agammaglobulinemia (also known as X-linked agammaglobulinemia [XLA]) in an 8-year-old male in 1952. Then, in 1993, it was discovered that this disease was related to mutations in a tyrosine kinase belonging to the Tec family. This protein was named Bruton's tyrosine kinase (BTK) and has since demonstrated critical roles in autoimmune diseases and B-cell receptor signaling (BCR).[126,130] Indeed, BTK has been implicated in a number of intracellular signaling pathways, including the adaptive immune response and trafficking of lymphocytes; however, the role of BTK extends beyond B-cells, to include other hematopoietic cells (e.g. myeloid cells, platelets).[131]

The first human BTK inhibitor, ibrutinib (PCI-32765), was developed in 2009 and demonstrated utility in treating B-cell malignancies. It was subsequently approved by the Food and Drug Administration for the treatment of chronic lymphocytic leukemia (CLL), mantle cell lymphomas, and lymphoplasmacytic lymphoma (Waldenström's macroglobulinemia).[131] This inhibitor reacts with a cysteine residue (C481) in the ATP binding site of BTK, which blocks the catalytic activity, and forces the kinase domain to assume an inactive conformation.[132] Nevertheless, while ibrutinib is often referred to as a first generation BTK inhibitor, ibrutinib can inhibit the kinase activities of numerous TFKs by irreversibly binding a conserved cysteine residue.[133]

Bone Marrow Tyrosine Kinase on Chromosome X (BMX): BMX is a protein that was initially discovered in granulocytic monocyte lineages within the hematopoietic system.[126] It was later revealed that BMX is widely expressed in epithelial and endothelial lineages, as well as brain, prostate, lung and heart.[129] In these capacities, BMX can function as a regulator in the immune response, secrete inflammatory mediators, and maintain stem-cells. Additionally, BMX has been found to be overexpressed in cancers (e.g. prostate, breast, colon, cervical carcinoma).[126,129]

One of the most potent inhibitors of BMX is BMX-IN-1. This is a covalent inhibitor that binds to reacts with a cysteine residue (C496) in the ATP binding site. It is important to note that this residue is found in all members of the TFKs. Likewise, BMX-IN-1 has a high affinity for BTK, as well as members from the EGFR family (EGFR, HER2, HER4), JAK3, BLK and MAP2K7.[129] It is possible that the structural homology of these receptors allow covalent inhibitors to promiscuously bind other TFKs.

1.11.2 Coagulation Factors XI(a) and XII(a) as Therapeutic Targets

Human epidemiological data suggest an important pathogenic role for FXI in the development of CVD, including stroke and heart attack.[134-136] Despite early studies failing to find a link between FXI deficiency and protection against myocardial infarction, follow on biomarker studies demonstrated that FXIa is associated with the risk of cardiovascular events in stable coronary artery disease patients. Along these lines, components of the kallikrein-kinin system, including FXI, have been shown to interact directly with multiple pathways complicit in CVD, including platelet activation and thromboinflammation.[52,137] Furthermore, previous studies by our group have demonstrated that FXI inhibition improves outcomes using *in vivo* mouse models of atherosclerosis,[138] sepsis,[54,139,140] ischemic stroke and ischemia-reperfusion injury.[1,141] Indeed, inhibiting FXI is antithrombotic in a primate model of thrombosis and is protective in sepsis.[2,142]

Based on the effectiveness of FXI inhibition in these models, it is possible that the mechanism of action of FXIa in vascular biology includes, but is not limited to, the enzymatic cleavage of FIX. In fact, FXIa substrates include members of the complement cascade,[143] TFPI,[144,145] and regulators of endothelial cell procoagulant activity, including ADAMTS-13.[146] The promiscuity of FXIa is also observed through its 'upstream' activation of FXII, thus in part redefining the traditional model of the coagulation cascade (**Figure 1.13**).

This activity suggests a novel pathway for FXIa as a reciprocal activator of FXII and the kallikrein-kinin system; thus, FXI may function as a bidirectional interface between thrombin generation and FXII activation (**Figure 1.14)**.

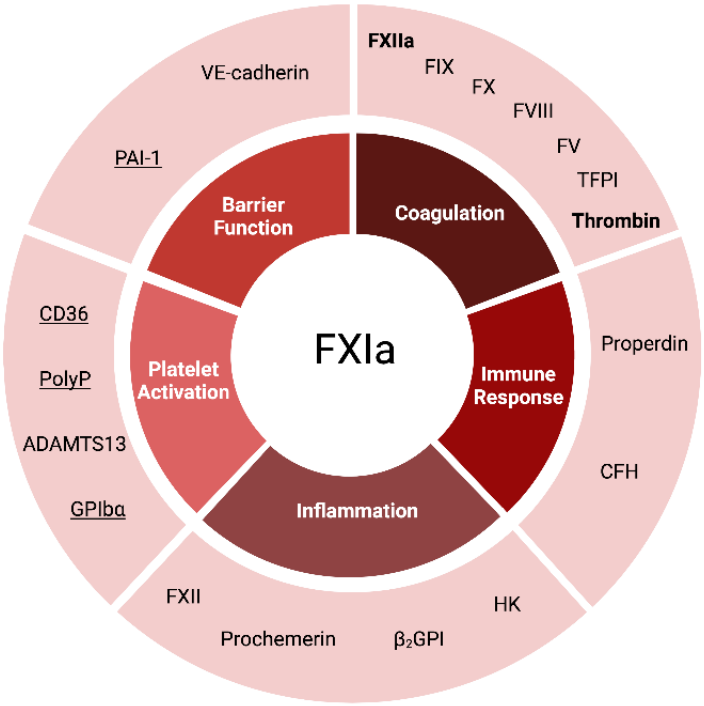

Figure 1.13 Function and substrates of coagulation factor XIa. FXIa is an enzyme that acts upon substrates (outer circle) to regulate physiological and pathological processes (inner circle). All substrates are downstream targets unless otherwise specified. FXI receptors and co-factors are distinguished by an underline. Upstream FXI interaction partners are distinguished by bolded text. TFPI, tissue factor pathway inhibitor; CFH, complement factor H; HK, high-molecular-weight kininogen; β_2GPI, beta2-glycoprotein I; GPIbα, platelet glycoprotein Ibα; polyP, polyphosphate; PAI-1, plasminogen activator inhibitor-1; VE-cadherin, vascular endothelial-cadherin. Reprinted with permission from Lira et al., *Semin Thromb Hemost*, 2022: in Press.[147]

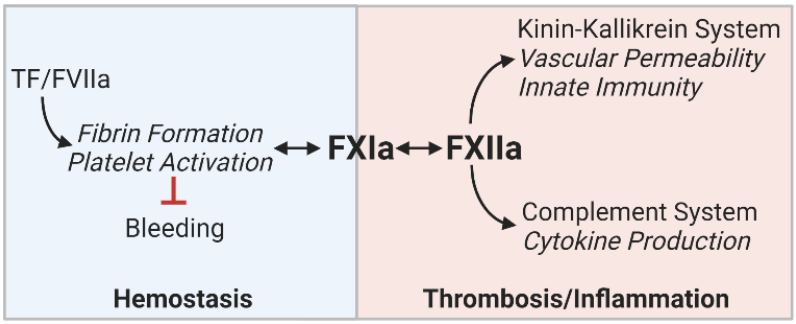

Figure 1.14 FXIa as a central regulator of hemostasis, thrombosis, and inflammation. Activated coagulation factor XI (FXIa) is positioned at the node between hemostasis and thrombosis/inflammation. FXIa responsible for amplifying thrombin generation, resulting in fibrin formation and platelet activation. When the balance tips in the setting of disease, the crossover and the activation of FXII (FXIIa) stimulates the activation of the kinin-kallikrein system and the complement system, resulting in thrombosis and inflammation. Figure created with BioRender.com by Tia C.L. Kohs.

The multifaceted function of FXIa provided a rationale for testing if FXI inhibition prevents thromboinflammation. Given the relatively mild bleeding disorder associated with FXI deficiency and the extremely low rates of bleeding observed in clinical trials of FXI inhibitors,[148,149] FXI inhibition does not seem to significantly compromise hemostasis. Moreover, individuals born without FXII have no apparent pathology, including bleeding diathesis or immunocompromise, and are generally identified through incidental detection of a prolonged activated partial thromboplastin time (aPTT); however, hyperactivity of FXII appears to be pathologic, as certain mutations in exon 9 provoke a rare form of hereditary angioedema.[150] Taken together, both FXI and FXII may represent attractive therapeutic targets.

1.12 Dissertation Overview

In my dissertation, I examined the complex interactions within the blood microenvironment, and how these interactions play integral roles in the settings of

vascular diseases and medical devices. Chapter 1 introduces some of the key players in the blood microenvironment - endothelial cells, platelets, and coagulation - and the mechanisms that govern the interactions between the various constituents. These interactions are discussed both under physiological conditions, as well as in the presence of foreign surfaces or in different models of disease. Chapter 2 then outlines the general materials and methods relevant to the subsequent research chapters. Chapters 3-8 highlight my first-author papers that were published/submitted during my time in graduate school.

In Chapter 3, I present the mechanisms by which TEC family kinases (TFKs) contribute to the thromboinflammatory processes in the setting of diet-induced obesity. For these studies, our team first investigated the role of TFKs in endothelial cell activation *in vitro* and found that VEGF-A induces VCAM-1 expression in a BMX-dependent manner. We then performed a pilot study in a nonhuman primate (NHP) model *in vivo* and observed that treatment with the TFK inhibitor, ibrutinib, inhibited platelet deposition and endothelial cell activation *in vivo*. Taken together, the findings detailed in Chapter 3 suggest that TFKs may contribute to the pathologies underlying atherosclerosis and could represent a novel therapeutic target.

Chapter 4 describes our study that investigated the role of coagulation factor (F) XI in sustaining the thromboinflammatory phenotype associated with chronic hyperlipidemia. For these experiments, we used the same NHP model of diet-induced obesity described in Chapter 3 and examined the effect of diet-induced obesity on platelet sensitivity and inflammatory markers. Pharmacological targeting of FXI using the monoclonal antibody,

humanized 1A6, reduced platelet priming for activation and inflammation. Taken together, this study demonstrates that FXI activation promotes vascular dysfunction in hyperlipidemia.

To further investigate the role of FXI in thromboinflammation, I turned my attention to thromboinflammation in the setting of multiple sclerosis (MS). In Chapter 5, I present the work evaluating if treatment with the anti-FXI monoclonal antibody, 14E11, could improve neurological function and attenuate CNS damage in a murine model of MS, experimental autoimmune encephalomyelitis (EAE). We found that pharmacological inhibition of FXI reduces disease severity, immune cell migration, axonal damage, and BBB disruption in mice with EAE. Thus, therapeutic agents targeting FXI and FXII may provide a useful approach for treating autoimmune and neurologic disorders.

Taking what I learned from targeting the intrinsic pathway of coagulation in disease settings, I shifted my focus to study vascular device-related thrombosis. In Chapter 6, I describe the development of over 400 antibodies that target FXII activation and FXIIa activity. Our team performed functional assays to characterize seven of the antibodies. Based on our findings, 1B2 was selected for further testing in a baboon model of vascular device-initiated thrombosis. We found that treatment with 1B2 inhibited platelet deposition and fibrin formation, which suggests that targeting the intrinsic pathway may reduce or prevent vascular-device associated thrombosis in a variety of clinical settings, including extracorporeal membrane oxygenators (ECMO).

In Chapter 7, I present the results from a single-center retrospective cohort study of patients on ECMO at Oregon Health & Science University. It is well established that

although ECMO treatment can provide lifesaving benefits to critically ill patients;[105,106] however, the issue of hemocompatibility is highly nuanced, as ECMO is associated with both vascular device-associated thrombosis and anticoagulation-associated bleeding.[107-109] Our work here focused on defining the incidence, predictors, and clinical consequences of severe thrombocytopenia (platelet count $<50 \times 10^9$/L) in patients on ECMO. Interestingly, we found that severe thrombocytopenia in adults undergoing ECMO treatment is predictive of thrombosis using a multivariate logistic regression model. Overall, this study provides insight into the prevalence and clinical consequences associated with severe thrombocytopenia in patients on ECMO.

The retrospective cohort study outlined in Chapter 8 was performed by querying the Extracorporeal Life Support Organization (ELSO) Registry from 2015 to 2019 to obtain a larger primary analysis population. Of the 16,453 ECMO patients documented during the designated study period, 9,538 of them were included in our analyses and thrombosis occurred in nearly a quarter of the cohort. We found that ECMO runs longer than 14 days and higher pump flow rates were associated with an increased risk of thrombosis, and that thrombosis increased likelihood of in-hospital mortality. Although this work is hypothesis generating, further studies are required to determine the true associations between clinical factors and thrombosis.

Finally, Chapter 9 provides conclusions from each of these studies and offers future directions for the projects detailed in my dissertation.

Chapter 2. General Materials & Methods

2.1 Ethical Considerations

Human studies were performed in accordance with an approved protocol from the Institutional Review Board of Oregon Health & Science University. Written consent was obtained from all subjects in accordance with the Declaration of Helsinki.

All studies using rodents and nonhuman primates, including rhesus macaques, were approved by the Institutional Animal Care and Use Committee of the Oregon Health & Science University prior to initiation. Rhesus macaques were housed at the Oregon National Primate Research Center (ONPRC) at Oregon Health & Science University. Wild-type male mice were housed in the Animal Resource Facility at the Portland Veterans Affairs Medical Center.

2.2 Common Reagents

Crosslinked collagen-related peptide (CRP-XL) was from Dr. Richard Farndale (Cambridge University, Cambridge, UK). Adenosine diphosphate (ADP) was from Sigma-Aldrich (St. Louis, MO, US). Thrombin receptor activator peptide 6 (TRAP-6) was from Tocris Bioscience (Bristol, UK). The activated partial thromboplastin time (aPTT) reagent and prothrombin time (PT) Dade Innovin were from Thermo Fisher Scientific (Middletown, VA, US) and Siemens Healthcare Diagnostics (Munich, Germany), respectively. Prostacyclin was obtained from Cayman Chemical (Ann Arbor, MI, USA). All other reagents were obtained from Sigma-Aldrich (St. Louis, MO, USA) or previously cited sources.[151]

2.3 Antibodies

The mouse anti-human PE CD62P (P-selectin) antibody used for flow cytometry was obtained from BD Biosciences (San Jose, CA, US). The mouse anti-human monoclonal IgG1 against VCAM-1 (1.G11B1) used for contrast-enhanced ultrasound (CEU) molecular imaging was obtained from Bio-Rad Antibodies (Hercules, CA, US).

2.4 Blood Collection and Processing

2.4.1 *Human Blood Collection*

Human venous blood was drawn by venipuncture from healthy subjects into 3.8% sodium citrate (1:10). To isolate platelets, acid-citrate-dextrose (85 mM sodium citrate, 100 mM glucose, 71 mM citric acid, 30°C) was added to the anticoagulated blood samples (1:10). Next, the samples were centrifuged at 200 *g* for 20 min to obtain platelet rich plasma (PRP). The PRP was centrifuged at 1000 *g* for 10 min in the presence of prostacyclin (0.1 µg/mL) and the platelet poor plasma (PPP) was decanted to obtain platelets. The platelet pellet was re-suspended in modified HEPES-Tyrode buffer (129 mM NaCl, 0.34 mM Na_2HPO_4, 2.9 mM KCl, 12 mM $NaHCO_3$, 20 mM HEPES, 5 mM glucose, 120 mM $MgCl_2$, pH 7.3), and washed via centrifugation at 1000 *g* for 10 min in the presence of prostacyclin (0.1 µg/mL). The washed platelets were re-suspended in modified HEPES-Tyrode buffer to the desired concentration

2.4.2 *Nonhuman Primate Samples*

Whole blood samples were collected from rhesus macaques by venipuncture into 3.2% sodium citrate, EDTA, or plastic vacutainers at designated study intervals. To isolate platelet poor plasma, blood samples anticoagulated with 3.2% sodium citrate or EDTA

were centrifuged at 2000 *g* for 8-10 min. The supernatant was removed and the remaining blood was centrifuged at 1000-2000 *g* for 3-10 min. To isolate serum, blood was drawn into a plastic vacutainer and allowed to sit for 30 min at room temperature. The blood clot was then removed by centrifuging the sample at 1000 *g* for 10 min. Blood plasma samples that were not immediately used for analyses were banked at -80°C for batch testing.

2.5 Flow Cytometry for Platelet Activation

Platelet function was measured by measuring integrin activation, granule secretion, and phosphatidylserine (PS) expression by flow cytometry. Whole blood samples anticoagulated with sodium citrate (3.2%-3.8%) were diluted in modified HEPES-Tyrode buffer (1:4). The samples were then incubated with an anti-CD62P PE (1:10), an anti-PAC-1 FITC (1:10) antibody, or FITC bovine lactadherin (1:10) for 20 min at 37°C in the presence of agonists that signal downstream of immunotyrosine activation motif (ITAM)- or G-protein coupled receptor (GPCR)- mediated pathways. These agonists included: the GPVI agonist, cross-linked collagen-related peptide (CRP-XL); the P2Y agonist, adenosine diphosphate (ADP); and/or the PAR-1 agonist, thrombin receptor activator peptide 6 (TRAP-6). The agonist concentrations can be found in the methods section for the research chapters. Reactions were stopped with the addition of paraformaldehyde (2%). Flow cytometry was performed on a FACSCanto II (BD Biosciences, Franklin Lakes, NJ, US) and analyses were performed on FlowJo software (version 10.7.1). The platelet populations were identified using logarithmic signaling amplification for forward and side scatter and platelet activation was presented as either mean fluorescence intensity or positive cell percentages.

2.6 Nonhuman Primate Model of Obesity and Hyperlipidemia

Adult male rhesus macaques were fed a high fat diet (45% carbohydrates, 18% protein, and 36% fat by caloric content LabDiet 5L0P, Purina Mills) for >2 years and were selected on the basis of having carotid intimal-medial thickening as a marker of early atherosclerotic changes. Anesthesia was induced with ketamine (10 mg/kg intramuscularly) and maintained with isoflurane (1.0-1.5%) to facilitate contrast enhanced ultrasound molecular imaging. At designated study intervals, animals underwent phlebotomy for analysis of lipid levels and inflammatory biomarkers, platelet aggregation studies, and whole blood flow cytometry.

2.6.1 *Lipid Levels and Complete Blood Counts*

Nonhuman primate blood samples obtained by venipuncture were used to measure lipids and inflammatory biomarker profiles. These assays were performed by the Clinical Pathology Laboratory at the Oregon National Primate Research Center using an ABX Pentra 400 Clinical Chemistry System (Horiba Medical, Irvine, CA, US).

2.6.2 *Inflammatory Biomarkers*

Inflammatory biomarkers were measured in either plasma or serum samples isolated from NHP samples obtained through venipuncture. Samples were analyzed for cytokines using custom Luminex panels (ThermoFisher, Waltham, MA, US; Millipore Sigma HNDG3MAG-36K, Burlington, MA) and an ELISA kit for C-reactive protein (ALPCO, Salem, NH, US). These analyses were performed in the Endocrine Technologies Core at the Oregon National Primate Research Center following the manufacturer's instructions. Briefly, 25 µL of each serum sample was diluted in assay diluent and incubated overnight

with antibody-coated, fluorescent-dyed capture microspheres specific for each analyte, followed by detection antibodies and streptavidin-phycoerythrin. Washed microspheres with bound analytes were resuspended in reading buffer and analyzed on a Milliplex LX-200 Analyzer (EMD Millipore, Billerica, MA, USA) bead sorter with XPonent Software version 3.1 (Luminex, Austin, TX, USA). Data were calculated using Milliplex Analyst software version 5.1 (EMD Millipore).

2.6.3 *Contrast Enhanced Ultrasound Molecular Imaging*

This molecular imaging technique relies on microbubbles with a gain-of-function VWF A1 domain or an antibody to VCAM-1 conjugated to the surface to target platelet GPIbα in vascular beds or inflamed endothelial cells, respectively.[152-154] The microbubbles were prepared by sonicating a gas-saturated aqueous suspension of distearoylphosphatidylcholine (2 mg/mL), polyoxyethylene-40-stearate (1 mg/mL), and distearoylphosphatidylethanolamine-PEG (2000) biotin (0.4 mg/mL). Ligands were conjugated to the microbubble surface using either a 15-amino acid cyclic peptide (CCP-015b) biotinylated at an added C-terminal lysine residue or a monoclonal antibody against VCAM-1 (1.G11B1). Microbubble concertation and size distribution between agents for each experiment were monitored using electrozone sensing (Multisizer III, Beckman-Coulter, Brea, CA, US).

Imaging was performed at the carotid bifurcation along the longitudinal access using multi-pulse, contrast-specific imaging at 7 MHz, a mechanical index of 1.9, a dynamic range of 55 dB, and a frame rate of 1 Hz (Sequoia, Siemens Medical Imaging, Mountain View, CA, US). Following the injection of the targeted microbubbles (1×10^8, i.v.), the

ultrasound was paused while a 2-D ultrasound at low power (mechanical index<0.10) was used to locate the carotid artery. Contrast-specific imaging was used to capture several frames and the first two frames were digitally averaged to quantify the signal for the retained microbubbles. To reduce the signal from microbubbles freely circulating, several frames acquired after >5 destructive pulse sequences (mechanical index 1.3) were averaged and subtracted.

2.7 Statistical Analysis

For datasets obtained from *in vitro* and *in vivo* experiments, data were first tested for normality and sphericity using Shapiro-Wilk and F-tests, respectively. Statistical analyses were performed using GraphPad Prism 9 (San Diego, CA, US) and statistical significance was considered for $P<0.05$. Statistical tests were chosen according to the criteria outlined in the flow diagram below (**Figure 2.1**).

For retrospective analyses, patient demographics were reported using standard descriptive statistics. Continuous variables were presented as a mean value plus or minus the standard deviation (SD) or standard error of mean (SEM). Categorical and dichotomous variables were presented as frequency and the percentage of total. To compare differences between cohorts, *P*-values were calculated Welch's t-tests, Fisher exact tests, Wilcoxon-Mann-Whitney tests. Statistical significance was defined as $P<0.05$ for simple demographic comparisons. Multivariate logistic regression was used to determine clinically meaningful predictors of both bleeding and thrombosis. Select risk factors for hemostatic compromise and thrombosis were selected a priori based on known relevance for the regression model. For multiple logistic regression models, statistical significance

was defined as an adjusted $P<0.05$. All statistics for retrospective analyses were calculated using R (R Foundation for Statistical Computing, version 3.6.2).

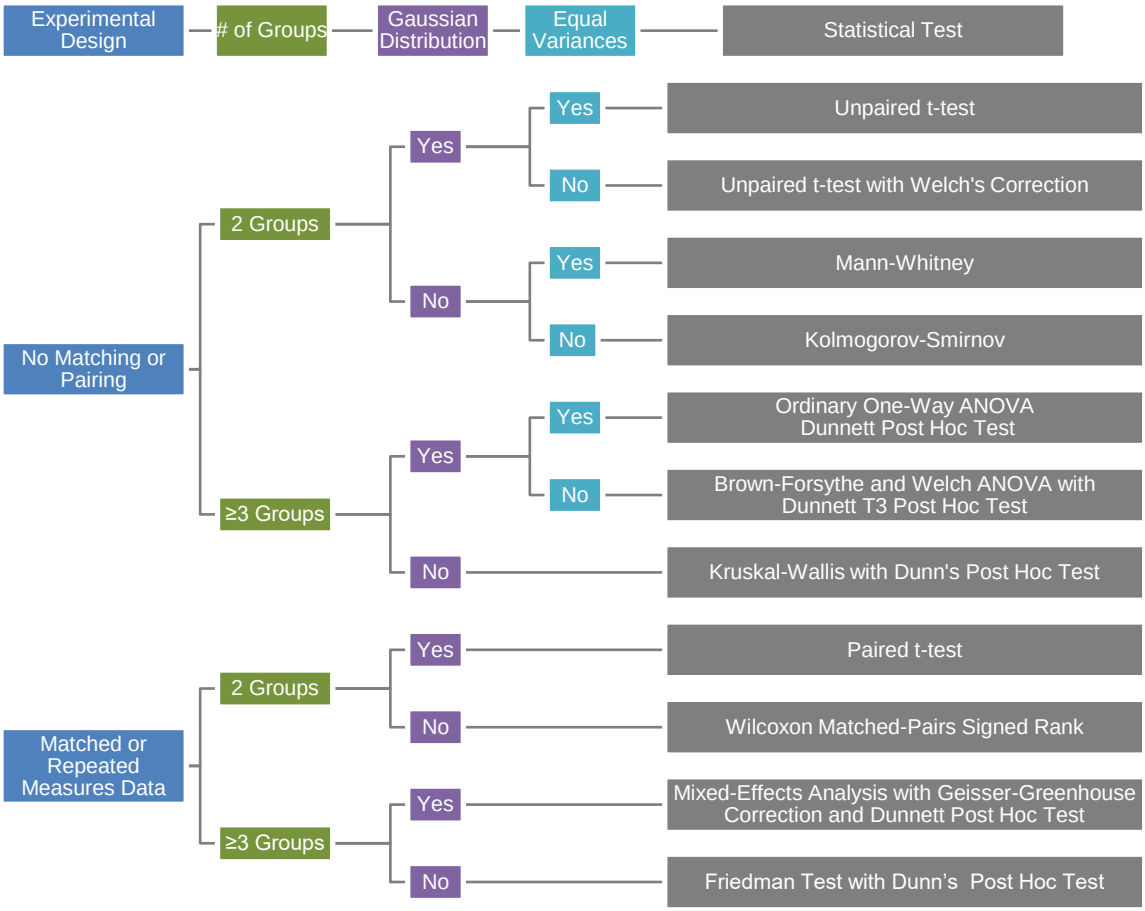

Figure 2.1 Statistical tests based on GraphPad Prism 9 guidance. GraphPad Prism 9 detects which type of data are entered (e.g., continuous, categorical, or survival data) and suggests appropriate statistical analyses based on the data type and experimental design.

Chapter 3. Ibrutinib inhibits BMX-dependent endothelial VCAM-1 expression *in vitro* and proatherosclerotic endothelial activation and platelet adhesion *in vivo*

Tia C. L. Kohs, Sven R. Olson, Jiaqing Pang, Kelley R. Jordan, Tony J. Zheng, Aris Xie, James Hodovan, Matthew Muller, Carrie McArthur, Jennifer Johnson, Bárbara B. Sousa, Michael Wallisch, Paul Kievit, Joseph E. Aslan, João D. Seixas, Gonçalo J. L. Bernardes, Monica T. Hinds, Jonathan R. Lindner, Owen J. T. McCarty, Cristina Puy, and Joseph J. Shatzel

This work was originally published by Springer Nature.
Cellular and Molecular Bioengineering, 2022; Volume 15, Pages 231-243
Reprinted with permission

3.1 Abstract

Inflammatory activation of the vascular endothelium leads to overexpression of adhesion molecules such as vascular cell adhesion molecule-1 (VCAM-1), contributing to the pro-thrombotic state underpinning atherogenesis. While the role of TEC family kinases (TFKs) in mediating inflammatory cell and platelet activation is well defined, the role of TFKs in vascular endothelial activation remains unclear. We investigated the role of TFKs in endothelial cell activation *in vitro* and in a nonhuman primate model of diet-induced atherosclerosis *in vivo*. *In vitro*, we found that ibrutinib blocked activation of the TFK member, BMX, by vascular endothelial growth factors (VEGF)-A in human aortic endothelial cells (HAECs). Blockade of BMX activation with ibrutinib or

pharmacologically distinct BMX inhibitors eliminated the ability of VEGF-A to stimulate VCAM-1 expression in HAECs. We validated that treatment with ibrutinib inhibited TFK-mediated platelet activation and aggregation in both human and primate samples as measured using flow cytometry and light transmission aggregometry. We utilized contrast-enhanced ultrasound molecular imaging to measure platelet GPIbα and endothelial VCAM-1 expression in atherosclerosis-prone carotid arteries of obese nonhuman primates. We observed that the TFK inhibitor, ibrutinib, inhibited platelet deposition and endothelial cell activation *in vivo*. Herein, we found that VEGF-A signals through BMX to induce VCAM-1 expression in endothelial cells, and that VCAM-1 expression is sensitive to ibrutinib *in vitro* and in atherosclerosis-prone carotid arteries *in vivo*. These findings suggest that TFKs may contribute to the pathogenesis of atherosclerosis and could represent a novel therapeutic target.

3.2 Graphical Abstract

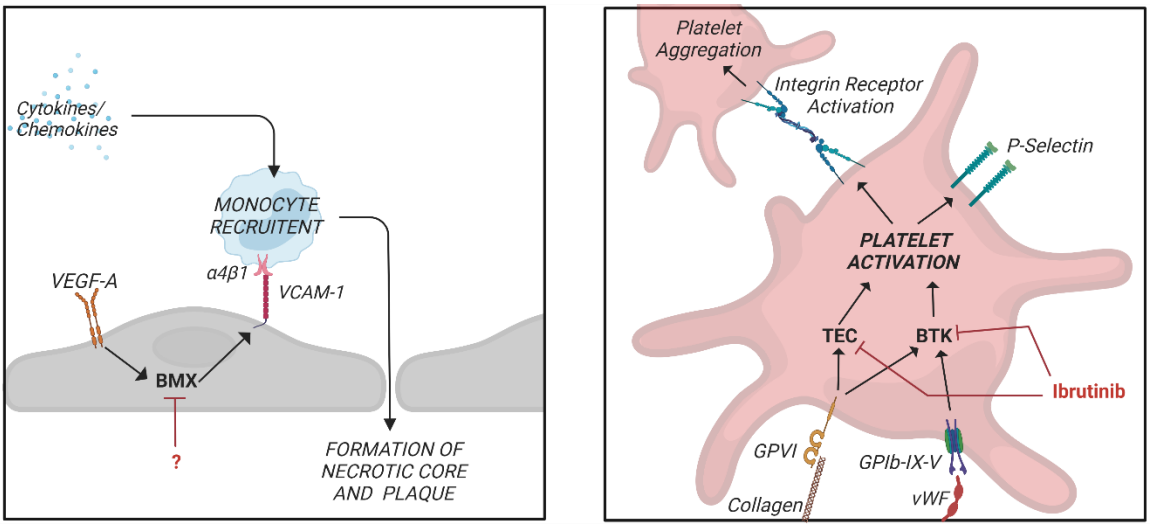

3.3 Introduction

In this chapter, our studies focused on elucidating the mechanisms by which TEC family kinases (TFKs) contribute to the thromboinflammatory processes in the setting of diet-induced obesity. We first investigated the role of TFKs in endothelial cell activation *in vitro* and found that VEGF-A induces VCAM-1 expression in a BMX-dependent manner. We then performed a pilot study in a nonhuman primate (NHP) model *in vivo* and observed that treatment with the TFK inhibitor, ibrutinib, inhibited platelet deposition and endothelial cell activation *in vivo*. Note, the rhesus macaque is a unique model for diet-induced obesity, as well as insulin resistance and pre-diabetes, based on metabolic similarities between humans and rhesus macaques.[155] These commonalities (e.g. white adipose tissue deposits, pattern of hyperlipidemia, control of lipolysis, and islet cell structure and function) are not shared by rodents.[156] Taken together, the findings detailed in this chapter suggest that pathways driven by the activation of select TFK pathways may contribute to the pathologies underlying atherosclerosis and could represent a novel therapeutic target.

3.4 Background

Atherosclerosis is a chronic inflammatory disease characterized by the accumulation of lipoproteins and smooth muscle cells in the arterial intima, endothelial cell activation, and leukocyte recruitment culminating in atheromatous plaque formation.[157] During the later stages of atherosclerosis, patients may experience significant complications from plaque rupture and thrombus formation.[157,158] Despite medical advances, atherosclerosis remains the leading cause of mortality in the United States.[159,160]

Endothelial activation contributes to the pro-thrombotic and pro-inflammatory milieu underlying atherogenesis. As platelets adhere to the vascular endothelium, pro-inflammatory endothelial activation occurs in concert with an overexpression of adhesion proteins involved in cell-cell interactions, such as intercellular adhesion molecule-1 (ICAM-1) and vascular cell adhesion molecule-1 (VCAM-1).[161,162] Elucidating the mechanisms that govern platelet-endothelial interactions, the release of endothelial-cell derived inflammatory factors and the expression of cell adhesion molecules may identify novel therapeutic targets to mitigate the progression of atherogenesis.

Due to their role in systemic inflammation and cytokine signaling, TEC family kinases (TFKs) represent promising targets for mitigating inflammatory disorders and autoimmune diseases.[163,164] The TFKs represent the second largest group of non-receptor tyrosine kinases and consist of five members: 1) BTK (Bruton's tyrosine kinase); 2) RLK (resting lymphocyte kinase; also known as TXK); 3) ITK (interleukin-2-inducible T-cell kinase); 4) TEC (tyrosine kinase expressed in hepatocellular carcinoma); and 5) BMX (bone-marrow tyrosine kinase gene on chromosome X; also known as ETK).[127] BTK is mainly expressed in B-cells, whereas RLK/TXK, and ITK are exclusively expressed in myeloid hematopoietic cells. TEC is expressed in certain somatic cells and BMX is specifically expressed by the cardiac endothelium and arterial endothelial cells.[165-167] BTK and TEC play important signaling roles in glycoprotein VI (GPVI)-mediated platelet activation, spreading, and aggregation.[168]

Within the last decade, the TEC family kinase and critical B-cell signaling molecule BTK has become a novel and effective therapeutic target in many hematologic malignancies.[169]

Indeed, the first-generation BTK inhibitor, ibrutinib, has demonstrated efficacy in treating several hematological malignancies, such as chronic lymphocytic leukemia, and chronic inflammatory conditions, such as graft-versus-host disease.[169,170] However, ibrutinib also imparts anti-platelet effects as BTK contributes to platelet signaling, with accumulating clinical data demonstrating the effects of TFK inhibition in platelets.[131] Additionally, ibrutinib exhibits off-target effects through inhibition of several other TFKs including TEC and BMX.[133]

Vascular endothelial cells express BMX but not BTK.[165] Both BMX and BTK play a role in systemic inflammation and cytokine signaling, leading to the investigation of several TFK inhibitors for inflammatory and autoimmune diseases.[163,164] In particular, inhibition of inflammatory cytokine activity has been demonstrated to mitigate cardiovascular morbidity in a major clinical trial.[171] Although it has been shown that BMX plays a role in signaling via the vascular endothelial growth factor receptors 1 and 2 (VEGFR1, VEGFR2) and that tumor necrosis factor-α (TNFα) induces a reciprocal activation between BMX and VEGFR2, it remains unknown if these mechanisms are sensitive to TFK inhibitors such as ibrutinib.[172,173] Since ibrutinib can also inhibit BMX activity by irreversibly binding a conserved cysteine residue,[133] we used ibrutinib as a functional tool to investigate the role of TFKs in the pathogenesis of atherosclerosis.

While TFKs appear to be novel, druggable targets to inhibit key pathways that mediate platelet signaling and activity, the effects of inhibiting these pathways on platelet-endothelial interactions and overall cardiovascular risk *in vivo* remain undescribed. We hypothesized that TFKs play a critical role in atherosclerosis formation via several

independent pathways: 1) pro-atherosclerotic vascular endothelial functions; 2) platelet function; and 3) regulation of pro-atherosclerotic cytokine production and systemic inflammation. We therefore aimed to evaluate the role of TFKs on these biochemical pathways.

3.5 Materials and Methods

3.5.1 *Reagents*

Primary human aortic endothelial cells (HAECs) and 0.1% gelatin solution were obtained from American Type Culture Collection (Manassas, VA, USA). VascuLife VEGF Endothelial Medium Complete Kit was obtained from Lifeline Cell Technology (Frederick, MD, USA). The irreversible BTK inhibitor, ibrutinib, was obtained from Selleck Chemicals (Houston, TX, USA). The irreversible BMX inhibitor, BMX-IN-1, was obtained from MedChemExpress (Monmouth Junction, NJ, USA). Recombinant human vascular endothelial growth factor (VEGF) and TNFα were obtained from R&D System (Minneapolis, MN, USA). CRP-XL was obtained from Dr. Richard Farndale (Cambridge University, Cambridge, UK). Protein A/G Sepharose and Protein A/G PLUS-agarose beads were from Santa Cruz Biotechnology (Dallas, TX, USA). Laemmli Sample Buffer was obtained from Bio-Rad Antibodies (Hercules, CA, USA). Accutase and human endothelial serum free media were obtained from Thermo Fisher Scientific (Waltham, MA, USA). Prostacyclin was obtained from Cayman Chemical (Ann Arbor, MI, USA). All other reagents were obtained from Sigma-Aldrich (St. Louis, MO, USA) or previously cited sources.[151]

3.5.2 *Antibodies*

The 15-amino acid cyclic peptide (CCP-015b) and the mouse anti-human monoclonal IgG1 against VCAM-1 (1.G11B1) used for contrast-enhanced ultrasound (CEU) molecular imaging were obtained from Dr. Gray D. Shaw (Quell Pharma Inc., Plymouth, MA, USA) and Bio-Rad Antibodies (Hercules, CA, USA), respectively. The PE mouse anti-human CD62P (P-selectin) and FITC mouse anti-human PAC-1 antibodies used for flow cytometry were obtained from BD Biosciences (San Jose, CA, USA). The APC anti-human CD62P (P-selectin) antibody used for flow cytometry was obtained from BioLegend (San Diego, CA, USA). The PE-Cyanine7 CD106 (VCAM-1) antibody used for flow cytometry was obtained from ThermoFisher Scientific (Waltham, MA, USA). The anti-p-Tyr antibody used for immunoprecipitation assays was from Santa Cruz Biotechnology (Dallas, TX, USA). The anti-ETK/BMX antibody and anti-p-STAT3 used for immunoprecipitation assays were from Cell Signaling Technology (Danvers, MA, USA). The anti-p-BMX antibody used for immunoprecipitation assays was from Abcam (Cambridge, UK). The anti-VCAM-1 antibody used for Western blotting was from Santa Cruz Biotechnology (Dallas, TX, USA).

3.5.3 *Flow Cytometry for VCAM-1 Expression*

HAECs were grown to confluence in 0.1% gelatin-coated 6-well plates with VascuLife VEGF Endothelial Medium Complete Kit. HAECs were serum-starved for 4 h and then pre-incubated with vehicle (DMSO) or ibrutinib (10 μM) for 30 min at 37°C. Cells were then stimulated with VEGF-A (100 ng/mL) or TNFα (5 ng/mL) in serum-free medium with 0.5% bovine serum albumin (BSA) for 6 h at 37°C. HAECs were washed with PBS, incubated with accutase to detach cells for 2 min at 37°C, and centrifuged at 1000 *g* for 5 min. Samples were re-suspended in 0.5% BSA in PBS and incubated with an anti-

VCAM-1 PE/Cy7 antibody (1:50) for 30 min at 37°C at 200 rpm. Samples were then diluted with 0.5% BSA in PBS, centrifuged at 1000 *g* for 5 min, and re-suspended in 2% PFA. Samples were analyzed by flow cytometry (FACSCanto II, BD Biosciences, Franklin Lakes, NJ, USA) and VCAM-1 expression was determined by flow cytometry analysis using FlowJo software (version 10.7.1).

3.5.4 *Immunopreciptation and Western Blotting*

HAECs were grown to confluence in 0.1% gelatin-coated 12-well plates with VascuLife VEGF Endothelial Medium Complete Kit. HAECs were serum-starved for 4 h before being stimulated with vehicle, VEGF-A (100 ng/mL), or TNFα (5 ng/mL) in serum-free medium with 0.5% BSA for 6 h at 37°C. Prior to stimulation, cells were pre-incubated with vehicle (DMSO) or the TFK inhibitors, JS25 (20, 40, 80 µM), BMX-IN-1 (20, 40 µM), or ibrutinib (10 µM) as indicated for 30 min at 37°C. Cells were lysed in Laemmli sample buffer containing 200 mM dithiothreitol. Protein sample were separated by SDS-PAGE, transferred to polyvinylidene difluoride (PVDF) membranes, and blotted with an anti-VCAM-1 antibody (0.4 µg/mL) and a horseradish peroxidase-conjugated secondary antibody (1:10,000).

For immunoprecipitation experiments, cells were seeded in 12-well plates and serum-starved for 4 h before being stimulated with vehicle or VEGF-A (100 ng/mL) in serum-free medium with 0.5% BSA for 5 to 60 min at 37°C. Cells were lysed with cold lysis buffer (10mM Tris/HCl, pH 7.4; 150 mM NaCl; 2 mM EDTA; 1% Triton X-100) containing PMSF (1:100) and phosphatase inhibitor (1:100) for 30 min at 4°C. HAEC lysates were then pre-cleaned with Protein A/G Sepharose and incubated with 2 µg of an

anti-p-Tyr antibody or nonspecific IgGs overnight at 4°C. Antibody-protein complexes were then captured with Protein A/G PLUS-agarose beads at 4°C for 2 h. At the end of the incubation period, the beads were washed three time in a lysis buffer. Precipitates were then eluted with Laemmli sample buffer supplemented with 200 mM dithiothreitol. Protein sample were separated by SDS-PAGE, and transferred to PVDF membranes and blotted with an anti-BMX antibody (0.1 µg/mL), an anti-p-BMX Y566 antibody (0.03 µg/mL), or an anti-p-STAT3 Y705 antibody (0.2 µg/mL), and horseradish peroxidase-conjugated secondary antibodies. Films were scanned and blots representative of 3-4 independent experiments are shown.

3.5.5 *Human Platelet Isolation*

Human venous blood was drawn by venipuncture from healthy subjects into 3.8% sodium citrate (1:10) and acid citrate dextrose (1:10) as previously described.[174,175] Written informed consent from volunteers was obtained in accordance with an approved protocol from the Institutional Review Board of Oregon Health & Science University. Platelet rich plasma (PRP) was isolated from whole blood by centrifugation at 200 *g* for 20 min. PRP was then centrifuged at 1000 *g* for 10 min in the presence of prostacyclin (0.1 µg/mL) and the platelet poor plasma (PPP) was decanted to obtain platelets. The platelet pellet was re-suspended in modified HEPES-Tyrode buffer (129 mM NaCl, 0.34 mM Na_2HPO_4, 2.9 mM KCl, 12 mM $NaHCO_3$, 20 mM HEPES, 5 mM glucose, 120 mM $MgCl_2$, pH 7.3), and washed via centrifugation at 1000 *g* for 10 min in the presence of prostacyclin (0.1 µg/mL) and acid citrate dextrose (1:10). The washed platelets were re-suspended in modified HEPES-Tyrode buffer to the desired concentration.

3.5.6 *Platelet Aggregation*

Platelet aggregation was measured in response to GPVI-agonist, cross-linked collagen-related peptide (CRP-XL). Platelet aggregation studies were performed by pre-incubating 300 µL of human washed platelets (3×10^8/mL) with inhibitors for 10 min at room temperature. Platelets were then stimulated with CRP-XL (1 µg/mL) and monitored under continuous stirring at 37°C. Platelet aggregation was measured by changes in light transmission using an aggregometer (Chrono-Log Corporation, Havertown, PA, USA). Data were presented as representative aggregation tracings. The averages of maximal platelet aggregation for 3 different experiments were analyzed for statistical significance by one-way ANOVA using GraphPad PRISM 8 software. For the NHP studies, 300 µL of PRP was warmed to 37°C and then stimulated with CRP-XL (1 µg/mL) under continuous stirring. Platelet aggregation was measured by changes in light transmission using an aggregometer (PAP-4, Bio/DataCorporation, Horsham, PA, USA). Data were presented as representative aggregation tracings.

3.5.7 *Flow Cytometry for Platelet Activation*

Platelet integrin activation and granule secretion in response to CRP-XL were measured using flow cytometry. Flow cytometry studies were performed with human whole blood anticoagulated with 3.8% sodium citrate and pre-incubated with either vehicle (DMSO) or ibrutinib (10 µM) for 10 min at 37°C. Human whole blood samples were diluted in modified HEPES-Tyrode buffer (1:4) and incubated with anti-CD62P PE (1:20) or anti-PAC-1 FITC (1:20) antibody for 20 min at 37°C in the presence of CRP-XL (5 µg/mL). Whole blood from rhesus macaques was also diluted in modified HEPES-Tyrode buffer (1:4) and incubated with anti-CD62P PE (1:10) or anti-PAC-1 FITC (1:10) antibody for

20 min at 37°C in the presence of CRP-XL (5 µg/mL). The reactions were stopped by adding 2% PFA and analyzed by flow cytometry (BD FACSCanto II, BD Biosciences, Franklin Lakes, NJ). Platelet activation was determined by flow cytometry analysis using FlowJo software (version 10.7.1) and presented as mean fluorescence intensity.

3.5.8 *Nonhuman Primate Model of Early Atherosclerosis*

This study was approved by the Institutional Animal Care and Use Committee of the Oregon Health & Science University (Approval Number: IP00002332) prior to initiation. Rhesus macaques (*Macaca mulatta*), were cared for and housed at the Oregon National Primate Research Center (ONPRC) at Oregon Health & Science University.

Adult male rhesus macaques (*n*=2; ages 14 and 18 years) were fed a high fat diet (45% carbohydrates, 18% protein, and 36% fat by caloric content LabDiet 5L0P, Purina Mills) for >2 years and were selected on the basis of having carotid intimal-medial thickening as a marker of early atherosclerotic changes. Animals were administered ibrutinib orally daily for 7 days at a dose of 10 mg/kg/day and studied at baseline and days 1 and 7 after drug administration. The dose used in this study was selected to test the maximal response of ibrutinib within the dose range of 1.25-12.5 mg/kg/day used in clinical studies ibrutinib.[176] Anesthesia was induced with ketamine (10 mg/kg intramuscularly) and maintained with isoflurane (1.0-1.5%) at two discrete time points during the study to facilitate CEU molecular imaging.

At designated study intervals, animals underwent phlebotomy for analysis of lipid levels and inflammatory biomarkers, platelet aggregation studies, and whole blood flow cytometry. Hematological analyses were also performed on adult male rhesus macaques

(*n*=3; ages 8, 12,15 years) fed a standard diet (58.52% carbohydrates, 26.82% protein, and 14.65% fat by caloric content LabDiet 5L0P, Purina Mills) as lean controls.

3.5.9 *Nonhuman Primate Blood Collection*

For the NHP studies, venous blood samples were collected from rhesus macaques by venipuncture into 3.2% sodium citrate or plastic vacutainers at baseline and days 1 and 7 following ibrutinib treatment. Platelet rich plasma (PRP) was isolated from blood samples anticoagulated with 3.2% sodium citrate by centrifugation of whole blood at 200 *g* for 8 min. The supernatant was removed, and platelet poor plasma (PPP) was obtained by further centrifugation of the remaining blood at 1000 *g* for 3 min. To isolate serum, blood was drawn into a plastic vacutainer and allowed to sit for 30 min at room temperature. The blood clot was then removed by centrifuging the sample at 1000 *g* for 10 min.

3.5.10 *Hematological Analysis for Lipid Profiles and Inflammatory Biomarkers*

Venous blood samples collected from rhesus macaques by venipuncture were used to measure lipids and inflammatory biomarker profiles. Serum samples were analyzed for lipid levels by the Clinical Pathology Laboratory at the ONPRC using an ABX Pentra 400 Clinical Chemistry System (Horiba Medical, Irvine, CA, USA). C-reactive protein (CRP) concentrations were assessed by an enzyme-linked immunosorbent assay (ELISA) kit, following the manufacturer's instructions (30-9710S, ALPCO, Salem, NH, USA). The assay range was 0.95-150 ng/mL and intra-assay CV was 3.6%.

Serum samples were analyzed for cytokines using a custom 9-plex monkey cytokine Luminex panel (ThermoFisher, Waltham, MA, USA), which included IL-1β, IL-2, IL-4,

IL-6, IL-8, IL-10, IL-12/IL-23p40, IFN-γ, and IFN-α. The analysis was performed by the Endocrine Technologies Core at the ONPRC. Briefly, 25 µL of each serum sample was diluted in assay diluent and incubated overnight with antibody-coated, fluorescent-dyed capture microspheres specific for each analyte, followed by detection antibodies and streptavidin-phycoerythrin. Washed microspheres with bound analytes were resuspended in reading buffer and analyzed on a Milliplex LX-200 Analyzer (EMD Millipore, Billerica, MA, USA) bead sorter with XPonent Software version 3.1 (Luminex, Austin, TX, USA). Data were calculated using Milliplex Analyst software version 5.1 (EMD Millipore). An in-house generated rhesus macaque serum pool was run in quadruplicate as a quality control. Intra-assay CVs were as follows: IL-1β, 4.7%; IL-2, 12.7%; IL-8, 1.6%; IL-10, 4.3%; IL-12/IL-23p40, 6.6%; IFN-γ, 12.8%; IFN-α, 3.2%. Intra-assay CVs for IL-4 and IL-6 were not calculated, as they were undetectable in the QC. Since all samples were analyzed in a single assay, no inter-assay variation was calculated.

3.5.11 *Targeted Molecular Imaging Agent Preparation*

For CEU molecular imaging, microbubbles targeted to platelet glycoprotein-Ibα (GPIbα), endothelial vascular cell adhesion molecule-1 (VCAM-1), or control microbubbles were prepared as previously described.[177-179] In brief, biotinylated lipid-shelled decafluorobutane microbubbles were prepared via sonication of a gas-saturated aqueous suspension of distearoylphosphatidylcholine (2 mg/mL), polyoxyethylene-40-stearate (1 mg/mL), and distearoylphosphatidylethanolamine-PEG (2000) biotin (0.4 mg/mL). Microbubbles targeted to platelet GPIbα or endothelial VCAM-1 were prepared by conjugating biotinylated ligands to the microbubble surface using either a 15-amino acid cyclic peptide (CCP-015b) biotinylated at an added C-terminal lysine residue or a

monoclonal antibody against VCAM-1 (1.G11B1), respectively. Microbubbles targeted to platelet GPIbα and endothelial VCAM-1 were previously validated using *in vitro* flow chamber assays and immunohistochemistry of spleen and carotid artery from rhesus macaques that were fed a high fat diet for 2 years, respectively.[177,179] Control microbubbles were unconjugated with no targeting ligand. Electrozone sensing was used to measure microbubble concentration and to ensure similar size distribution between agents for each experiment (Multisizer III, Beckman-Coulter, Brea, CA, USA).

3.5.12 *Carotid Molecular Imaging*

We utilized CEU molecular imaging at the carotid bifurcation to measure endothelial VCAM-1 and platelet GPIbα before and after treatment with the TFK inhibitor ibrutinib as previously described.[177-179] In brief, longitudinal-axis imaging at the carotid bifurcation was performed using multi-pulse, contrast-specific imaging at 7MHz, a mechanical index of 1.9, a dynamic range of 55dB, and a frame rate of 1 Hz (Sequoia, Siemens Medical Imaging, Mountain View, CA, USA). Intravenous injections of microbubbles targeted to endothelial VCAM-1 or platelet GPIbα (1×10^8) were performed in a random order. Following injection of targeted microbubbles, the ultrasound was paused for 1 min before locating the carotid artery using two-dimensional ultrasound at low power (mechanical index<0.10) and activating contrast-specific imaging for several frames. The signal for the retained microbubbles was quantified by digitally averaging the first two frames acquired and then subtracting several averaged frames acquired after >5 destructive pulse sequences (mechanical index 1.3) to mitigate signal from freely circulating microbubbles. Data from regions-of-interest at the near and far walls of the common carotid artery were averaged.

3.5.13 *Statistical Analysis*

Data were tested for normality using a Shapiro-Wilk test. Two group data presented in the study were not normally distribution and were analyzed by a Mann-Whitney test. For three or more groups, data were analyzed by one-way ANOVA with a Dunnett's post-hoc test. Statistical significance was considered for $P<0.05$. For all the experiments, n indicates the number of independent experiments performed. Individual data from the NHP experiments were not evaluated statistically to avoid overpowering the analysis given the small size of the animal cohort. Statistical analyses were performed using GraphPad PRISM 9 (San Diego, CA, USA).

3.6 Results

3.6.1 *Effects of VEGF-A on Endothelial Cell VCAM-1 Expression*

Tyrosine kinases play a central role in endothelial cell signal transduction by phosphorylating cellular proteins to facilitate growth and differentiation signal cascades, as well as to regulate vessel tone, expression of adhesion molecules, and chemoattractants.[163] Endocardial and arterial endothelial cells express the TEC family kinase (TFK), BMX. BMX is known to be involved in signaling downstream of VEGFR1 and VEGFR2.[172,173] Since VEGF-A, the ligand for the aforementioned receptors, is upregulated in atherosclerotic plaques and enhance atherosclerosis, we studied whether VEGF-A-mediated VCAM-1 expression by endothelial cells was mediated by BMX.

First, we validated that VCAM-1 expression was increased in response to VEGF-A using flow cytometry. As seen in **Figure 3.1A**, VCAM-1 expression was upregulated in response to VEGF-A (100 ng/mL) compared to vehicle; VCAM-1 expression was

confirmed to be upregulated by the cytokine TNFα (5 ng/mL). We next confirmed that VEGF-A-induced phosphorylation of BMX (**Figure 3.1B**) Previous studies have shown that BMX mediates STAT3 activation,[133,180] and that STAT3 contributes to a number of cardiovascular diseases, including atherosclerosis, cardiac hypertrophy, and heart failure.[181] Indeed, as shown in **Figure 3.1B**, VEGF-A stimulation of HAECs upregulated phosphorylation of both BMX and STAT3 as a function of time, providing a mechanistic link between the initiator involvement of BMX as well as the pathological roles of STAT3 in atherosclerosis.

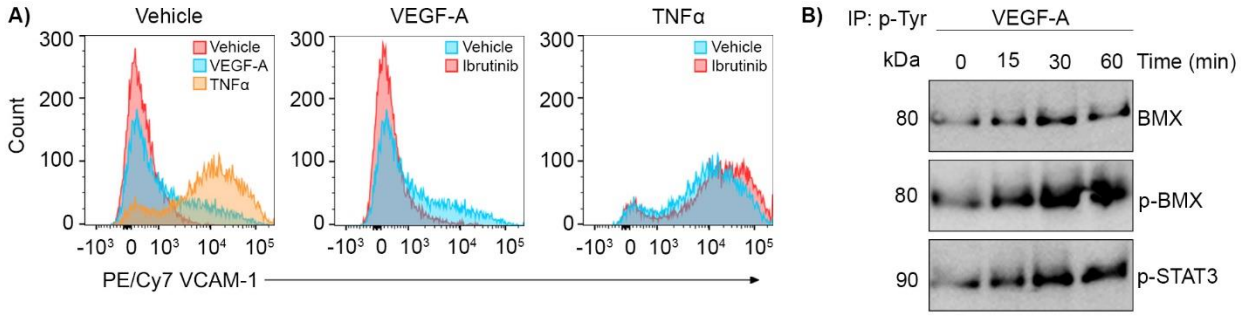

Figure 3.1 VCAM-1 expression in human aortic endothelial cells (HAECs) following exposure to VEGF-A or TNFα. (A) Representative flow cytometry histograms from HAECs stimulated with vehicle, VEGF-A (100 ng/mL), or TNFα (5 ng/mL). In select experiments, HAECs were pre-incubated with ibrutinib (20 μM). (B) Phosphorylation of BMX (p-BMX) and STAT3 (p-STAT3) immunoprecipitated from HAECs stimulated with VEGF-A (100 ng/ml) for 0, 15, 30, or 60 min. Representative blots for at least *n*=3. IP indicates immunoprecipitation.

3.6.2 *Effects of BMX Inhibition on Endothelial Cell VCAM-1 Expression*

When the endothelium is activated, adhesion molecules (e.g. E-selectin, ICAM-1, and VCAM-1) are expressed on the surface. VCAM-1 represents the most prevalent adhesion molecule in atherosclerosis and is present in early atherosclerotic lesions.[162] Since VEGF-A stimulates VCAM-1 expression in HAECs (**Figure 3.1A**) and VEGF-A signals through

BMX and STAT3 (**Figure 3.1B**), we next tested if the kinase pathway downstream of VEGF-A stimulation is sensitive to BMX inhibition. Our results show that pharmacological inhibition of BMX with the BMX inhibitors, JS25 and BMX-IN-1, reduced VCAM-1 expression in response to VEGF (**Figure 3.2A**). Along these lines, VEGF-A-induced VCAM-1 expression was also sensitive to ibrutinib (**Figure 3.2A**). With the exception of the higher concentration of JS25 (40 µM), VCAM-1 expression in response to TNFα was not affected by any of the aforementioned inhibitors (**Figure 3.2B**). Taken together, our data demonstrate that VEGF-A-mediated endothelial VCAM-1 expression is sensitive to pharmacological inhibition of BMX.

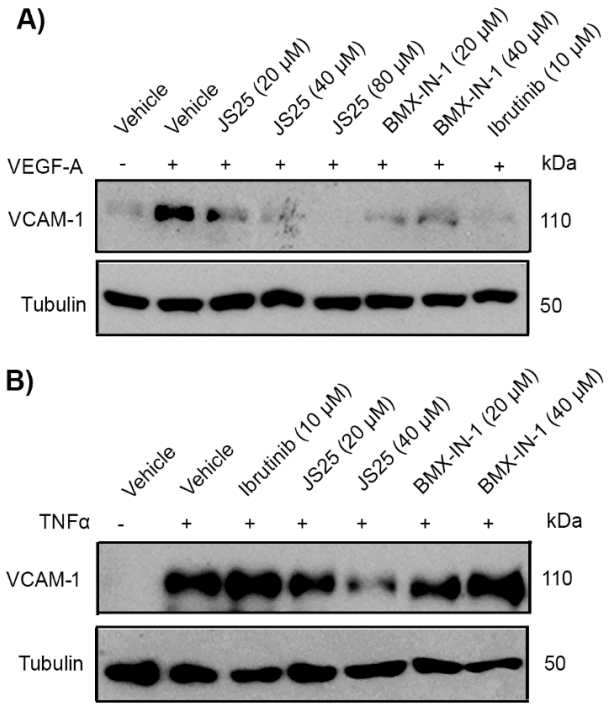

Figure 3.2 Effect of ibrutinib on VEGF-A-induced VCAM-1 expression in human aortic endothelial cells (HAECs). (A) HAECs were stimulated with either VEGF-A (100 ng/mL) or (B) with TNFα (5 ng/mL) for 6 h in the presence of different concentrations of BMX inhibitors (JS25 or BMX-IN-1) or ibrutinib (10 µM). Representative blots for at least *n*=3.

3.6.3 *Effects of TFK Inhibition on Platelet Aggregation*

To advance toward *in vivo* testing in a nonhuman primate (NHP) model, we first validated the effect of ibrutinib on known platelet pathways in response to ITAM-mediated agonists, including CRP-XL. CRP-XL mediates platelet activation in a receptor tyrosine kinase-dependent manner.[182] We found that pre-incubation of human washed platelets with ibrutinib significantly abrogated platelet aggregation in response to CRP-XL (1 µg/mL) (**Figure 3.3A**) (P=0.029). Next, we examined the effect of TFK inhibition on NHP platelet aggregation in response to CRP-XL. Our data show robust aggregation of NHP platelets in response to CRP-XL (1 µg/mL) prior to administration of ibrutinib (**Figure 3.3B, Baseline**). Platelet aggregation in response to CRP-XL (1 µg/mL) was abrogated following one week of treatment with the BTK inhibitor, ibrutinib (**Figure 3.3B, Ibrutinib**). These data validate that ibrutinib inhibits GPVI-mediated platelet aggregation.

3.6.4 *Effects of TFK Inhibition on Platelet P-selectin and PAC-1 Expression*

Upon activation, platelets release α-granules containing numerous substances including P-selectin (CD62P).[175,183] Therefore, we used flow cytometry to quantify P-selectin expression as a marker of GPVI-mediated platelet activation. We first pre-incubated human whole blood with ibrutinib (10 µM) before stimulating with CRP-XL and staining with an anti-P-selectin antibody. Flow cytometry analyses confirmed that ibrutinib significantly decreased P-selectin expression in response to CRP-XL relative to control (P=0.012) (**Figure 3.3C)**. Stimulation of NHP whole blood with CRP-XL upregulated P-selectin surface expression at baseline, and dramatic inhibition of CRP-XL-induced P-

selectin expression was observed as early as one day following the initial dose of ibrutinib (**Figure 3.3D**).

Downstream of the initial GPVI-mediated platelet activation, intracellular signaling events promote "inside-out" activation of platelet integrins such as αIIbβ3 that bind to fibrinogen, vWF, and matrix proteins with RGD-like sequences.[34] These processes mediate stable platelet adhesion and aggregation, as well as thrombus formation.[175] To monitor platelet surface integrin αIIbβ3 activation, whole blood samples were treated as previously described and an anti-PAC-1 antibody was used to recognize the active conformation of platelet integrin αIIbβ3. We confirmed that PAC-1 expression in human samples treated with ibrutinib decreased relative to control (P=0.042) (**Figure 3.3E**). Indeed, PAC-1 expression in the NHP samples was elevated at baseline and dramatically inhibited as early as one day following the initial dose of ibrutinib (**Figure 3.3F**). Taken together, these results confirm that inhibiting TFK blocks platelet GPVI-mediated α-granule secretion and integrin activation.

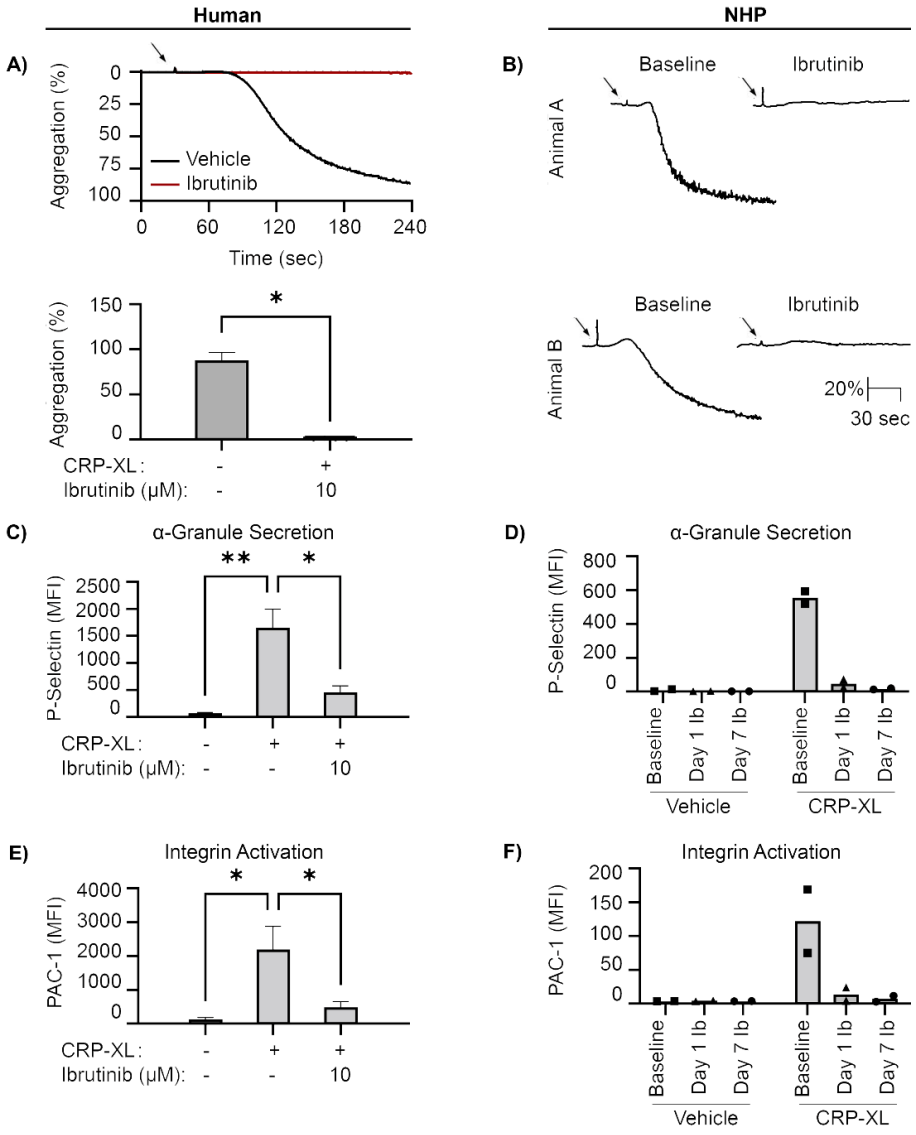

Figure 3.3 Platelet aggregation and activation in response to the GPVI-agonist, CRP-XL. (A) Human washed platelets ($3x10^8$/mL) were pre-treated with ibrutinib for 10 min at room temperature and stimulated with CRP-XL (1 μg/mL). Representative tracings from human washed platelets pre-incubated with ibrutinib (*n*=3) prior to stimulation with CRP-XL (arrow). Maximal aggregation from human washed platelets pre-incubated with ibrutinib (*n*=3). (B) Platelet rich plasma from obese NHPs (*n*=2) was stimulated with CRP-XL (1 μg/mL). Traces are shown for primates at baseline and after one week of ibrutinib treatment following the addition of CRP-XL (arrow). Flow cytometry analysis of P-selectin (C-D) and PAC-1 (E-F) expression from human (*n*=3) or NHP (*n*=2) whole blood samples stimulated with CRP-XL (5 μg/mL). MFI, mean fluorescent intensity. * indicates $P<0.05$. ** indicates $P<0.01$. *n* indicates the number of independent experiments using blood from different donors. Error bars indicate SEM.

3.6.5 *Effects of TFK Inhibition on Body Weight, Lipid Profiles, and Inflammatory Biomarkers*

Although TFKs represent an attractive target to reduce platelet activation, the effects of inhibiting these pathways on platelet-endothelial interactions and overall cardiovascular risk *in vivo* remains unknown. Having validated the efficacy of ibrutinib with respect to platelet activity *in vitro*, we next sought to perform a pilot experiment examining the systemic effects of BTK inhibition using a model of obese NHPs exhibiting an atherosclerotic phenotype **(Figure 3.4A**). The two rhesus macaques in this pilot study were fed a high fat diet for a minimum of two years, resulting in the development of detectable atherosclerotic lesions in the aorta, coronary, carotid and renal arteries.[179]

At baseline, animals on the high fat diet had a greater body mass compared to lean control animals. The obese animals had elevated levels of C-reactive protein and interleukin (IL)-4 compared to the lean control animals, while IL-8 levels were not elevated compared to lean controls. Treatment of obese animals with ibrutinib for one week did not consistently alter the body mass, lipid levels, or levels of various inflammatory biomarkers (**Table 3.1**).

Table 3.1 Body weight, lipid profiles, and inflammatory biomarkers in obese NHPs at baseline and after one week of ibrutinib treatment. LDL, low-density lipoprotein; HDL, high-density lipoprotein; CRP, C-reactive protein; IL, interleukin. Data are shown as mean ± SD. *Historic data from Chadderdon et al.[179]

	Lean	Obese			
		Animal A		Animal B	
		Baseline	Ibrutinib	Baseline	Ibrutinib
Weight, kg	11.0 ± 1.9 *	20.5	20.5	23.8	23.9
Total Cholesterol, mg/dL	134 ± 21 *	137	138	162	187
LDL Cholesterol, mg/dL	58 ± 11 *	67	75	74	98
HDL Cholesterol, mg/dL	65 ± 15 *	30	34	72	82
CRP, ng/mL	380.53 ± 150.29	890.60	1109.00	924.80	922.20
IL-4, pg/mL	1.14 ± 0.13	1.53	2.06	5.47	5.18
IL-8, pg/mL	196.9 ± 95.2	91.4	74.4	175	135

3.6.6 *Effects of TFK Inhibition on Carotid Endothelial Activation and Platelet Adhesion*

Previous studies have demonstrated that obese NHPs exhibit a significant increase in platelet GPIbα and endothelial VCAM-1 compared to lean control animals, indicating local platelet adhesion and endothelial inflammation.[177] It has also been shown that endothelial expression of VCAM-1 increases over time in NHPs feed a high fat diet.[179] We performed a pilot study to determine the effects of TFK inhibition on local platelet activation and endothelial inflammation, we used a non-invasive molecular imaging technique to measure platelet GPIbα and endothelial VCAM-1 at the carotid bifurcation before and after treatment with ibrutinib in a NHP model of diet-induced obesity. On visual inspection, a decrease in VCAM-1 expression was observed in the presence of ibrutinib (**Figure 3.4B**). Quantification of intensity per unit area showed a decrease from intensity levels at or above 1.8 V/U to below 1.6 V/U in the presence of ibrutinib. The quantification of platelet deposition at baseline indicated a variable response with a high of 19.5 V/U to a low of -2.5 V/U. The maximum intensity recorded for GPIbα was near 2.3 V/U in the presence of ibrutinib V/U (**Figure 3.4C**).

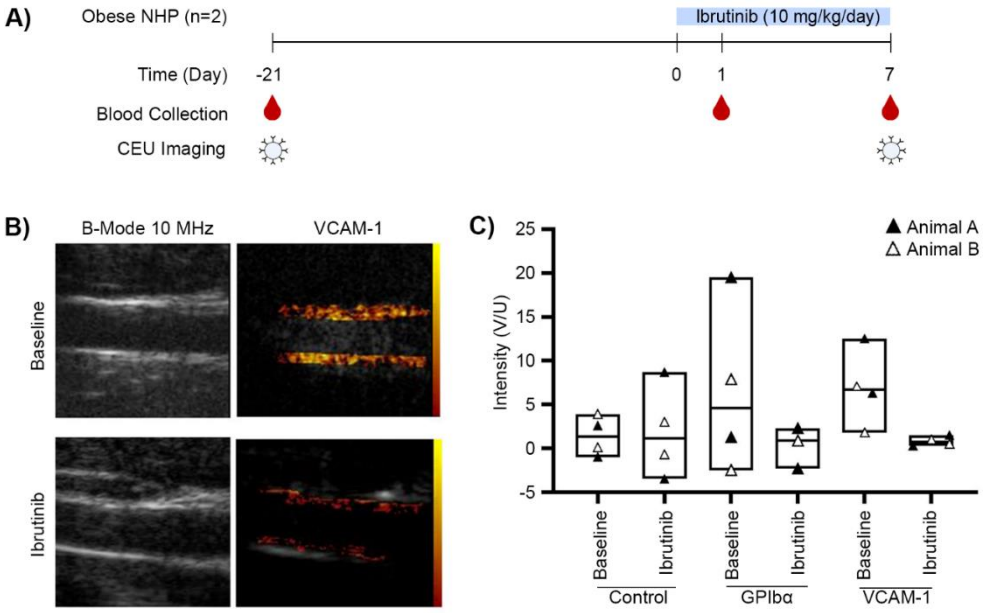

Figure 3.4 Experimental design and targeted contrast-enhanced ultrasound molecular imaging. (A) Experimental design for the *in vivo* study using an NHP model of early atherosclerosis. (B) Examples obtained at baseline and after 1 week of ibrutinib showing non-contrast, two-dimensional image of the carotid artery at the bifurcation (left) and a background-subtracted color-coded image (right) obtained after injecting VCAM-1-targeted microbubbles. (C) Background subtracted video intensity for VCAM-1 and GPIbα-targeted microbubbles in obese rhesus macaques (*n*=2) treated with TEC family kinase inhibitor, ibrutinib, compared to vehicle. Floating bar plots illustrating the median (bar), and the maxima and minimum (box) for CEU molecular imaging. NHP, nonhuman primate; CEU, contrast-enhanced ultrasound.

3.7 Discussion

This study examined the effects of TFK inhibition on endothelial activity *in vitro* and makers of endothelial cell activation in atherosclerosis-prone arteries in NHPs *in vivo*. Our findings suggest that the TFK inhibitor, ibrutinib, inhibited VEGF-A-mediated endothelial VCAM-1 expression, as well as GPVI-mediated platelet aggregation, integrin activation, and granule secretion *in vitro*. In a pilot study using an NHP model of diet-induced atherosclerosis, ibrutinib also decreased markers of vascular endothelial cell activation and platelet adhesion compared to baseline *in vivo*. While the systemic and

global platelet inhibition demonstrated in this work can be a major cause of bleeding risks *in vivo,* previous studies have shown that inhibition of BTK with ibrutinib analogs in an NHP model did not result in bleeding, capillary abnormalities, or thrombocytopenia.[183] Similarly, clinical trials for ibrutinib reported predominantly low-grade bleeding events in humans.[169,184] The sample size for this pilot experiment was small (n=2) due to the limited resources available to study NHP models of early atherosclerosis. This is a caveat to the findings from these preliminary studies that generate a hypothesis that TFKs contribute to the pathogenesis of atherosclerosis and that BTK represents an efficacious and safe target to prevent atherothrombosis.

During the progression of atherosclerosis, a number of pro-inflammatory signaling cascades are implicated through the release of cytokines and growth factors (e.g. interleukins, TNF, VEGF), and the expression of adhesion proteins (e.g. E-selectin, ICAM-1, VCAM-1).[162,185] For example, VEGF can signal through the PLCγ-sphingosine kinase-PKC cascade or the PI3K/AKT/MAPK cascade to activate NF-kB and induce VCAM-1 expression.[186,187] Furthermore, VEGF signals through the TEC family kinase member, BMX, via VEGFR1 and VEGFR2.[172,173] Indeed, our *in vitro* studies showed that VEGF-A-mediated VCAM-1 expression is sensitive to pharmacological inhibition of BMX with selective BMX inhibitors or ibrutinib. The fact that ibrutinib inhibited VCAM-1 expression induced by VEGF-A may explain the effect of ibrutinib on the endothelium *in vivo*. Alternatively, TNFα can induce activation of BMX via TNFR2, and the formation of a reciprocally activated complex between BMX and VEGFR2; this in turn elicits the common PI3K/AKT pathway.[173] Of note, TNFR2 is tightly regulated compared to its ubiquitous counterpart, TNFR1. TNFR1-mediated pathways have been

extensively studied as the main receptor for TNFα on endothelial cells; nevertheless, induction of VCAM-1 expression by TNFα-TNFR1 seems to be independent of BMX.[173,188]

Although it has been suggested that both TNFα and VEGF increase phosphorylation of BMX on Y566, our studies indicate that TNFα-mediated VCAM-1 expression is not affected by pharmacological inhibition of BMX. One possible explanation is that, compared to VEGF, TNFα induces phosphorylation at fewer tyrosine residues. More specifically, TNFα induces Tyr(P)-1054/1059 on VEGFR2, but neither TNFα nor BMX induce phosphorylation at Tyr(P)-1175, a site that is critical for VEGF-mediated activation of PI3K/AKT and PLCγ pathways upstream of VCAM-1.[129] Taken together, this suggests that while BMX is dispensable in TNFα-mediated VCAM-1 expression, BMX plays a role in VEGF-mediated VCAM-1 expression on aortic endothelial cells, and as such is sensitive to ibrutinib. Furthermore, the observed decrease in VCAM-1 expression following one week of treatment with ibrutinib suggests that ibrutinib disrupts an inflammatory signaling pathway driving endothelial cell activation, or at least markers of activation, *in vivo*.

Although ibrutinib is often referred to as a first generation BTK inhibitor, previous studies showed that ibrutinib inhibits the kinase activities of numerous TFKs including BMX by irreversibly binding a conserved cysteine residue.[133] The TFKs share a common domain organization that consists of: 1) an N-terminal pleckstrin-homology domain; 2) a TEC-homology domain with a BTK motif and one to two proline-rich regions; 3) SRC homology 3 and 2 domains; and 4) a carboxy-terminal kinase domain.[127,128] Within the

kinase domain, the residues in the ATP binding site share 40–65% identity and 60–80% similarity.[129] Ibrutinib reacts with a cysteine residue (C481) within the ATP binding site, thus blocking the catalytic activity of BTK by forcing the BTK kinase domain to adopt an inactive conformation.[132] Similarly, the covalent BMX inhibitors, BMX-IN-1 and JS25, bind a cysteine residue (C496) in the ATP binding site. This residue is a unique occurrence found in the ATP binding pocket and is present in all five members of the TFKs (BTK, ITK, RLK/TXK and TEC), as well as members from the EGFR family (EGFR, HER2, HER4), JAK3, BLK and MAP2K7.[129] By virtue of structural homology, BMX-IN-1 and JS25 could also be covalent inhibitors of the other kinases in the TEC family.[129]

Beyond compromised endothelial function, atherosclerosis is characterized by dysregulated platelet-endothelial interactions, which encourages aberrant leukocyte recruitment.[151,189] In this setting, platelets facilitate monocyte adhesion to the vascular endothelium and subsequent transmigration through the endothelial cell layer to facilitate the shift of lipid-laden macrophages to foam cells. Additionally, neutrophils as well as neutrophil-platelet interactions are implicated in the progression of atherogenesis.[190,191] Although the pro-atherosclerotic phenotype imparted by endothelial cell activation and the secretion of growth factors/chemokines/cytokines by platelets to facilitate leukocyte recruitment has been extensively studied, the role of TFKs in this system as a whole remains poorly defined. Since TFKs are not only expressed by hematopoietic cells, but also by other somatic cells, and ibrutinib promiscuously inhibits TFKs, the utility of ibrutinib could extend beyond its use in treating hematological malignancies and quelling endothelial dysfunction to more global effects within the blood microenvironment.

Chapter 4. Pharmacologically targeting of coagulation FXI in a hyperlipidemia model inhibits endothelial inflammation and priming of platelet activation

Tia C.L. Kohs, Helen H. Vu, Kelley R. Jordan, Iván Parra-Izquierdo, Monica T. Hinds, Joseph J. Shatzel, Paul Kievit, Terry K. Morgan, Samuel Tassi Yunga, Thuy T.M. Ngo, Joseph E. Aslan, Michael Wallisch, Christina U. Lorentz, Erik I. Tucker, Cristina Puy, David Gailani, Jonathan R. Lindner, and Owen J.T. McCarty

This work is currently under review by

Research and Practice in Thrombosis and Haemostasis.

4.1 Abstract

Background: Hyperlipidemia is associated with chronic inflammation and thromboinflammation. This is an underlying cause of several cardiovascular diseases, including atherosclerosis. In diseased blood vessels, rampant thrombin generation results in the initiation of the coagulation cascade, activation of platelets, and endothelial cell dysfunction. Coagulation factor (F) XI represents a promising therapeutic target to reduce thromboinflammation as it is uniquely positioned at an intersection between inflammation and thrombin generation.

Objectives: Investigate the role of FXI in promoting platelet and endothelial cell activation in a model of hyperlipidemia.

Methods: Nonhuman primates (NHPs) were fed a standard chow diet (lean, n=6) or a high-fat diet (obese, n=8) to establish a model of hyperlipidemia. Obese NHPs were

intravenously administered a FXI blocking antibody at 2mg/kg and studied at baseline, 1, 7, 14, 21, and 28 days after drug administration. Platelet activation and inflammatory markers were measured using FACS or ELISA. Molecular imaging was used to quantify vascular cell adhesion molecule 1 (VCAM-1) expression at the carotid bifurcation.

Results: Obese NHPs demonstrated increased sensitivity for platelet P-selectin expression and phosphatidylserine exposure in response to platelet GPVI or PAR agonists compared to lean NHPs. Obese NHPs exhibited elevated levels of C-reactive protein, cathepsin D, and myeloperoxidase compared to lean NHPs. Following pharmacological inhibition of FIX activation by FXIa, platelet priming for activation by GPVI or PAR agonists, C-reactive protein levels, and endothelial VCAM-1 levels were reduced in obese NHPs.

Conclusions: FXI activation promotes the proinflammatory phenotype of hyperlipidemia by priming platelet activation and inciting endothelial cell dysfunction.

4.2 Introduction

Hyperlipidemia and obesity are associated with chronic vascular inflammation and thrombosis. Thus, the studies outlined here were designed to investigate the role of coagulation factor (F) XI in sustaining the thromboinflammatory phenotype associated with chronic hyperlipidemia. For these experiments, we used the same nonhuman primate (NHP) model of diet-induced obesity described in Chapter 2 and examined the effect of diet-induced obesity on platelet sensitivity and inflammatory markers. Pharmacological targeting of FXI using the monoclonal antibody, humanized 1A6, reduced platelet

priming for activation and inflammation. In conclusion, our study demonstrated that inhibition of FXI activation reduces vascular dysfunction in hyperlipidemia.

4.3 Background

Thromboinflammation associated with hyperlipidemia is an underlying cause of cardiovascular diseases (CVD), including atherosclerosis.[158] In the setting of atherosclerosis, lipid accumulation within the blood vessel walls prompts endothelial cell dysfunction.[65,67,69] Concomitantly, select chemokines and chemoattractants are upregulated and secreted, which results in aberrant recruitment of leukocytes into the intima.[65,69] Circulating lipoproteins are readily oxidized and internalized by macrophages, thereby generating foam cells in the nascent atheroma and secreting additional inflammatory cytokines and reactive oxygen species.[70] Mature plaques with a necrotic core form following the accumulation of dying macrophages. The rupture of these plaques is highly thrombogenic and is a common cause of myocardial infarction or stroke.[71,72]

Thrombin generation is central for the homeostasis and regulation of barrier function and protection against vessel damage. In the setting of diseased blood vessels, rampant acceleration and propagation of thrombin generation results in: 1) occlusive thrombus formation; 2) onset of inflammation; and 3) deleterious loss of endothelial barrier function.[192] By way of amplifying thrombin generation, coagulation factor (F) XI has been shown to play a detrimental role in promoting thromboinflammation, in part by creating a thrombin amplification loop. FXI is activated by thrombin, which by then activating FIX, FXIa feeds forward to generate more thrombin.[193] Yet, the enzymatic

function of FXIa has been shown to extend beyond an exclusive partnership with FIX. These functions range from degradation of inhibitors of thrombin generation (e.g. tissue factor pathway inhibitor [TFPI]) to activation of 'upstream' members of the coagulation cascade (e.g. FXII).[2,144,145] In fact, it has become apparent that FXIa acts on a litany of substrates to amplify local thrombin generation, platelet activation, and endothelial cell barrier function, thereby serving as a valued member in the maintenance of homeostasis.[147] In the setting of hyperlipidemia, these processes are imbalanced, creating a pathologic thromboinflammatory phenotype.

The multifaceted function of FXIa has provided the rationale for testing if inhibition of FXI activation or FXIa activity is anti-inflammatory in addition to being antithrombotic. Indeed, it has been observed that FXI inhibition improves outcomes in *in vivo* mouse models of atherosclerosis,[138] sepsis,[54,139,140] ischemic stroke and myocardial infarction.[1,141] Moreover, inhibition of either FXII or FXI activation prevented an acute inflammatory response, platelet consumption, and reduced markers of endothelial dysfunction in a baboon model of systemic inflammatory response syndrome.[2,52,142] This anti-inflammatory signature of FXI inhibition was observed in clinical trials, wherein a reduction in C-reactive protein levels was observed in end-stage renal disease patients on chronic hemodialysis on a FXI inhibitor.[194] Based on these observations, we interrogated if pharmacological inhibition of FXI activation by FXIIa and FIX activation by FXIa with the anti-FXI antibody, humanized 1A6 (h1A6), would reduce thromboinflammation in a nonhuman primate model of hyperlipidemia.

4.4 Material and Methods

4.4.1 *Reagents*

Crosslinked collagen-related peptide (CRP-XL) was from Dr. Richard Farndale (Cambridge University, Cambridge, UK). Adenosine diphosphate (ADP) was from Sigma-Aldrich (St. Louis, MO, US). Thrombin receptor activator peptide 6 (TRAP-6) was from Tocris Bioscience (Bristol, UK). The activated partial thromboplastin time (aPTT) reagent and prothrombin time (PT) Dade Innovin were from Thermo Fisher Scientific (Middletown, VA, US) and Siemens Healthcare Diagnostics (Munich, Germany), respectively. The polystyrene bead standards used for nanoscale flow cytometry, Megamix-Plus FSC and Megamix-Plus SSC, were from BioCytex (Marseille, France).

4.4.2 *Antibodies*

The mouse anti-human PE CD62P (P-selectin) antibody used for flow cytometry was obtained from BD Biosciences (San Jose, CA, US). The FITC bovine lactadherin used for flow cytometry was obtained from Haematologic Technologies (Essex Junction, VA, US) and BioLegend (San Diego, CA, US), respectively. The mouse anti-human monoclonal IgG1 against VCAM-1 (1.G11B1) used for contrast-enhanced ultrasound (CEU) molecular imaging was obtained from Bio-Rad Antibodies (Hercules, CA, US).

4.4.3 *Generation of Anti-FXI Monoclonal Antibodies*

The anti-FXI monoclonal antibody, 1A6, was generated as previously described.[195] This antibody binds to the apple 3 domain of FXI, and blocks FXIIa-mediated activation of FXI as well as FXIa-mediated activation of FIX and FV. Note, although 1A6 does not inhibit feedback activation of FXI by thrombin, and thus does not block the generation of

FXIa, the downstream enzymatic action of FXIa on FIX in particular is eliminated. The humanized form of the antibody, h1A6 (BAY 1831865), was a generous gift from Bayer AG (Wuppertal, Germany).

4.4.4 *Nonhuman Primate (NHP) Model of Hyperlipidemia*

All rhesus macaque (*Macaca mulatta*) studies were approved by the Oregon Health & Science University Institutional Animal Care and Use Committee (IP00002332). The rhesus macaques were housed and cared for by the Oregon National Primate Research Center (ONPRC) at Oregon Health & Science University.

Adult male rhesus macaques were placed in lean (n=6) and obese (n=8) cohorts. The lean cohort was fed a standard diet (58% carbohydrates, 27% protein, and 15% fat by caloric content LabDiet 5L0P, Purina Mills), whereas the obese cohort was fed a high-fat diet (45% carbohydrates, 18% protein, and 36% fat by caloric content LabDiet 5L0P, Purina Mills) for an average of 7.6±1.6 years.

From the obese cohort, five rhesus macaques were administered the humanized anti-FXI monoclonal IgG 1A6 (h1A6) at 2mg/kg on day 0. This dose was selected based on prior works showing that 1A6 administered to a baboon at 2mg/kg inhibited >99% of FXI activity for at least 10 days.[195] Thus, to ensure maximal inhibition was maintained throughout a 28-day time course, we administered an additional maintenance dose of h1A6 (2 mg/kg) on day 14 following blood collection. Hematological analyses were performed at designated study intervals (**Supplemental Figure 4.1**).

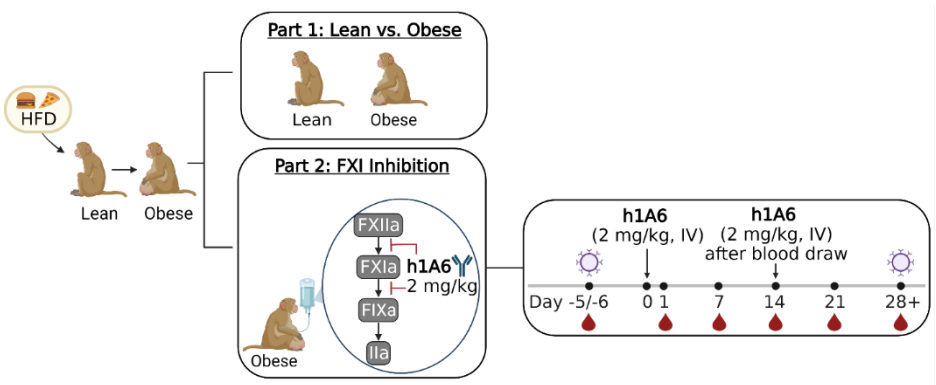

Supplemental Figure 4.1 Experimental design for nonhuman primate studies. The first part of this study compared adult male rhesus macaques were administered either a standard chow diet (n=6, lean) or a high-fat diet (n=8, obese). In the second part of this work, obese rhesus macaques (n=5) were administered the anti-FXI monoclonal IgG humanized 1A6 (h1A6) at 2 mg/kg intravenously. Contrast enhanced ultrasound imaging was performed at days -5/6 and 28+ relative to the first dose of h1A6. Hematological analyses were performed at designated study intervals.

4.4.5 *Blood Collection*

Blood Collection

Venous blood samples were collected by venipuncture into 3.2% sodium citrate or EDTA vacutainers prior to administration of h1A6 at time = 0 (day 0), and at days 1, 7, 14, 21, and 28 following h1A6 treatment. Platelet poor plasma (PPP) was obtained by centrifugation of whole blood for 10 min at 2000*g*, removal of the supernatant, and centrifugation of the remaining plasma for 10min at 2000*g*. Plasma samples that were not immediately used for analyses were banked at -80°C for batch testing.

4.4.6 *Hematological Analysis for Complete Blood Counts and Lipid Levels*

Whole blood samples were analyzed for lipid levels and complete blood counts by the Clinical Pathology Laboratory at the ONPRC using an ABX Pentra 400 Clinical Chemistry System (Horiba Medical, Irvine, CA, US).

4.4.7 *Plasma Clotting Assays and Quantification of Coagulation Factor Activation*

Clotting times were measured in PPP isolated from whole blood anticoagulated with 3.2% sodium citrate. In brief, PPP was incubated with activated partial thromboplastin time (aPTT) reagent for 3 min at 37°C. Clotting was initiated by the addition of $CaCl_2$ (25 mM) and measured using a KC4 Coagulation Analyzer (Bray, Co. Wicklow, Ireland). To measure the prothrombin time (PT), clotting of PPP was initiated by the equivolume addition of Dade Innovin reagent.

FXIIa-antithrombin (AT), FXIa-AT, and T-AT complexes were quantified in PPP isolated from whole blood anticoagulated with EDTA as described previously [2]. FXIIa-AT, FXIa-AT, and T-AT standards were prepared by incubating FXIIa (1µM) or FXIa (1µM) or thrombin (1µM) with antithrombin (5µM), EDTA (1mM) and heparin (5U/mL) for 2h at 37°C. Standards were defined as 1µM of protease-antithrombin complex.[196] Terminal complement complex (C5b-9) was quantified as described previously.[197]

4.4.8 *Flow Cytometry for Platelet Activity*

Platelet activation state was assessed by measuring α-granule secretion and phosphatidylserine (PS) expression by flow cytometry. Whole blood anticoagulated with 3.2% sodium citrate was diluted in modified HEPES-Tyrode buffer (1:4). Platelet P-selectin (CD62P) expression was used as a marker for α-granule secretion and was analyzed with an anti-CD62P PE (1:20) antibody at baseline or following stimulation with in the GPVI agonist CRP-XL (0.3, 1.0µg/mL), ADP (1.0, 3.0µM), or a PAR-1 agonist TRAP-6 (30, 100µM) for 20 min at 37°C. PS exposure on the membrane was used as a marker of a procoagulant platelet phenotype and analyzed with FITC bovine lactadherin (1:10) in the presence of a combination of CRP-XL (1.0µg/mL) and TRAP-6

(100µM). To stop reactions, samples were diluted with paraformaldehyde (2%). Flow cytometry was performed on a FACSCanto II (BD Biosciences, Franklin Lakes, NJ).

Data were analyzed using FlowJo software (version 10.7.1). To measure platelet activation, platelet populations were first identified by logarithmic signal amplification for forward and side scatter. Using a within-subject design, with each animal serving as its own control to minimize individual variations, data were presented as percentage of platelets expressing CD62P or PS on the membrane. Activated platelets on the surface of leukocytes were determined by quantifying staining for CD62P+ platelets in the leukocyte population.

4.4.9 *Hematological Analysis for Inflammatory Biomarkers*

NHP EDTA-plasma samples were analyzed for inflammatory biomarkers by the Endocrine Technologies Core (ETC) at the ONPRC. Plasma samples were analyzed for C-reactive protein using an ELISA kit (ALPCO, Salem, NH, US) following the manufacturer's instructions. The assay range was 0.95-150 ng/mL and intra-assay CV was 2.7%. The inter-assay CV for the C-reactive protein ELISA was 11.1%. Plasma samples were also analyzed for cathepsin D, myeloperoxidase, and soluble VCAM-1 using a custom Luminex panel (Millipore Sigma HNDG3MAG-36K, Burlington, MA). The analysis was performed following the manufacturer's instructions. Briefly, 25µL of each plasma sample was diluted in assay diluent and incubated overnight with antibody-coated, fluorescent-dyed capture microspheres specific for each analyte, followed by incubation with detection antibodies and streptavidin-phycoerythrin. Washed microspheres with bound analytes were resuspended in reading buffer and analyzed on a

Milliplex LX-200 Analyzer (EMD Millipore, Billerica, MA, US) bead sorter with XPonent Software version 3.1 (Luminex, Austin, TX, US). Data were calculated using Milliplex Analyst software version 5.1 (EMD Millipore). Intra-assay CVs were as follows: cathepsin D, 5.6%; MPO, 9.0%; sVCAM-1, 8.0%. Since all the samples were analyzed in a single assay, no inter-assay variation was calculated for this study.

4.4.10 *Nanoparticle Tracking Analysis*

Total particle concentrations in EDTA-plasma samples were measured by nanoparticle tracking analysis using the ZetaView PMX-420 instrument (Particle Metrix, Germany) according to manufacturer guidelines. The instrument was calibrated daily using 100nm alignment particles supplied by Particle Metrix. Plasma samples were diluted 10,000-fold in 0.1µm-filtered PBS. Settings of 70% camera sensitivity and 30 frame rate were selected based on manufacturer recommendations and maintained constant through all runs. Recorded concentrations were adjusted for dilution factor to obtain the particle concentration in the original undiluted plasma and expressed as particles per mL.

4.4.11 *Nanoscale Flow Cytometry of Extracellular Vesicles*

Nanoscale flow cytometry imaging and counting of stained extracellular vesicles (EVs) was performed as previously described.[198-200] Briefly, PPP was isolated from whole blood anticoagulated with EDTA and was obtained by centrifugation of whole blood for 10 min at 2500*g*, removal of the supernatant, and centrifugation of the remaining plasma for 10 min at 2500*g*. EVs were stained with an anti-CD62P APC (1:100), anti-CD41 FITC (1:500), anti-CD41 APC (1:2000), anti-CD9 PE (1:100), or anti-CD31 BV421 (1:1000) antibody for 1h at RT. Samples were then diluted 1:200 with 200 nm bead buffer (FACS

sorting 200 nm beads in PBS) to avoid coincident events and keep the abort rate under 10%. The 200 nm bead sample dilution buffer was used to provide both an internal relative size and volume of sample tested standard for all stained samples. Megamix (100-900 nm, GFP-labeled polystyrene beads) and molecules of equivalent soluble fluorophores (MESF) beads for each fluorophore conjugate were also used to standardize instrument settings. Flow cytometry was performed on a FacsAria Fusion (BD Biosciences, Haryana, India) with a ZenPure PureFlow Mini Capsule PES 0.1 µm filter (Manassas, Virginia, US).

Relative EV sizes were approximated by comparing EV side scatter with polystyrene beads and assuming the refractive index of small EVs is >1.5 and large EVs closer to 1.4. Positive antibody staining was used to distinguish EVs from other unlabeled, similarly sized nanoparticles (e.g. lipoproteins, non-specific cell fragments). The expression of $CD62P^{+}/CD41^{+}/CD9^{+}$ and $CD31^{+}/CD41^{-}$ expression were used as markers for EVs derived from activated platelet and endothelial, respectively. Stained PBS, conjugated isotype controls, and unstained plasma samples served as negative controls. Data were collected based on uniform 200 nm bead sample dilution buffer bead counts, which provided test volumes for each sample. Data were reported as gated events per microliter of starting plasma. The mean of duplicate experiments for each sample was employed for statistical analyses. Data were log transformed to adjust for geometric variance with the mean.

4.4.12 *Targeted Molecular Imaging Agent Preparation*

Lipid-shelled decafluorobutane microbubbles targeted to endothelial vascular cell adhesion molecule-1 (VCAM-1) were prepared as previously described.[177,179,201] Briefly,

the microbubbles were derived by sonicating a gas-saturated aqueous suspension of distearoylphosphatidylcholine (2mg/mL), polyoxyethylene-40-stearate (1mg/mL), and distearoylphosphatidylethanolamine-PEG (2000) biotin (0.4mg/mL). Targeting was achieved using a streptavidin bridge to conjugate a biotinylated anti-VCAM-1 antibody (1.G11B1) to the microbubble surface. The cross reactivity of the VCAM-1 antibody with macaque epitopes was evaluated by immunohistochemistry of banked spleen and carotid artery samples from animals that were fed a high-fat diet for two years [179]. Control microbubbles were unconjugated with no targeting ligand. Electrozone sensing was used to measure microbubble concentration and to ensure similar size distribution between the agents for each experiment (Multisizer III, Beckman-Coulter, Brea, CA, US).

4.4.13 *Contrast Enhanced Ultrasound (CEU) Molecular Imaging*

Contrast enhanced ultrasound (CEU) molecular imaging at the carotid bifurcation was used to measure endothelial VCAM-1 as a marker of endothelial cell activation before and after treatment with h1A6, as previously described.[177,179,201] In brief, we performed longitudinal-axis imaging at the carotid bifurcation using multi-pulse, contrast-specific imaging at 7 MHz, a mechanical index of 1.9, a dynamic range of 55 dB, and a frame rate of 1 Hz (Sequoia, Siemens Medical Imaging, Mountain View, CA, US). Microbubbles targeted to endothelial VCAM-1 (1×10^8) were intravenously injected and the ultrasound was paused for 1 min before locating the carotid artery. We located the carotid artery using 2-D ultrasound at low power (mechanical index <0.10) and activated contrast-specific imaging for several frames. The signal for retained microbubbles was quantified by taking a digital average of the first two frames acquired. To distinguish the signal from

microbubbles freely circulating, we subtracted several averaged frames that were acquired after >5 destructive pulse sequences (mechanical index 1.3). Data from regions-of-interest at the near and far walls of the common carotid artery were averaged.

4.4.14 *Statistical Analysis*

Data were tested for normality and sphericity using Shapiro-Wilk and F-tests. Two group data that were normally distributed with equal standard deviations were analyzed by an unpaired t-test. If the standard deviations were not equal, then Welch's correction was applied. Data that were not normally distributed were analyzed by a Mann-Whitney test. For three or more groups, normally distributed data were analyzed by a repeated measures one-way ANOVA with a Dunnett's post-hoc test. Data that were not normally distributed were analyzed by a Friedman test with a Dunn's post-hoc test. Statistical significance was considered for $P<0.05$. For all experiments, n indicates the number of independent experiments performed. Statistical analyses were performed using GraphPad Prism 9 (San Diego, CA, US).

4.5 Results

4.5.1 *Effects of Diet-induced Hyperlipidemia on Platelet Activity and Thrombin Generation*

We first sought to examine biomarkers of platelet activation and coagulation factor activation in a model of diet-induced hyperlipidemia. When platelets are activated, the contents of their granules, including P-selectin and ADP, which are stored in platelet alpha and dense granules, respectively, are translocated to the platelet surface.[175,183] Therefore, for both obese and lean cohorts, we quantified P-selectin expression at baseline as well as in response to subthreshold concentrations of platelet agonists that

signal downstream of immunotyrosine activation motif (ITAM)- or G-protein coupled receptor (GPCR)-linked receptors, GPVI or PAR-1, respectively (**Figure 4.1A-B, D**). While the baseline level of platelet activation was equivalent for both lean and obese cohorts, hyperlipidemia primed platelet activation in response to the GPVI agonist, CRP-XL, or PAR-1 agonist (TRAP-6), as evidenced by a substantial increase in platelet P-selectin expression observed in the obese cohort compare to the lean cohort at an equivalent dose of agonist. Platelet P-selectin expression in response to ADP was variable and insensitive to hyperlipidemia (**Figure 4.1C**).

When platelets become activated, intracellular signaling events facilitate phosphatidylserine (PS) exposure on the platelet surface. These processes confer a procoagulant scaffold for coagulation factors to assemble, a requisite step for thrombin generation and subsequent fibrin formation.[202,203] Thus, systemic platelet coagulability was measured by quantifying PS exposure in response to agonists that signal through GPVI and PAR-1. We found that agonist-induced PS expression levels were elevated in NHP platelets on a high-fat diet compared to platelets from NHPs on a standard chow diet (**Figure 4.1E**)**.** Taken together, these results confirm that hyperlipidemia increases the sensitivity of platelets for activation by either GPVI- or PAR-1 agonists.

We next examined the effect of hyperlipidemia on coagulation factor activity. We did not observe any differences in activated partial thromboplastin time (aPTT) or prothrombin time (PT) in plasma from the obese or lean cohorts (**Figure 4.2A-B**). The level of FXIIa-AT and T-AT complexes were insensitive to diet-induced hyperlipidemia (**Figure 2C, 2E**). However, when profiling the procoagulant phenotype of our obese NHP cohort, we found an increase in FXIa-AT complexes at baseline in the obese cohort (**Figure 4.2D)**.

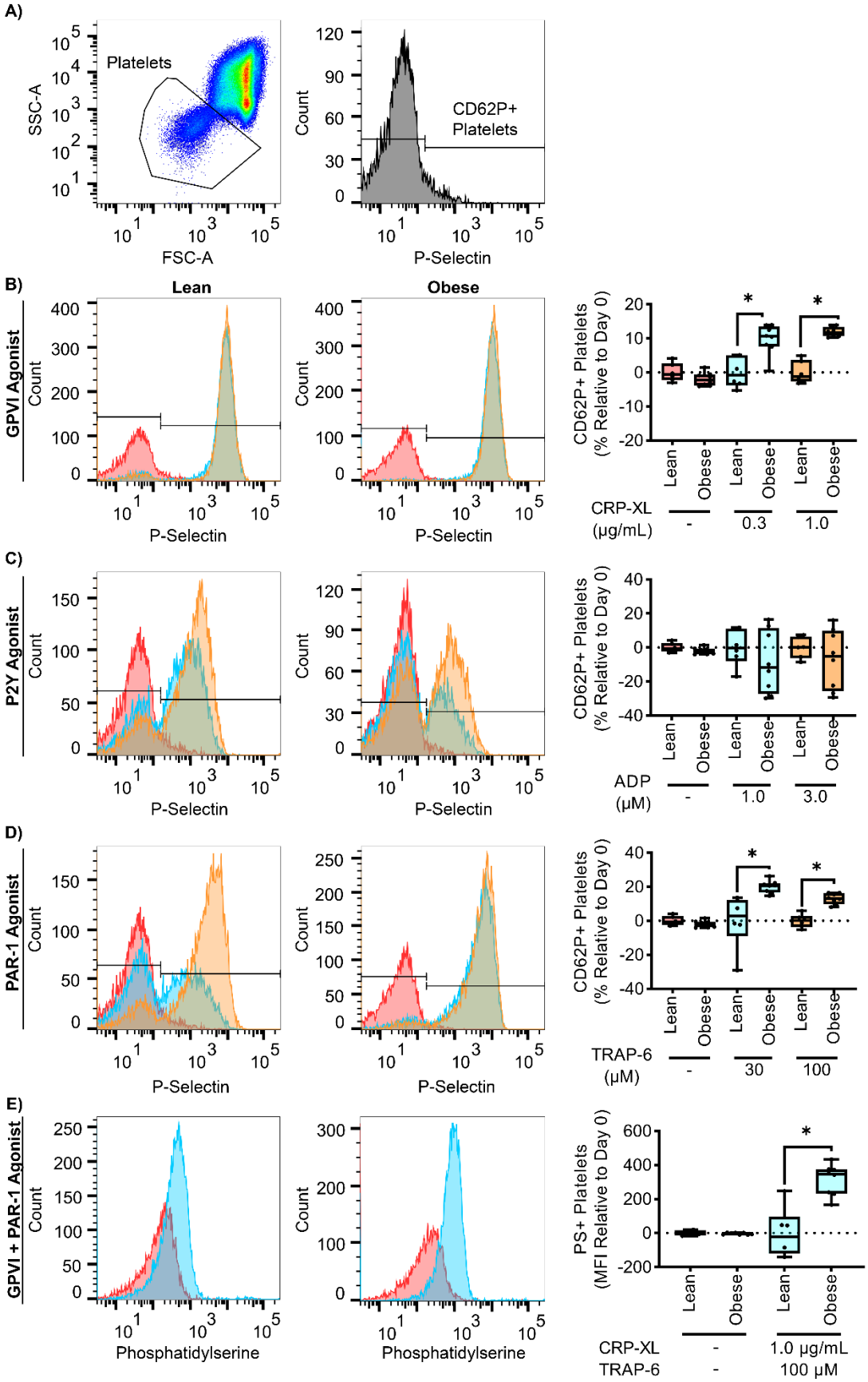
A)
Platelets
SSC-A
FSC-A
CD62P+
Platelets
Count
P-Selectin
B)
Lean
Obese
GPVI Agonist
Count
P-Selectin
CD62P+ Platelets
(% Relative to Day 0)
CRP-XL
(μg/mL)
-
0.3
1.0
C)
P2Y Agonist
ADP
(μM)
1.0
3.0
D)
PAR-1 Agonist
TRAP-6
(μM)
30
100
E)
GPVI + PAR-1 Agonist
Phosphatidylserine
PS+ Platelets
(MFI Relative to Day 0)
1.0 μg/mL
100 μM

Figure 4.1 Hyperlipidemia primes platelet activation by GPVI or PAR-1 agonists. The platelet population was identified using forward versus side scatter (FSC-A vs. SSC-A*)* gating (A). Whole blood samples from NHPs on a standard chow diet (n=6, lean) or NHPs on a high-fat diet (n=8, obese) were stained with an anti-CD62P PE antibody (B-D) or FITC bovine lactadherin (E). Samples were then stimulated with a GPVI agonist (0.3, 1.0 µg/mL), a P2Y agonist (1.0, 3.0 µM), or a PAR-1 agonist (30, 100 µM). Flow cytometry was used to measure platelet surface expression of P-selectin and phosphatidylserine (PS) as markers of platelet activation or coagulability, respectively. Statistical analyses were conducted using an unpaired t-test, Welch's t-test, or a Mann-Whitney test. Statistical significance is indicated by one asterisk (*) for $P<0.05$. Data are shown as mean ± SEM.

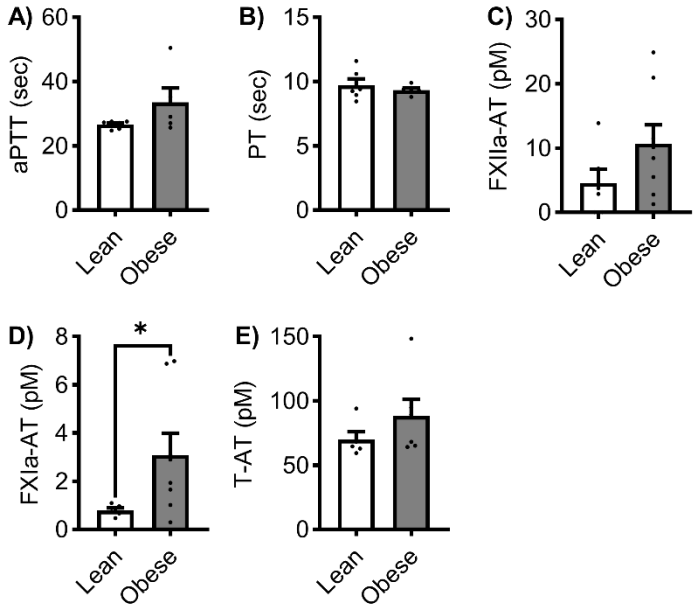

Figure 4.2 Levels of activated FXI were elevated in a model of hyperlipidemia. Platelet poor plasma (PPP) was isolated from NHPs on a standard chow diet (n=6, lean) or NHPs on a high-fat diet (n=8, obese). Clotting times were measured by incubating PPP with an aPTT reagent followed by $CaCl_2$ to initiate clot formation (A) or stimulating PPP with Dade Innovin reagent to measure prothrombin time (PT). Activated coagulation protease species, FXIIa-AT, FXIa-AT, and T-AT were measured using a custom ELISA (C-D). Statistical analyses were conducted using a Mann-Whitney test or an unpaired t-test. Statistical significance is indicated by one asterisk (*) for $P \leq 0.05$. Data are shown as mean ± SEM. aPTT, activated partial thrombospondin time; prothrombin time (PT).

4.5.2 *Effects of Diet-induced Hyperlipidemia on Inflammation*

Hematological analyses showed that relative to the lean controls, NHPs with diet-induced hyperlipidemia had significantly higher levels of hemoglobin, hematocrit, and red blood cells; interestingly, however, the obese NHPs showed a reduction in white blood cells (**Supplemental Table 4.1**). On biochemical analysis, obese NHPs also had elevated levels of alanine transaminase, chloride, total cholesterol, low-density lipoprotein and high-density lipoprotein relative to lean NHPs (**Supplemental Table 4.2**). These findings are in line with previous studies comparing lean versus obese NHPs [179,204].

Supplemental Table 4.1 Complete blood counts in a model of hyperlipidemia following FXI inhibition. Complete blood counts for lean (n=6) and obese (n=5) NHPs at baseline (day 0) and at days 1, 7, 14, 21, and 28+ following treatment with humanized 1A6 (h1A6). Statistical significance is indicated by one asterisk (*) for $P < 0.05$. One asterisk (*) is used to designate $P < 0.05$ for lean NHPs versus obese NHPs at day 0. One dagger (†) is used to designate $P < 0.05$ for obese NHPs at day 0 versus days 1, 14, 21, or 28. Note, neutrophils in obese NHPs at day 0 were not compared to day 7 measurements due to an insufficient number of samples at day 7 (n=1). Data are presented as mean ± SEM. NHP, nonhuman primate; WBC, white blood cell; HGB, hemoglobin; HCT, hematocrit; RBC, red blood cell; PLT, platelet; MCV, mean corpuscular volume; MCH, mean corpuscular hemoglobin; MCHC, mean corpuscular hemoglobin concentration; RDW, red cell distribution width; MPV, mean platelet volume.

	Lean NHPs	**Obese NHPs + h1A6 (2 mg/kg)**					
		0	**1**	**7**	**14**	**21**	**28**
WBC (k/μ)	5.8 ± 0.5	4.0 ± 0.3 *	6.5 ± 0.2 †	5.6 ± 0.5	6.0 ± 0.5	6.4 ± 0.6	4.9 ± 0.1
HGB (k/μ)	13.4 ± 0.3	15.3 ± 0.5 *	15.2 ± 0.4	15.9 ± 0.3	15.0 ± 0.4	15.0 ± 0.4	14.6 ± 0.3
HCT (k/μ)	40.9 ± 0.9	46.5 ± 1.5 *	46.7 ± 1.3	47.6 ± 0.5	45.6 ± 1.0	46.2 ± 1.2	44.7 ± 0.8
RBC (k/μ)	5.55 ± 0.13	6.17 ± 0.15 *	6.22 ± 0.14	6.32 ± 0.00	6.06 ± 0.09	6.13 ± 0.11	5.96 ± 0.09
Lymphocyte (k/μ)	2.37 ± 0.38	1.48 ± 0.18	3.75 ± 0.23 †	3.25 ± 0.11	3.00 ± 0.44	3.51 ± 0.47 †	2.12 ± 0.12
Monocyte (k/μ)	0.29 ± 0.05	0.24 ± 0.03	0.41 ± 0.08	0.28 ± 0.05	0.44 ± 0.07 †	0.40 ± 0.06	0.34 ± 0.06
Neutrophil (k/μ)	2.99 ± 0.31	2.21 ± 0.32	2.15 ± 0.27	1.68	2.37 ± 0.34	2.27 ± 0.22	2.24 ± 0.14
Eosinophil (k/μ)	0.11 ± 0.03	0.11 ± 0.04	0.20 ± 0.10	0.38 ± 0.19	0.19 ± 0.10	0.24 ± 0.12	0.14 ± 0.07
Basophil (k/μ)	0.03 ± 0.01	0.02 ± 0.00	0.05 ± 0.01	0.04 ± 0.00	0.02 ± 0.01	0.04 ± 0.01	0.02 ± 0.00
PLT (k/μ)	310 ± 23	311 ± 32	355 ± 30	241 ± 55	350 ± 25	327 ± 48	355 ± 28 †
MCV (fL)	74 ± 1	75 ± 1	75 ± 1	76 ± 1	75 ± 1	75 ± 1	75 ± 1
MCH (pg)	24.2 ± 0.4	24.7 ± 0.4	24.4 ± 0.3	25.1 ± 0.4	24.7 ± 0.3	24.5 ± 0.4	24.5 ± 0.3
MCHC (g/dL)	32.7 ± 0.1	32.8 ± 0.1	32.6 ± 0.2	33.3 ± 0.2	32.9 ± 0.1	32.5 ± 0.2	32.7 ± 0.1
RDW (%)	12.8 ± 0.1	12.9 ± 0.3	12.7 ± 0.3	12.5 ± 0.3	12.6 ± 0.3	12.7 ± 0.4	12.6 ± 0.3 †
MPV (fL)	9.2 ± 0.3	8.8 ± 0.3	8.8 ± 0.3	9.6 ± 0.3	8.8 ± 0.2	9.2 ± 0.5	8.8 ± 0.3

Supplemental Table 4.2 Lipid profiles and metabolic changes in the setting of hyperlipidemia following FXI inhibition. Chemistry panels for lean (n=6) and obese (n=5) NHPs at baseline (day 0) and at days 1, 7, 14, 21, and 28 following treatment with humanized 1A6 (h1A6). One asterisk (*) is used to designate $P < 0.05$ for lean NHPs versus obese NHPs at day 0. One dagger (†) is used to designate $P < 0.05$ for obese NHPs at day 0 versus days 1, 7, 14, 21, or 28. Data are presented as mean ± SEM. NHP, nonhuman primate; ALKP, alkaline phosphatase; ALT, alanine transaminase; AST, aspartate aminotransferase; GCT, glucose challenge test; BUN, blood urea nitrogen; LDL, low-density lipoprotein; HDL, high-density lipoprotein.

	Lean NHPs	**Obese NHPs + h1A6 (2 mg/kg)**					
		0	**1**	**7**	**14**	**21**	**28**
Total Protein (g/dL)	6.5 ± 0.2	6.7 ± 0.2	6.9 ± 0.2	7.3 ± 0.2	7.2 ± 0.1	7.3 ± 0.1 †	7.0 ± 0.1
Albumin (g/dL)	4.0 ± 0.1	3.7 ± 0.1	4.0 ± 0.1	4.0 ± 0.1	4.0 ± 0.1	3.9 ± 0.1	4.0 ± 0.1
ALKP (U/L)	178 ± 35	87 ± 9	88 ± 6	90 ± 7	97 ± 11	90 ± 9	86 ± 7
ALT (U/L)	25 ± 4	92 ± 15 *	98 ± 13	87 ± 14	93 ± 13	89 ± 13	74 ± 9
AST (U/L)	40 ± 2	47 ± 4	47 ± 6	32 ± 6 †	44 ± 5	36 ± 4	40 ± 5
GGT (IU/L)	51 ± 4	65 ± 6	65 ± 7	62 ± 7	65 ± 6	62 ± 6	60 ± 5
Total Bilirubin (mg/dL)	0.18 ± 0.01	0.20 ± 0.03	0.28 ± 0.08	0.19 ± 0.04	0.17 ± 0.02	0.21 ± 0.03	0.17 ± 0.02
Glucose (mg/dL)	50 ± 4	62 ± 13	86 ± 13	99 ± 17 †	71 ± 16	93 ± 16	60 ± 10
BUN (mg/dL)	16.2 ± 0.5	14.0 ± 0.8	14.0 ± 1.6	13.2 ± 0.8	13.8 ± 0.9	12.6 ± 0.9	12.4 ± 0.8
Creatine (µmol/L)	0.8 ± 0.0	0.9 ± 0.1	0.8 ± 0.1	0.8 ± 0.0	0.8 ± 0.1	0.8 ± 0.0	0.9 ± 0.1
Potassium (mmol/L)	3.6 ± 0.1	3.7 ± 0.1	3.7 ± 0.1	4.1 ± 0.1	4.1 ± 0.1	4.2 ± 0.1	3.7 ± 0.1
Sodium (mmol/L)	144 ± 0	145 ± 1	144 ± 1	143 ± 0	145 ± 0	144 ± 1	145 ± 1
Chloride (mmol/L)	104 ± 1	109 ± 1 *	107 ± 1	107 ± 1	108 ± 1	107 ± 1	109 ± 1
Magnesium (mg/dL)	1.7 ± 0.1	1.6 ± 0.1	1.8 ± 0.0	1.8 ± 0.1	1.7 ± 0.0	1.7 ± 0.0	1.6 ± 0.1
Phosphate (mg/dL)	4.8 ± 0.2	4.2 ± 0.2	5.4 ± 0.4	4.7 ± 0.3	4.4 ± 0.3	4.4 ± 0.3	4.3 ± 0.3
Cholesterol (mg/dL)	116 ± 7	280 ± 47 *	274 ± 35	273 ± 43	272 ± 40	279 ± 41	283 ± 39
LDL (mg/dL)	58 ± 6	160 ± 43 *	147 ± 31	144 ± 37	144 ± 34	145 ± 35	156 ± 35
HDL (mg/dL)	60 ± 5	105 ± 10 *	110 ± 12	102 ± 12	105 ± 11	110 ± 13	117 ± 12
Triglycerides (mg/dL)	48 ± 9	142 ± 57	174 ± 62	236 ± 85 †	207 ± 69	203 ± 69	147 ± 43

4.5.3 *Effects of Diet-induced Hyperlipidemia on Inflammation*

Systemic inflammation is a hallmark of hyperlipidemia and is accompanied by the upregulation of cytokines and the release of growth factors.[205,206] Accordingly, we measured inflammatory markers known to contribute to plaque instability and the inflammatory tone of atherosclerotic lesions. Confirming the findings from our previous study where NHPs were transitioned to a high-fat diet,[179] an increase in plasma levels of C-reactive protein levels were observed in the obese cohort as compared to the lean animals (**Figure 4.3A**). Cathepsin D and myeloperoxidase levels also increased in obese NHPs compared to lean NHPs (**Figure 4.3B-C**). Complement activation, as measured by

levels of C5b-9 soluble terminal complement complex, was elevated in in the setting of hyperlipidemia (**Figure 4.3D**). While the release of extracellular vesicles (EVs) is reflective of a pro-inflammatory state, we did not observe any differences in total EV or endothelial ($CD31^{+}/CD41^{-}$) or activated platelet ($CD62P^{+}/CD41^{+}/CD9^{+}$) EV subset particle count between obese and lean cohorts (**Figure 4.3E-G**). These data confirmed that hyperlipidemia increased select markers of inflammation, including C-reactive protein, and the complement system in our NHP model.

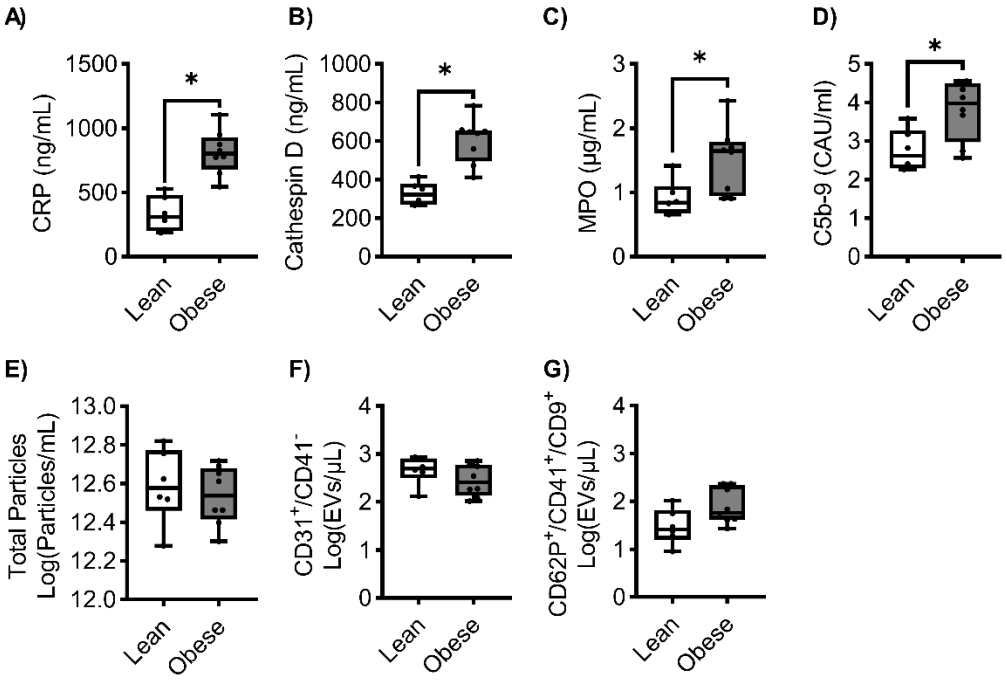

Figure 4.3 Diet-induced hyperlipidemia increased markers of systemic inflammation. Platelet poor plasma (PPP) samples were isolated from NHPs on a standard chow diet (n=6, lean) or NHPs on a high-fat diet (n=8, obese). Plasma levels of C-reactive protein (A), cathepsin D (B), myeloperoxidase (C), and C5b-9 (D) in NHPs on a standard chow diet (n=6, lean) or NHPs on a high-fat diet (n=8, obese) were measured. For the analysis of extracellular vesicles, we measured total particle concentration (E), endothelial EVs (F), or platelet EVs (G). Statistical analyses were conducted using an unpaired t-test, Welch's test, or a Mann-Whitney test. Statistical significance is indicated by one asterisk (*) for $P<0.05$. Data are shown as mean ± SEM.

4.5.4 *Effects of Pharmacological Targeting of FXI on the Thromboinflammatory Phenotype of Hyperlipidemia*

As hyperlipidemia was associated with an increase in circulating markers of FXI activation in our model, we evaluated whether pharmacological targeting of FXI would provide an antiplatelet and anti-inflammatory benefit. We first confirmed that aPTT clotting times were increased following treatment of obese primates with the anti-FXI antibody, h1A6, which inhibits FXI activation by FXIIa as well as FIX and FV activation by FXIa (**Figure 4.4A**). Conversely, h1A6 did not affect PT clotting times, confirming that this antibody does not affect the extrinsic pathway coagulation (**Figure 4.4B**). Along these lines, h1A6 was unable to reduce the degree of activated FXIa in the obese primate cohort, in line with the fact that this antibody does not prevent thrombin-mediated activation of FXI (**Figure 4.4C**). Likewise, we did not observe a reduction in T-AT levels in the presence of h1A6 (**Figure 4.4D**).

We next examined the effect of FXI inhibition on platelet reactivity in our model of hyperlipidemia. As seen in **Figures 4.5A** and **4.5C**, the increase in P-selectin expression in responses to GPVI or PAR-1 agonists was diminished after one day of treatment with the FXI antibody, h1A6, relative to baseline (day 0). These findings suggest that the sensitization of platelets for activation in the setting of hyperlipidemia was reversed by a FXI inhibitor. Yet, this inhibitory effect was only seen at the 24h timepoint, while changes in PS exposure at 24h in the presence of the FXI mAb h1A6 were not statistically significant (**Figure 4.5D**). Platelet P-selectin expression in response to ADP stimulation remained varied and was largely insensitive to the presence of hA16 (**Figure 4.5B**).

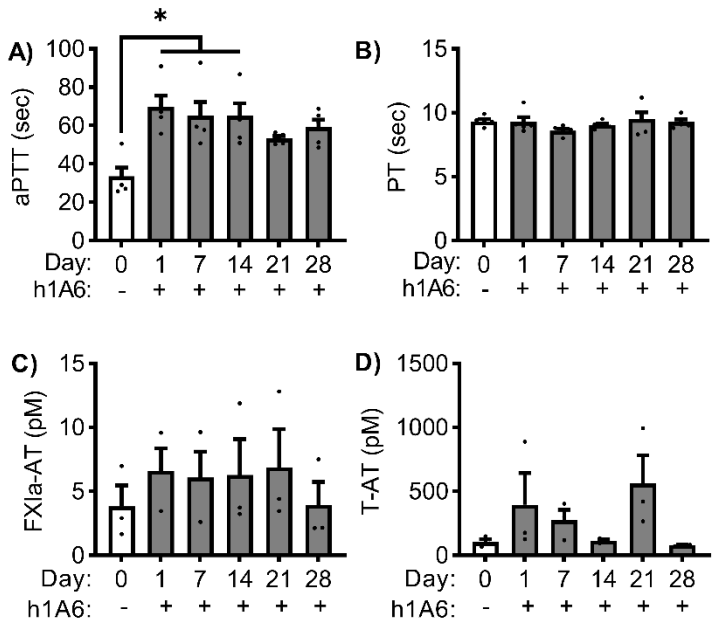

Figure 4.4 FXI inhibition prolonged aPTT clotting times in a model of hyperlipidemia. Platelet poor plasma (PPP) was isolated from NHPs on a high-fat diet (n=5) treated with a FXI function-blocking antibody. Clotting times were measured by incubating PPP with an aPTT reagent followed by $CaCl_2$ to initiate clot formation (A) or stimulating PPP with Dade Innovin reagent to measure PT (B). Activated coagulation protease species, FXIa-AT and T-AT, were measured using a custom ELISA (C-D). Statistical analyses were conducted using a Friedman test with a Dunn's post-hoc test or a repeated measures one-way ANOVA with a Dunnett's post-hoc test. Statistical significance is indicated by one asterisk (*) for $P \leq 0.05$. Data are shown as mean ± SEM.

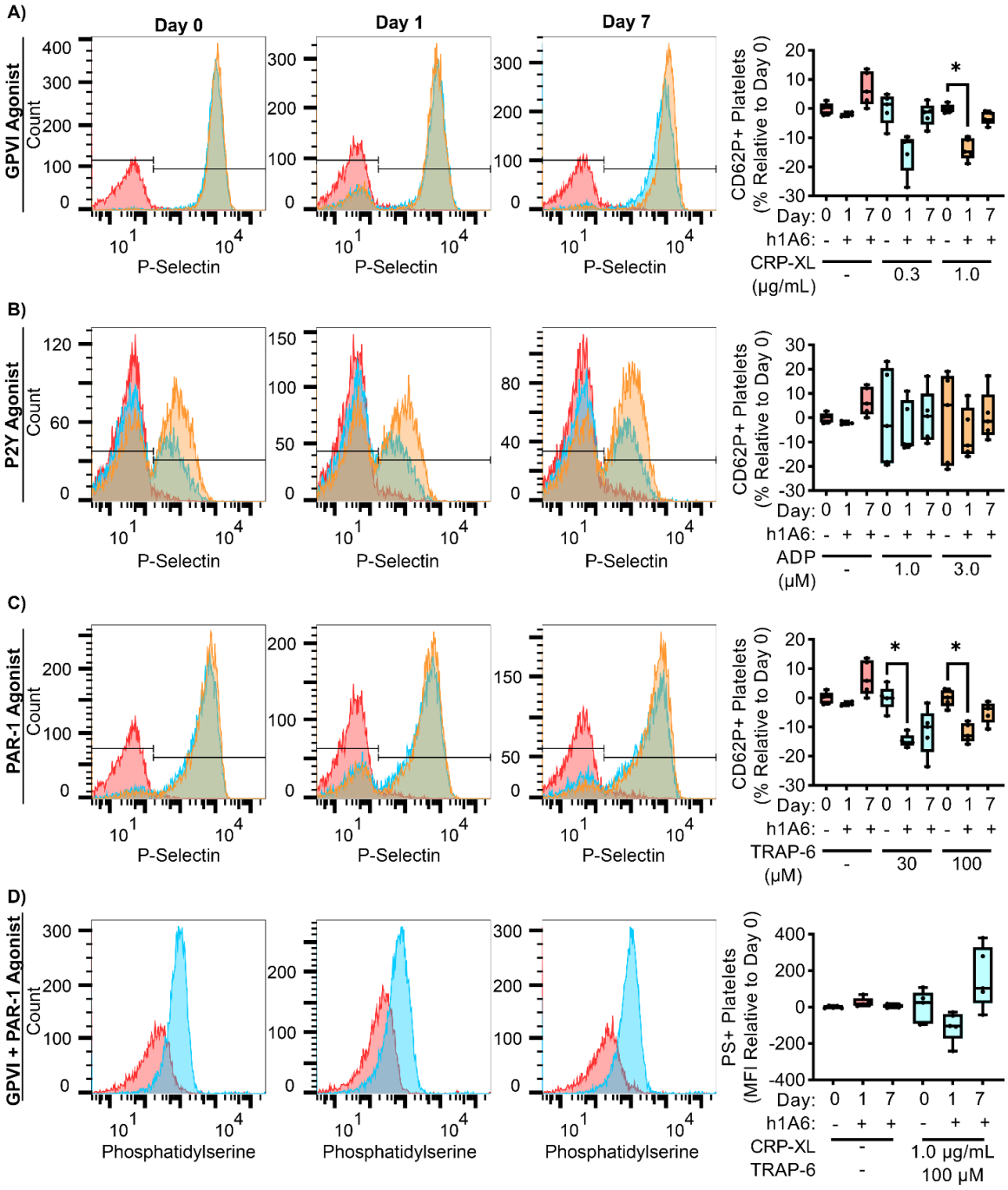

Figure 4.5 The sensitization of platelets for activation by GPVI or PAR-1 agonists in the setting of hyperlipidemia was reversed following treatment with a FXI inhibitor. The platelet population was identified using forward versus side scatter (*FSC-A vs. SSC-A*) gating (A). Whole blood samples from NHPs on a high-fat diet (n=5) were stained with an anti-CD62P PE antibody (B-D) or FITC bovine lactadherin (E). Samples were then stimulated with a GPVI agonist (0.3, 1.0 µg/mL), a P2Y agonist (1.0, 3.0 µM), or a PAR-1 agonist (30, 100 µM). Flow cytometry was used to measure platelet surface

expression of P-selectin and phosphatidylserine (PS) as markers of platelet activation or coagulability, respectively. Statistical analyses were conducted using a a mixed-effects analysis with Geisser-Greenhouse correction or a Friedman test with a Dunn's post-hoc test. Statistical significance is indicated by one asterisk (*) for $P<0.05$. Data are shown as mean ± SEM.

Additional hematological analyses showed that there was a significant increase in white blood cells and lymphocytes after one day of treatment with the FXI antibody, h1A6, relative to baseline (day 0). This was followed by later increases in monocytes, platelets, red cell distribution width, glucose, and triglycerides, and a decrease in aspartate aminotransferase at day 7 (**Supplemental Tables 4.1-4.2**). However, note that there were substantial variations in these markers over the study period.

We next evaluated if pharmacological targeting of FXI would reduce the inflammatory phenotype observed in our diet-induced obese primate cohort. Akin to our observations that a function blocking anti-FXI mAb reduced C-reactive protein levels in end-stage renal disease patients on dialysis,[194] we observed a decrease in C-reactive protein levels after three and continuing to four weeks relative to baseline (day 0) of treatment with the anti-FXI mAb, h1A6 (**Figure 4.6A**). Yet, we did not observe any additional effects of FXI therapy on the elevated plasma levels of cathepsin D, myeloperoxidase, or C5b-9 soluble terminal complement complex nor levels of platelet- or endothelial cell-derived EVs found in this model of hyperlipidemia (**Figure 4.6B-G**).

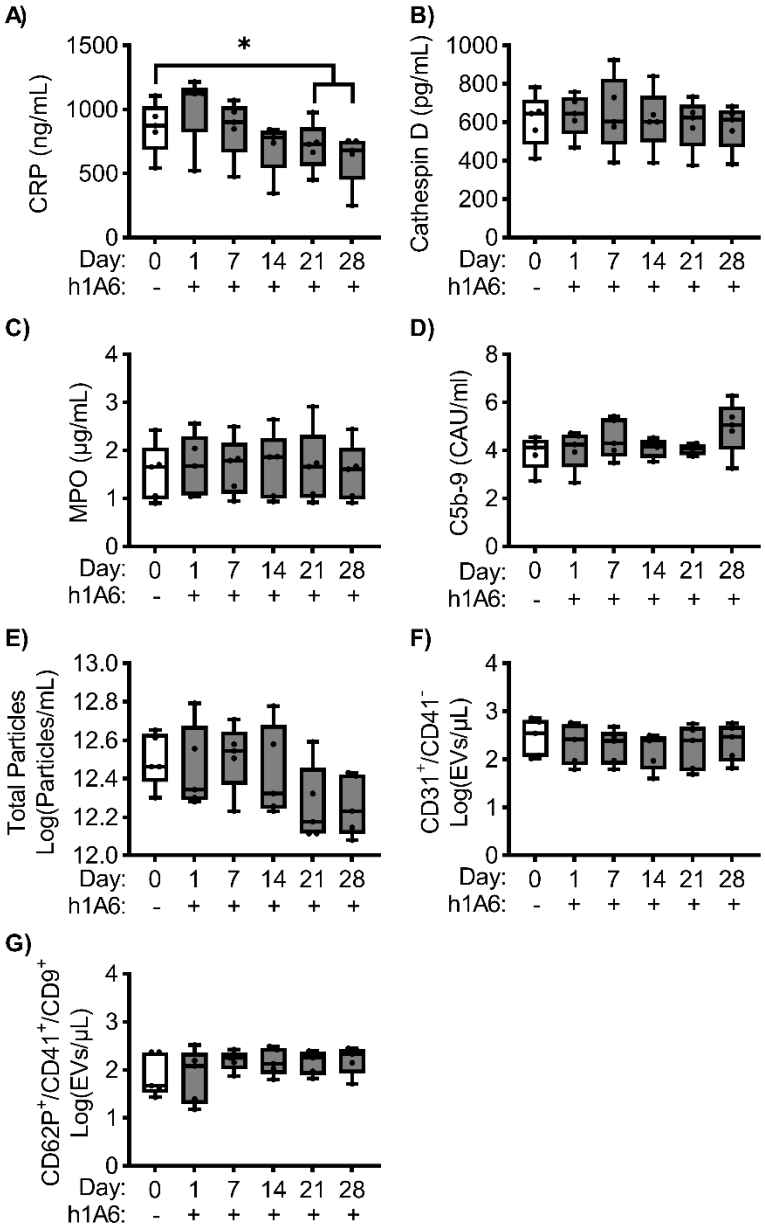

Figure 4.6 FXI inhibition prevented the increase in C-reactive protein levels in a model of hyperlipidemia. Platelet poor plasma (PPP) was isolated from NHPs on a high-fat diet (n=5) treated with a FXI function-blocking antibody. Plasma levels of C-reactive protein (A), cathepsin D (B), myeloperoxidase (C), and C5b-9 (D) in NHPs on a high-fat diet (n=5) treated with a FXI function-blocking antibody were measured. For the analysis of extracellular vesicles, we measured total particle concentration (E), endothelial EVs (F), or platelet EVs (G). Data presented at Day 0 served as the baseline for comparison, allowing us to establish a reference point for evaluating the effects of FXI inhibition. Statistical analyses were conducted using a repeated measures one-way ANOVA with a

Dunnett's post-hoc test or a Friedman test with a Dunn's post-hoc test. Statistical significance is indicated by one asterisk (*) for $P<0.05$. Data are shown as mean ± SEM. CRP, C-reactive protein; MPO, myeloperoxidase; EV, extracellular vesicle.

4.5.5 *Effects of Pharmacological Targeting of FXI on Endothelial Inflammatory Markers*

Endothelial cell dysfunction is one of the hallmarks of hyperlipidemia leading to atherosclerosis. This is recapitulated in the primate model of hyperlipidemia used in the current study; we have previously shown that NHPs on a high-fat diet have increased expression of endothelial cell vascular cell adhesion molecule-1 (VCAM-1) compared to NHPs on a standard-chow diet.[179] Using a non-invasive molecular imaging technique to quantify local VCAM-1 expression at the carotid bifurcation, we confirmed that obese primates were characterized by a positive though variable increase in endothelial cell VCAM-1 expression levels at baseline. When evaluated following four weeks of treatment with the anti-FXI mAb, h1A6, we found an absence of VCAM-1 signal (**Figure 4.7A**). Congruent with prior studies showing that diet-induced obesity induced a reduction in soluble levels of VCAM-1 as compared to lean animals,[179] presumably due to the fact that VCAM-1 remains endothelial cell surface associated in the setting of chronic inflammation,[207] we found a decrease in circulating VCAM-1 levels in our hyperlipidemic cohort as compared to our lean cohort. Yet, the anti-FXI mAb, h1A6, was unable to reverse this trend in sVCAM-1 levels, suggesting that using sVCAM-1 as a biomarker is unable to detect the ability of pharmacological targeting of FXI to acutely pacify endothelial cell VCAM-1 levels (**Figure 4.7B**).

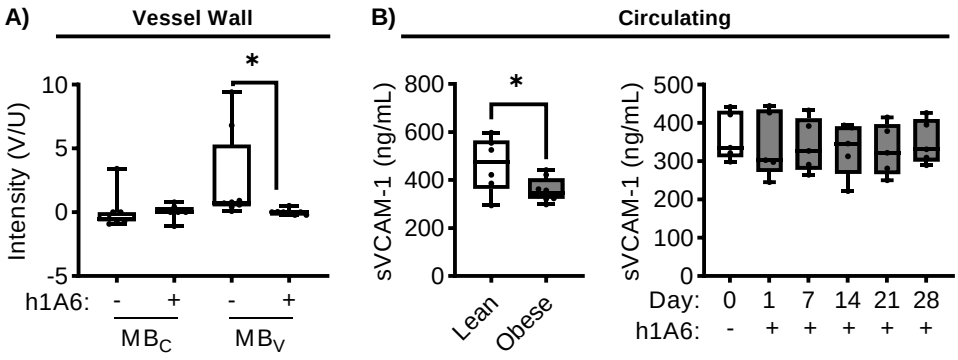

Figure 4.7 Treatment with a FXI inhibitor reduced VCAM-1 expression at the inflamed vessel wall surface in the setting of hyperlipidemia. We used a non-invasive ultrasound-based molecular imaging technique to measure VCAM-1 expression at the vessel wall surface as a marker of local activation in NHPs on a high-fat diet (n=5) treated with a FXI function-blocking antibody Data are presented as box and whisker plots showing the background subtracted video intensity for control (MB_C) and VCAM-1-targeted (MB_V) microbubbles (A). Systemic activation was determined by measuring circulating levels of VCAM-1 (sVCAM-1) in both NHPs on a standard chow diet (lean) and NHPs on a high-fat diet (obese) treated with a FXI function-blocking antibody (B). Statistical analyses were conducted using a Wilcoxon test, an unpaired t-test, or a Friedman test with a Dunn's post-hoc test. Statistical significance is indicated by one asterisk (*) for $P<0.05$. Data are shown as mean ± SEM.

4.6 Discussion

This study investigated the role of FXI in sustaining thromboinflammation associated with chronic hyperlipidemia. Using a function blocking antibody that prevented FXI activation by FXIIa as well as FIX and FV activation by FXIa, we found that pharmacological targeting of FXI reduced the levels of C-reactive protein, platelet reactivity to activation by GPVI and PAR-1 agonists, and endothelial cell activation as measured by VCAM-1 levels. These data suggest that the therapeutic effects of targeting FXI may extend beyond anticoagulation and include antiplatelet and anti-inflammatory benefit.

Herein, we observed a selective reduction in markers of inflammation in a NHP model of diet-induced hyperlipidemia. Indeed, we found that the elevated C-reactive protein levels in an obese NHP cohort were reduced by a ~25% following 4-weeks of anti-FXI therapy. These results are consistent with the findings of Lorentz *et al*., which reported that administration of the anti-FXI antibody, AB023, decreased C-reactive protein levels and also attenuated T-AT levels in end-stage renal disease patients on hemodialysis.[194] Along these lines, preliminary results from our clinical trial evaluating FXI inhibition for prevention of catheter-associated thrombosis also found that treatment with AB023 blunted the increased levels of C-reactive protein as well as T-AT levels following central line placement.[208] The efficacy of FXI inhibition observed in those studies may be in part attributed to the mechanism-of-action by which medical devices activate FXII to initiate thrombin generation in a FXI-dependent manner. The mechanism-of-action of the procoagulant and inflammatory phenotype observed in the setting of hyperlipidemia is perhaps multifaceted and includes several inciting factors, including tissue factor (TF) expressed on inflamed endothelium and circulating leukocyte or EVs. Along the lines of T-AT levels being insensitive to FXI inhibition in this model, the markers of activated leukocytes including elevated levels of cathepsin D and MPO observed in the obese NHP cohort were not affected by treatment with the anti-FXI antibody. It appears that FXI inhibition was unable to reduce the baseline levels of procoagulant and select inflammatory activity in this model of hyperlipemia.

While C-reactive protein is a useful biomarker for inflammation, the either direct or indirect mechanisms by which C-reactive protein levels are regulated or related to FXIa activity remain to be defined. Perhaps a partial explanation lies in the crosstalk between

FXI, inflammation, and the complement cascade. Indeed, we have previously shown that FXIa neutralizes complement factor H (CFH) by specific cleavage of the R341/R342 bonds, leading to enhanced cleavage of complement components, including C3b.[143] This may in part explain why inhibiting either FXI or FXII activation in a baboon model of systemic inflammatory response syndrome prevented complement activation including C3b and C5b-9.[2,142] As CFH is known to bind C-reactive protein to attenuate its proinflammatory activity,[209] perhaps inhibiting FXI with h1A6 disturbed the crosstalk between CFH and C-reactive protein, as well as activation of the complement cascade. Taken together, the reduction in C-reactive protein levels may represent both a biomarker, as well as a mechanism, for the anti-inflammatory effects observed following the blockade of FXI. Additionally, platelet inhibitors (e.g. clopidogrel and eptifibatide) have been shown to provide an anti-inflammatory benefit in patients, including the reduction of C-reactive protein levels [210]. It may be that the antiplatelet effects of FXI inhibition likewise cause a reduction in inflammatory markers, including C-reactive protein.

By way of accelerating and propagating thrombin generation, we have shown that FXI promotes platelet activation and single platelet consumption in shear flow.[211] For instance, in a NHP model of thrombus formation on a collagen-coated vascular graft, we found that pharmacological inhibition of FXIa activation of FIX with h1A6 reduced single platelet consumption in the bloodstream distal to a site of thrombus formation.[211] This mechanism was conserved in a baboon model of systemic inflammatory response syndrome, where inhibition of FXI activation by FXIIa prevented *Staphylococcus aureus*-induced platelet and fibrinogen consumption.[52] Along these lines, the current

study demonstrates that pharmacological targeting FXI with h1A6 reduced platelet reactivity, as measured by expression of P-selectin in response to GPVI and PAR-1 agonists, in a NHP model of hyperlipidemia. Given the variable expression of platelet P-selectin in response to a P2Y1 agonist, future studies may benefit from measuring additional markers of platelet activation (e.g. GPIIb/IIIa). It is important to highlight that while the interaction of FXIa with the platelet surface may induce an allosteric modulation of FXIa, our previous experiments demonstrate that these anti-FXI monoclonal antibodies do not exhibit any observable effects on FXI-platelet binding or activation.[212-214] Moreover, since platelets provide a procoagulant surface to amplify and propagate thrombin generation, perhaps pharmacological targeting of FXI produces an antiplatelet benefit via both direct and indirect means.

By serving to facilitate adhesion and transmigration of inflammatory cells to sites of endothelial cell damage or dysfunction, VCAM-1 represents both a proinflammatory biomarker and perhaps even a therapeutic target for vascular diseases including atherosclerosis. Endothelial cell VCAM-1 expression is known to be induced by angiotensin II and thrombin.[215,216] More recently, Kossman *et al*. described a role for thrombin-mediated FXI activation in potentiating vascular inflammation and dysfunction in a rodent model of arterial hypertension.[216] Moreover, while FXIa can directly bind and be internalized by the vascular endothelium,[217] there may be signaling mechanisms downstream that depend on FXIa beyond its role in amplifying thrombin generation. Indeed, endothelial cell inactivation of FXIa may indirectly regulate endothelial barrier function by way of activation of the membrane-bound metalloproteinase, ADAM10. This proposed mechanism may explain our prior observation that pharmacological targeting of

FXI preserved endothelial barrier function in a murine model of atherogenesis [138], and herein reducing endothelial cell VCAM-1 expression in non-human primate model of hyperlipidemia associated with early atherosclerosis.

To evaluate coagulation activation, we measured aPTT, PT, FXIIa-AT, FXIa-AT and T-AT complexes. Following treatment with h1A6, we observed prolonged aPTT clotting times up to day 14 post-treatment. Despite the maintenance dose of h1A6 following the day 14 blood draw and the unexplained elevation in T-AT levels at day 21, the aPTT prolongation did not reach statistical significance on days 21 and 28. This inconsistency may be attributed to an usually high aPTT measured for one of the animals in the day 0 group. Unfortunately, due to limited sample volume, we were not able to measure additional serine-protease complexes. It is worth noting that we specifically chose to measure FXIa-AT complexes due to their longer half- compared to other inhibitory complexes (e.g. C1-esterase inhibitor, alpha-1-antitrypsin and alpha 2-antiplasmin) and based on our prior experience measuring FXIa-AT in NHP plasma.[2,142] Although our findings provide insights into the role of FXIa activity in the setting of diet-induced hyperlipidemia, future work would benefit from assessing downstream effects of FXIa activity, including the activation of FIX as measured by FIX-AT levels.

Our study has several limitations. One of the limitations is that this work was designed as a composite study comprised of two parts- one comparing lean versus obese NHPs and the second examining the effect of inhibiting FXI. This experimental design choice was largely due to a scarcity of resources available to study NHP models of hyperlipidemia. Thus, the small sample size did not allow us to evaluate inhibition of FXI in the lean cohort, nor account for sex or age as biological variables. Indeed, only male NHPs were

used in these studies, as nonhuman primates are recognized by the National Institute of Health as an “acutely scarce resource”, with females being prioritized for breeding. Additionally, NHPs in the lean cohort were significantly younger on average than NHPs in the obese cohort (8.2 vs.18.6 years, $P<0.0001$). An additional limitation of this study is the use of a single pharmacological agent, h1A6, for these studies. As FXIa has been shown to act on substrates involved in the regulation of inflammation, platelet activation, barrier function and the immune response, a comprehensive understanding of the role of FXI in hyperlipidemia-induced thromboinflammation will require use of additional tools including reducing FXI levels and targeting the active site of FXIa. Even taking these limitations into account, our findings indicate that FXI may represent a safe therapeutic target to quell the thromboinflammatory mechanisms that promote atherogenesis.

Chapter 5. Pharmacological targeting of coagulation factor XI attenuates experimental autoimmune encephalomyelitis in mice

Tia C.L. Kohs, Meghan E. Fallon, Ethan C. Oseas, Laura D. Healy, Xiaolin Yu, Erik I. Tucker, Owen J.T. McCarty, David Gailani, Halina Offner-Vandenbark, and Norah G. Verbout

This work was originally published by Springer Nature.

Metabolic Brain Disease, 2023: in Press

Reprinted with permission

5.1 Abstract

Multiple sclerosis (MS) is the most common disabling neurological disorder in young adults worldwide. MS pathophysiologies include the formation of inflammatory lesions, axonal damage and demyelination, and blood brain barrier (BBB) disruption. Coagulation proteins, including factor (F)XII, can serve as important mediators of the adaptive immune response during neuroinflammation. Indeed, plasma FXII levels are increased during relapse in relapsing-remitting MS patients, and previous studies showed that reducing FXII levels was protective in a murine model of MS, experimental autoimmune encephalomyelitis (EAE). Our objective was to determine if pharmacological targeting of FXI, a major substrate of activated FXII (FXIIa), improves neurological function and attenuates CNS damage in the setting of EAE. EAE was induced in male mice using murine myelin oligodendrocyte glycoprotein peptides combined with heat-inactivated

Mycobacterium tuberculosis and pertussis toxin. Upon onset of symptoms, mice were treated every other day intravenously with anti-FXI antibody, 14E11, or saline. Disease scores were recorded daily until euthanasia for *ex vivo* analyses of inflammation. Compared to the vehicle control, 14E11 treatment reduced the clinical severity of EAE and total mononuclear cells, including $CD11b^{+}CD45^{high}$ macrophage/microglia and $CD4^{+}$ T cell numbers in brain. Following pharmacological targeting of FXI, BBB disruption was reduced, as measured by decreased axonal damage and fibrin(ogen) accumulation in the spinal cord. These data demonstrate that pharmacological inhibition of FXI reduces disease severity, immune cell migration, axonal damage, and BBB disruption in mice with EAE. Thus, therapeutic agents targeting FXI and FXII may provide a useful approach for treating autoimmune and neurologic disorders.

5.2 Introduction

To further investigate the role of factor (F) XI thromboinflammation, we turned our attention to thromboinflammation in the setting of multiple sclerosis (MS). In this chapter, we evaluated if treatment with the anti-FXI monoclonal antibody, 14E11, could improve neurological function and attenuate CNS damage in a murine model of MS, experimental autoimmune encephalomyelitis (EAE). It is important to note that although the EAE lesions lack the heterogeneity and spontaneity of MS lesions, EAE is the most extensively studied animal model of autoimmune disease; moreover, EAE has been used to develop three approved MS treatments (glatiramer acetate, mitoxantrone and natalizumab).[218] Thus, EAE remains a suitable model for questions related to the function of immune and inflammatory components, as well immune-mediated tissue injury, during autoimmune CNS disease. In our studies, we found that pharmacological inhibition of FXI reduces disease severity,

immune cell migration, axonal damage, and BBB disruption in mice with EAE. Thus, therapeutic agents targeting FXI and FXII may provide a useful approach for treating autoimmune and neurologic disorders.

5.3 Background

Multiple sclerosis (MS) is a neurodegenerative, demyelinating disease of the central nervous system (CNS) that affects approximately 2.2 million individuals globally.[86] MS is characterized by inflammatory lesions, axonal damage, and leukocyte trafficking across the blood-brain barrier (BBB). The pathophysiology of MS is believed to be caused in part by increased BBB vascular permeability, leading to the transmigration of peripheral T cells into the brain parenchyma that induce lesions and subsequent demyelination.

Recent evidence suggests that in addition to immune cells, other factors contribute to the pathophysiology of MS. In particular, clinical observations of MS patients and studies using animal models have advanced a connection between the coagulation cascade and inflammatory processes in MS.[87] The coagulation cascade is a series of enzymatic reactions in which a zymogen precursor becomes activated to its enzyme form, which then catalyzes the next reaction in the pathway, ultimately activating thrombin and forming a fibrin clot.

Two distinct activation pathways are recognized to lead to the formation of thrombin, with elements of both pathways found to be associated in the pathogenesis of MS. For example, increased levels of thrombin activity have been documented within the plasma of MS patients.[219,220] Likewise, studies using an animal model of MS, experimental

autoimmune encephalomyelitis (EAE), suggest that thrombin activity may contribute to MS pathology by influencing BBB permeability and myelination.[221-223] Prothrombin, the zymogen precursor of thrombin, and coagulation factor X (FX) have also been found to be elevated in the plasma of patients with MS.[219,224] In addition, relapsing-remitting MS patients experiencing relapse were found to have markedly higher plasma levels of coagulation factor XII (FXII), which was correlated with their disease activity.[225] Further evidence that components of the coagulation system play a role in the MS disease state is described in studies demonstrating the presence of the blood plasma factors fibrinogen, tissue factor, and protein C inhibitor in active MS lesions and plaques.[226-229] These observations from MS patient studies are further supported by data from disease models, in which constituents of the blood coagulation system, including platelets, fibrinogen, activated coagulation factor X (FXa), FXII, as well as the proinflammatory kallikrein-kinin system have been shown to contribute to EAE pathologies.[96,230-232]

Therapeutic strategies that inhibit thrombin activity reduce disease severity in both MS patients and EAE models. Historically, the anticoagulant heparin was used to treat MS with mixed success.[233,234] In experimental models, anticoagulation with heparin, warfarin, or rivaroxaban have been shown to ameliorate the clinical course of EAE.[228,235,236] Similarly, treatments that directly target FXa,[232,236] platelets,[230] fibrin formation,[237] or FXII [238] have been shown to ameliorate EAE. Though effective in disease models, traditional anticoagulants may pose additional risks to MS patients, in particular increased bleeding. Thus, they may be unsuitable for long-term clinical use. Strategies that target both inflammation and fibrin formation within the CNS without impairing hemostasis significantly may have therapeutic value.

Coagulation factor XI (FXI) is a major substrate of activated FXII (FXIIa), the initiator of the intrinsic pathway of coagulation. In various animal models, decreasing or eliminating FXI activity through gene knockout, pharmacologic inhibition, or antisense oligonucleotide mediated knockdown has been shown to be antithrombotic without impairing hemostasis.[195,239-242] We have previously demonstrated that targeting FXI with 14E11, a mouse monoclonal antibody that selectively inhibits the activation of FXI by FXIIa and reciprocal activation of FXII by FXIa *in vitro*,[1,2] has antithrombotic effects in multiple disease models. 14E11 improves outcomes in mouse polymicrobial sepsis,[54] acute ischemic stroke,[243] acute myocardial ischemia,[1] atherosclerosis,[138] and deep vein thrombosis.[244] Additionally, the humanized version of 14E11, AB023, has been shown to reduce markers of thrombin generation and inflammation in renal failure patients undergoing hemodialysis (Lorentz 2021), underscoring the potential utility of pharmacologic inhibition of FXI in conditions where thrombin activity is increased. In the present study, we evaluated if treatment with 14E11 improves neurologic outcomes in a mouse model of EAE. We found that 14E11 improved disease scores and prevented both axonal damage and fibrin accumulation in the spinal cord. Our results show that pharmacologic inhibition of FXI reduces disease severity in EAE and suggests that contact activation of FXI through FXIIa has a pathogenic role in the progression of autoimmune disorders of the CNS.

5.4 Material and Methods

5.4.1 *Reagents*

The anti-FXI monoclonal antibody, 14E11, was generated and purified as previously described.[212]

5.4.2 *Animals*

The animal care and procedures in this study were performed in accordance with the National Institutes of Health *Guide for the Care and Use of Laboratory Animals* and the regulations of the Oregon Health & Science University Institutional Animal Care and Use Committee.[245] The male C57BL/6 mice used in this study were housed at the Portland Veterans Affairs Medical Center in the Animal Resource Facility (Portland, OR, US) according to guidelines set by the National Research Council and the Committee on Care and Use of Laboratory Animals of the Institute of Laboratory Animal Resources.

5.4.3 *EAE Induction and 14E11 Treatment*

EAE was induced by inoculating C57BL/6 mice subcutaneously with mouse myelin oligodendrocyte glycoprotein, peptides 35–55 (MOG35–55) combined with complete Freund's adjuvant containing heat-inactivated *M. tuberculosis*, as previously described.[246] On days 0 and 2 relative to immunization, mice were intraperitoneally injected with 75 ng and 200 ng of pertussis toxin (PTX), respectively. To quantify the symptoms of EAE, a disease score was assigned to each mice daily. The scale used to assess EAE symptoms was as follows: 0, normal; 1, limp tail or mild hind limb weakness; 2, moderate hind limb weakness or mild ataxia; 3, moderately severe hind limb weakness; 4, severe hind limb weakness or mild forelimb weakness or moderate ataxia; 5, paraplegia with no more than moderate forelimb weakness; and 6, paraplegia with severe forelimb weakness or severe ataxia or moribund condition.

At the onset of clinical signs of EAE (disease score ≥ 2.5, typically between days 10–13), mice were randomized into two groups. The mice were then administered either the anti-

FXI antibody, 14E11 (1 mg/kg, n=9), or vehicle (saline, n=7) at the same volume intravenously (**Figure 5.1a**). The 14E11 dose level was selected based on previous work [212]. The mice were monitored for changes in disease score by an investigator blinded to treatment status until mice were euthanized for *ex vivo* analyses. In accord with efforts to replace, reduce, and refine the use of animals, the saline-treated animal cohort concurrently served as a vehicle control for two treatment arms: 1) 14E11 presented herein and 2) the thrombin mutant W215A/E217A. These three cohorts were run simultaneously; the data from the vehicle cohort was previously published as part of Verbout *et al.* study comparing the vehicle and the W215A/E217A cohort and thus technically used herein as a historic control.

5.4.4 *Flow Cytometry*

Flow cytometry was used to measure markers of inflammation in the CNS and periphery during EAE just prior to euthanasia. To quantify the population of mononuclear cells in the CNS, Percoll density gradient centrifugation was used to isolate mononuclear cells.[247] The CNS cells (n=3 per group) were then pooled to achieve sufficient numbers for the antibody staining protocol. To measure the activation of the macrophage subpopulation of splenocytes, spleen tissue was homogenized and single cell suspensions were prepared. Cells (1×10^6) were washed with a staining media comprised of PBS with NaN_3 (0.1%) and BSA (1%) and stained with combinations of anti-CD4, anti-CD45, anti-ICAM-1 and anti-CD11b antibodies. These antibodies were obtained from sources previously described.[248]

5.4.5 *Immunohistochemistry*

To perform *ex vivo* analyses following vehicle or 14E11 treatment, mice were euthanized with an isoflurane overdose until respiration ceased. They were then heparinized, transcardially perfused with 100 mL of 4% paraformaldehyde (mass/volume in sodium phosphate buffer [0.1 M, pH 7.4]), and fixed at 4°C for 24 hours. Mice then underwent necropsy, and intact spinal columns were removed. Spinal cord sections 1-2 mm in length were dissected from the thoracic and lumbar regions from one representative animal per treatment group to analyze CNS pathology and fibrin(ogen) accumulation, respectively.

To assess CNS pathology, thoracic spinal cord tissues were re-fixed in 5% glutaraldehyde (mass/volume in sodium phosphate buffer [0.1 M, pH 7.4]) at 4°C for 72 hours, post-fixed in 1% osmium tetroxide for 3.5 hours, rehydrated in ethanol, and embedded in plastic. Then, 0.5 μm semithin sections were obtained with a microtome, mounted onto precleaned microscope slides, and stained with toluidine blue to visualize nerve structures. Spinal sections were imaged at 20× and manually stitched into a complete composite of the section. To assess for axonal damage within the thoracic tissue, composite images were analyzed by a trained, blinded user as described previously.[249] Briefly, regions of interest within the white matter tracts were segmented for areas of tissue damage, which included demyelinated axons, degenerating axons, and disrupted compact myelin. Percent area of tissue damage was quantified by measuring area of damaged white matter and total area of white matter (damaged and intact).

To assess fibrin(ogen) accumulation within the CNS, lumbar spinal cord tissues were fixed and embedded in paraffin for sectioning. Sections were blocked in 10% normal goat serum containing 1% bovine serum albumin and 0.025% Triton-X at room temperature

for 45 minutes to decrease nonspecific staining. Tissue sections were then incubated with a primary antibody to fibrin(ogen) (1:50 in goat serum, rabbit polyclonal, MP Biomedicals) overnight at 4°C followed by goat anti-rabbit IgG Alexa Fluor 488 (Molecular Probes). Slides were rinsed, mounted in aqueous media, and imaged at 20× with a Zeiss Axiovert fluorescent microscope. 20× images were processed identically in SlideBook (ver. 5.5) and manually stitched into a composite of the entire section using Photoshop. Quantitative analysis of fibrin(ogen) accumulation was performed on composite images using ImageJ (ver. 2.3.0). Color channels were split, and the green channel intensity histogram data were obtained and utilized to determine the background threshold value. Mean gray values corresponding to fibrin(ogen) signal were measured above the threshold value. Corrected integrated density was determined by subtracting background and accounting for area of fibrin(ogen).

5.4.6 *Statistical Analysis*

Shapiro-Wilk and F-tests were used to test for normality and compare variances in the data. If the data were normally distributed with equal standard deviations, unpaired t-tests were used to compare vehicle and 14E11-treated mice. If the data were not normally distributed, the data were compared by a Mann-Whitney test. A *P* value less than 0.05 was considered statistically significant. GraphPad Prism 9 (ver. 9.5.0) was used to perform statistical analyses.

5.5 Results

5.5.1 *Effect of FXI Inhibition on Clinical Signs of EAE*

Patients with MS experience discrete episodes, also referred to as ‘attacks’ or ‘relapses’, during which they present with varying clinical symptoms (e.g. changes in gait, muscle weakness, and incoordination).[250] Clinical rating scales are commonly used to assess the severity of neurological dysfunction and inform treatment strategies in humans, as well as monitor disease progression in animal models.[251,252] To quantify the effects of FXI inhibition on EAE symptoms, EAE mice were administered 14E11 or vehicle control at peak disease every other day for four days (**Figure 5.1a**). Mice treated with 14E11 had an average peak disease score of 2.4, whereas mice in the control cohort had an average peak disease score of 3.5, which represents a 31.4% reduction (**Figure 5.1b**). To further quantify this effect, we calculated cumulative disease index (CDI) by summing daily disease scores for each cohort. Mice treated with 14E11 had a mean CDI of 15.3, while mice in the control group had a mean CDI of 26.9, representing a 43% decrease in mean CDI with 14E11 treatment (**Figure 5.1c**). These data confirm that targeting FXI reduced clinical symptom severity in a mouse model of MS.

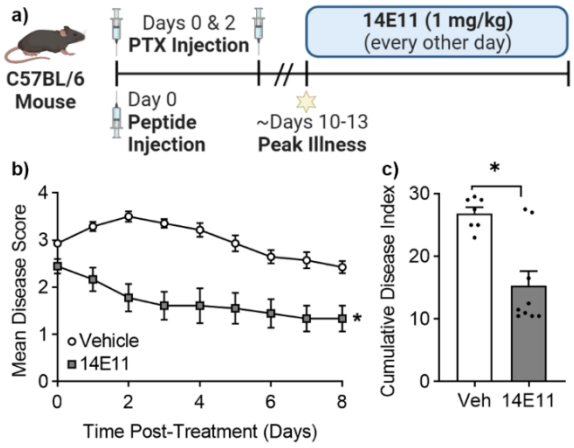

Figure 5.1 EAE symptoms attenuated by treatment with 14E11. Male C57BL/6 mice immunized with MOG/CFA/PTX were monitored and assigned a disease score daily. At peak disease onset (disease score ≥ 2.5), mAb 14E11 (1 mg/kg) was administered every other day for four days (a). The mean disease scores (b) and the cumulative disease index (c) for 14E11-treated mice were significantly lower compared to mice treated with vehicle (c). Data are presented as mean ± SEM for two independent experiments, where *n* = 7-9. Statistical analyses were performed using Mann-Whitney tests on GraphPad Prism 9. Statistical significance is indicated by a single asterisk (*) for $P \leq 0.05$.

5.5.2 *Effect of FXI Inhibition on EAE-Induced Inflammation*

Since activated macrophages and microglia have been shown to upregulate demyelination in the early stages of MS (Wang et al. 2019), we next evaluated the role of FXI in mediating the inflammatory response in EAE. To do this, we first quantified the population of activated macrophages/microglia (CD11b/CD45^{high} cells) and CD4+ T-cells in brain samples from vehicle control and 14E11 treated mice. Note, to overcome the lower limit of CNS cells required for the antibody staining protocol, the CNS cells (n=3 per group) were pooled (n=1 per group) before flow cytometry analyses. Compared to the vehicle-treated group, total numbers of mononuclear cells recovered from the 14E11 treated group were reduced by ~50% (from 3.2M to 1.6M cells) and absolute numbers of infiltrating CD11b/CD45^{high} cells in the CNS were reduced by 24% (from

188,800 to 142,880 cells) and $CD4^+$ T cells by 44% (from 115,520 to 65,120 cells), respectively **(Figure 5.2a-b)**. Additionally, we measured macrophage subpopulation activation in splenocytes harvested from mice with EAE. No differences were observed for $CD11b^+$ macrophages expressing TNFα or ICAM-1 following treatment with 14E11 **(Figure 5.2c-d)**. These results suggest that FXI plays a role in reducing EAE-induced inflammation in the CNS, but not in the peripheral splenocytes.

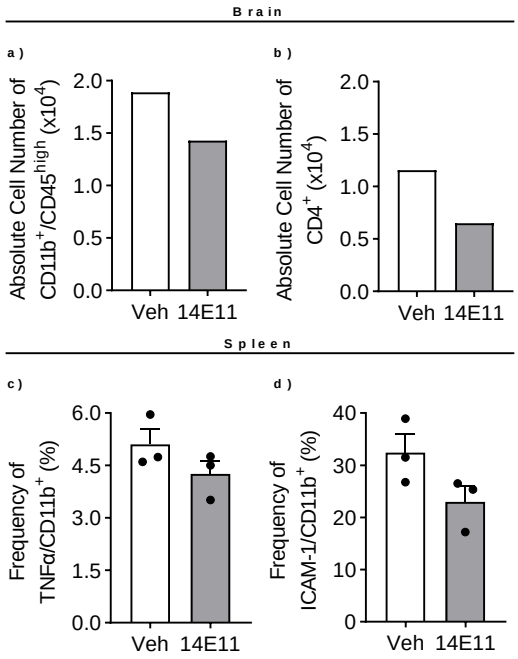

Figure 5.2 Treatment with 14E11 reduced inflammation caused by EAE in the CNS, but not in splenic macrophages. CNS cells and splenocytes were obtained from mice with EAE treated with either vehicle or 14E11 (1 mg/kg, i.v.). To achieve sufficient cell numbers for antibody staining, CNS cells were pooled (n=3 per group). Flow cytometry was used to measure the population of activated macrophages/microglia ($CD11b^+/CD45^{high}$) (a) and T cells ($CD4^+$) (b) within the brain. Data are presented as the absolute numbers of infiltrating cells in the pooled CNS samples. To study macrophage activation in the spleen, flow cytometry was used to measure the expression of TNFα (c) and intercellular adhesion molecule-1 (ICAM-1) (d) on $CD11b^+$ macrophages. Data are presented as mean ± SEM from $n = 3$. Statistical analyses were conducted using unpaired t-tests on GraphPad Prism 9. Statistical significance is indicated by a single asterisk (*) for $P \leq 0.05$.

5.5.3 *Effect of FXI Inhibition on Demyelination in the Thoracic Spinal Cord*

The progression of MS is marked by increasing instances of demyelinated lesions in the CNS that result in the debilitating loss of nervous system function.[250] To determine the effect of FXI inhibition on myelination, we stained spinal cord cross sections with toluidine blue and used light microscopy to assess myelination. As shown in **Figure 5.3**, there appeared to be a notable reduction in demyelination in the spinal cord sections of mice treated with 14E11 compared to mice in the control group. Indeed, we quantified demyelination damage as percent of damaged white matter in a representative spinal cord image (n=1) from each group. The percent of white matter area damaged was reduced from 13.6% in vehicle treated controls to 2.14% in 14E11 treated mice, representing an 84.3% decrease in damage with 14E11 treatment. Note, due to the limitation of a single sample size per group, cautious interpretation of these findings is warranted. Nonetheless, these results suggest that targeting FXI may preserve myelination in the spinal cords of EAE mice.

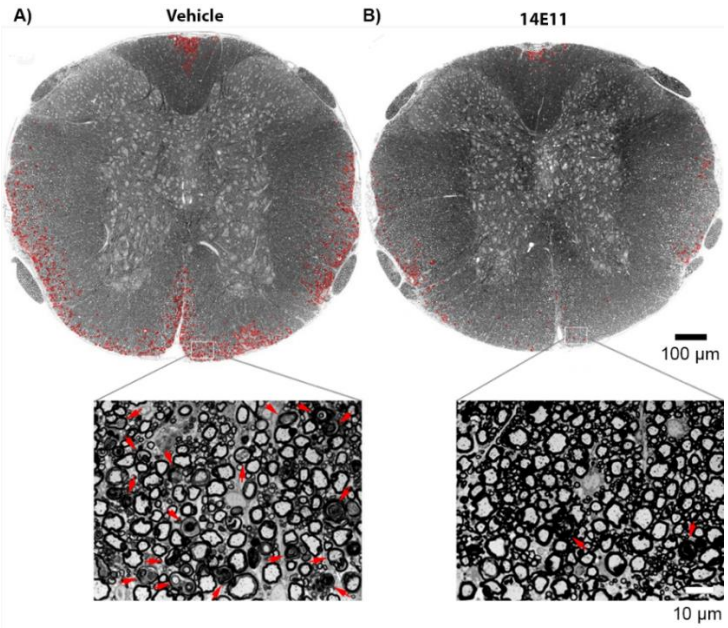

Figure 5.3 Axonal damage and demyelination in the thoracic spinal cord is reduced following treatment with 14E11. Damage to the myelin in spinal cord sections was assessed by staining the tissues with toluidine blue and using light microscopy to image the semithin sections at 20×. A complete view of the spinal cord cross section was obtained by stitching photographs together in Adobe Photoshop. The representative images shown are from mice treated with 14E11 (a) and vehicle (a). Tissue damage in the white matter is denoted in red. The scale bar in the composite image is 100 µm and the scale bar in the magnified view (63×) is 10 µm.

5.5.4 *Effect of FXI Inhibition on Fibrin(ogen) Accumulation in the CNS*

Accumulation of the plasma protein fibrin(ogen) in the CNS is a prominent feature of BBB disruption and MS pathology. Studies have shown that fibrinogen accumulation correlates with axonal damage in the mouse models of EAE.[237] Since we saw a reduction in the percent area of damaged white matter, we investigated the effects of FXI inhibition on fibrin(ogen) deposition in the lumbar region of the CNS (**Figure 5.4**). Percent area positive for fibrin(ogen) signal was reduced from 4.88% in the vehicle control to 2.55% for 14E11 treatment. Additionally, we found the corrected fluorescent integrated density reduced from 5.48E7 RFUs to 2.59E7 RFUs for vehicle and 14E11 treatments,

respectively. This corresponds to a 52.7% reduction in intensity of fibrin(ogen) signal for 14E11 treatment compared to vehicle control. These preliminary findings suggest that pharmacological targeting of FXI may preserve barrier function in the setting of EAE.

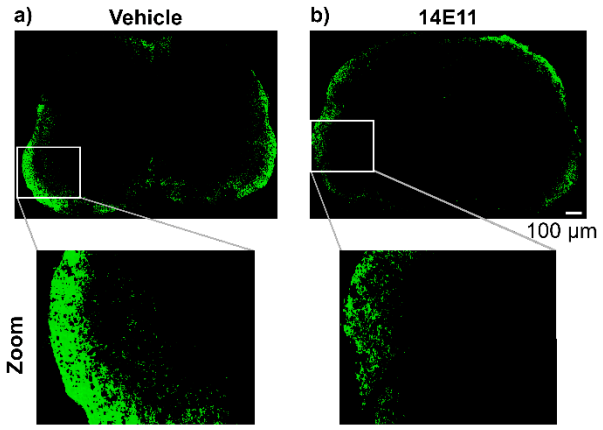

Figure 5.4 Effects of pharmacologic targeting of FXI by 14E11 treatment on fibrin(ogen) deposition in the spinal cord. Sections of the lumbar region of the spinal cord were stained for fibrin(ogen) deposition from one representative animal per treatment group. 20× images were manually stitched into composites and thresholded for background fluorescence for vehicle (a) or 14E11 treatment (b). Representative images show a reduction in area positive for fibrin(ogen) signal as well as corrected fluorescent integrated density for 14E11 treatment compared to vehicle. Scale bar indicates 100 µm.

5.6 Discussion

Clinical and experimental evidence suggest that coagulation components play a role in exacerbating the pathologies associated with MS.[87,88,253] Indeed, the intrinsic pathway of coagulation has been implicated in MS and EAE pathologies, as plasma FXII levels or activity have been shown to be elevated in MS patients,[89] and FXII deficiency is protective in EAE.[90] However, the mechanism by which the intrinsic pathway of coagulation contributes to EAE through FXII remains ill-defined. Therefore, we evaluated the effects of pharmacologically targeting of FXI on autoimmune responses in EAE. At the onset of symptoms (disease score ≥ 2.5), EAE mice were treated with the

anti-FXI monoclonal antibody, 14E11. Following treatment with 14E11, we observed a reduction in the clinical severity of EAE symptoms, axonal damage and demyelination, and fibrin(ogen) accumulation in the CNS. Our findings indicate that FXI may be a potential therapeutic target in treating the progression of autoimmune disorders of the CNS.

Our results indicate that pharmacological targeting of FXI improves disease scores of EAE. Treatment with 14E11 significantly attenuated clinical symptom severity over the course of eight days, which corresponded to approximately a 40% reduction in the cumulative disease index. These data are consistent with other studies in which targeting components of the coagulation cascade improved disease severity in EAE, including FXII,[254] FXa,[232] thrombin,[228,255] fibrin,[256] and activated protein C (APC).[228] Previous findings by Göbel *et al*. showed that there were no significant differences in clinical disease scores between FXI-deficient mice and wild-type mice.[225] One possible explanation for the difference between these studies is that Göbel *et. al.* evaluated the effect of complete FXI deficiency, while our study employed a strategy to pharmacologically target FXI at peak disease. Incorporating prophylactic 14E11 treatment as a future direction may resolve the discrepancies between our current study and the prior work using a FXI-null mouse model and provide valuable mechanistic insights.

Treatment with 14E11 also resulted in a trend towards a reduction in EAE-induced inflammation. During the early stages of MS, fibrinogen infiltrates the CNS and activates microglia through the integrin receptor, CD11b/CD18,[257] resulting in an M1-like

activation and pro-inflammatory phenotype.[227,229,257] Therefore, CD11b+ macrophage expression of TNFα and ICAM-1 were measured as markers of activated macrophages/microglia found to be causative in early stages of EAE. Interestingly, only modest decreases of TNFα or ICAM-1 macrophage expression were observed between 14E11 and vehicle treatment. This observation may be due to an evaluation of cells isolated from peripheral splenic tissue rather than within the CNS itself. Nonetheless, this suggests that inhibition of FXI by 14E11 does not provoke significant attenuation of the primary, peripheral immune response after EAE induction. We next quantified the population of activated macrophages/microglia (CD11b/CD45^{high} cells) and CD4+ T cells in pooled murine brain samples. Not only did treatment with 14E11 reduce the total number of mononuclear cells in the brain by 50%, but we also observed reduced percentages of activated CNS macrophages/microglia and T cells. These results strongly support the conclusion that inhibition of FXI plays an important role in limiting EAE-induced inflammation.

Additionally, we found that 14E11-treated mice had reduced demyelination in the white matter of spinal cord tissue compared to the vehicle cohort. Previous studies have found that the inhibition of oligodendrocyte progenitor cell (OPC) maturation contributes to demyelination processes, and that OPC maturation and recruitment to demyelinating lesions is negatively regulated by thrombin in a PAR1-dependent manner.[224,258] Since thrombin activity is upregulated in the CNS of MS patients, and FXI is positioned upstream of thrombin generation, it is possible that targeting FXI reduces the amount of thrombin generated.[220] Indeed, the reduction in demyelination observed in the 14E11-treated mice may be attributed to decreased levels of FXIa-mediated thrombin generation.

However, we did not evaluate thrombin activity nor the effect of 14E11 on thrombin generation in this study.

FXI inhibition also reduced BBB disruption, as measured by fibrin(ogen) accumulation in the spinal cord. Under physiological conditions, BBB integrity is modulated by intercellular junction proteins (e.g. gap, adherens, or tight junctions) and matrix metalloproteinases (MMP). These proteins can signal through a number of receptors on the surface of cerebral vascular endothelium, including the thrombin receptors PAR-1 and PAR-4.[87] Previous studies have demonstrated that blocking PAR-1 in the setting of EAE prevents BBB disruption by downregulating MMP9 and attenuating the loss of tight junctions.[259] Therefore, it is possible that targeting FXI reduces BBB permeability by reducing the amount of thrombin generated. Alternatively, we have recently shown that FXIa activity increases endothelial permeability both *in vitro* and *in vivo* by downregulating vascular endothelial-cadherin (VE-cadherin) expression and increasing endothelial permeability.[138] Thus, targeting FXIa activity with 14E11 may have elicited a protective effect on barrier function by preventing VE-cadherin inhibition.

There are several limitations of this study. One issue is that limited numbers of mononuclear cells in CNS required pooling of cells from three mice in order to overcome detection thresholds needed for FACs analysis of cell subtypes. Although such pooling gave a greater sampling of smaller subsets, it also precluded biological replicates. Pooling samples can decrease study power, modify the mean values and standard deviations of the data, and mask outliers within a heterogeneous population. Another limitation of this study is that we evaluated treatment with 14E11 at one dose level and at one timepoint,

which precludes a full evaluation of the treatment window and effect level. It is conceivable that prophylactic treatment with 14E11, which would more closely mimic therapeutic strategies to combat and treat disease clinically, could have strengthened our findings.

Overall, treatment with 14E11 decreased severity of EAE clinical signs, axonal damage, and fibrin(ogen) deposition within the CNS. However, no significant differences were found in splenic immune responses, indicating that FXI may have a limited role in peripheral EAE-associated inflammatory responses. Taken together, 14E11 may be acting as a BBB-protective agent to influence EAE pathology. Yet, a caveat to BBB-protective agents in therapeutic use is that if they are administered after the initial disruption of the BBB, they will not target insoluble fibrin deposited in the CNS prior to treatment. Therefore, future work should investigate the role of feedback activation of FXIa by thrombin in EAE pathology to further delineate the function of the intrinsic pathway in EAE pathology and progression. In conclusion, the results reported herein support pharmacological targeting of FXI as a therapeutic strategy to facilitate the treatment of MS and other neurological autoimmune diseases.

Chapter 6. Development of coagulation FXII antibodies for inhibiting vascular device-related thrombosis

Tia C.L. Kohs, Christina U. Lorentz, Jennifer Johnson, Cristina Puy, Sven R. Olson, Joseph J. Shatzel, David Gailani, Monica T. Hinds, Erik I. Tucker, Andras Gruber, Owen J.T. McCarty, and Michael Wallisch

This work was originally published by Springer Nature.
Cellular and Molecular Bioengineering, 2020; Volume 14, Pages 161-175
Reprinted with permission

6.1 Abstract

Vascular devices such as stents, hemodialyzers, and membrane oxygenators can activate blood coagulation and often require the use of systemic anticoagulants to selectively prevent intravascular thrombotic/embolic events or extracorporeal device failure. Coagulation factor (F)XII of the contact activation system has been shown to play an important role in initiating vascular device surface-initiated thrombus formation. As FXII is dispensable for hemostasis, targeting the contact activation system holds promise as a significantly safer strategy than traditional antithrombotics for preventing vascular device-associated thrombosis. The objective of this study was to generate and characterize anti-FXII monoclonal antibodies that inhibit FXII activation or activity. Monoclonal antibodies against FXII were generated in FXII-deficient mice and evaluated for their binding and anticoagulant properties in purified and plasma systems, in whole

blood flow-based assays, and in an in vivo nonhuman primate model of vascular device-initiated thrombus formation. A FXII antibody screen identified over 400 candidates, which were evaluated in binding studies and clotting assays. One non-inhibitor and six inhibitor antibodies were selected for characterization in functional assays. The most potent inhibitory antibody, 1B2, was found to prolong clotting times, inhibit fibrin generation on collagen under shear, and inhibit platelet deposition and fibrin formation in an extracorporeal membrane oxygenator deployed in a nonhuman primate. These results suggest that selective contact activation inhibitors hold potential as useful tools for research applications as well as safe and effective inhibitors of vascular device-related thrombosis.

6.2 Introduction

Taking what we have learned from the previous studies targeting the intrinsic pathway of coagulation in disease settings, we shifted our focus to study vascular device-related thrombosis. In this chapter, we report the development of potent neutralizing monoclonal antibodies targeting FXII activation and FXIIa activity. FXII(a) was selected as the drug target because individuals born without FXII have no apparent pathology, including bleeding diathesis or immunocompromise; however, hyperactivity of FXII appears to be pathologic, as certain mutations in exon 9 provoke a rare form of hereditary angioedema.[150] In our screen of over 400 candidates, we performed functional assays for the characterization of seven select antibodies. Based on our preliminary findings, 1B2 was selected to assess the effects of in a model of vascular device-initiated thrombosis in a pediatric membrane oxygenator inserted into a high flow arteriovenous shunt in a baboon. We found that treatment with 1B2 inhibited platelet deposition and fibrin

formation, which suggests that targeting the intrinsic pathway may reduce or prevent vascular-device associated thrombosis in a variety of clinical settings, including extracorporeal membrane oxygenators (ECMO).

6.3 Background

Vascular devices, including ventricular assist devices (VAD), stents, and extracorporeal membrane oxygenators (ECMO), are prone to surface-initiated thrombus formation.[58,59] While these devices provide needed cardiovascular support to patients, their use inevitably exposes blood to non-biological surfaces and non-physiological shear stress, creating a highly pro-coagulant environment.[57] The current standard of care to prevent thrombotic complications for some vascular devices, including venous and arterial thromboembolism, or occlusions within extracorporeal vascular device circuits (extracorporeal organ support, ECOS) sometimes mandates the administration of anticoagulation. Currently available anticoagulants (e.g. heparin, warfarin, direct coagulation factor (F) X inhibitors) target enzymes in the extrinsic, intrinsic, and common pathways of blood coagulation. While these anticoagulants prevent vascular device-associated thrombosis, the extrinsic and common pathways are critical for hemostasis, their inhibition universally increase the risk of bleeding, including life-threatening hemorrhage.[59] Therefore, there is an urgent need to develop new strategies for safer anticoagulation capable of preventing vascular device-associated thrombosis. Our study was designed to develop and characterize inhibitors of the contact activation system (CAS), and in particular, FXII, which is activated by foreign surfaces, including vascular devices, yet is not required for normal hemostasis.[57] Our efforts in developing exclusively intrinsic pathway inhibitors, including FXII, are consistent with the original concept that

an anticoagulation strategy targeting FXII or activated FXII (FXIIa) could provide thromboprotection without hemostasis impairment.[260-262]

FXII (Hageman factor) is an 80 kDa, 596 residue long single-chain glycoprotein proenyzme that is produced and secreted by hepatocytes. It is encoded by a 12 kb gene comprised of 13 introns and 14 exons, located at chromosome 5q33-qter. Upon activation, it is cleaved into a 353-residue heavy chain joined to a 243 residue long light chain, which contains part of the catalytic domain joined by a disulfide bond (α-FXIIa) (**Figure 6.1A**). There are seven structural domains: a fibronectin domain type II, 2 epidermal growth factor (EGF) domains, a fibronectin domain type I, a kringle domain, a proline-rich region, and the protease (catalytic) domain.[51] The physiologic plasma concentration of FXII in humans is in the range of 30-40 μg/mL.[263] Phylogenetic studies have demonstrated that FXII likely arose as a genetic duplication event; FXII is conserved across a number of species, including human, opossum, platypus, and frog, but is absent in birds and many sea creatures.[264] Humans and mice with congenital deficiencies in FXII exhibit *in vitro* prolongation of the activated partial thromboplastin time (aPTT), yet lack an abnormal bleeding phenotype, in stark contrast to other coagulation factor deficiencies such as FVIII and FIX (hemophilia A and B, respectively).[265] Pharmacologic inhibition or genetic knockout of FXII has been shown to reduce thrombus formation in both *in vitro* and *in vivo* experimental models, again whilst leaving hemostasis intact.[266,267]

When blood contacts negatively charged surfaces, including a number of biological molecules and artificial materials such as those that comprise vascular devices, the

zymogen FXII is cleaved after Arg353, which generates the serine protease α-FXIIa.[268] The fate of α-FXIIa is several-fold: 1) α-FXIIa cleaves factor XI (FXI) to form FXIa and ultimately produces thrombin (factor IIa [FIIa]) to drive platelet activation and fibrin formation; 2) α-FXIIa activates prekallikrein (PK) to form α-kallikrein, which both converts FXII to α-FXIIa in a reciprocal feedback mechanism, and activates major components of complement system C3 and C5, which subsequently activate both the classical and alternative complement activation pathways;[57] moreover, kallikrein cleaves the cofactor high molecular weight kininogen (HK) to release bradykinin (BK), a systemic vasoregulatory and inflammatory mediator;[58,59] 3) α-FXIIa is cleaved after Arg334 to generate β-FXIIa, which is comprised of the α-FXIIa catalytic domain and a 2 kDa heavy chain remnant (**Figure 6.1B**); and 4) β-FXIIa, while unable to generate FXIa, is additionally able to activate PK to form α-kallikrein.

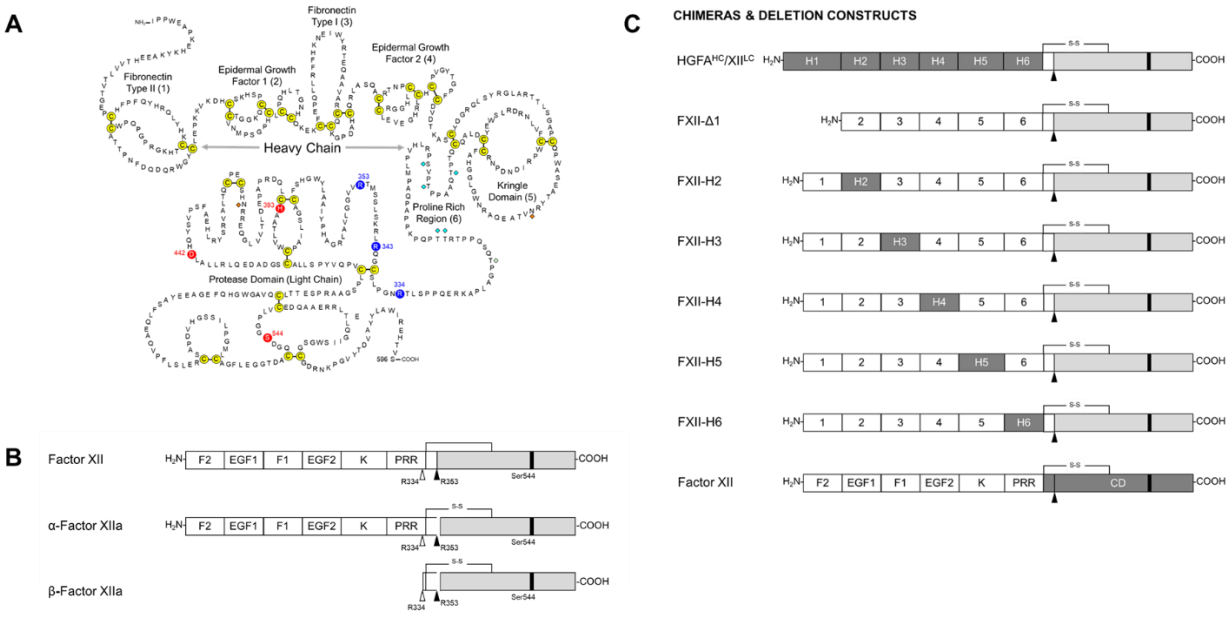

Figure 6.1 Human FXII. (A) Primary and secondary structure of FXII. (B) Schematic diagrams comparing the domain structures of FXII, α- FXIIa, and β- FXIIa. (C) Chimera and deletion constructs. Dark gray shading indicates the HGFA domains introduced into FXII to create FXII /HGFA chimeras.

Herein, we describe the generation and characterization of antibodies against FXII used to study FXII activation pathways and the function of FXII in promoting thrombus formation under shear flow. We also validate that inhibiting FXII activity prevents platelet deposition and fibrin formation in blood perfused membrane oxygenators.

6.4 Material and Methods

6.4.1 *Generation of Anti-FXII Monoclonal Antibodies*

Antibodies against FXII were generated as previously described.[51] In brief, three FXII-deficient Balb-C mice were immunized with an intraperitoneal (IP) injection of a 30 µg mixture of recombinant murine and human FXII in Freund's complete adjuvant on day 0, and 20 µg mixture in Freund's incomplete adjuvant on day 18. A 10 µg booster dose in saline was administered on day 46. Spleens were harvested on day 49, and a standard

polyethylene glycol-based protocol was used to fuse lymphocytes with P3X63Ag8.653 myeloma cells. Production runs of 50 – 400 mL hybridoma cultures were grown and antibodies were purified using a protein A matrix.

6.4.2 *Expression of Recombinant FXII and Antibody Mapping*

Complementary DNA (cDNA) from human FXII was inserted into vector pJVCMV.[264] Using polymerase chain reaction (PCR), the sequence encoding individual domains from the FXII homolog hepatocyte growth factor activator (HGFA) was amplified from the human HGFA cDNA and used to replace the corresponding sequence in the FXII cDNA (**Figure 6.1C**).[265] HEK293 fibroblasts (ATCC-CRL1573) were transfected with pJVCMV/ FXII-HGFA constructs as described.[264] Anti-FXII monoclonal antibodies were used as the primary antibody in Western blots to detect FXII in human and mouse plasma, as well as purified α- and β-FXII. Purified FXII antibodies were size-fractionated on 10% polyacrylamide–sodium dodecyl sulfate gels, and chemiluminescent Western blots were prepared using 1D7, 5C12, 7G11, 9G3, 15D10, or goat polyclonal–anti-human FXII immunoglobulin G (IgG) for detection.

6.4.3 *Western Blot of Plasma FXII*

Platelet-poor plasma (PPP) was obtained as previously described from the following wide range of species: giant anteater (Myrmecophaga tridactyla), cattle (Bos taurus), horse (Equus ferus caballus), pig (Sus scrofa domestica), rabbit (Oryctolagus cuniculus), raccoon (Procyon lotor), Amur tiger (Panthera tigris altaica), human (Homo sapiens), baboon (Papio anubis), domestic cat (Felis silvestris catus), chicken (Gallus gallus domesticus), domestic dog (Canis lupus familiaris), African elephant, (Loxodonta

africana), llama (Lama glama), cynomolgus monkey (Macaca fascicularis), rhesus macaque (Macaca mulatta), rat (Rattus norvegicus domestica), African green monkey (Chlorocebus aethiops), and marmoset (Callithrix jacchus).[212] One μL PPP was size fractionated on SDS-polyacrylamide gels under reducing or non-reducing conditions, followed by Western blotting using the different monoclonal antibodies.

6.4.4 *Activated Partial Thromboplastin Time (aPTT)*

Nine parts venous blood was drawn by venipuncture from healthy male and female adult volunteers into one part 3.2% sodium citrate in accordance with the OHSU (Oregon Health & Science University) Institutional Review Board (No. 1673). Informed consent was received from all human blood donors. Platelet-poor plasma was prepared by centrifugation of citrated whole blood at 2150×g for 10 minutes. Further centrifugation of the plasma fractions at 2150×g for 10 minutes yielded platelet-poor plasma, which was pooled and stored at −80°C until use.

aPTT measurements were made in duplicate using SynthASil (Instrumentation Laboratory, Bedford, MA, USA) and a KC4 Analyzer. Activated clotting time (ACT) of blood was determined in duplicates using LupoTek KCT (r2-Diagnostics, South Bend, IN, USA). Prothrombin time (PT) assay was conducted with Dade® Innovin® (Siemens Healthcare Diagnostics, Flanders, NJ, USA) according to the manufacturer's protocol. PT of plasma samples was quantified using a KC4 Analyzer. Plasma thrombin-antithrombin complex (TAT) were measured with ELISA kits from Siemens (Flanders, NJ, USA) as previously described.

In separate studies, citrated platelet-poor plasma was obtained from the following species: human (*Homo sapiens*), baboon (Papio anubis), cynomolgus monkey (Macaca fascicularis), rhesus macaque (Macaca mulatta), mouse (Mus musculus), rat (Rattus norvegicus), and rabbit (Oryctolagus cuniculus) was serially diluted into FXII-depleted human plasma (Affinity Biologicals). These dilutions were incubated with 20 µg/mL anti-FXII monoclonal antibody and aPTT was measured using a KC-4 coagulometer (Tcoag, Ltd, Ireland; SynthasIL Reagent, Instrumentation Laboratory) as described above.

6.4.5 *Non-activated Thromboelastometry Analysis (NATEM)*

NATEM was measured immediately after venous blood collection (within 5-10 minutes). Human blood was taken into syringes containing 3.2% (w/v) sodium citrate (one-tenth of blood volume) and FXII antibodies (40 µg/mL, final concentration) were added prior to recalcification (300 µL blood re-calcified with 20 µL 200 mM $CaCl_2$) for use in the NATEM assay following standard protocols.

6.4.6 *FXII Activation and FXIIa Inhibition*

FXII activation and FXIIa inhibition were measured as previously described.[217] In brief, to measure activation of FXII, human FXII (40 nM; Haematologic Technologies, Inc., Essex Junction, VT) was incubated with an anti-FXII monoclonal antibody (mAb) (0-80 nM) for 10 minutes at room temperature, followed by dextran sulfate (1 µg/mL) for 20 minutes at 37°C. Spectrozyme FXIIa (0.5 mM; Sekisui Diagnostics GmbH, Germany) was then added to measure hydrolysis by activated FXII (FXIIa). To assess the effect on FXII activation by polyphosphates, FXII (100nM) was co-incubated with an anti-FXII

mAb (0-200 nM) for 10 minutes at room temperature. The mixture was diluted 50/50 with HK (12.5 nM, Enzyme Research Laboratories, South Bend, IN), PK (12.5 nM, Enzyme Research Laboratories, South Bend, IN), and polyphosphates [long (> 1000 phosphate units) or short (~70-100 phosphate units)].[269] The antibody solution (10 µM, final concentration) was incubated for 60 minutes at 37°C. Polybrene (120 µg/mL, Sigma-Aldrich, Saint Louis, MO) and soybean trypsin inhibitor (1mg/mL, Sigma, Sigma-Aldrich, Saint Louis, MO) were added to the antibody solution and the amidolytic activity was quantified. To test FXIIa inhibition, Spectrozyme FXIIa was added to mixtures of FXIIa (20 nM) and anti-FXII mAb (0-40 nM). The samples were read at 405 nm.

6.4.7 *Flow Chamber Analysis*

Glass capillary tubes (0.2 × 2 × 50 mm; VitroCom, Mountain Lakes, NJ, USA) were coated with 100 µg/mL of fibrillar type I collagen (Chrono-Log Corp, Havertown, PA, USA) for 1 hour at room temperature (RT), then washed with PBS and blocked with 5 mg/mL denatured bovine serum albuminutes for 1 hour at RT. The capillary tubes were connected to a blood reservoir and a syringe pump. Human venous blood was collected by venipuncture into syringes containing 3.8% (w/v) sodium citrate (one-tenth of blood volume). Blood was incubated with 100 µg/mL 1B2, 1D7, or 5A12 for 10 minutes at RT. Re-calcification buffer (1:9, buffer:blood; 75 mmol/L $CaCl_2$ and 37.5 mmol/L $MgCl_2$) was added to allow for coagulation prior to perfusion at venous shear rate of 300 s^{-1} for 10 minutes at 37 °C. Capillaries were washed with PBS, fixed with 4% paraformaldehyde and sealed with Fluoromount-G Mounting Medium (ThermoFisher Scientific). Platelet aggregates and fibrin formation in the capillaries were imaged for analysis using a 63×

Zeiss Axio Imager M2 microscope (Carl Zeiss MicroImaging GmbH, Germany) as previously described.[52]

6.4.8 *Anticoagulation of Baboons*

All animal experiments were approved by the Institutional Animal Care and Use Committee of Oregon Health & Science University. To establish the time course of coagulation parameters, one anti-FXII antibody that binds the FXII catalytic domain (1B2), and one that bind the FXII heavy chain (1D7) were selected. 1B2 (n = 2) or 1D7 (n = 1) were administered to baboons (*Papio anubis*) in subsequent i.v. doses of 1 mg/kg every 40 minutes over a 4-hour period, totaling six doses. A baseline measurement was made prior to drug administration at time = 0. Blood samples were collected for up to three weeks post administration and aPTT, ACT, PT, TAT levels were measured. Complete blood count (CBC) was also measured to determine platelet count, hematocrit concentration, white blood cell count, and red blood cell count.

6.4.9 *Baboon Model of Thrombogenesis in Extracorporeal Membrane Oxygenators*

All animal experiments were approved by the Institutional Animal Care and Use Committee of Oregon Health & Science University. Two juvenile baboons (*Papio anubis*) were repeatedly employed for the perfusion experiments. Baboons were implanted with exteriorized femoral arteriovenous shunts as described previously.[239,270,271] In brief, ^{111}In-labeled autologous platelets and ^{125}I-labeled homologous fibrinogen were used for measurement of thrombus formation in the saline-primed oxygenator cartridge that was interposed in the exteriorized shunt loop (Terumo-CAPIOX® RX05, coated hollow fiber design, Terumo Cardiovascular Group, Ann

Arbor, MI). Animals were administered 1B2 intravenously at a 5 mg/kg initial dose with 2 mg/kg daily maintenance dose. The vehicle control experiments were performed in week one, prior to antibody treatment in week two. Platelet radioactivity within the oxygenator was recorded in real-time using gamma camera imaging (GE-Brivo NM 615 interfaced with Xeleris 3.1 software, GE Healthcare, Chicago, IL). Platelet deposition was calculated as previously described.[195,239,271,272] For quantification of ^{125}I-fibrin content at the 60 minutes endpoint, the cartridge was removed, rinsed, dried, and stored refrigerated until processing. In brief, the oxygenators were filled with digest buffer (10 mM Tris-H3PO4 pH 7.0, 35 mM SDS) for 3 days. The radioactivity of the digest solution was measured using a gamma counter (Wizard-3, PerkinElmer, Shelton, CT), and the amount of trapped fibrin/fibrinogen was calculated as previously described.[239,272] Bleeding times were evaluated twice during each administration of 1B2 using the adult Surgicutt® device (International Technidyne, Piscataway, NJ), as described previously. Template bleeding time (BT) was recorded twice during each experiment and averaged.[273,274] Briefly, a pressure cuff at 40 mm Hg was applied to the upper arm, and a 5 mm long × 1 mm deep incision was made on the volar surface of the lower arm. Blood drops were collected on a Whatman® filter paper every 30 seconds until the bleeding stopped.

6.5 Results

6.5.1 *Generation and Characterization of Monoclonal FXII Antibodies*

FXII antibodies were generated by immunization of FXII knock-out mice with a mixture of human and mouse FXII zymogen. A total of 463 monoclonal antibodies were identified in an ELISA screen as binders of murine and/or human FXII. Using an aPTT

clotting assay, we screened the cell culture supernatants using platelet-poor plasma serially diluted into FXII-deficient plasma (1:128 dilution), which gave a baseline aPTT of ~50-70 sec. Of these, 78 clones were shown to prolong aPTT of human platelet-poor plasma (>2-fold increase in clotting times over baseline); these antibodies were then tested for cross-reactivity with mouse FXII in plasma. We identified two antibodies that robustly prolonged aPTT of human plasma only (1B2 and 5C12) and four that prolonged the aPTT of both human and mouse plasma (1D7, 7G11, 15D10, and 9G3). Additionally, 5A12, despite binding FXII, did not prolong the aPTT of human platelet-poor plasma.

The binding epitopes for these antibodies on human and mouse FXII were determined by Western blot. We used plasma-derived α- and β-FXIIa to identify the binding region. Our data showed that only two human-specific antibodies, 1B2 and 5C12, recognized β-FXIIa, which only contains the catalytic domain of α-FXII; neither bound to murine FXII. The antibodies 1D7, 7G11, 9G3, 15D10, and 5A12 recognized both human and mouse FXII and did not bind β-FXIIa, which suggests that they bind to the heavy chain of FXII (**Figure 6.2A-B**).

We next used FXII/HGFA chimeras to identify the FXII regions containing the binding sites for the anti-FXII antibodies. As the *F12* gene arose from a duplication of the *HGFA* gene, FXII and HGFA have similar domain structures with the exception that FXII has a proline-rich region not found in HGFA. We prepared FXII with individual domains replaced by corresponding HGFA domains as previously described (**Figure 6.1C**).[262] The antibody 1D7 was the only antibody which recognized both the reduced and non-reduced forms of human FXII (**Figure 6.2A**); 1D7 was found to recognize the second epidermal

growth factor (EGF2) domain, as evidenced by the reduction in detection when this domain was swapped out for the H4 domain of HGFA. Similarly, 5A12 detected the second EGF2 domain of FXII. Deletion or exchange of the fibronectin type 2 (F2), as well as the first and second EGF domains (EGF1, EGF2) of FXII regions with the HGFA homologous region reduced the detection of these FXII chimeras by the antibodies 7G11, 9G3, and 15D10 by Western blot (**Figure 6.2C**).

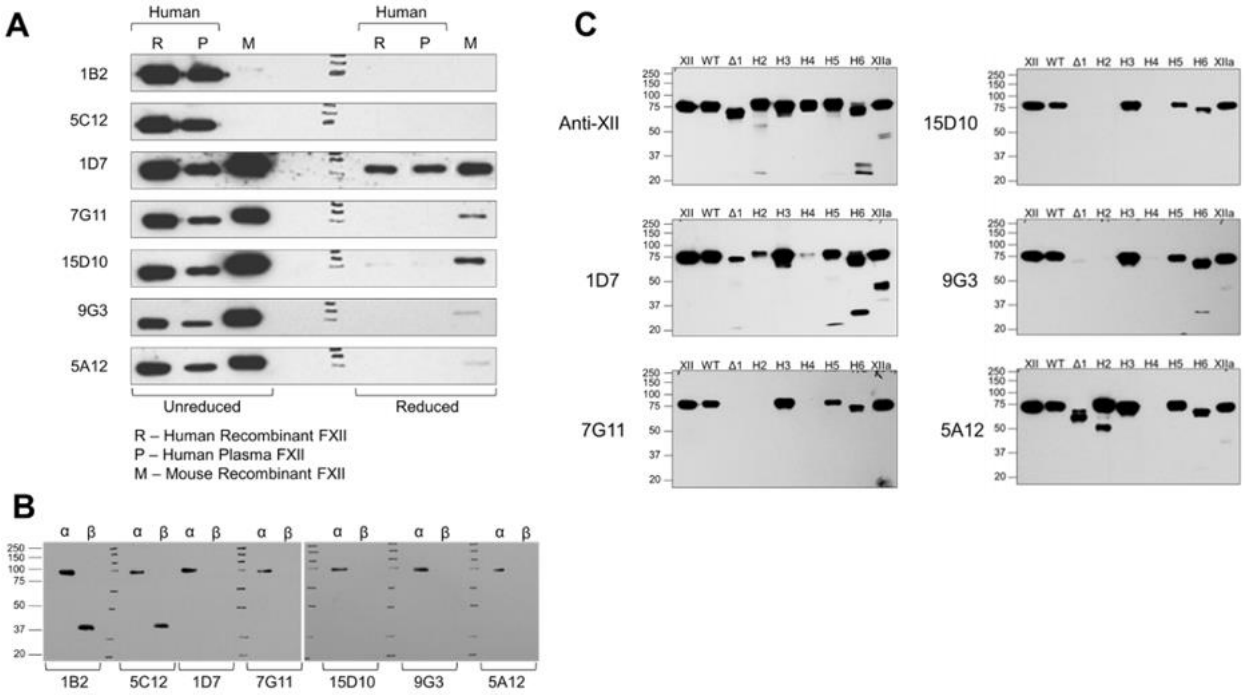

Figure 6.2 Western blots of human and mouse FXII. (A) Western blots of FXII unreduced and reduced human recombinant FXII (R), human plasma FXII (P), and mouse recombinant FXII (M)-fractionated by sodium dodecyl sulfate-PAGE. (B) Western blots of human α- and β- FXII. (C) Western blots of FXII and FXII/HGFA chimeras.

6.5.2 *Cross-reactivity of Monoclonal FXII Antibodies*

As antibodies were raised in FXII-deficient mice, it is possible that some of them recognize epitopes on FXII that are conserved between species. We evaluated the species

cross-reactivity of the anti-FXII antibodies with FXII derived from a range of vertebrate animals (**Figure 6.3A**). The most universal antibodies in our set were 7G11 and 15D10, which recognized FXII from giant anteater, cattle, horse, pig, raccoon, tiger, baboon, dog, elephant, and llama. A slight band was detected by 7G11 and 15D10 for rabbit FXII. Despite 9G3 binding to the same three domains as 7G11 and 15D10, 9G3 was only found to detect FXII in plasma from raccoon, tiger, dog, elephant, and llama. 9G3 detected FXII from human but not baboon plasma. The antibody 1D7 detected FXII in the plasma from cattle, horse, rabbit, raccoon, tiger, baboon, dog, elephant, llama, and uniquely, cat FXII. The antibody 5A12 detected FXII in plasma from cattle, pig, rabbit, tiger, baboon, elephant, and llama. The antibodies 1B2 and 5C12 were shown to detect FXII in plasma from giant anteater and baboon. All of the antibodies were shown to detect both the positive control (human FXII), with FXII-depleted plasma serving as a negative control (**Figure 6.3A**). These studies confirm that immunizing mice with a protein in which they are deficient can generate antibodies that cross-react with presumed conserved epitopes across species.

We extended our study to characterize the binding of a subset of anti-FXII antibodies to plasmas from animals commonly used in preclinical research including NHPs. Our data showed that 1B2 and 5C12 detected FXII in plasma from African green monkeys in addition to baboons and humans (**Figure 6.3B**). Likewise, the antibodies 1D7 and 5A12 detected FXII in plasma from baboons and humans as well as cynomolgus monkey, rat, and marmoset; a slight band was shown for both antibodies for detection of rhesus macaque FXII. 5A12 detected FXII from African green monkey, while 1D7 detected FXII in beagle plasma (**Figure 6.3B**).

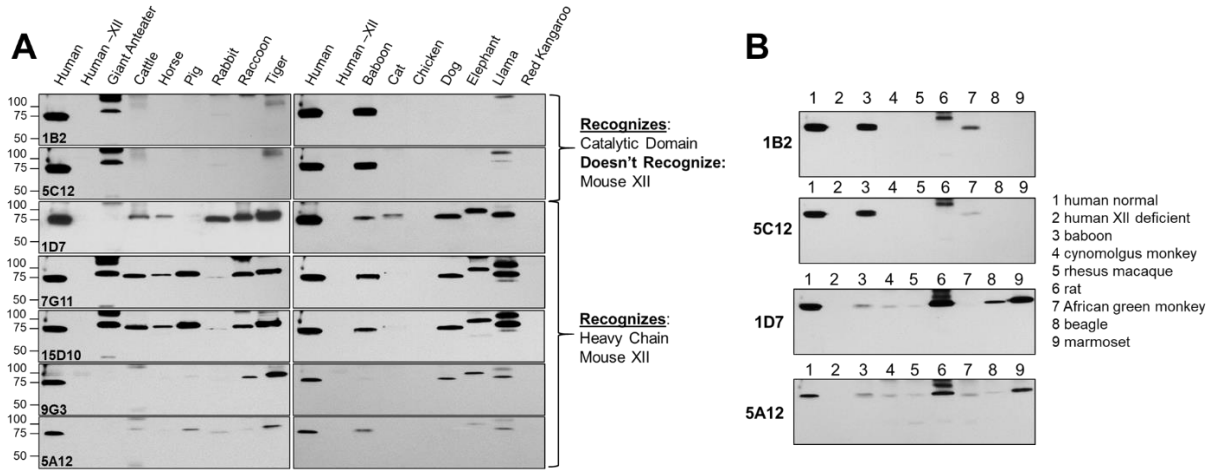

Figure 6.3 Western blots of FXII from mammalian plasmas. Western blots of non-reducing 7.5% polyacrylamide gels of FXII for a variety of animal species (A) and commonly used preclinical research animal models (B).

6.5.3 *Effect of Monoclonal FXII Antibodies on Clotting Times of Plasma and Whole Blood*

We measured the effect of each antibody on the aPTT using pooled human platelet-poor plasmas (PPP) that were serially diluted with human FXII-depleted PPP. Our reference data, serially diluted normal pooled human plasma with FXII-depleted plasma alone, showed that aPTT remained near 30 secs until the level of FXII was reduced by >95%, at which point there is a sharp increase in aPTT that exceeded 250-300 sec as the amount of FXII remaining fell near or below 1% of normal (**Figure 6.4A**). This pattern was conserved across the seven species tested (human, baboon, mouse, rat, cynomolgus, rhesus macaque, and rabbit (**Figure 6.4B-H**).

The diluted aPTT assay was employed to detect the potential inhibitory effects of the FXII antibodies on clotting. In human plasma, the aPTT began increasing upon reduction of FXII to 10% or less, and plateaued at approximately 260 sec once FXII was reduced to

0.01%. Of note, the antibodies were used at a concentration of 20 µg/mL (125 nM), thus roughly four times lower than the concentration of FXII in plasma (~40 µg/mL, 500 nM). The anti-FXII mAbs 1B2 and 5C12 caused a leftwards shift in the curve for human and baboon plasma clotting times indicative of an inhibitory effect (**Figure 6.4B-C**). Antibodies 1D7, 7G11 and 15D10 inhibited the aPTT in human, baboon, cynomolgus, rhesus macaque, mouse, rat, and rabbit plasmas (**Figure 6.4B-H**), although it should be noted that the degree of inhibition as reflected by the aPTT prolongation in human and baboon plasmas was less than observed for 1B2 and 5C12. An inhibitory effect was also observed for 9G3 in human, baboon, cynomolgus, rhesus macaque, and mouse plasmas (**Figure 6.4B-F**). The FXII antibody 5A12 did not affect clotting times in any of the plasmas tested (**Figure 6.4B-H**).

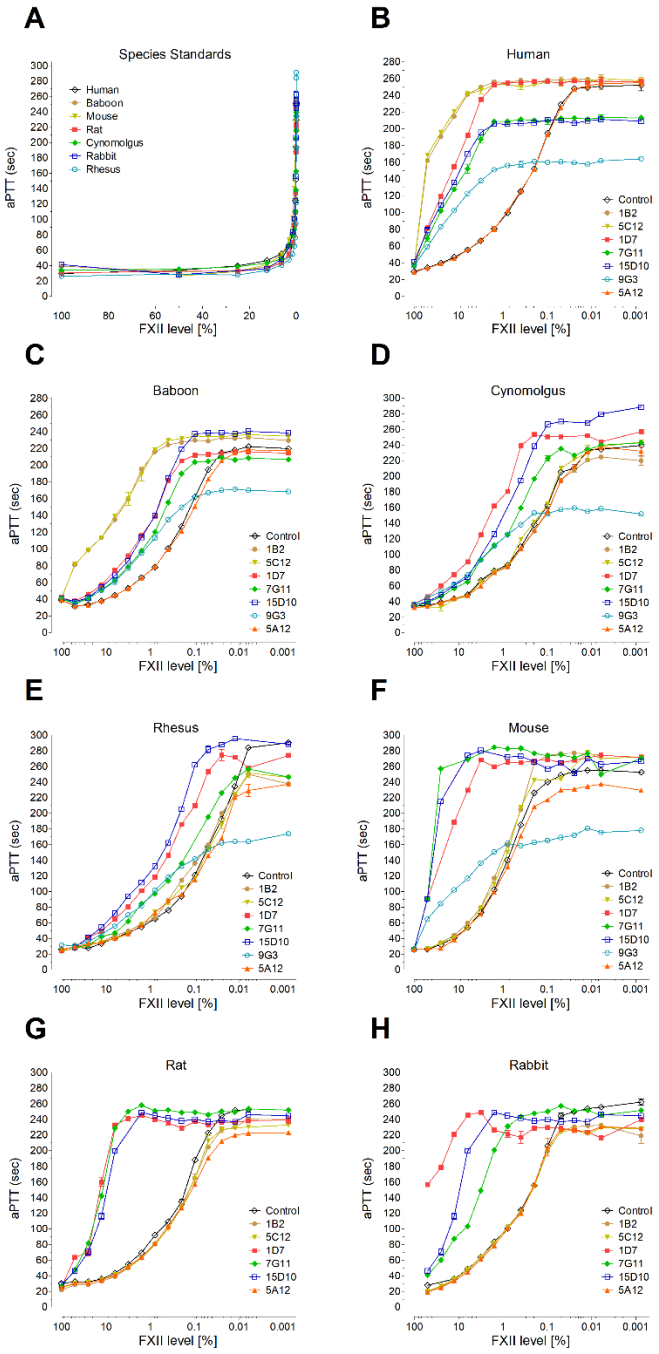

Figure 6.4 Clotting times were measured using aPTT. Platelet-poor plasma from (A) human, (B) baboon, (C) cynomolgus, (D) rhesus, (E) mouse, (F) rat, or (G) rabbit was serially diluted into FXII-deficient human plasma. These dilutions were incubated with 20 µg/mL of FXII antibody candidates. Clotting times were measured following addition of an aPTT reagent. Changes in aPTT were plotted as a function of FXII levels on a logarithmic scale.

We next employed non-activated thromboelastometry analysis (NATEM) to measure the effect of the panel of FXII antibodies on clotting time (CT), clot formation time (CFT), the time to reach a clot strength of 20 mm force, maximum clot firmness (MCF), time to reach maximum clot firmness (MCF-t), and the time from start of clotting to maximum velocity (α-angle). We first performed an aPTT assay using whole human blood, wherein we confirmed that the FXII antibodies 1B2, 5C12, 1D7, 7G11, 15D10, and 9G3 prolonged clotting times, with the greatest level of inhibition observed for 1B2 and 5C12 (**Figure 6.5A**). For NATEM assay (for schematic, see **Figure 6.5B**), we used an antibody concentration of 40 μg/mL, thus roughly half the equimolar concentration to antigen FXII levels in whole blood.

The clotting time (CT), and the CT added to the clot formation time (CT+CFT) measured via NATEM, was prolonged for 1B2, 5C12, 1D7, 7G11, and 15D10, whereas 9G3 and 5A12 did not affect the CT (**Figure 6.5C, E**). No increases for CFT alone, MCF-t, MCF or α-angle were observed for 1B2, 5C12, 1D7, 7G11, and 15D10 (**Figure 6.5D, F-H**). 5A12 did not affect any of the parameters measured (**Figure 6.5C-H**).

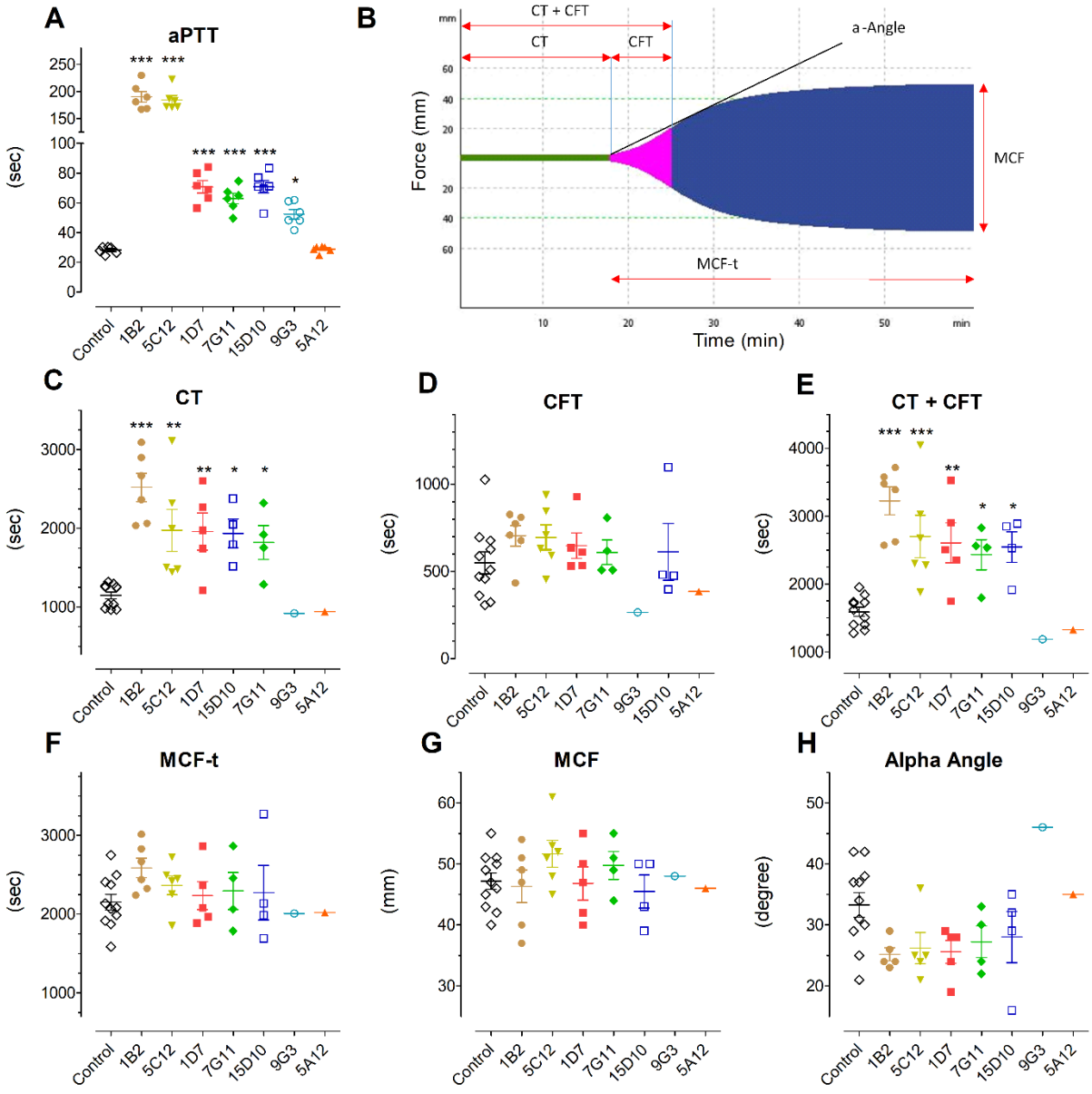

Figure 6.5 Thrombus formation and growth was measured using non-activated thromboelastometry (NATEM). Human plasma from healthy volunteers was inhibited with 40 µg/mL antibody. (A) FXII inhibition confirmed by aPTT; (B) thromboelastometry curve explaining the parameters reported below; (C) clotting time; (D) clot formation time, (E) time to 20 mm clot firmness; (F) maximum clot firmness; (G) time to maximum clot firmness; (H) time to maximum velocity. Data represents mean ± SEM and were analyzed using one-way ANOVA (GraphPad Software, San Diego, CA) with Dunnett's posthoc analysis versus control. * $P<0.05$, ** $P<0.01$, *** $P<0.001$.

6.5.4 *Effect of Monoclonal FXII Antibodies on FXII Activation and FXIIa Activity*

We assessed the ability of the anti-FXII antibodies to inhibit FXII activation or activity. Dextran sulfate or long- or short-chain polyphosphates (polyP) were added to purified FXII to induce FXII activation and amidolytic activity toward a FXIIa-specific chromogenic substrate. We found that FXII activation or activity was inhibited by 1B2, 5C12, 1D7, 7G11, and 15D10 as measured by the amidolytic activity of FXIIa (Figure 6A-C) regardless of whether FXII was activated by long- or short-chain polyP or dextran sulfate. Differing degrees of efficacy were observed for the antibodies with the greatest potency being reported for 1B2 and 5C12. 1D7 was observed to inhibit FXII activation by short-chain polyP as compared to long-chain polyP or dextran sulfate, whereas 9G3 was ineffective in blocking FXII activation by dextran sulfate while exhibiting inhibitory effects against long- or short-chain polyP-mediated activation of FXII (**Figure 6.6A-C**). FXII activation was unaffected 5A12. Lastly, we characterized the effect of the anti-FXII antibodies on inhibiting FXIIa activity directly in a purified system. Only the antibodies that bound to the catalytic domain of FXII, 1B2 and 5C12, were capable of inhibiting the amidolytic activity of purified FXIIa (**Figure 6.6D**).

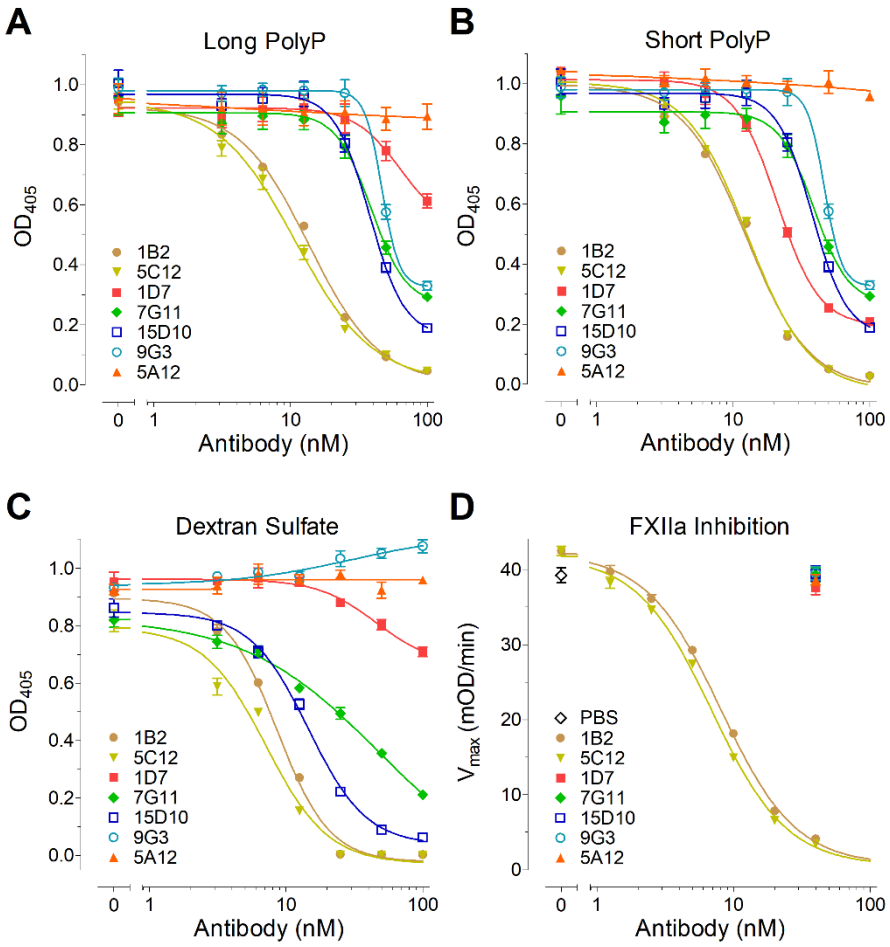

Figure 6.6 Anti-FXII antibodies inhibit FXIIa activity. Increasing concentrations of anti-FXII antibodies were added to a solution of purified FXII. FXII was activated by either long PolyP (A), short PolyP (B), or dextran sulfate (C). Amidolytic activity was quantified as hydrolysis of the chromogenic substrate Spectrozyme FXIIa. Activated FXII (FXIIa; 20 nM) was incubated with increasing concentrations of anti-FXII antibodies for 5 minutes before addition of Spectrozyme FXIIa. The velocity of hydrolysis was measured for 20 minutes and V_{max} was calculated for each reaction (D). Each data point was measured in duplicate. Data represent mean ± SEM from $n = 2$.

6.5.5 *Effect of Monoclonal FXII Antibodies on an In Vitro Model of Thrombus Formation Under Flow*

Experiments were designed to examine the effect of anti-FXII antibodies on fibrin generation and platelet deposition in an *in vitro* model of thrombus formation under flow.

Sodium citrate-anticoagulated whole human blood was recalcified prior to perfusion over immobilized collagen for 10 minutes at a shear rate of 300 sec^{-1} to produce fibrin- and platelet-rich clots (**Figure 6.7**). Consistent with a necessary role for FXII activation and activity in this assay,[52,275] the anti-FXII antibodies 1B2, 5C12, and 1D7 abrogated fibrin formation on collagen under flow; only platelet aggregates were observed in the presence of these antibodies. In contrast, the anti-FXII antibody, 5A12, did not affect the extent of fibrin deposition or thrombus formation.

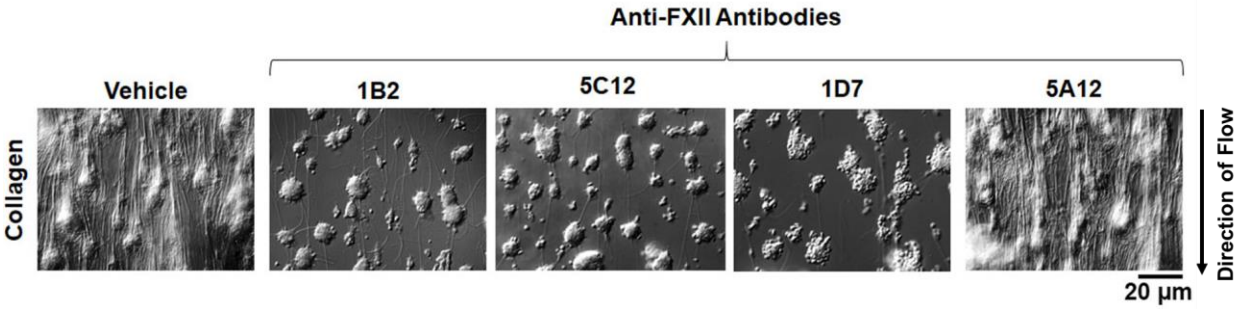

Figure 6.7 Effect of anti-FXII antibodies on fibrin and thrombus formation under shear. Re-calcified, citrated whole blood pretreated with anti-FXII antibody (100 µg/mL, 10 minutes) was perfused through collagen-coated chambers at 300s^{-1}. Representative images from $n = 3$.

6.5.6 *Effect of Monoclonal FXII Antibodies on an In Vitro Model of Vascular Device-initiated Thrombus Formation*

We next selected two anti-FXII antibodies for advancement for testing in a baboon NHP model. We have already demonstrated the efficacy of antibody 5C12 in this model.[268] Based on favorable binding and inhibitory profiles in the *in vitro* assays, we chose one antibody that binds the FXII catalytic domain (1B2), and one that binds the FXII heavy chain (1D7). In a preliminary dose range finding study, both 1B2 and 1D7 were administered to baboons in a stepwise manner consisting of six doses of 1 mg/kg given

40 minutes apart. Our results show that 1D7 caused a 1.5 fold increase in the plasma aPTT above baseline after the sixth dose, while 1B2 caused a greater than three-fold increase in the plasma aPTT from baseline after the second dose (**Figure 6.8A**). Corresponding increases in activated clotting time (ACT) were noted after 4 hours (**Figure 6.8B**). Neither of the antibodies altered the PT, circulating TAT levels, platelet count, hematocrit, or WBC or RBC levels (**Figure 6.8D-H**). Based on the favorable pharmacodynamic profile of 1B2 over 1D7, 1B2 was chosen for use in the baboon model of vascular device-initiated thrombus formation.

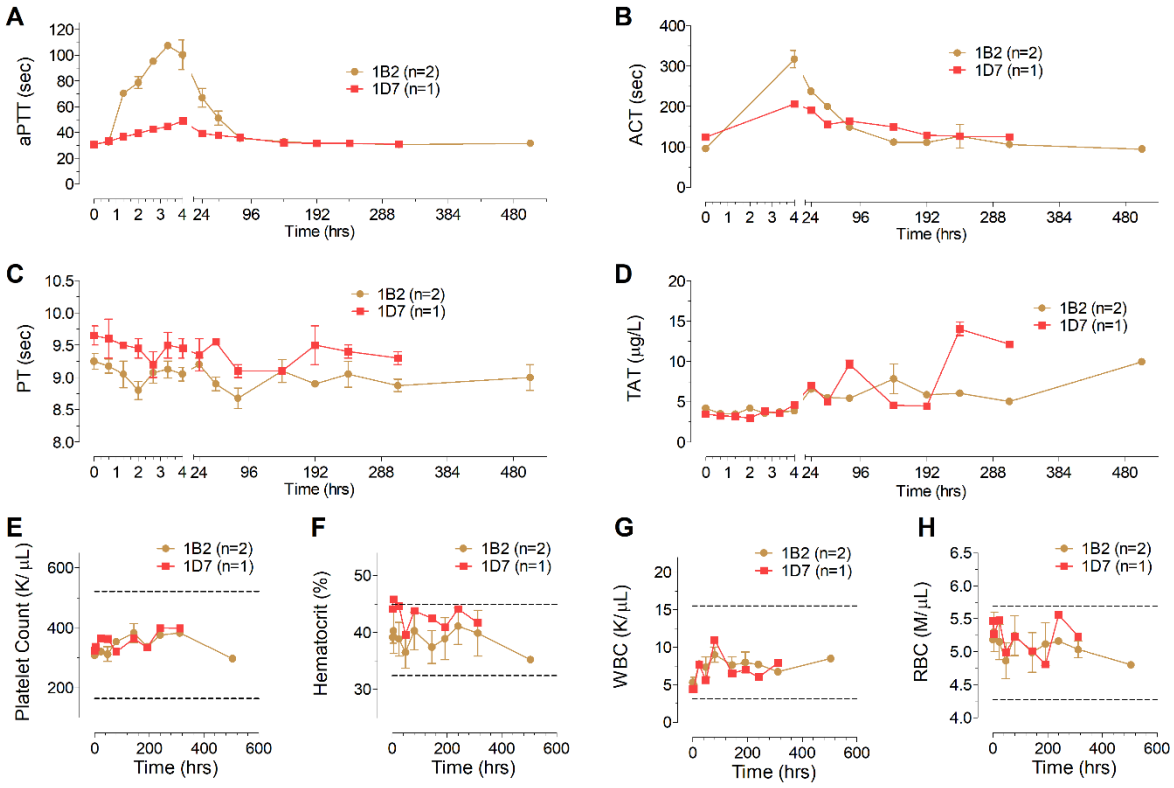

Figure 6.8 Time course of coagulation parameters after 1B2 or 1D7 administration in a nonhuman primate. Baboons were administered i.v. doses of 1 mg/kg 1B2 or 1D7 every 40 minutes over a 4-hour period. Blood samples were collected for up to three weeks post administration. (A) aPTT, (B) ACT, (C) PT, and (D) TAT levels were measured. Complete blood count (CBC) was measured: (E) platelet counts, (F)

hematocrit, (G) white blood cell count, and (H) red blood cell count. The upper and lower limits of reference values are indicated by dashed lines. aPTT, activated partial thromboplastin time; ACT, activated clotting time; PT, prothrombin time; TAT, thrombin-antithrombin complex.

A pediatric extracorporeal membrane oxygenator was inserted into the loop of an exteriorized arteriovenous shunt implanted in a baboon. We quantified autologous radiolabeled platelet deposition in the oxygenator in the absence of an anticoagulant, finding that after 30 minutes over 1.5 billion platelets per minute were being deposited in the oxygenator, resulting in the retention of upwards of 80 billion platelets in the oxygenator by 60 minutes (**Figure 6.9A-B**). Robust fibrin formation was observed in the oxygenator at the 60-minute time point under non-anticoagulant conditions (**Figure 6.9C**). Our data show that pretreatment of the baboon with 1B2 resulted in a significant reduction in both the rate (0.86 ± 0.03 billion platelets per minute) and the extent of platelet deposition and fibrin formation (**Figure 6.9A-C**). We did not detect any change in template bleeding time following treatment with 1B2 as compared to vehicle control (**Figure 6.9E**).

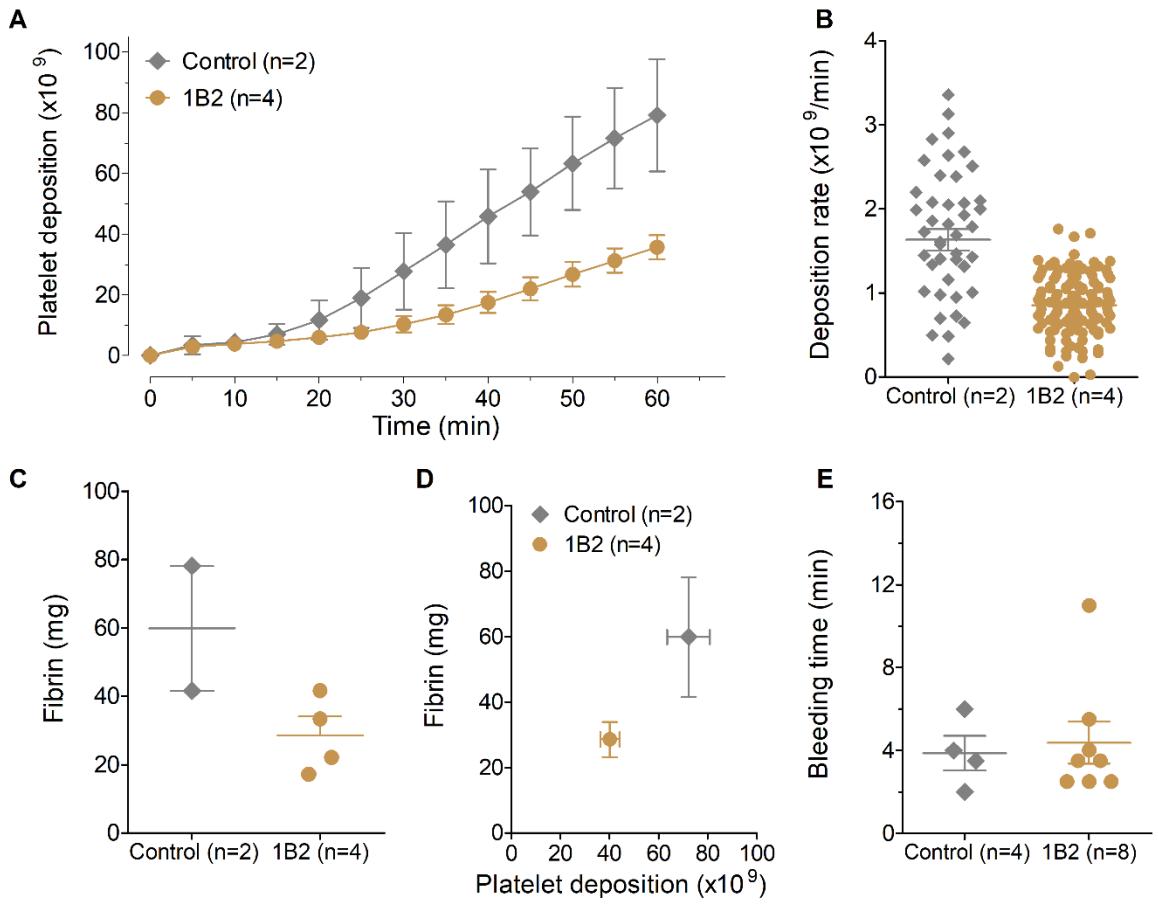

Figure 6.9 Effect of 1B2 on platelet deposition and fibrin formation in ECMO. (A) Real-time platelet deposition was monitored in an ECMO device inserted in the extended loop of a chronic AV shunt. Study arms included vehicle control (n = 2) or 1B2 (5 mg/kg initial day + 2 mg/kg on the following days 30 minutes before perfusion, n = 4). (B) Average platelet deposition rate was calculated from 30 to 60 min. (C) Measurement of terminal fibrin content in the oxygenator and (D) correlation of fibrin and platelet content. (E) Two Surgicutt® bleeding time measurements were performed during each experiment and each data point represents the average of the two measurements. ECMO, extracorporeal membrane oxygenator; AV, arteriovenous; FXII, factor XII.

6.6 Discussion

In this study, a library of monoclonal antibodies against FXII were generated in FXII-deficient mice. One non-inhibitory and six inhibitory antibodies were selected for further characterization. The relative potencies of the inhibitors on FXII activation and activity

were determined using functional assays. These antibodies exhibited cross-reactivity with FXII from a variety of vertebrate animals as assessed by Western blots of mammal plasmas. We used aPTT and NATEM assays to characterize the inhibitory effects of the antibodies on initiation, strengthening, and growth of clots. A series of activity assays, including an *in vitro* flow chamber model, were employed to define the effect of the antibodies on FXII activation and activity. Based on the results, two antibodies that bind to the catalytic domains of FXII, α-FXIIa and β-FXIIa, 1B2 and 5C12, were chosen to assess the effects of FXII inhibition in a model of vascular device-initiated thrombus formation using a pediatric membrane oxygenator inserted into a high flow arteriovenous shunt in a baboon. Results for 5C12 were reported previously.[268] Here we discuss results with antibody 1B2.

Vascular interventions that involve placement of artificial devices such as intravenous access catheters, stents, vascular grafts, valves, and ventricular assist devices (VADs) may be complicated by thrombosis. Prothrombotic effects of some vascular devices, which can cause both device failure and thromboembolic complications, include: 1) non-physiologic, shear-stress induced platelet activation as shown by an increase in soluble P-selectin and enhanced platelet aggregation; 2) release of thrombotic platelet microparticles; 3) excessive red blood cell hemolysis; 4) complement activation; 5) inflammation; and 6) exaggerated coagulation via contact-driven FXII activation and thrombin generation.[276,277] Several of these effects also paradoxically contribute to the non-trivial bleeding diathesis occasionally encountered with some types of vascular devices, most notably: consumptive coagulopathy; platelet shedding of hemostatic surface molecules including GPVI, GPIb, and CD63; and non-physiologic shear-

mediated loss of high molecular weight von Willebrand factor multimers.[278,279] As a result, both thrombosis and major bleeding rates encountered in patients with VADs, ECMO, or CPB are high. For instance, rates of oxygenator thrombosis, arterial thrombosis, and major bleeding in ECMO approach 16%, 10%, and 30%, respectively.[276,277] Here we found that inhibiting the contact activation system by blocking FXIIa activity has an anti-platelet effect in a model of vascular device-initiated thrombus formation. This suggests that when blood comes in contact with foreign surfaces such as an ECMO circuit, inhibiting the initial events that trigger activation of the coagulation cascade that lead to thrombin generation may be an effective route for dampening deleterious platelet activation.

Vascular-device associated thrombosis or outright device failure remain important complications of these medical technologies, and systemic anticoagulation during their use has traditionally been mandated. Although numerous potent anticoagulant drugs are widely available that can reduce the incidence of these complications if given at effective doses, all have dose-limiting hemorrhagic toxicities.[280] This has inspired researchers to develop vascular technologies with improved biocompatible surfaces, alternative dosing protocols for anticoagulants, and entirely new therapeutic agents aimed at blunting the pathologic processes implicated in bleeding and thrombosis.[276,277] FXII, of the CAS, has emerged as a promising target due to an abundance of pre-clinical and early clinical data supporting the efficacy and safety of agents targeting the protein. Murine and NHP models have demonstrated that pharmacologic inhibition or genetic knockout of FXII substantially reduces collagen- and $FeCl_3$-induced experimental venous and arterial thrombosis, respectively.[212,265] Perhaps more compelling is the demonstration that

inhibiting FXII activation or activity is useful in reducing device failure in animal models where membrane oxygenators were perfused with blood to induce clot formation.[57,268] Herein, we validate this hypothesis by demonstrating that the anti-FXII monoclonal antibody 1B2 inhibits platelet deposition and fibrin formation in an extracorporeal membrane oxygenator deployed in nonhuman primates. These studies, and our prior work with the anti-FXII mAb 5C12, suggest that targeting the catalytic domain of FXII may be a useful approach for limiting vascular-device associated thrombosis.

In addition to inciting thrombosis, vascular devices including ECMO and hemodialysis circuits induce a pro-inflammatory process similar in some aspects to that observed in sepsis. Indeed, in patients with extracorporeal devices or sepsis, excessive cytokine release as part of the overwhelming inflammatory response may result in organ damage and contribute to morbidity. We observed that the CAS, and specifically crosstalk between FXII and FXI, serves as a nexus between thrombosis and inflammation in animal models of severe infection and bacterial challenge.[2,54] In these models, selective inhibition of FXII activation significantly blunted the inflammatory response, exemplified by a nearly 6-fold reduction in interleukin (IL)-6 levels. Since increased IL-6 levels are associated with poorer survival in patients undergoing ECMO,[281-283] the CAS may prove an effective target to reduce vascular device-associated inflammation, in addition to its anticoagulant properties.

Translational approaches for reducing vascular device-associated thrombosis by targeting and inhibiting the CAS must take into account the effects of anti-FXII antibodies on FXII activation and activity in the absence of a surface. In the absence of surface, some

antibodies directed at the FXII heavy chain accelerate the reciprocal activation of PK and FXII in plasma. While this does not lead to clotting, it could potentiate the release of bradykinin as a consequence of kallikrein cleavage of HK. An example of this effect was observed for the anti-FXII antibody, 15H8, which interferes with contact activation by preventing FXII from binding to surfaces. Previously, we demonstrated that 15H8 prevented thrombus formation *in vitro* on collagen as well as *in vivo* in an AV shunt thrombosis model.[262] Yet, addition of 15H8 to human plasma was found to potentiate FXII-mediated activation of PK leading to the complete cleavage of the HK. In the absence of a surface the FXII heavy chain serves an important regulatory function that prevents FXII from activating. 15H8 interferes with that function, setting off brisk reciprocal activation with PK. 15H8 binds to the N-terminal fibronectin type 2 domain of FXII, which has been shown to be important in preventing FXII activation in the absence of a surface.[284] Thus, caution is advised when developing therapies directed at the FXII heavy chain, as they may promote activities with a detrimental effect on patients.

In summary, we have generated a panel of anti-FXII antibodies with varying affinity and specificity for FXII; the functional effects of these antibodies were screened and evaluated for their anticoagulant and antithrombotic properties in *in vitro*, *ex vivo*, and *in vivo* models. Our data provides rationale for targeting the contact activation system to reduce or prevent vascular-device associated thrombosis in a variety of clinical settings, including ECMO.

Chapter 7. Severe thrombocytopenia in adults undergoing extracorporeal membrane oxygenation is predictive of thrombosis

Tia C.L. Kohs, Patricia Liu, Vikram Raghunathan, Ramin Amirsoltani, Michael Oakes, Owen J.T. McCarty, Sven R. Olson, Luke Masha, David Zonies, and Joseph J. Shatzel

This work was originally published by Taylor & Francis.
Platelets, 2022; Volume 33, Pages 570-576
Reprinted with permission

7.1 Abstract

Extracorporeal membrane oxygenation (ECMO) provides lifesaving circulatory support and gas exchange, although hematologic complications are frequent. The relationship between ECMO and severe thrombocytopenia (platelet count <50 × 109/L) remains ill-defined. We performed a cohort study of 67 patients who received ECMO between 2016 and 2019, of which 65.7% received veno-arterial (VA) ECMO and 34.3% received veno-venous (VV) ECMO. All patients received heparin and 25.4% received antiplatelet therapy. In total, 23.9% of patients had a thrombotic event and 67.2% had a hemorrhagic event. 38.8% of patients developed severe thrombocytopenia. Severe thrombocytopenia was more common in patients with lower baseline platelet counts and increased the likelihood of thrombosis by 365% (OR 3.65, 95% CI 1.13–11.8, *P*=0.031), while the type of ECMO (VA or VV) was not predictive of severe thrombocytopenia (*P*=0.764). Multivariate logistic regression controlling for additional clinical variables found that

severe thrombocytopenia predicted thrombosis (OR 3.65, CI 1.13–11.78, *P*=0.031). Over a quarter of patients requiring ECMO developed severe thrombocytopenia in our cohort, which was associated with an increased risk of thrombosis and in-hospital mortality. Additional prospective observation is required to clarify the clinical implications of severe thrombocytopenia in the ECMO patient population.

7.2 Introduction

In this chapter, we continued our study of extracorporeal membrane oxygenators (ECMO) by performing a retrospective cohort study at Oregon Health & Science University. It is well established that although ECMO treatment can provide lifesaving benefits to critically ill patients;[105,106] however, the issue of hemocompatibility is highly nuanced, as ECMO is associated with both vascular device-associated thrombosis and anticoagulation-associated bleeding.[107-109] Our work here focused on defining the incidence, predictors, and clinical consequences of severe thrombocytopenia (platelet count $<50 \times 10^9$/L) in patients on ECMO. Interestingly, we found that severe thrombocytopenia in adults undergoing ECMO treatment is predictive of thrombosis using a multivariate logistic regression model. Overall, this study provides insight on the prevalence and clinical consequences associated with severe thrombocytopenia in patients on ECMO.

7.3 Background

Extracorporeal membrane oxygenation (ECMO) can provide lifesaving circulatory support and gas exchange via a cardiopulmonary bypass circuit to critically ill and postsurgical patients; however, significant rates of hematologic complications

compromise its use. There are two predominant types of ECMO: veno-arterial (VA) and veno-venous (VV). In VA ECMO, deoxygenated blood is directed through the ECMO circuit and an external oxygenator before returning to the body via arterial cannulation, thus replacing both oxygenation and circulatory support. In contrast, VV ECMO provides only gas exchange via VV cannulation techniques.

Thrombosis and hemorrhage are exceedingly common, with overall bleeding rates as high as 60% reported in patients on ECMO.[123] The pathophysiology of ECMO-associated hemorrhage is complex, involving the mandated use of parenteral anticoagulation, consumption of coagulation factors, acquired deficiency of von Willebrand factor, platelet activation/dysfunction, and subsequent platelet consumption leading to thrombocytopenia.[58,285] Paradoxically, thrombosis (both venous and arterial) is similarly common in the critically ill population requiring ECMO, with rates of cannula-associated deep vein thrombosis approaching 85%.[286] Thus, ECMO results in a precarious balance between hemostasis and thrombosis, contributing to high rates of morbidity and mortality.

Thrombocytopenia is a well-described phenomenon associated with ECMO, with an estimated prevalence of 21%; severe thrombocytopenia (platelet count $<50 \times 10^9$/L) in patients on ECMO, however, is not as well characterized and has a reported prevalence of 6.3-26.6% in the literature.[287] While thrombocytopenia and severe thrombocytopenia have been associated with reduced survival in patients on ECMO, the relationship between severe thrombocytopenia and specific clinical outcomes such as bleeding and thrombosis has not been fully evaluated.[287] Additionally, the contribution of platelet

counts to the complex milieu of ECMO-associated bleeding and thrombosis is poorly understood.

We performed the following retrospective cohort study to better define the incidence, predictors, and clinical consequences of severe thrombocytopenia in patients on ECMO.

7.4 Material and Methods

7.4.1 *Study Design and Data Source*

This study protocol was approved by the Oregon Health and Science University (OHSU) Institutional Review Board prior to study initiation (Study Number 00019765). We performed a retrospective cohort study of adults (age ≥18 years) who received ECMO (either VA or VV) for any indication at OHSU between March 1, 2016 and September 30, 2019. All data were obtained by extraction from the hospital's electronic medical record.

7.4.2 *Study Population*

A total of 69 patients were treated with ECMO during the study period. Patients who had a documented ECMO course between 1 and 90 days were included, resulting in a final study population of 67 adult patients.

7.4.3 *Data Collection*

Data were extracted by direct medical record review including patient demographics, laboratory parameters, clinical indication for ECMO use, duration of treatment, ECMO parameters, anticoagulant and antiplatelet use and monitoring parameters (partial thromboplastin time (aPTT) and anti-Factor Xa assay (anti-FXa), and safety. Clinical outcomes assessed included overall survival, rate of hemorrhage, thrombosis, and blood

transfusion requirements while on ECMO. Hemorrhage was defined by the International Society on Thrombosis and Haemostasis (ISTH) consensus criteria.[288] Both venous and arterial thrombosis were included, as well as thrombotic events within the extracorporeal circuit that mandated a circuit exchange. The first 30 complete blood counts obtained while on ECMO were evaluated in order to determine the incidence of thrombocytopenia and platelet trends over time. On average, there were 3.7 platelet checks per day in the cohort. The average duration of ECMO treatment in the cohort was 7.0 ± 5.0 days.

7.4.4 *ECMO Anticoagulation Protocols*

In the absence of a major contradiction (bleeding within a critical site or life-threatening bleeding), heparin is administered in conjunction with ECMO to achieve a therapeutic anti-FXa level of 0.35–0.70 IU/mL for VA ECMO and 0.30–0.50 IU/mL for VV ECMO. Antiplatelet therapy and cannulation strategy were determined at the discretion of the treating physicians. The majority of patients received ECMO via the Maquet Cardiohelp life support system.

7.4.5 *Statistical Analysis*

Patient demographics were reported in total and by type of ECMO (VA vs. VV) using standard descriptive statistics. Continuous data were presented as a mean value with standard deviation (SD). Continuous and dichotomous variables were compared between VV and VA ECMO with Welch's t-tests and Fisher exact tests, respectively. Statistical significance was defined as a two-sided *P* value of <0.05 for all analyses.

Univariate logistic regression analysis was used to identify risk factors for the following specific clinical outcomes of interest; the presence of documented bleeding events, major

hemorrhage by ISTH criteria,[288] and thrombosis. The following variables were selected apriori to be assessed in the model: (i) mean platelet count, (ii) platelet count range, or (iii) severe thrombocytopenia (platelet count $<50 \times 10^9$/L).

Multiple logistic regression analysis was then used to identify risk factors for the aforementioned outcomes, and for the development of severe thrombocytopenia. The following variables were selected apriori and considered as independent predictors in the model: (i) age, (ii) concurrent use of antiplatelet drugs, (iii) duration of ECMO, (iv) body mass index (BMI), (v) severe thrombocytopenia, and (vi) mean albumin level.

All statistics were calculated using R (R Foundation for Statistical Computing, version 3.6.2).

7.5 Results

7.5.1 *Patient Demographics and Clinical Outcomes*

During the 43-month study period, 67 adult patients treated with ECMO met inclusion criteria. Within this cohort, 44 (65.7%) received VA ECMO and 23 (34.3%) received VV ECMO. The cohort had a mean age of 51.1 years and 65.7% of the entire study population identified as male. The mean duration of ECMO was 7.0 days. The mean platelet count while on ECMO was 118×10^9/L. However, patients who went on to develop severe thrombocytopenia had lower baseline platelet counts (199×10^9/L vs. 110×10^9/L, $P<0.001$). In total, only 58% of patients on ECMO survived, with similar survival rates between VV and VA ECMO. Additional demographic characteristics and treatment parameters are outlined in **Table 7.1.**

Within the cohort, patients on VA ECMO were older than those on VV ECMO (55.5 years vs. 42.7 years, *P*=0.002), with higher mean albumin levels (2.2 g/dL vs. 1.8 g/dL, *P*=0.016) and higher incidences of bleeding (77.3% vs. 47.8%, *P*=0.027). Patients on VV ECMO had higher mean platelet counts (138.8 x 10^9/L vs. 107.3 x 10^9/L, *P*=0.033), therapeutic anti-FXa levels (54.6% vs. 33.9%, *P*=0.002), days on ECMO (9.0 days vs. 5.9 days, *P*=0.033), and mean daily heparin use (35,268 units/day vs. 20,282 units/day, *P*=0.033). The average platelet count for the entire cohort at the first thrombotic event was $105 \pm 45 \times 10^9$/L, and the average platelet count for individuals who had at least one instance of severe thrombocytopenia and developed a thrombus was $85 \pm 32 \times 10^9$/L. Of the 69 patients in the cohort, 13 patients had PF4 and 4 patients had SRA labs sent. Among these patients, 3 (21%) were PF4-positive and 1 (8%) had a confirmatory SRA. Patients undergoing cardiac surgery were more likely to have severe thrombocytopenia (*P*=0.008) while those with ARDS were less likely (*P*=0.047) (**Table 7.1**). The most common indications for ECMO were acute respiratory distress syndrome (25.4%), post-cardiotomy circulatory support (23.9%), acute myocardial infarction (19.4%), and decompensated heart failure (13.4%). Less common indications are also detailed in **Table 7.1**.

Table 7.1 Demographic and clinical characteristics of 67 adult patients on ECMO.

Variable	Total (*n*=67)	No Severe Thrombocytopenia (*n*=41)	Severe Thrombocytopenia (*n*=26)	*P*-Value
Patient Demographics				
Age, years	51.1 ± 15.9	51.6 ± 16.0	50.4 ± 16.0	0.759
Male, *n* (%)	44 (65.7)	28 (68.3)	16 (61.5)	0.606
Body Mass Index, kg/m^2	32.7 ± 9.7	33.0 ± 10.3	32.3 ± 8.9	0.762
Weight, kg	99.2 ± 32.9	99.9 ± 34.4	98.2 ± 31.1	0.833
Patients on Antiplatelet Drugs, *n* (%)	17 (25.4)	12 (29.3)	5 (19.2)	0.403
Aspirin, *n* (%)	16 (23.9)	11 (26.8)	5 (19.2)	0.565
Clopidogrel, *n* (%)	7 (10.4)	2 (4.9)	5 (19.2)	0.099
Prasugrel, *n* (%)	1 (1.5)	1 (2.4)	0 (0.0)	N/A
Mean Initial Platelet Count, x 10^9/L	164.6 ± 91.5	199.0 ± 91.2	110.5 ± 61.9	< 0.001†
Mean Platelet Count, x 10^9/L	118.1 ± 49.6	122.0 ± 43.7	111.4 ± 58.1	0.414
Mean aPTT, seconds	95.3 ± 37.2	93.4 ± 38.6	98.4 ± 35.3	0.587
Therapeutic anti-FXa*, %	40.7 ± 25.0	40.3 ± 26.3	41.5 ± 23.1	0.854
Mean Albumin, g/dL	2.0 ± 0.5	2.1 ± 0.5	2.0 ± 0.5	0.421
Reason for ECMO				
Post-cardiotomy, *n* (%)	16 (23.9)	5 (12.2)	11 (42.3)	0.008 †
Acute myocardial infarction, *n* (%)	12 (17.9)	10 (24.4)	2 (7.7)	0.109
Decompensated heart failure, *n* (%)	9 (13.4)	6 (14.6)	3 (11.5)	1.000
Sepsis, *n* (%)	2 (3.0)	1 (2.4)	1 (3.8)	1.000
Refractory arrhythmia, *n* (%)	2 (3.0)	2 (4.9)	0 (0.0)	N/A
Pulmonary embolism, *n* (%)	2 (3.0)	0 (0.0)	2 (7.7)	N/A
Acute respiratory distress, *n* (%)	17 (25.4)	14 (34.1)	3 (11.5)	0.047 †
Pneumonia, *n* (%)	4 (6.0)	2 (4.9)	2 (7.7)	0.638
Trauma, *n* (%)	2 (3.0)	1 (2.4)	1 (3.8)	1.000
Parameters of ECMO Treatment				
Venoarterial ECMO, *n* (%)	44 (65.7)	24 (58.5)	20 (76.9)	0.187
Average Flow Rate, mL/hour	3846 ± 643	3889 ± 697	3776 ± 551	0.467
Duration, days	7.0 ± 5.0	7.4 ± 5.5	6.2 ± 4.2	0.310
Mean Daily Heparin, units/day	25427 ± 15341	25507 ± 15562	25301 ± 15290	0.958
Average Number of Platelet Checks/Day	3.8 ± 1.7	3.5 ± 1.4	4.1 ± 1.9	0.174
Efficacy and Safety				
Incidence of Bleeding, *n* (%)	45 (67.2)	25 (61.0)	20 (76.9)	0.196
ISTH Major Bleed, *n* (%)	37 (55.2)	19 (46.3)	18 (69.2)	0.082
Thrombosis, *n* (%)	16 (23.9)	6 (14.6)	10 (38.5)	0.039 †
Number of RBCs	8.9 ± 10.1	8.1 ± 9.7	10.3 ± 10.8	0.390
Survive ECMO, *n* (%)	39 (58.2)	24 (58.5)	15 (57.7)	1.000

† Significant at *P*=0.05

Data represents mean ± SD

Note: several patients received multiple antiplatelet agents while on ECMO

7.5.2 *Thrombotic and Hemorrhagic Events*

Thrombotic and hemorrhagic events were common within our cohort. Documented bleeding was recorded in 45 (67.2%) patients, and of these, 37 (55.2%) patients suffered a major bleed, as defined by the ISTH consensus criteria.[289] Clinically evident thrombosis occurred in 16 (23.9%) patients. Additional clinical outcomes are described in **Table 7.1.** The mean number of units of red blood cells transfused was 8.9 units and 17 (25.4% of

patients) received concurrent antiplatelet therapy while on ECMO. Due to the limitations of the retrospective analysis we were unable to evaluate the platelet transfusions.

Of our entire study population, thrombotic events most commonly occurred in arterial sites (10.4%), followed by venous (9.0%) Major hemorrhagic events were common in the cannula site (7.5%) and the GI tract (7.5%). Additional sites of thrombotic and hemorrhagic events are outlined in **Table 7.2.**

Table 7.2 Site of thrombotic and hemorrhagic events.

Variable	Total (*n*=67)	VA (*n*=44)	VV (*n*=23)	*P*-Value
Site of thrombotic event				
Venous	6 (9.0)	0 (0.0)	6 (26.1)	N/A
Arterial	7 (10.4)	6 (13.6)	1 (4.3)	0.408
Device	1 (1.5)	1 (2.3)	0 (0.0)	N/A
Intracardiac	3 (4.5)	3 (6.8)	0 (0.0)	N/A
Cerebrovascular accident	1 (1.5)	1 (2.3)	0 (0.0)	N/A
Other	1 (1.5)	0 (0.0)	1 (4.3)	N/A
Site of any hemorrhagic event				
Retroperitoneum	2 (3.0)	1 (2.3)	1 (4.3)	1.000
Mediastinum	2 (3.0)	2 (4.5)	0 (0.0)	N/A
GI tract	6 (9.0)	6 (13.6)	0 (0.0)	N/A
Cannula site	6 (9.0)	5 (11.4)	1 (4.3)	0.656
Other	18 (26.9)	12 (27.3)	6 (26.1)	1.000
Pulmonary	5 (7.5)	2 (4.5)	3 (13.0)	0.330
Surgical Site	6 (9.0)	6 (13.6)	0 (0.0)	N/A
Site of major hemorrhagic event				
Retroperitoneum	2 (3.0)	1 (2.3)	1 (4.3)	1.000
Mediastinum	1 (1.5)	1 (2.3)	0 (0.0)	N/A
GI tract	5 (7.5)	5 (11.4)	0 (0.0)	N/A
Cannula site	5 (7.5)	4 (9.1)	1 (4.3)	0.653
Other	17 (25.4)	9 (20.5)	8 (34.8)	0.243
Pulmonary	3 (4.5)	2 (4.5)	1 (4.3)	1.000
Surgical Site	3 (4.5)	3 (6.8)	0 (0.0)	N/A

Note: several patients had multiple sites of thrombotic and hemorrhagic events while on ECMO

7.5.3 *Incidence and Clinical Ramifications of Thrombocytopenia*

In our cohort, 26 patients (38.8%) developed severe thrombocytopenia (platelet count $<50 \times 10^9$/L) for at least one day while on ECMO. Of the 26 patients that developed severe thrombocytopenia, 20 (76.9%) were receiving VA ECMO and 6 (23.1%) were receiving VV ECMO. The mean daily heparin dose was not significantly different in patients who developed severe thrombocytopenia versus those who did not (25,301 vs.

25,507 units, *P*=0.958). Antiplatelet drug usage was not statistically significant between those who developed severe thrombocytopenia compared to those who did not (23.1% vs. 43.9%, *P*=0.403). Univariate analysis showed that developing severe thrombocytopenia significantly increased the odds of a thrombotic event (OR 3.65, 95% CI 1.13-11.77, *P*=0.031) and decreased the odds of surviving hospitalization (OR 0.288, 95% CI 0.100-0.835, *P*=0.022) (**Table 7.3**). Additionally, the development of severe thrombocytopenia significantly increased the odds of a major hemorrhagic event in patients on VA ECMO (OR 5.59, 95% CI 1.27-24.58, *P*=0.023). Using multivariate logistic regression and controlling for age, concurrent use of antiplatelet drugs, duration of ECMO, body mass index (BMI), and mean albumin level, we found that age and severe thrombocytopenia were risk factors for thrombotic events (**Table 7.4**).

Table 7.3 Univariate logistic regression assessing the relationship between platelet count and relevant clinical outcomes.

Outcome	Total (*n*=67)			VA (*n*=44)			VV (*n*=23)		
	OR	**95% CI**	***P*-Value**	**OR**	**95% CI**	***P*-Value**	**OR**	**95% CI**	***P*-Value**
Mean Platelet Count									
Thrombosis	1.003	0.992-1.014	0.570	0.996	0.976-1.016	0.675	1.004	0.989-1.019	0.635
Major Bleed	1.001	0.991-1.011	0.807	0.995	0.981-1.010	0.541	1.010	0.995-1.027	0.198
Incidence of Bleeding	1.002	0.991-1.012	0.751	1.001	0.984-1.019	0.882	1.010	0.995-1.027	0.198
Platelet Count Range									
Thrombosis	0.992	0.983-1.001	0.098	0.995	0.982-1.008	0.422	0.991	0.978-1.004	0.166
Major Bleed	0.999	0.992-1.005	0.640	0.991	0.981-1.000	0.061	1.007	0.997-1.018	0.174
Incidence of Bleeding	1.001	0.994-1.007	0.869	0.993	0.984-1.003	0.170	1.007	0.997-1.018	0.174
Severe Thrombocytopenia									
Thrombosis	3.646	1.129-11.774	0.031 †	4.714	0.832-26.723	0.080	6.500	0.850-49.687	0.071
Major Bleed	2.605	0.926-7.331	0.070	5.600	1.432-21.894	0.013 †	0.444	0.063-3.112	0.414
Incidence of Bleeding	2.133	0.705-6.456	0.180	4.500	0.831-24.373	0.081	0.444	0.063-3.112	0.414

† Significant at *P*=0.05

Table 7.4 Multivariate logistic regression to predict outcome variables.

Outcome	Total (*n*=67)			VA (*n*=44)			VV (*n*=23)		
	OR	**95% CI**	***P*-Value**	**OR**	**95% CI**	***P*-Value**	**OR**	**95% CI**	***P*-Value**
Predictors of Any Bleeding *									
Age	1.02	0.98-1.06	0.400	1.06	0.98-1.14	0.170	0.91	0.83-1.01	0.070
Antiplatelet Drugs	0.60	0.15-2.34	0.459	0.47	0.07-2.89	0.411	0.44	0.02-9.65	0.602
Duration of ECMO	1.07	0.94-1.23	0.322	1.16	0.86-1.58	0.330	1.36	0.97-1.92	0.078
Body Mass Index	1.02	0.96-1.09	0.442	1.08	0.95-1.21	0.234	0.92	0.79-1.08	0.326
Severe Thrombocytopenia	2.46	0.74-8.22	0.144	6.61	0.93-46.84	0.059	0.25	0.01-5.24	0.375
Albumin	3.00	0.89-10.16	0.077	5.43	0.86-8.08	0.073	0.08	0.00-4.82	0.223
Predictors of Major Bleeds *									
Age	0.99	0.96-1.03	0.65	1.00	0.94-1.07	0.904	0.91	0.83-1.01	0.070
Antiplatelet Drugs	0.35	0.09-1.35	0.13	0.22	0.04-1.21	0.082	0.44	0.02-9.65	0.602
Duration of ECMO	1.05	0.93-1.18	0.40	0.95	0.76-1.18	0.632	1.36	0.97-1.92	0.078
Body Mass Index	1.00	0.95-1.06	0.93	1.00	0.94-1.08	0.889	0.92	0.79-1.08	0.326
Severe Thrombocytopenia	2.68	0.87-8.25	0.09	5.59	1.27-24.58	0.023 †	0.25	0.01-5.24	0.375
Albumin	1.67	0.55-5.04	0.37	1.77	0.39-8.08	0.463	0.08	0.00-4.82	0.223
Predictors of Thrombosis *									
Age	0.94	0.90-0.99	0.011 †	0.95	0.87-1.03	0.216	0.91	0.80-1.04	0.165
Antiplatelet Drugs	2.49	0.49-12.70	0.274	4.50	0.48-42.09	0.187	1.39	0.05-37.61	0.844
Duration of ECMO	1.03	0.91-1.18	0.629	0.93	0.69-1.24	0.608	0.98	0.79-1.21	0.847
Body Mass Index	1.00	0.93-1.08	0.945	0.93	0.82-1.06	0.258	1.08	0.90-1.30	0.401
Severe Thrombocytopenia	5.30	1.30-21.68	0.02 †	5.82	0.74-46.09	0.095	665.09	0.71-620026.09	0.062
Albumin	1.20	0.35-4.09	0.771	0.78	0.12-5.17	0.799	146.33	1.16-18499.85	0.043 †
Predictors of Severe Thrombocytopenia **									
Age	1.00	0.96-1.03	0.933	0.98	0.93-1.04	0.561	0.94	0.85-1.04	0.234
Antiplatelet Drugs	0.50	0.13-1.94	0.316	0.58	0.13-2.57	0.475	0.00	0.00-Inf	0.996
Duration of ECMO	0.91	0.80-1.04	0.182	0.98	0.80-1.21	0.879	0.76	0.49-1.18	0.220
Body Mass Index	0.98	0.93-1.04	0.521	0.98	0.92-1.05	0.627	1.12	0.94-1.33	0.214
Albumin	0.77	0.26-2.25	0.628	0.71	0.17-2.89	0.632	0.00	0.00-1.22	0.058

ECMO, extracorporeal membrane oxygenation; Body Mass Index, body mass index; OR, odds ratio; CI, confidence interval. For continuous variables, odds ratios are in terms of changes in odds as a result of a one-unit change in the variable.

† Significant at *P*=0.05

* Adjusted for age, antiplatelet drugs, duration of ECMO, Body Mass Index, severe thrombocytopenia, and albumin level

** Adjusted for age, antiplatelet drugs, duration of ECMO, Body Mass Index, and albumin level

The mean platelet count lay outside the physiologic range (150-400 × 10^9/L) nearly 100% of the time and tended to decrease over time on ECMO (**Figure 7.1**). When analyzed by type of ECMO, patients on VA ECMO trended consistently below the physiologic range, whereas patients on VV experienced an initial dip followed by a rise in platelet count. No statistically significant difference in platelet count was observed between patients with and without thrombotic events (*P*=0.630) (**Figure 7.1**).

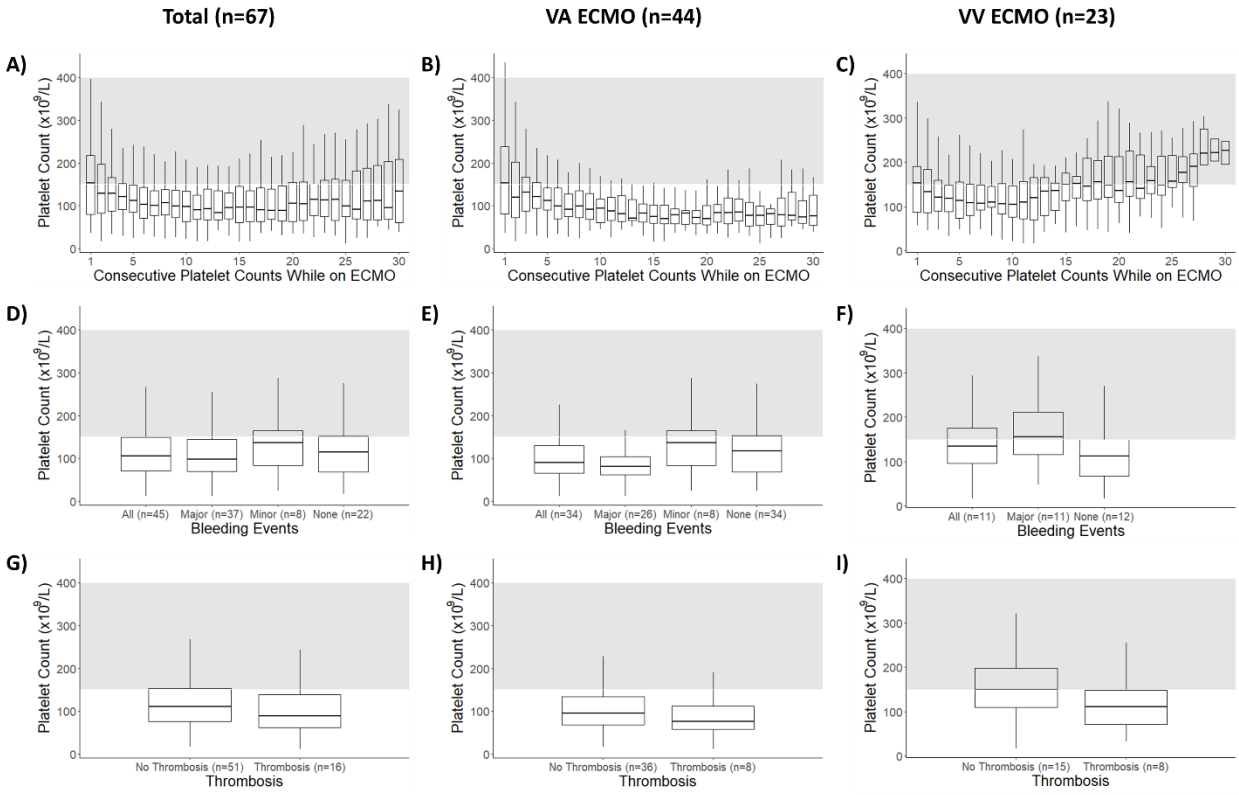

Figure 7.1 Platelet counts stratified by VA and VV ECMO. Consecutive platelet counts while undergoing ECMO treatment (A-C). Platelet counts stratified by hemorrhagic (D-F) and thrombotic (G-I) events. The gray region represents the physiologic platelet count range (150-400 × 10^9/L).

7.6 Discussion

In the outlined cohort study of 67 patients, we found that severe thrombocytopenia was common in patients undergoing ECMO and is predictive of mortality. After controlling for possible confounding variables in multivariate analysis, severe thrombocytopenia also predicted major bleeding in VA ECMO (although not in the entire cohort), and surprisingly was a risk factor for thrombotic events in the entire cohort. Our study provides new insight on the prevalence and clinical consequences of severe thrombocytopenia in patients on ECMO that have not previously been reported. Of the

patients in our study, 38.8% developed severe thrombocytopenia. Notably, of the 26 patients that developed severe thrombocytopenia, 20 (76.9%) were receiving VA ECMO and 6 (23.1%) were receiving VV ECMO. While limited by the small sample size, the duration of ECMO was not associated with the development of thrombocytopenia, consistent with previous studies.[287,290]

Thrombocytopenia is not uncommon in critically ill patients. Prior analysis have suggested incidences of thrombocytopenia up to 50% at some time point in critically ill patients admitted to the intensive care unit, with 5% to 20% of patients developing severe thrombocytopenia.[291] Multiple potentially overlapping mechanisms have been suggested to explain the worsening thrombocytopenia seen in critically ill patients including platelet clumping, hemodilution, underproduction, destruction or consumption.[292] Prior analysis have also suggests thrombocytopenia to be a predictor of both mortality and hemorrhage in critically ill patients, similar to our findings in patients on ECMO.[293] While disproportionately composed of patients on VA-ECMO, the overall survival of 58% in our cohort is similar to the survival reported by the Extracorporeal Life Support Organization Registry International Report 2016 of 58.7% in all adults on VV and VA ECMO.[294]

At first glance, it may seem counter intuitive that subjects with severe thrombocytopenia developed more thrombotic complications; however, there is some literature to suggest that the association between thrombocytopenia and ECMO use is confounded by the subjects' severity and duration of critical illness. One study found that 22% of subjects developed severe thrombocytopenia while receiving ECMO, but they also showed that a

higher initial severity of critical illness, lower baseline platelet count, and the development of hepatic or renal failure accounted for that association. It is possible that severe thrombocytopenia develops in patients who are more systemically ill and in more severe underlying proinflammatory and prothrombotic states.[290]Alternatively, it is plausible that the finding of severe thrombocytopenia led to less aggressive anticoagulation strategies and increased risk of thrombosis. Indeed, while the level of anticoagulation appeared to be unaffected in our cohort, the use of antiplatelet therapy was numerically diminished in patients who developed severe thrombocytopenia. Lastly, as we did not evaluate the temporal relationship of thrombocytopenia to thrombosis, thrombocytopenia may be a result of thrombosis rather than a cause. Equally plausible is the possibility that thrombocytopenia was a harbinger of still-occult thrombosis.

In regards to bleeding, several studies have demonstrated impaired platelet function during ECMO. Reduced expression of adhesion receptors GPIbα and GPVI and decreased levels of biomarkers of platelet activation, PF4 and ß-thromboglobulin during ECMO have been suggested as mechanisms for disrupted functional and structural thrombocyte integrity and aggregation in ECMO patients.[295,296]

The findings from this study are hypothesis generating and clinically relevant for several reasons. First, thrombosis and hemorrhage are common and severe complications of ECMO, and while acquired platelet dysfunction has previously been implicated,[297] platelet count remains a practical variable that can be easily tracked, and adjusted with transfusion or risk factor modification. However, previous studies have suggested that platelet transfusion may paradoxically increase the risk of thrombosis.[298] For instance,

Cashen et al. used a multivariable analysis to demonstrate that platelet transfusion volume was independently associated with increased daily thrombotic risk.[299]

Additionally, the role of anticoagulation in ECMO is not fully clear, given increasing reports of ECMO ran without anticoagulation highlighting the complex hemostatic milieu brought about by blood-device interactions and non-physiologic blood rheology provoked by the extracorporeal circuit.[300,301] As anticoagulant free ECMO seems increasingly feasible, it may seem plausible that severe thrombocytopenia is an indication to safely pause anticoagulation. However, our study found that the differences in mean daily heparin dose and the use of antiplatelet drugs were not statistically significant in patients who developed severe thrombocytopenia versus those who did not (P=0.958, P=0.403), suggesting that, at least at our center, there is a perceived need to continue heparin as much as possible. Although the ideal anticoagulation strategy for patients on ECMO therapy remains unclear, recommendations from the Extracorporeal Life Support Organization (ELSO) recommend UFH in all patients on ECMO.[302-304] A clinical trial is underway comparing traditional anticoagulation to anticoagulant free VV-ECMO which may provide insight into the true risks and benefits of anticoagulation in this population (NCT04273607). While further analysis is needed before definitive conclusions can be drawn, the finding that severe thrombocytopenia is associated with thrombosis suggests that continuing anticoagulation may be a consideration in ECMO patients who develop severe thrombocytopenia.

These findings should be taken in the context of the limitations of the analysis, including the small size of our cohort and the retrospective nature of our analysis. The

generalizability of these findings is likely constrained due to the small sample size. Furthermore, the data were collected retrospectively and therefore, one cannot control for all clinical factors that may have affected outcomes or may serve as residual confounders. A proportion of ECMO patients may have received left ventricular impellas as well, which were unaccounted for in this analysis. As impellas may represent an independent risk factor for bleeding, thrombosis, and thrombocytopenia this may be a confounder to our analysis. Moreover, due to the limitations of our data capture methods, we considered only the first 30 consecutive platelet counts when evaluating if patients developed severe thrombocytopenia; however, only two patients developed severe thrombocytopenia for a non-sustained period of time beyond the first 30 counts. In addition, asymptomatic ECMO patients were not routinely screened for thrombotic events; it is possible that more event would have been observed with this diagnostic strategy. Future studies should also incorporate validated ECMO risk scores such as APACHE II, SAVE, or PRESERVE to provide further information on disease severity and prediction of survival. Nonetheless, the results from this analysis should be considered as a larger prospective analysis evaluating the complex derangements of hemostasis and thrombosis associated with ECMO. As further data are generated, clinicians should be conscious of platelet count in patients on ECMO and consider potential strategies to mitigate the significant risks of hemorrhage and thrombosis associated with ECMO.

Chapter 8. Predictors of venous thrombosis in VV ECMO: an analysis of the ELSO Registry 2015-2019

Tia C.L. Kohs, Benjamin R. Weeder, Boris I. Chobrutskiy, Owen J.T. McCarty, David Zonies, Bishoy M. Zakhary, and Joseph J. Shatzel

This work is currently under review by the *Journal of Thrombosis and Thrombolysis*.

8.1 Abstract

Venovenous extracorporeal membrane oxygenation (VV-ECMO) is a life-saving therapy for critically ill patients, but it carries an increased risk of thrombosis due to blood interacting with non-physiological surfaces. While the relationship between clinical variables and thrombosis remains unclear, our study aimed to identify which factors are most predictive of thrombosis. The Extracorporeal Life Support Organization (ELSO) Registry was queried to obtain a cohort of VV-ECMO patients aged 18 years and older from 2015 to 2019. Patients who were over 80-years-old, at the extremes of weight, who received less than 24 hours of ECMO, multiple rounds of ECMO, or had missing data were excluded. Multivariate logistic regression modeling was used to assess predictors of thrombosis and mortality. Of the 16,453 patients who received VV-ECMO during the inclusion period, 9,538 patients were included in the analysis, with a mean age of 47.0±15.1 years and an average ECMO run time of 305±347 hours. Thrombosis occurred in 23% of the cohort, with circuit thrombosis and membrane lung failure being the most common. Multivariate analysis showed that ECMO runs over 14 days (OR: 3.18,

P<0.001) and higher pump flow rates (OR: 1.05, *P*=0.048) were associated with an increased risk of thrombosis. Additionally, patients with thrombosis were at increased likelihood of in-hospital mortality (OR: 1.49, *P*<0.001). This study confirmed well-known thrombotic risk factors in VV-ECMO and suggested that higher ECMO flow rates may increase the risk of thrombosis. Future studies investigating the impact of pump flow rate on blood rheology and hemostasis would be illuminating.

8.2 Graphical Abstract

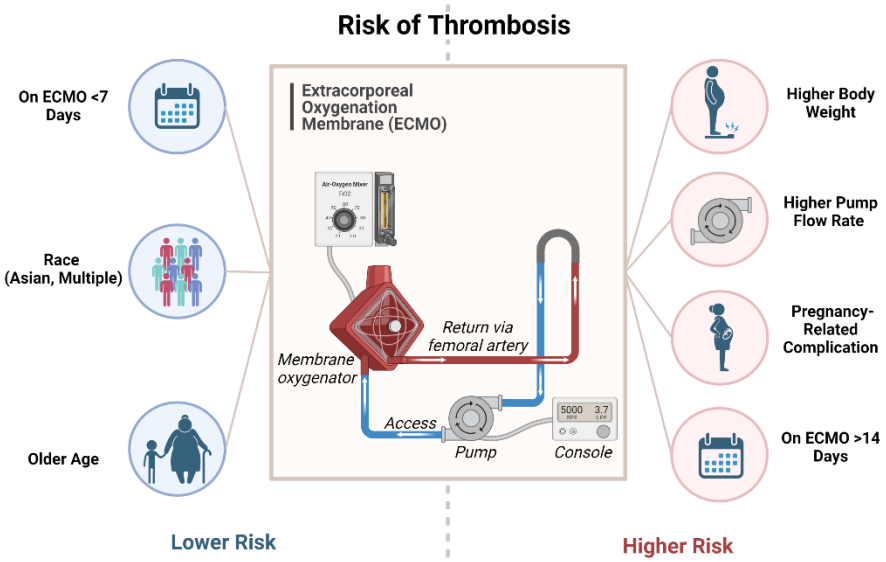

8.3 Introduction

For the last chapter of my dissertation, we performed additional multiple logistic regression analyses to assess predictors of thrombosis and mortality. In this retrospective cohort study, we queried the Extracorporeal Life Support Organization (ELSO) Registry from 2015 to 2019 to obtain a larger primary analysis population. Of the 16,453 ECMO patients documented during the designated study period, 9,538 of them were included in our analyses and thrombosis occurred in nearly a quarter of the cohort. We found that

ECMO runs longer than 14 days and higher pump flow rates were associated with an increased risk of thrombosis, and that thrombosis increased likelihood of in-hospital mortality. Although this work is hypothesis generating, further studies are required to determine the true associations between clinical factors and thrombosis. Nonetheless, these findings highlight the importance of effectively identifying, preventing and treating thrombotic events.

8.4 Background

Venovenous extracorporeal membrane oxygenation (VV ECMO) is a form of mechanical life support for patients with severe respiratory failure.[305] The use of VV ECMO has increased significantly in recent years, in part to support patients with coronavirus disease 2019 (COVID-19) experiencing severe respiratory failure.[306 307] However, despite the potentially lifesaving benefits of ECMO,[105,106] pathologic blood clotting (thrombosis) is a well-known complication of ECMO, with reported incidences of over 25% in some studies.[308-310] Clot buildup can lead to decreased or ceased circuit blood flow, membrane lung failure, and pulmonary or systemic emboli, all of which can result in significant morbidity and mortality.[305]

The incidence of thrombotic complications during ECMO can be influenced by a variety of patient-, circuit-, and management-related factors. For example, patients receiving frequent transfusions of blood products or who develop severe thrombocytopenia, a marker of critical illness, are at increased risk for thrombotic events while on ECMO.[308,311] Additionally, ECMO exposes blood to non-biologic material and non-pulsatile flow; this in turn leads to platelet activation and initiation of the intrinsic

pathway of coagulation and systemic inflammatory responses [312,313]. Inappropriate maintenance of the circuit (e.g. insufficient monitoring for air bubbles, tube compression or kinks, etc.) can contribute to thrombosis.[307] Lastly, the intensity and duration of anticoagulation therapy, as well as the type of anticoagulant used, may also impact the risk of clotting in ECMO, although these decisions underscore the precarious balance regarding the risk of bleeding imparted by anticoagulation.[308] At present, there is no evidence-based consensus for anticoagulation practices or monitoring coagulation status in ECMO patients.[313,314] The risk of clotting with ECMO use is a multifactorial issue that requires careful attention to patient-, circuit-, and management-related factors to optimize outcomes. Additionally, our current ability to identify the subset of patients with the highest risk of thrombosis, and who could benefit the most from prophylaxis or targeted interventions, is limited.

Our hypothesis is that by utilizing data from the ELSO Registry, we will be able to identify clinically relevant variables that accurately predict thrombosis in adult patients receiving VV-ECMO for respiratory failure. Specifically, the objective of this work is to determine which clinical factors are most predictive of thrombosis in this patient population.

8.5 Material and Methods

8.5.1 *Study Design and Data Source*

We queried the ELSO Registry for adults (≥ 18 years old) on VV ECMO between 1/1/2015 and 12/31/2019. Data included information on patient demographics, cannulation strategies, ECMO specific factors, and clinical outcomes. Patients were

excluded if their records were missing critical data, including: age, weight, sex, race, history of cardiac arrest and transplant, duration and year on ECMO, primary diagnosis, discharge status (survival), support type, run number, and cannulation site. We also excluded patients if they were ≥ 80 years old, had a weight outside of the limits defined by the ELSO Registry (< 10.0 kg or > 500.0 kg), or received multiple ECMO runs (**Figure 8.1**).

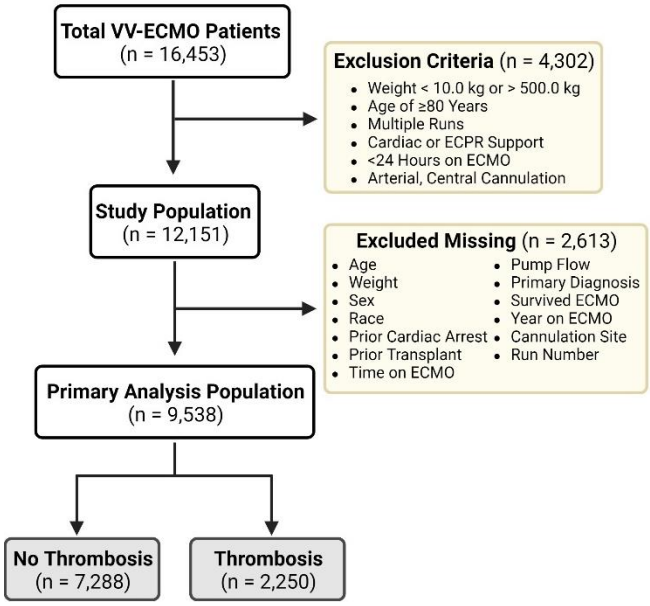

Figure 8.1 Exclusion criteria used for defining the primary analysis population. VV ECMO, venovenous extracorporeal membrane oxygenation. ECPR, extracorporeal cardiopulmonary resuscitation.

8.5.2 *Thrombotic Events*

We defined thrombotic events using the Complications Codes and the Registry Data Definitions provided by ELSO (**Supplemental Table 8.1**).[315,316] Thrombotic events were classified as: circuit thrombosis, membrane failure, circuit exchange, hemolysis, CNS infarction, hemofilter clot, ischemia, or pump failure.

Supplemental Table 8.1 ECLS Codes used to define the thrombosis subgroups included in the analyses.

Code	Description
101	Membrane Lung Failure
104	Blood Pump Failure
114	Hemofilter Clot
132	Circuit Change
133, 134	Circuit Thrombosis
321	CNS Infarction
211, 822, 823	Hemolysis
901	Ischemia

8.5.3 *Statistical Analysis*

For continuous variables, data were reported as mean ± standard deviation (SD). For categorical variables, data were reported as frequency and the percentage of total. Since pump flow rates were correlated to body weight (**Supplemental Figure 8.1**), normalized flow rates were calculated for unadjusted analyses by dividing the pump flow rates at 24 hours by the weight of the patients. To compare differences between cohorts, *P*-values were calculated using Fisher exact tests, Wilcoxon-Mann-Whitney tests, or t-tests. Statistical significance was defined as $P < 0.05$ for simple demographic comparisons.

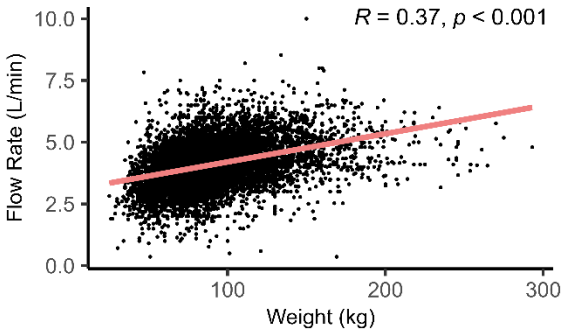

Supplemental Figure 8.1 Scatterplot showing a positive correlation between pump flow rate at 24 hours and body weight.

A multivariate logistic regression model was used to determine clinically meaningful predictors of thrombosis. Select risk factors for thrombosis were selected a priori based on known relevance for the regression model. Variable categories with a low frequency of observations (< 1%) were binned as "other", with the exception of cannulation sites as these were primary predictors of interest. For multiple logistic regression models, statistical significance was defined as an adjusted $P<0.05$. The covariates in the final model were evaluated for collinearity using the variance inflation factor. All statistics were calculated using R (R Foundation for Statistical Computing, Version 4.2).

8.6 Results

8.6.1 *Primary Analysis Population Characteristics*

There were 16,453 ECMO patients in the ELSO Registry during the five-year study period. After excluding patients missing data or met exclusion criteria, the primary analysis population was 9,538 patients. This population was stratified by incidence of a thrombotic event (**Figure 8.1**). The mean age of patients in the primary analysis population was 47.0 (± 15.1) years old and the cohort was predominantly male (61.2%). A full list of the cohort demographics is included in **Table 8.1.**

Table 8.1 Demographic information for adult patients on VV-ECMO
VV-ECMO, venovenous (VV) extracorporeal membrane oxygenation. VAD, ventricular assist device.

Characteristic	All Patients N = 9538[1]	No Thrombosis N = 7,288[1]	Thrombosis N = 2,250[1]	P-Value[2]
Age (years)	46.99 (15.11)	47.26 (15.18)	46.13 (14.85)	0.002
Weight (kg)	89.63 (29.82)	88.94 (29.33)	91.86 (31.27)	<0.001
Sex				
Male	5,838 (61.2%)	4,427 (60.7%)	1,411 (62.7%)	0.094
Female	3,700 (38.8%)	2,861 (39.3%)	839 (37.3%)	0.097
Race				
White	5,682 (59.6%)	4,319 (59.3%)	1,363 (60.6%)	0.269
Black	1,217 (12.8%)	949 (13.0%)	268 (11.9%)	0.170
Asian	1,161 (12.2%)	910 (12.5%)	251 (11.2%)	0.097
Middle Eastern or North African	138 (1.4%)	91 (1.2%)	47 (2.1%)	0.005
Native American	36 (0.4%)	21 (0.3%)	15 (0.7%)	0.017
Native Pacific Islander	15 (0.2%)	14 (0.2%)	1 (0.0%)	0.218
Hispanic	717 (7.5%)	533 (7.3%)	184 (8.2%)	0.185
Multiple	318 (3.3%)	260 (3.6%)	58 (2.6%)	0.022
Other	254 (2.7%)	191 (2.6%)	63 (2.8%)	0.653
Prior Cardiac Arrest	829 (8.7%)	674 (9.2%)	155 (6.9%)	<0.001
Prior Transplant	516 (5.4%)	391 (5.4%)	125 (5.6%)	0.709
Time on ECMO (hours)	304.55 (346.88)	245.37 (256.14)	496.24 (499.57)	<0.001
Pump Flow Rate (L/min)	4.08 (0.91)	4.05 (0.90)	4.19 (0.92)	<0.001
Primary Diagnosis				
Diseases of the respiratory system	7,055 (74.0%)	5,367 (73.6%)	1,688 (75.0%)	0.197
Injury and poisoning	469 (4.9%)	353 (4.8%)	116 (5.2%)	0.540
Infectious and parasitic diseases	453 (4.7%)	345 (4.7%)	108 (4.8%)	0.910
Diseases of the circulatory system	452 (4.7%)	362 (5.0%)	90 (4.0%)	0.061
Pregnancy related complication	130 (1.4%)	89 (1.2%)	41 (1.8%)	0.037
Endocrine, nutritional and metabolic diseases	121 (1.3%)	93 (1.3%)	28 (1.2%)	1.000
Other	858 (9.0%)	679 (9.3%)	179 (8.0%)	0.052
Survived ECMO	6,340 (66.5%)	5,046 (69.2%)	1,294 (57.5%)	<0.001
Year on ECMO				<0.001
2015	1,123 (11.8%)	814 (11.2%)	309 (13.7%)	0.001
2016	1,550 (16.3%)	1,125 (15.4%)	425 (18.9%)	<0.001
2017	1,703 (17.9%)	1,311 (18.0%)	392 (17.4%)	0.550
2018	2,375 (24.9%)	1,862 (25.5%)	513 (22.8%)	0.009
2019	2,787 (29.2%)	2,176 (29.9%)	611 (27.2%)	0.014
Cannulation Site				
Femoral Vein	6,513 (68.3%)	4,985 (68.4%)	1,528 (67.9%)	0.678
Internal Jugular Vein	7,367 (77.2%)	5,600 (76.8%)	1,767 (78.5%)	0.095
Subclavian Vein	122 (1.3%)	103 (1.4%)	19 (0.8%)	0.041
Discontinuation Reason				
Expected Recovery	6,771 (71.0%)	5,366 (73.6%)	1,405 (62.4%)	<0.001
Died or Poor Prognosis	2,497 (26.2%)	1,710 (23.5%)	787 (35.0%)	<0.001
Organ Transplant	104 (1.1%)	91 (1.2%)	13 (0.6%)	0.007
ECMO Complication	81 (0.8%)	52 (0.7%)	29 (1.3%)	0.012
Resource Limitation	13 (0.1%)	8 (0.1%)	5 (0.2%)	0.202
Transition to VAD Support	6 (0.1%)	5 (0.1%)	1 (0.0%)	1.000
Unknown	66 (0.7%)	56 (0.8%)	10 (0.4%)	0.111

[1] Mean (SD); n (%)
[2] Wilcoxon rank sum test; Pearson's Chi-squared test

8.6.2 *Prevalence of Thrombotic Complications*

Of the patients in the primary analysis population, 2,250 patients had a qualifying thrombotic event (23.6%). The most common thrombotic events were circuit thrombosis (8.6%) followed by membrane lung failure (6.1%). Other, less frequent patient-specific thrombotic events include CNS infaction (1.4%), hemofilter clot (1.1%), ischemia (1.0%), and blood pump failure (0.9%). The full breakdown of thrombotic events is listed in **Table 8.2**.

Table 8.2 Thrombotic complications for adult patients on VV-ECMO.

Characteristic	All Patients N = 9538[1]
Circuit Thrombosis	819 (8.6%)
Membrane Lung Failure	579 (6.1%)
Circuit Change	514 (5.4%)
Hemolysis	482 (5.1%)
CNS Infarction	131 (1.4%)
Hemofilter Clot	103 (1.1%)
Ischemia	95 (1.0%)
Blood Pump Failure	85 (0.9%)

[1] Mean (SD); n (%)

Patients were more likely to have a thrombotic event if they were on ECMO longer (P<0.001), had a higher weight (P<0.001), or had a higher flow rate at 24 hours after starting ECMO (P<0.001). Unadjusted data visualizing the distributions of pump flow rates at 24 hours is presented in **Figure 2.** Higher blood flow rates at 24 hours were associated with an increased incidence of hemolysis, circuit exchange, and mortality (P<0.001 for all).

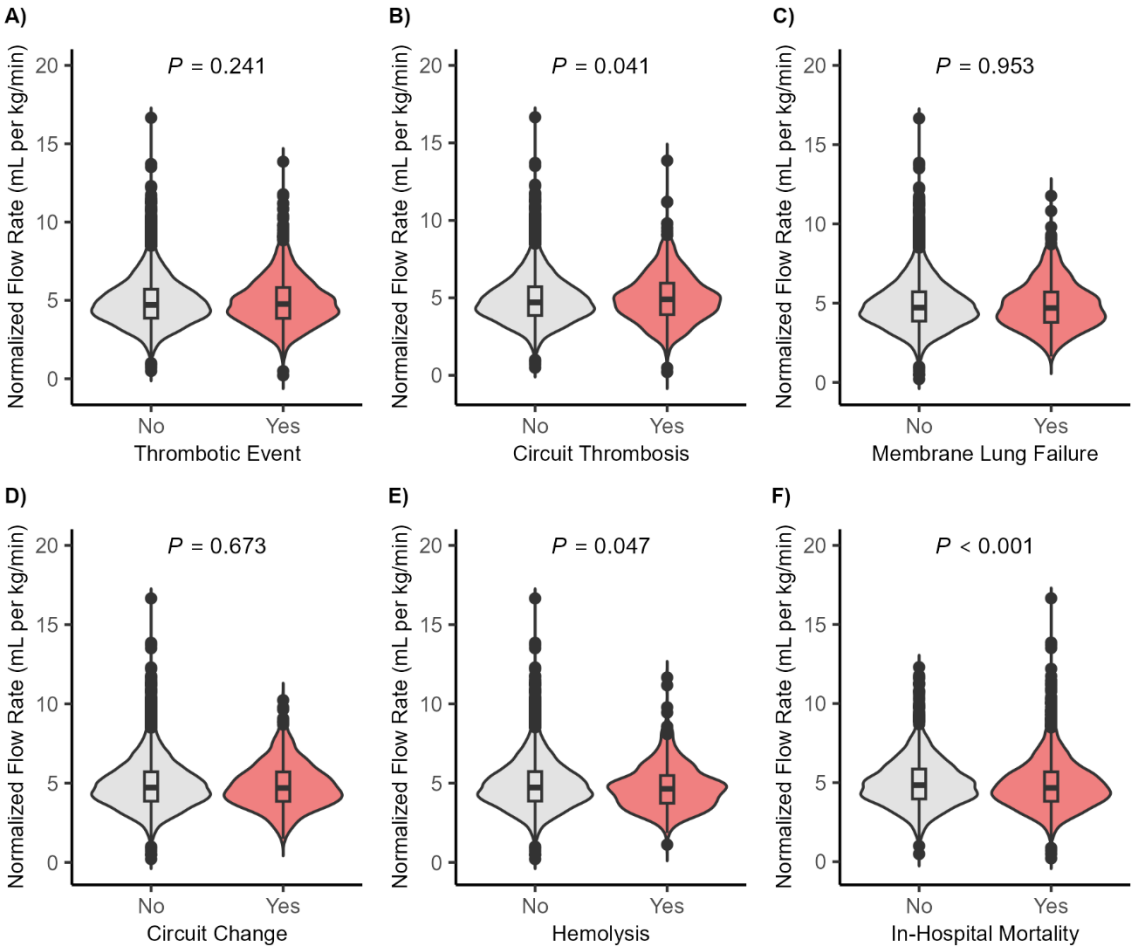

Figure 8.2 Violin plot showing the flow rate at 24 hours for patients stratified by the incidence of thrombotic events or in-hospital mortality. Violin plot showing normalized flow rates stratified by the incidence of a thrombotic event (A), circuit clot/air emboli (B), membrane lung failure (C), circuit change (D), hemolysis (E), or in-hospital mortality (F). Statistical significance is indicated by one asterisk (*) for $P<0.05$.

8.6.3 *Predictors of Thrombosis (As a Composite of All Thrombotic Events)*

After controlling for potential risk factors for thrombotic events, risk factors included higher body weight (OR: 1.02 [1.01-1.04], $P<0.001$), higher pump flow rates at 24 hours (OR: 1.05 [1.00-1.10], $P=0.048$), being on ECMO greater than 14 days (OR: 3.18 [2.82-3.58], $P<0.001$), and a primary diagnosis of pregnancy-related complications (OR: 1.57 [1.04-2.33], $P=0.028$). Patients that were older (up to 80 years old) (OR: 0.96 [0.93-

1.00], *P*=0.028) or on ECMO for less than 7 days (OR: 0.52 [0.46-0.60], *P*<0.001) were at a lower risk for thrombotic events (**Figure 8.3**).

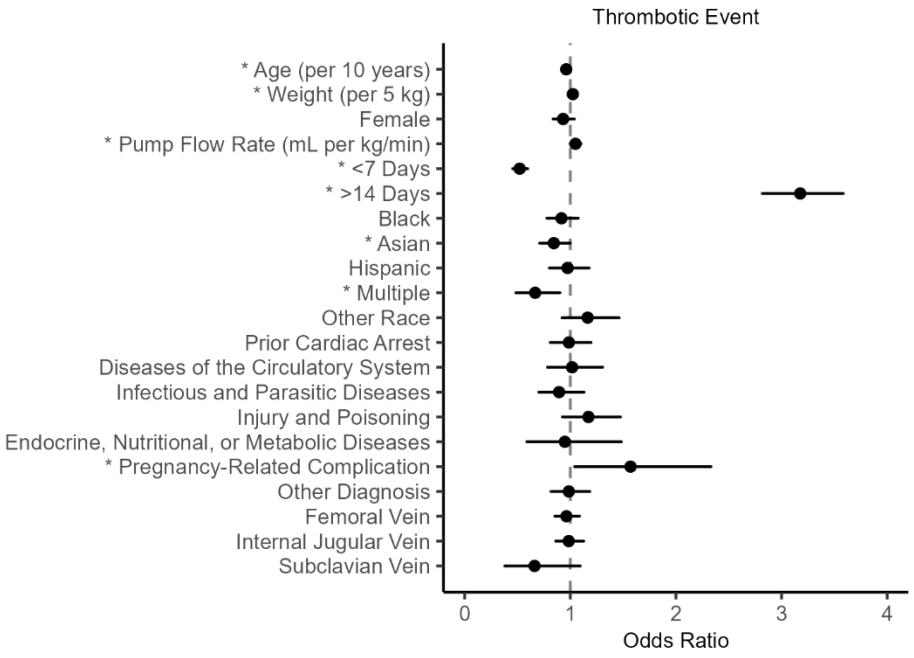

Figure 8.3 Clinical characteristics and cannulation sites associated with thrombotic events. Forest plot showing the effect of covariates on the incidence of a thrombotic event. The closed symbol represents the odds ratio and the whiskers represent the 95% confidence interval. The dashed line indicates the covariate had no effect compared to the reference patient. Statistical significance is indicated by one asterisk (*) for *P<0*.05.

8.6.4 *Predictors of Circuit Thrombosis and Membrane Lung Failure*

Risk factors for circuit thrombosis included higher pump flow rates at 24 hours (OR: 1.07 [1.00-1.15], *P*=0.039), being on ECMO greater than 14 days (OR: 2.18 [1.83-2.59], *P*<0.001), a primary diagnosis of a pregnancy-related complications (OR: 2.69 [1.66-4.21], *P*<0.001), a primary diagnosis of injury or poisoning necessitating ECMO use (OR: 1.81 [1.34-2.42], *P*<0.001), and cannulation of the internal jugular vein relative to cannulation of the femoral vein (OR: 1.25 [1.02-1.54], *P*=0.037). Patients on ECMO for less than 7 days (OR: 0.50 [0.41-0.62], *P*<0.001) or had a cannula placed in the femoral

vein (OR: 0.82 [0.69-0.97], *P*=0.018) were at a lower risk for of circuit thrombosis (**Figure 8.4A**).

Risk factors for membrane lung failure included higher body weight (OR: 1.02 [1.00-1.04], *P*=0.022) and being on ECMO greater than 14 days (OR: 3.73 [3.03-4.61], *P*<0.001). Patients that were older (up to 80 years old) (OR: 0.93 [0.87-0.99], *P*=0.018), on ECMO for less than 7 days (OR: 0.35 [0.26-0.48], *P*<0.001), or female (0.73 [0.61-0.89], *P*=0.002) were at a lower risk for membrane lung failure (**Figure 8.4B**).

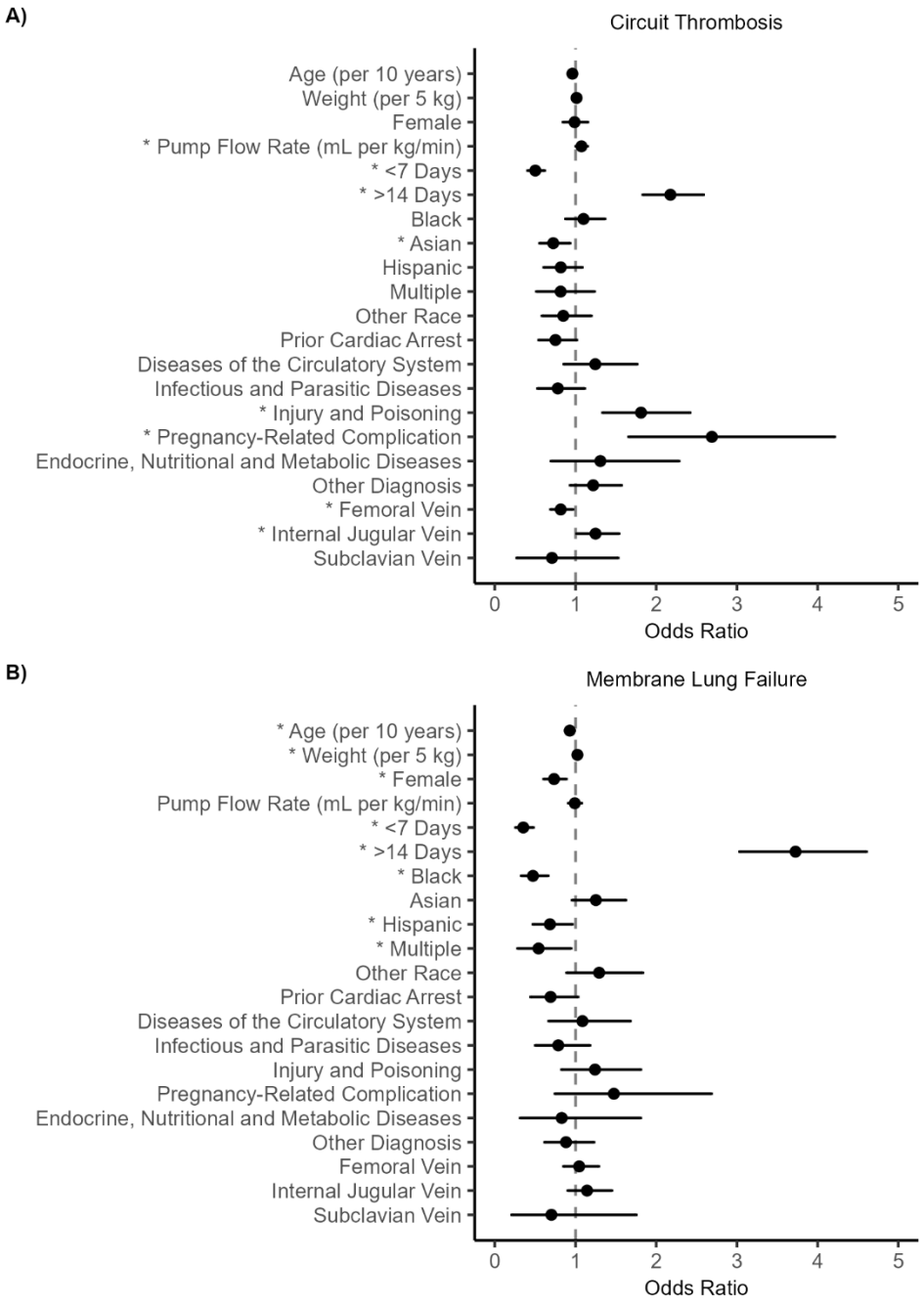

Figure 8.4 Clinical characteristics and cannulation sites associated with circuit clots or air emboli. Forest plot showing the effect of covariates on the incidence of a circuit clot/air embolus (A) or membrane lung failure (B). The closed symbol represents the odds ratio and the whiskers represent the 95% confidence interval. The dashed line indicates the covariate had no effect compared to the reference patient. Statistical significance is indicated by one asterisk (*) for $P<0.05$.

8.6.5 *Predictors of In-Hospital Mortality*

Risk factors for in-hospital mortality included thrombosis (OR: 1.49 [1.33-1.65], *P*<0.001), older age (OR: 1.38 [1.33-1.42], *P*<0.001), being on ECMO greater than 14 days (OR: 1.95 [1.73-2.19], *P*<0.001), having a history of cardiac arrest (OR: 1.69 [1.45-1.97], *P*<0.001) or organ transplant (OR: 1.26 [1.04-1.53], *P*=0.040), a primary diagnosis of infectious and parasitic diseases necessitating ECMO (OR: 1.35 [1.10-1.65], *P*=0.012), and cannulation at the internal jugular vein (OR: 1.15 [1.02-1.30], *P*=0.040). Patients with a higher body weight (OR: 0.98 [0.97-0.99], *P*=0.022) were at a lower risk for in-hospital mortality (**Figure 8.5**).

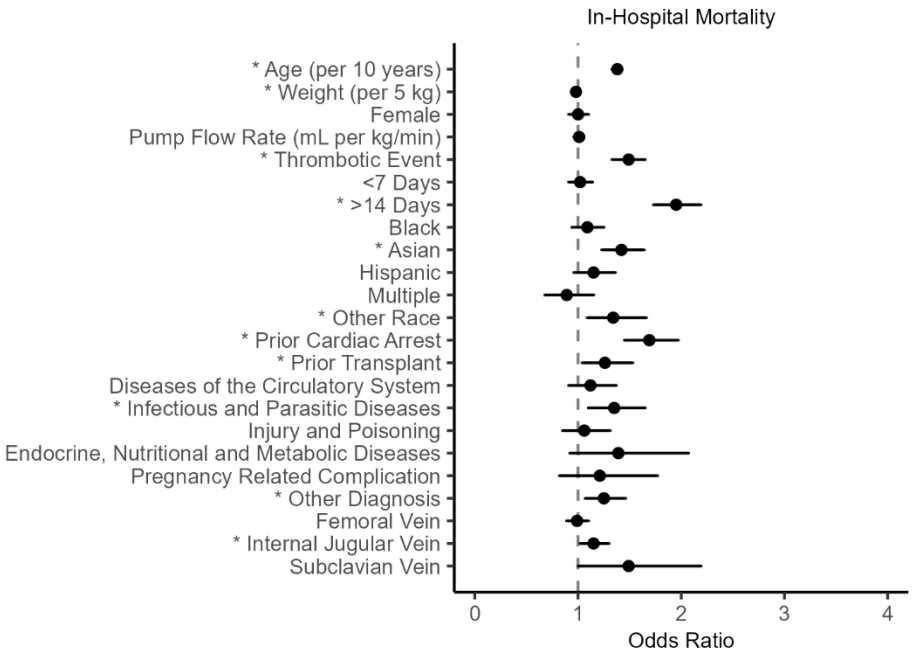

Figure 8.5 Clinical characteristics and cannulation sites associated with in-hospital mortality. Forest plot showing the effect of covariates on the incidence of in-hospital mortality. The closed symbol represents the odds ratio and the whiskers represent the 95% confidence interval. The dashed line indicates the covariate had no effect compared to the reference patient. Statistical significance is indicated by one asterisk (*) for *P<0.*05.

8.7 Discussion

In this analysis of patients on VV ECMO, we corroborated other studies which found that time on ECMO and weight are predictive of thrombosis.[317-319] Likewise, our analysis identified well known thrombotic risk factors, such as pregnancy.[320] Unique to our analysis, we found that pump flow rate at 24 hours was predictive of thrombotic device failure, hemolysis, and mortality, which, to the best of our knowledge, has not been reported previously. This work adds to the growing literature showing that both patient-specific and device-specific risk factors are predictive of thrombosis in VV ECMO. Notably, we found that patients who developed a thrombotic event had a higher mortality, highlighting the critical need to effectively identify, prevent and treat thrombotic events.

Multiple variables determine ECMO blood flow rate including patient size, native cardiac output, and target arterial oxygen content.[321] After controlling for patient weight and other confounders, we determined that higher ECMO blood flow rates at 24 hours were predictive of thrombotic device occlusion. This is initially counterintuitive as blood stasis and low flow states are well-known risk factors for thrombosis;[322,323] however, extracorporeal devices have significant and often unpredictable effects on blood rheology and hemostatic balance. For instance, preclinical work using *ex vivo* ECMO models demonstrate that lower flow rates (2.5 L/min vs. 4 L/min) increased hemolysis and lead to the loss of low high-molecular weight vWF multimers and ristocetin-induced platelet aggregation.[324] This observation by Ki *et al.* suggests that lower flow rates may tip the hemostatic balance towards bleeding. There are potential confounders for this observation that we were unable to measure due to a lack of available data in the ELSO

Registry. For instance, it is possible patients on higher blood flow rates are less predisposed to be on anticoagulation or receive lower doses of anticoagulation then those receiving lower flow rates.

There are several limitations of our analysis that should be noted. While comprehensive, the ELSO Registry has the potential for incomplete data, biases that can limit the translatability of the findings, and limited clinical variables that may impact study findings. For instance, the inability to control for anticoagulation use (to assess for the absence of anticoagulation, as well as the type and dose used) and to assess for peripheral thrombosis (e.g. deep vein thrombosis, pulmonary embolism) is a major limitation. Another limitation is the ability to only assess blood flow rate at a finite time point, as mean blood flow rates for longer observation periods may be more informative.

In conclusion, this large analysis of patients on VV-ECMO showed that higher pump flow rates at 24 hours correlated with an increased risk of circuit thrombosis. Thus, larger translational work assessing the impact of blood flow rate on blood rheology and hemostasis would be illuminating. This work is hypothesis generating, but requires further study to determine the true associations between ECMO blood flow rate and thrombosis.

Chapter 9. Conclusions and Future Directions

9.1 Conclusions

In my dissertation, I investigated the nuanced interactions between the various players in the blood microenvironment (e.g. endothelial cells, platelets, coagulation factors), and how these interactions impact vascular diseases and responses to medical devices. These efforts were directed toward developing tools to target both the intracellular and extracellular pathways implicated here, as well as identifying relevant predictors of adverse clinical outcomes to inform patient care.

In the first two studies, we utilized a nonhuman primate (NHP) model of diet-induced hyperlipidemia to study the contributions of Tec family kinases (TFKs) and coagulation factor (F) XI to the thromboinflammatory milieu. More specifically, we initially focused on targeting platelet activation through the TFK, Bruton's tyrosine kinase (Btk), using ibrutinib. Although ibrutinib is regarded as a first generation Btk inhibitor with known effects on platelet signaling,[131] ibrutinib can also bind to the conserved cysteine residue and inhibit the kinase activities of numerous TFKs.[133] Indeed, our preliminary *in vitro* work led us to a discovery on endothelial cell signal transduction in which VEGF-A induced endothelial activation, as measured by VCAM-1 expression, in a manner that was dependent upon the endothelial TFK, bone marrow tyrosine kinase on chromosome X (Bmx). We then observed that treatment ibrutinib inhibited platelet deposition and endothelial cell activation our NHP model. Taken together, this suggest that TFKs may contribute to the pathologies underlying atherosclerosis and could represent a novel therapeutic target.

Building upon what we observed with the TFK work in the NHP model, we next investigated the role of FXI in sustaining the thromboinflammatory phenotype associated with chronic hyperlipidemia. In this study, we pharmacologically targeted FXI using the monoclonal antibody, humanized 1A6. This antibody prevents FXI activation by FXIIa as well as FIX and FV activation by FXIa. We found that treatment with h1A6 reduced: 1) levels of inflammatory biomarker, C-reactive protein; 2) platelet reactivity to activation by GPVI and PAR-1 agonists; and 3) endothelial cell activation as measured by VCAM-1 levels. These data suggest that therapeutic agents targeting FXI may extend beyond anticoagulation to include both antiplatelet and anti-inflammatory benefits.

We continued our investigation of FXI in the setting of thromboinflammation as we pivoted to a murine model of multiple sclerosis (MS), experimental autoimmune encephalomyelitis (EAE). For this work, we treated EAE mice with the monoclonal antibody, 14E11, which has been shown to selectively inhibits the activation of FXI by FXIIa and reciprocal activation of FXII by FXIa *in vitro*.[1,2] The objective was to evaluate if pharmacological targeting of FXI could improve neurological function and attenuate CNS damage. Our results demonstrated that targeting FXI reduced disease severity, immune cell migration, axonal damage, and BBB disruption in mice with EAE. These findings suggest that therapeutic agents targeting FXI and FXII may also provide a useful approach for treating autoimmune and neurologic disorders.

We next shifted our focus from the role intrinsic pathway of coagulation in the setting of diseases to the setting of vascular devices. More specifically, we performed functional assays to characterize anti-FXII antibodies developed by our group. Based on the

findings from initial screenings, 1B2 was selected for further testing in a baboon model of vascular device-initiated thrombosis. Following treatment with 1B2, we observed a reduction in platelet deposition and fibrin formation. Thus, targeting FXII activation and FXIIa activity may reduce or prevent vascular-device associated thrombosis in a variety of clinical settings, including extracorporeal membrane oxygenators (ECMO).

Following in on this, the next section detailed a single-center retrospective cohort study of patients on ECMO at Oregon Health & Science University (OHSU). The objective of this study was to define the incidence, predictors, and clinical consequences of severe thrombocytopenia (platelet count $<50 \times 10^9$/L) in ECMO patients. Using a multivariate logistic regression model, we found that severe thrombocytopenia is predictive of thrombosis in adults undergoing ECMO treatment. This finding is important because it provides insight on the prevalence and clinical consequences associated with severe thrombocytopenia in patients on ECMO.

We then performed a retrospective cohort study that built upon the analyses from the single-center study described above. For this set of analyses, we queried the Extracorporeal Life Support Organization (ELSO) Registry from 2015 to 2019 to obtain a larger primary analysis population. During the designated study period, there were 16,453 ECMO patients, of which 9,538 of them were included in our analyses. We then developed a multivariate logistic regression model to identify predictors of thrombosis. We found that ECMO runs that exceeded 14 days and higher pump flow rates were associated with an increased thrombotic risk, and that thrombosis increased likelihood of in-hospital mortality.

Overall, these studies provide new insights regarding the interplay between endothelial cells, platelets, and coagulation in the blood microenvironment. The studies described in the 'Future Directions' section are suggested to better delineate if FXI activation or FXIa activity drives inflammation and platelet function.

9.2 Future Directions

9.2.1 *Platelet Priming for Activation as a Product of FXI Activation or FXIa Activity*

In Chapter 4, we showed that platelets in hyperlipidemic primates are sensitized toward activation, as measured by platelet P-selection expression to a GPVI agonist (CRP-XL) or a PAR-1 agonist (TRAP-6), as compared to platelets from a lean cohort (**Figure 4.1B, D**). Following treatment of obese primates with h1A6, an antibody that blocks FXIIa-mediated activation of FXI and FXIa-mediated activation of FIX and FV, platelet sensitization to CRP-XL and TRAP-6 was reversed (**Figure 4.5A, C**). Despite these findings, it remains unclear if the platelet sensitization was dependent on FXI activation or FXIa activity, as thrombin can still feedback to activate additional FXI and platelets. Thus, to better delineate the mechanistic underpinnings driving platelet function, future studies may benefit from comparing 3G3 (an antibody that blocks FXIIa-mediated activation of FXI) to abelacimab (MAA 868, an antibody that locks FXI into a zymogen state and inhibits FXIa activity). In addition to measuring P-selectin expression as a marker of platelet activation, it may also be useful to measure platelet aggregation and platelet-leukocyte interactions. This would include tasks such as quantifying cytokine levels, leukocyte activation, and markers of NETs formation including MPO and citrullinated histones.[325,326]

9.2.2 *The Role of FXI Activation or FXIa Activity in Inflammation*

In Chapter 4, we demonstrated that pharmacological inhibition of FXI reduced inflammatory markers, including the hallmark biomarker C-reactive protein, in our NHP model of diet-induced obesity. More specifically, we showed that the elevated levels of CRP in the obese cohort were reduced by ~25% following 4-weeks of anti-FXI therapy (**Figure 9.1A**). Moreover, our team has demonstrated that pharmacological inhibition of FXI lowered CRP levels in a clinical trial in end-stage renal disease patients on hemodialysis (**Figure 9.1B**).[194] Continuing this theme, preliminary data from our clinical trial evaluating FXI inhibition for the prevention of catheter-associated thrombosis show that inhibition of FXI activation blunted the rise in CRP levels following placement of an indwelling catheter (**Figure 9.1C**). Taken together, these findings provide evidence of a link between the FXI activation and inflammation.

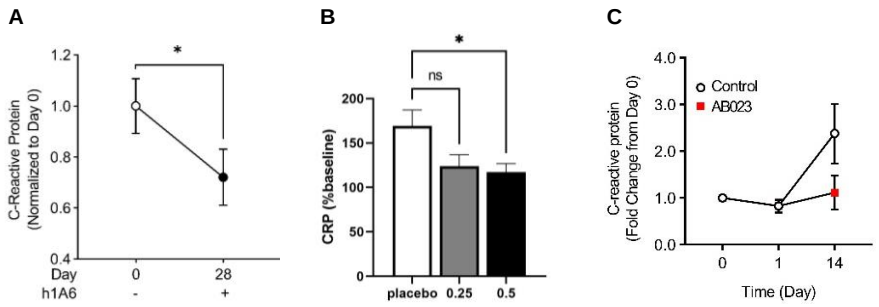

Figure 9.1 FXI inhibition blunts C-reactive protein levels. (A) FXI inhibition with h1A6 decreases CRP levels in a nonhuman primate model of diet-induced hyperlipidemia. (B) FXI inhibition with AB023 blunts CRP levels in patients on dialysis. CRP levels on study day 0- and 24-hours post-dose, expressed as % of baseline in placebo or 0.25 or 0.5 mg/kg AB023 group. Reprinted with permission from Lorentz et al., *Blood* 2021 Dec 2;138(22):2173-2184.[194] (C) FXI inhibition with AB023 blunts CRP in patients following catheter insertion. CRP levels measured on study day 0 and 1 and 14 days after insertion of an indwelling catheter, expressed as fold-change from baseline in the placebo group and the 2 mg/kg AB023 group. Unpublished data. Data are shown as mean ± SEM. **P*<0.05.

Although CRP levels can be an informative biomarker for gauging inflammatory responses, the mechanisms relating C-reactive protein and coagulation FXI remain ill-defined. To date, we know that C-reactive protein dissociates to regulate the innate immune system by way of the complement cascade and to serve as an effector in thrombosis [327-329]. Indeed, our group has shown that FXIa can inactivate one of the central inhibitors of the complement system, complement factor H (CFH).[143] Furthermore, inhibition of FXI activation in a NHP sepsis model abrogated the rise in C3b and C5b-9 levels in response to a bacterial challenge.[2,142] Thus, we hypothesize that inhibiting FXI activation or FXIa activity will preserve the active state of CFH, which will enhance complement activity by preserving CRP-CFH interactions.

To test this hypothesis, one could measure levels of CFH and complement system members, (e.g. C3b and C5b-9) in the obese primates at baseline and following treatment with FXI activation or FXIa activity inhibitors. It would also be illuminating to study the converse of this hypothesis—that inhibition of the complement system will reduce levels of FXIa as well as kallikrein and FXIIa in this model of diet-induced hyperlipidemia, as measured in enzyme complexes with C1-INH. Defining the mechanisms by which FXI has a role in propagating inflammation would provide insight into if FXI inhibition has potential therapeutic anti-inflammatory benefits in CVD and in particular, hyperlipidemia.

References

1. Lorentz CU, Verbout NG, Cao Z, et al. Factor XI contributes to myocardial ischemia-reperfusion injury in mice. *Blood advances*. 2018;2(2):85.

2. Silasi R, Keshari RS, Lupu C, et al. Inhibition of contact-mediated activation of factor XI protects baboons against S aureus-induced organ damage and death. *Blood Adv*. Feb 26 2019;3(4):658-669. doi:10.1182/bloodadvances.2018029983

3. Claesson-Welsh L, Dejana E, McDonald DM. Permeability of the Endothelial Barrier: Identifying and Reconciling Controversies. *Trends Mol Med*. Apr 2021;27(4):314-331. doi:10.1016/j.molmed.2020.11.006

4. Galley HF, Webster NR. Physiology of the endothelium. *British Journal of Anaesthesia*. 2004;93(1):105-113. doi:10.1093/bja/aeh163

5. Sandoo A, van Zanten JJ, Metsios GS, Carroll D, Kitas GD. The endothelium and its role in regulating vascular tone. *Open Cardiovasc Med J*. Dec 23 2010;4:302-12. doi:10.2174/1874192401004010302

6. Gale AJ. Continuing Education Course #2: Current Understanding of Hemostasis. *Toxicol Pathol*. Jan 2011;39(1):273-80. doi:10.1177/0192623310389474

7. Versteeg HH, Heemskerk JWM, Levi M, Reitsma PH. New Fundamentals in Hemostasis. *Physiological Reviews*. 2013;93(1):327-358. doi:10.1152/physrev.00016.2011

8. Moore EE, Moore HB, Kornblith LZ, et al. Trauma-induced coagulopathy. *Nature Reviews Disease Primers*. 2021/04/29 2021;7(1):30. doi:10.1038/s41572-021-00264-3

9. Krüger-Genge A, Blocki A, Franke RP, Jung F. Vascular Endothelial Cell Biology: An Update. *Int J Mol Sci*. Sep 7 2019;20(18)doi:10.3390/ijms20184411

10. Rahimi N. Defenders and Challengers of Endothelial Barrier Function. *Front Immunol*. 2017;8:1847. doi:10.3389/fimmu.2017.01847

11. Bazzoni G, Dejana E. Endothelial Cell-to-Cell Junctions: Molecular Organization and Role in Vascular Homeostasis. *Physiological Reviews*. 2004;84(3):869-901. doi:10.1152/physrev.00035.2003

12. Hautefort A, Pfenniger A, Kwak BR. Endothelial connexins in vascular function. *Vascular Biology*. 03 Dec. 2019 2019;1(1):H117-H124. doi:10.1530/vb-19-0015

13. Okamoto T, Usuda H, Tanaka T, Wada K, Shimaoka M. The Functional Implications of Endothelial Gap Junctions and Cellular Mechanics in Vascular Angiogenesis. *Cancers*. 2019;11(2):237.

14. Zhou JZ, Jiang JX. Gap junction and hemichannel-independent actions of connexins on cell and tissue functions--an update. *FEBS Lett*. Apr 17 2014;588(8):1186-92. doi:10.1016/j.febslet.2014.01.001

15. Soon A, Chua J, Becker D. Connexins in endothelial barrier function – novel therapeutic targets countering vascular hyperpermeability. *Thrombosis and Haemostasis*. 2016:852-867.

16. Lampugnani MG. Endothelial adherens junctions and the actin cytoskeleton: an 'infinity net'? *J Biol*. 2010;9(3):16. doi:10.1186/jbiol232

17. Brasch J, Harrison OJ, Ahlsen G, Carnally SM, Henderson RM, Honig B, Shapiro L. Structure and Binding Mechanism of Vascular Endothelial Cadherin: A Divergent Classical Cadherin. *Journal of Molecular Biology*. 2011/04/22/ 2011;408(1):57-73. doi:https://doi.org/10.1016/j.jmb.2011.01.031

18. Cummins PM. Occludin: one protein, many forms. *Mol Cell Biol*. Jan 2012;32(2):242-50. doi:10.1128/mcb.06029-11

19. Furuse M, Hirase T, Itoh M, Nagafuchi A, Yonemura S, Tsukita S, Tsukita S. Occludin: a novel integral membrane protein localizing at tight junctions. *J Cell Biol*. Dec 1993;123(6 Pt 2):1777-88. doi:10.1083/jcb.123.6.1777

20. Bauer H-C, Krizbai IA, Bauer H, Traweger A. "You Shall Not Pass"—tight junctions of the blood brain barrier. Review. *Frontiers in Neuroscience*. 2014-December-03 2014;8doi:10.3389/fnins.2014.00392

21. Krause G, Winkler L, Mueller SL, Haseloff RF, Piontek J, Blasig IE. Structure and function of claudins. *Biochimica et Biophysica Acta (BBA) - Biomembranes*. 2008/03/01/ 2008;1778(3):631-645. doi:https://doi.org/10.1016/j.bbamem.2007.10.018

22. Bazzoni G. The JAM family of junctional adhesion molecules. *Current Opinion in Cell Biology*. 2003/10/01/ 2003;15(5):525-530. doi:https://doi.org/10.1016/S0955-0674(03)00104-2

23. Ebnet K, Suzuki A, Ohno S, Vestweber D. Junctional adhesion molecules (JAMs): more molecules with dual functions? *J Cell Sci*. Jan 1 2004;117(Pt 1):19-29. doi:10.1242/jcs.00930

24. Weber C, Fraemohs L, Dejana E. The role of junctional adhesion molecules in vascular inflammation. *Nature Reviews Immunology*. 2007/06/01 2007;7(6):467-477. doi:10.1038/nri2096

25. Félétou M, Vanhoutte PM. Endothelium-derived hyperpolarizing factor: where are we now? *Arterioscler Thromb Vasc Biol*. Jun 2006;26(6):1215-25. doi:10.1161/01.ATV.0000217611.81085.c5

26. Ruggeri ZM, Mendolicchio GL. Adhesion Mechanisms in Platelet Function. *Circulation Research*. 2007;100(12):1673-1685. doi:doi:10.1161/01.RES.0000267878.97021.ab

27. Rumbaut RE, Thiagarajan P. *Platelet-Vessel Wall Interactions in Hemostasis and Thrombosis*. Morgan & Claypool Life Sciences; 2010.

28. Ruggeri ZM. The role of von Willebrand factor in thrombus formation. *Thrombosis Research*. 2007/01/01/ 2007;120:S5-S9. doi:https://doi.org/10.1016/j.thromres.2007.03.011

29. Zhou Y-F, Eng ET, Zhu J, Lu C, Walz T, Springer TA. Sequence and structure relationships within von Willebrand factor. *Blood, The Journal of the American Society of Hematology*. 2012;120(2):449-458.

30. Frantz C, Stewart KM, Weaver VM. The extracellular matrix at a glance. *J Cell Sci*. Dec 15 2010;123(Pt 24):4195-200. doi:10.1242/jcs.023820

31. Ricard-Blum S. The collagen family. *Cold Spring Harb Perspect Biol*. Jan 1 2011;3(1):a004978. doi:10.1101/cshperspect.a004978

32. Undas A, Ariëns RAS. Fibrin Clot Structure and Function. *Arteriosclerosis, Thrombosis, and Vascular Biology*. 2011;31(12):e88-e99. doi:doi:10.1161/ATVBAHA.111.230631

33. Kattula S, Byrnes JR, Wolberg AS. Fibrinogen and Fibrin in Hemostasis and Thrombosis. *Arteriosclerosis, Thrombosis, and Vascular Biology*. 2017;37(3):e13-e21. doi:doi:10.1161/ATVBAHA.117.308564

34. Li Z, Delaney MK, O'Brien KA, Du X. Signaling during platelet adhesion and activation. *Arterioscler Thromb Vasc Biol*. Dec 2010;30(12):2341-9. doi:10.1161/ATVBAHA.110.207522

35. Hantgan R, Hindriks G, Taylor R, Sixma J, de Groot P. Glycoprotein Ib, von Willebrand factor, and glycoprotein IIb:IIIa are all involved in platelet adhesion to fibrin in flowing whole blood. *Blood*. 1990;76(2):345-353. doi:10.1182/blood.V76.2.345.345

36. Li R, Emsley J. The organizing principle of the platelet glycoprotein Ib-IX-V complex. *J Thromb Haemost*. Apr 2013;11(4):605-14. doi:10.1111/jth.12144

37. Li Z, Delaney MK, O'Brien KA, Du X. Signaling During Platelet Adhesion and Activation. *Arteriosclerosis, Thrombosis, and Vascular Biology*. 2010;30(12):2341-2349. doi:doi:10.1161/ATVBAHA.110.207522

38. Rayes J, Watson SP, Nieswandt B. Functional significance of the platelet immune receptors GPVI and CLEC-2. *J Clin Invest*. Jan 2 2019;129(1):12-23. doi:10.1172/jci122955

39. Watson SP, Auger JM, McCarty OJT, Pearce AC. GPVI and integrin αIIbβ3 signaling in platelets. *Journal of Thrombosis and Haemostasis*. 2005;3(8):1752-1762. doi:https://doi.org/10.1111/j.1538-7836.2005.01429.x

40. Offermanns S. Activation of Platelet Function Through G Protein–Coupled Receptors. *Circulation Research*. 2006;99(12):1293-1304. doi:doi:10.1161/01.RES.0000251742.71301.16

41. Woulfe DS. Review Articles: Platelet G protein-coupled receptors in hemostasis and thrombosis. *Journal of Thrombosis and Haemostasis*. 2005;3(10):2193-2200. doi:https://doi.org/10.1111/j.1538-7836.2005.01338.x

42. Golebiewska EM, Poole AW. Platelet secretion: From haemostasis to wound healing and beyond. *Blood Rev*. May 2015;29(3):153-62. doi:10.1016/j.blre.2014.10.003

43. Thomas MR, Storey RF. The role of platelets in inflammation. *Thromb Haemost*. Aug 31 2015;114(3):449-58. doi:10.1160/th14-12-1067

44. Yun SH, Sim EH, Goh RY, Park JI, Han JY. Platelet Activation: The Mechanisms and Potential Biomarkers. *Biomed Res Int*. 2016;2016:9060143. doi:10.1155/2016/9060143

45. Lavergne M, Janus-Bell E, Schaff M, Gachet C, Mangin PH. Platelet Integrins in Tumor Metastasis: Do They Represent a Therapeutic Target? *Cancers*. 2017;9(10):133.

46. Huang J, Li X, Shi X, et al. Platelet integrin αIIbβ3: signal transduction, regulation, and its therapeutic targeting. *Journal of Hematology & Oncology*. 2019/03/07 2019;12(1):26. doi:10.1186/s13045-019-0709-6

47. Joo S-J. Mechanisms of Platelet Activation and Integrin αIIβ3. *Korean Circ J*. 5/ 2012;42(5):295-301.

48. Jackson SP. The growing complexity of platelet aggregation. *Blood*. 2007;109(12):5087-5095. doi:10.1182/blood-2006-12-027698

49. Monroe DM, Hoffman M. What Does It Take to Make the Perfect Clot? *Arteriosclerosis, Thrombosis, and Vascular Biology*. 2006;26(1):41-48. doi:doi:10.1161/01.ATV.0000193624.28251.83

50. Gailani D, Renné T. The intrinsic pathway of coagulation: a target for treating thromboembolic disease? *Journal of Thrombosis and Haemostasis*. 2007;5(6):1106-1112. doi:https://doi.org/10.1111/j.1538-7836.2007.02446.x

51. Stavrou E, Schmaier AH. Factor XII: what does it contribute to our understanding of the physiology and pathophysiology of hemostasis & thrombosis. *Thromb Res*. Mar 2010;125(3):210-5. doi:10.1016/j.thromres.2009.11.028

52. Zilberman-Rudenko J, Reitsma SE, Puy C, et al. Factor XII Activation Promotes Platelet Consumption in the Presence of Bacterial-Type Long-Chain Polyphosphate In Vitro and In Vivo. *Arterioscler Thromb Vasc Biol*. Aug 2018;38(8):1748-1760. doi:10.1161/ATVBAHA.118.311193

53. Renne T, Stavrou EX. Roles of Factor XII in Innate Immunity. *Front Immunol*. 2019;10:2011. doi:10.3389/fimmu.2019.02011

54. Tucker EI, Verbout NG, Leung PY, Hurst S, McCarty OJ, Gailani D, Gruber A. Inhibition of factor XI activation attenuates inflammation and coagulopathy while improving the survival of mouse polymicrobial sepsis. *Blood*. May 17 2012;119(20):4762-8. doi:10.1182/blood-2011-10-386185

55. Weidmann H, Heikaus L, Long AT, Naudin C, Schluter H, Renne T. The plasma contact system, a protease cascade at the nexus of inflammation, coagulation and immunity. *Biochim Biophys Acta Mol Cell Res*. Nov 2017;1864(11 Pt B):2118-2127. doi:10.1016/j.bbamcr.2017.07.009

56. Irmscher S, Doring N, Halder LD, et al. Kallikrein Cleaves C3 and Activates Complement. *J Innate Immun*. 2018/3// 2018;10(2):94-105. doi:10.1159/000484257

57. Larsson M, Rayzman V, Nolte MW, et al. A factor XIIa inhibitory antibody provides thromboprotection in extracorporeal circulation without increasing bleeding risk. *Sci Transl Med*. Feb 5 2014;6(222):222ra17. doi:10.1126/scitranslmed.3006804

58. Raffini L. Anticoagulation with VADs and ECMO: walking the tightrope. *Hematology Am Soc Hematol Educ Program*. Dec 8 2017;2017(1):674-680. doi:10.1182/asheducation-2017.1.674

59. Tillman B, Gailani D. Inhibition of Factors XI and XII for Prevention of Thrombosis Induced by Artificial Surfaces. *Semin Thromb Hemost*. Feb 2018;44(1):60-69. doi:10.1055/s-0037-1603937

60. Kohs TCL, Lorentz CU, Johnson J, et al. Development of Coagulation Factor XII Antibodies for Inhibiting Vascular Device-Related Thrombosis. *Cell Mol Bioeng*. Apr 2021;14(2):161-175. doi:10.1007/s12195-020-00657-6

61. Mohammed BM, Matafonov A, Ivanov I, et al. An update on factor XI structure and function. Thrombosis Research: Elsevier Ltd; 2018. p. 94-105.

62. Adams RLC, Bird RJ. Review article: Coagulation cascade and therapeutics update: Relevance to nephrology. Part 1: Overview of coagulation, thrombophilias and history of anticoagulants. *Nephrology*. 2009;14(5):462-470. doi:https://doi.org/10.1111/j.1440-1797.2009.01128.x

63. Ross R. Atherosclerosis—an inflammatory disease. *New England journal of medicine*. 1999;340(2):115-126.

64. Virani SS, Alonso A, Benjamin EJ, et al. Heart Disease and Stroke Statistics—2020 Update: A Report From the American Heart Association. *Circulation*. 2020;141(9):e139-e596. doi:doi:10.1161/CIR.0000000000000757

65. Geovanini GR, Libby P. Atherosclerosis and inflammation: overview and updates. *Clin Sci (Lond)*. Jun 29 2018;132(12):1243-1252. doi:10.1042/cs20180306

66. Hansson GK, Libby P, Tabas I. Inflammation and plaque vulnerability. *J Intern Med*. Nov 2015;278(5):483-93. doi:10.1111/joim.12406

67. Quillard T, Franck G, Mawson T, Folco E, Libby P. Mechanisms of erosion of atherosclerotic plaques. *Curr Opin Lipidol*. Oct 2017;28(5):434-441. doi:10.1097/mol.0000000000000440

68. Randolph GJ. Mechanisms that regulate macrophage burden in atherosclerosis. *Circ Res*. May 23 2014;114(11):1757-71. doi:10.1161/circresaha.114.301174

69. Viola J, Soehnlein O. Atherosclerosis - A matter of unresolved inflammation. *Semin Immunol*. May 2015;27(3):184-93. doi:10.1016/j.smim.2015.03.013

70. Moriya J. Critical roles of inflammation in atherosclerosis. *J Cardiol*. Jun 12 2018;doi:10.1016/j.jjcc.2018.05.010

71. Jing L, Shu-Xu D, Yong-Xin R. A review: Pathological and molecular biological study on atherosclerosis. *Clin Chim Acta*. Jun 1 2022;531:217-222. doi:10.1016/j.cca.2022.04.012

72. Zieleniewska NA, Kazberuk M, Chlabicz M, Eljaszewicz A, Kaminski K. Trained Immunity as a Trigger for Atherosclerotic Cardiovascular Disease-A Literature Review. *J Clin Med*. Jun 12 2022;11(12)doi:10.3390/jcm11123369

73. Bonetti PO, Lerman LO, Lerman A. Endothelial dysfunction: a marker of atherosclerotic risk. *Arteriosclerosis, thrombosis, and vascular biology*. 2003;23(2):168-175.

74. Davignon J, Ganz P. Role of endothelial dysfunction in atherosclerosis. *Circulation*. 2004;109(23_suppl_1):III-27-III-32.

75. Quek L, Bolen J, Watson S. A role for Bruton's tyrosine kinase (Btk) in platelet activation by collagen. *Current biology*. 1998;8(20):1137-S1.

76. Wagner DD, Burger PC. Platelets in inflammation and thrombosis. *Arteriosclerosis, thrombosis, and vascular biology*. 2003;23(12):2131-2137.

77. Gawaz M, Langer H, May AE. Platelets in inflammation and atherogenesis. *The Journal of clinical investigation*. 2005;115(12):3378-3384.

78. Berger PB, Bhatt DL, Fuster V, et al. Bleeding complications with dual antiplatelet therapy among patients with stable vascular disease or risk factors for vascular disease: results from the Clopidogrel for High Atherothrombotic Risk and Ischemic Stabilization, Management, and Avoidance (CHARISMA) trial. *Circulation*. 2010;121(23):2575-2583.

79. Khurram Z, Chou E, Minutello R, et al. Combination therapy with aspirin, clopidogrel and warfarin following coronary stenting is associated with a significant risk of bleeding. *The Journal of invasive cardiology*. 2006;18(4):162-164.

80. Landefeld CS, Beyth RJ. Anticoagulant-related bleeding: clinical epidemiology, prediction, and prevention. *The American journal of medicine*. 1993;95(3):315-328.

81. Jourdi G, Lordkipanidze M, Philippe A, Bachelot-Loza C, Gaussem P. Current and Novel Antiplatelet Therapies for the Treatment of Cardiovascular Diseases. *Int J Mol Sci*. Dec 3 2021;22(23)doi:10.3390/ijms222313079

82. Jones WS, Mulder H, Wruck LM, et al. Comparative Effectiveness of Aspirin Dosing in Cardiovascular Disease. *N Engl J Med*. May 27 2021;384(21):1981-1990. doi:10.1056/NEJMoa2102137

83. Graipe A, Ulvenstam A, Irevall AL, Soderstrom L, Mooe T. Incidence and predictors of serious bleeding during long-term follow-up after acute coronary syndrome in a population-based cohort study. *Sci Rep*. Nov 9 2021;11(1):21967. doi:10.1038/s41598-021-01525-7

84. Kargiotis O, Tsivgoulis G. The 2020 breakthroughs in early secondary prevention: dual antiplatelet therapy versus single antiplatelet therapy. *Curr Opin Neurol*. Feb 1 2021;34(1):45-54. doi:10.1097/WCO.0000000000000878

85. Collaborators GN. Global, regional, and national burden of neurological disorders, 1990-2016: a systematic analysis for the Global Burden of Disease Study 2016. *Lancet Neurol*. May 2019;18(5):459-480. doi:10.1016/s1474-4422(18)30499-x

86. Collaborators GMS. Global, regional, and national burden of multiple sclerosis 1990-2016: a systematic analysis for the Global Burden of Disease Study 2016. *Lancet Neurol*. Mar 2019;18(3):269-285. doi:10.1016/s1474-4422(18)30443-5

87. Jordan KR, Parra-Izquierdo I, Gruber A, et al. Thrombin generation and activity in multiple sclerosis. *Metab Brain Dis*. Mar 2021;36(3):407-420. doi:10.1007/s11011-020-00652-w

88. Plantone D, Inglese M, Salvetti M, Koudriavtseva T. A Perspective of Coagulation Dysfunction in Multiple Sclerosis and in Experimental Allergic Encephalomyelitis. *Frontiers in Neurology*. 2019;9(JAN)doi:10.3389/fneur.2018.01175

89. Zamolodchikov D, Bai Y, Tang Y, McWhirter JR, Macdonald LE, Alessandri-Haber N. A Short Isoform of Coagulation Factor XII mRNA Is Expressed by Neurons in the

Human Brain. *Neuroscience*. Aug 10 2019;413:294-307. doi:10.1016/j.neuroscience.2019.05.040

90. Ziliotto N, Baroni M, Straudi S, et al. Coagulation factor XII levels and intrinsic thrombin generation in multiple sclerosis. *Frontiers in Neurology*. 2018;9(APR)doi:10.3389/fneur.2018.00245

91. Erickson MA, Wilson ML, Banks WA. In vitro modeling of blood–brain barrier and interface functions in neuroimmune communication. *Fluids and Barriers of the CNS*. 2020/03/30 2020;17(1):26. doi:10.1186/s12987-020-00187-3

92. Erickson MA, Banks WA. Neuroimmune Axes of the Blood-Brain Barriers and Blood-Brain Interfaces: Bases for Physiological Regulation, Disease States, and Pharmacological Interventions. *Pharmacol Rev*. 2018;70(2):278-314. doi:10.1124/pr.117.014647

93. Huber JD, Egleton RD, Davis TP. Molecular physiology and pathophysiology of tight junctions in the blood–brain barrier. *Trends in Neurosciences*. 2001/12/01/ 2001;24(12):719-725. doi:https://doi.org/10.1016/S0166-2236(00)02004-X

94. Stamatovic SM, Keep RF, Andjelkovic AV. Brain endothelial cell-cell junctions: how to "open" the blood brain barrier. *Curr Neuropharmacol*. 2008;6(3):179-192. doi:10.2174/157015908785777210

95. Ziliotto N, Bernardi F, Jakimovski D, Zivadinov R. Coagulation Pathways in Neurological Diseases: Multiple Sclerosis. Review. *Frontiers in Neurology*. 2019-April-24 2019;10(409)doi:10.3389/fneur.2019.00409

96. Göbel K, Pankratz S, Asaridou C-M, et al. Blood coagulation factor XII drives adaptive immunity during neuroinflammation via CD87-mediated modulation of dendritic cells. *Nature Communications*. 2016/05/18 2016;7(1):11626. doi:10.1038/ncomms11626

97. Harlow DE, Honce JM, Miravalle AA. Remyelination Therapy in Multiple Sclerosis. *Frontiers in neurology*. 2015;6:257-257. doi:10.3389/fneur.2015.00257

98. Keough MB, Jensen SK, Yong VW. Experimental demyelination and remyelination of murine spinal cord by focal injection of lysolecithin. *J Vis Exp*. 2015;(97):52679. doi:10.3791/52679

99. McMurran CE, Jones CA, Fitzgerald DC, Franklin RJM. CNS Remyelination and the Innate Immune System. Review. *Frontiers in Cell and Developmental Biology*. 2016-May-03 2016;4(38)doi:10.3389/fcell.2016.00038

100. Plantone D, Inglese M, Salvetti M, Koudriavtseva T. A Perspective of Coagulation Dysfunction in Multiple Sclerosis and in Experimental Allergic Encephalomyelitis. *Frontiers in neurology*. 2019;9:1175-1175. doi:10.3389/fneur.2018.01175

101. Traiffort E, Kassoussi A, Zahaf A, Laouarem Y. Astrocytes and Microglia as Major Players of Myelin Production in Normal and Pathological Conditions. *Front Cell Neurosci*. 2020;14:79-79. doi:10.3389/fncel.2020.00079

102. Garg N, Smith TW. An update on immunopathogenesis, diagnosis, and treatment of multiple sclerosis. *Brain Behav*. 2015;5(9):e00362-e00362. doi:10.1002/brb3.362

103. Lequier L, Horton SB, McMullan DM, Bartlett RH. Extracorporeal membrane oxygenation circuitry. *Pediatr Crit Care Med*. Jun 2013;14(5 Suppl 1):S7-12. doi:10.1097/PCC.0b013e318292dd10

104. Gajkowski EF, Herrera G, Hatton L, Velia Antonini M, Vercaemst L, Cooley E. ELSO Guidelines for Adult and Pediatric Extracorporeal Membrane Oxygenation Circuits. *ASAIO Journal*. 2022;68(2):133-152. doi:10.1097/mat.0000000000001630

105. Combes A, Hajage D, Capellier G, et al. Extracorporeal Membrane Oxygenation for Severe Acute Respiratory Distress Syndrome. *New England Journal of Medicine*. 2018;378(21):1965-1975. doi:10.1056/NEJMoa1800385

106. Peek GJ, Mugford M, Tiruvoipati R, et al. Efficacy and economic assessment of conventional ventilatory support versus extracorporeal membrane oxygenation for severe adult respiratory failure (CESAR): a multicentre randomised controlled trial. *Lancet*. Oct 17 2009;374(9698):1351-63. doi:10.1016/s0140-6736(09)61069-2

107. Caprarola SD, Ng DK, Carroll MK, et al. Pediatric ECMO: unfavorable outcomes are associated with inflammation and endothelial activation. *Pediatr Res*. Nov 3 2021;doi:10.1038/s41390-021-01817-8

108. Figueroa Villalba CA, McMullan DM, Reed RC, Chandler WL. Thrombosis in Extracorporeal Membrane Oxygenation (ECMO) Circuits. *ASAIO J*. Dec 1 2021;doi:10.1097/MAT.0000000000001605

109. Vieira JL, Ventura HO, Mehra MR. Mechanical circulatory support devices in advanced heart failure: 2020 and beyond. *Prog Cardiovasc Dis*. Sep - Oct 2020;63(5):630-639. doi:10.1016/j.pcad.2020.09.003

110. Giani M, Arcadipane A, Martucci G. Challenges in the Extracorporeal Membrane Oxygenation Era. *Membranes (Basel)*. Oct 27 2021;11(11)doi:10.3390/membranes11110829

111. Shudo Y, Elde S, Lingala B, et al. Extracorporeal Membrane Oxygenation Bridge to Heart-Lung Transplantation. *ASAIO J*. May 27 2021;doi:10.1097/MAT.0000000000001457

112. Kato C, Oakes M, Kim M, Desai A, Olson SR, Raghunathan V, Shatzel JJ. Anticoagulation strategies in extracorporeal circulatory devices in adult populations. *Eur J Haematol*. Jan 2021;106(1):19-31. doi:10.1111/ejh.13520

113. Burki S, Adachi I. Pediatric ventricular assist devices: current challenges and future prospects. *Vasc Health Risk Manag*. 2017;13:177-185. doi:10.2147/VHRM.S82379

114. Miera O, Schmitt KL, Akintuerk H, et al. Antithrombotic therapy in pediatric ventricular assist devices: Multicenter survey of the European EXCOR Pediatric Investigator Group. *Int J Artif Organs*. Jul 2018;41(7):385-392. doi:10.1177/0391398818773040

115. Luscher TF, Davies A, Beer JH, et al. Towards personalized antithrombotic management with drugs and devices across the cardiovascular spectrum. *Eur Heart J*. Oct 8 2021;doi:10.1093/eurheartj/ehab642

116. Lippi G, Gosselin R, Favaloro EJ. Current and Emerging Direct Oral Anticoagulants: State-of-the-Art. *Seminars in thrombosis and hemostasis*. Jul 2019;45(5):490-501. doi:10.1055/s-0039-1692703

117. Bernard M, Jubeli E, Pungente MD, Yagoubi N. Biocompatibility of polymer-based biomaterials and medical devices - regulations, in vitro screening and risk-management. *Biomater Sci*. Jul 24 2018;6(8):2025-2053. doi:10.1039/c8bm00518d

118. Reviakine I, Jung F, Braune S, Brash JL, Latour R, Gorbet M, van Oeveren W. Stirred, shaken, or stagnant: What goes on at the blood-biomaterial interface. *Blood Rev*. Jan 2017;31(1):11-21. doi:10.1016/j.blre.2016.07.003

119. Colace TV, Tormoen GW, McCarty OJ, Diamond SL. Microfluidics and coagulation biology. *Annu Rev Biomed Eng*. 2013;15:283-303. doi:10.1146/annurev-bioeng-071812-152406

120. Palmerini T, Biondi-Zoccai G, Della Riva D, et al. Stent thrombosis with drug-eluting and bare-metal stents: evidence from a comprehensive network meta-analysis. *Lancet*. Apr 14 2012;379(9824):1393-402. doi:10.1016/s0140-6736(12)60324-9

121. Holmes DR, Jr., Kereiakes DJ, Garg S, et al. Stent thrombosis. *J Am Coll Cardiol*. Oct 19 2010;56(17):1357-65. doi:10.1016/j.jacc.2010.07.016

122. Negrier C, Dargaud Y, Bordet JC. Basic aspects of bypassing agents. *Haemophilia*. Dec 2006;12 Suppl 6:48-52; discussion 52-3. doi:10.1111/j.1365-2516.2006.01366.x

123. Aubron C, DePuydt J, Belon F, et al. Predictive factors of bleeding events in adults undergoing extracorporeal membrane oxygenation. *Ann Intensive Care*. 2016;6(1):97-97. doi:10.1186/s13613-016-0196-7

124. Dalton HJ, Reeder R, Garcia-Filion P, et al. Factors Associated with Bleeding and Thrombosis in Children Receiving Extracorporeal Membrane Oxygenation. *Am J Respir Crit Care Med*. Sep 15 2017;196(6):762-771. doi:10.1164/rccm.201609-1945OC

125. Wood KL, Ayers B, Gosev I, Kumar N, Melvin AL, Barrus B, Prasad S. Venoarterial-Extracorporeal Membrane Oxygenation Without Routine Systemic Anticoagulation Decreases Adverse Events. *Ann Thorac Surg*. May 2020;109(5):1458-1466. doi:10.1016/j.athoracsur.2019.08.040

126. Yin Z, Zou Y, Wang D, et al. Regulation of the Tec family of non-receptor tyrosine kinases in cardiovascular disease. *Cell Death Discovery*. 2022/03/16 2022;8(1):119. doi:10.1038/s41420-022-00927-4

127. Schwartzberg PL, Finkelstein LD, Readinger JA. TEC-family kinases: regulators of T-helper-cell differentiation. *Nature Reviews Immunology*. 2005/04/01 2005;5(4):284-295. doi:10.1038/nri1591

128. Yang W-C, Collette Y, Nunès JA, Olive D. Tec Kinases: A Family with Multiple Roles in Immunity. *Immunity*. 2000;12(4):373-382. doi:10.1016/S1074-7613(00)80189-2

129. Seixas JD, Sousa BB, Marques MC, et al. Structural and biophysical insights into the mode of covalent binding of rationally designed potent BMX inhibitors. 10.1039/D0CB00033G. *RSC Chemical Biology*. 2020;1(4):251-262. doi:10.1039/D0CB00033G

130. Ponader S, Burger JA. Bruton's tyrosine kinase: from X-linked agammaglobulinemia toward targeted therapy for B-cell malignancies. *J Clin Oncol*. Jun 10 2014;32(17):1830-9. doi:10.1200/jco.2013.53.1046

131. Shatzel JJ, Olson SR, Tao DL, McCarty OJT, Danilov AV, DeLoughery TG. Ibrutinib-associated bleeding: pathogenesis, management and risk reduction strategies. *J Thromb Haemost*. May 2017;15(5):835-847. doi:10.1111/jth.13651

132. Joseph RE, Amatya N, Fulton DB, Engen JR, Wales TE, Andreotti A. Differential impact of BTK active site inhibitors on the conformational state of full-length BTK. *eLife*. 2020/11/23 2020;9:e60470. doi:10.7554/eLife.60470

133. Shi Y, Guryanova OA, Zhou W, et al. Ibrutinib inactivates BMX-STAT3 in glioma stem cells to impair malignant growth and radioresistance. *Science translational medicine*. 2018;10(443):eaah6816. doi:10.1126/scitranslmed.aah6816

134. Gailani D, Bane CE, Gruber A. Factor XI and contact activation as targets for antithrombotic therapy. *J Thromb Haemost*. Aug 2015;13(8):1383-95. doi:10.1111/jth.13005

135. Gailani D, Gruber A. Factor XI as a Therapeutic Target. *Arterioscler Thromb Vasc Biol*. Jul 2016;36(7):1316-22. doi:10.1161/ATVBAHA.116.306925

136. Puy C, Rigg RA, McCarty OJ. The hemostatic role of factor XI. *Thromb Res*. May 2016;141 Suppl 2:S8-S11. doi:10.1016/S0049-3848(16)30354-1

137. Zilberman-Rudenko J, Itakura A, Wiesenekker CP, et al. Coagulation Factor XI Promotes Distal Platelet Activation and Single Platelet Consumption in the Bloodstream Under Shear Flow. *Arterioscler Thromb Vasc Biol*. Mar 2016;36(3):510-7. doi:10.1161/ATVBAHA.115.307034

138. Ngo ATP, Jordan KR, Mueller PA, et al. Pharmacological targeting of coagulation factor XI mitigates the development of experimental atherosclerosis in low-density lipoprotein receptor-deficient mice. *Journal of Thrombosis and Haemostasis*. 2021;19(4):1001-1017. doi:https://doi.org/10.1111/jth.15236

139. Bane CE, Jr., Ivanov I, Matafonov A, et al. Factor XI Deficiency Alters the Cytokine Response and Activation of Contact Proteases during Polymicrobial Sepsis in Mice. *PLoS One*. 2016/4// 2016;11(4):e0152968. doi:10.1371/journal.pone.0152968

140. Luo D, Szaba FM, Kummer LW, et al. Factor XI-deficient mice display reduced inflammation, coagulopathy, and bacterial growth during listeriosis. *Infection and immunity*. 2012;80(1):91-99.

141. Leung PY, Hurst S, Berny-Lang MA, et al. Inhibition of factor XII-mediated activation of factor XI provides protection against experimental acute ischemic stroke in mice. *Translational Stroke Research*. 2012/09// 2012;3(3):381-389. doi:10.1007/s12975-012-0186-5

142. Silasi R, Keshari RS, Regmi G, et al. Factor XII plays a pathogenic role in organ failure and death in baboons challenged with Staphylococcus aureus. *Blood*. Jul 15 2021;138(2):178-189. doi:10.1182/blood.2020009345

143. Puy C, Pang J, Reitsma SE, et al. Cross-Talk between the Complement Pathway and the Contact Activation System of Coagulation: Activated Factor XI Neutralizes Complement Factor H. *J Immunol*. Apr 15 2021;206(8):1784-1792. doi:10.4049/jimmunol.2000398

144. Puy C, Tucker EI, Ivanov IS, et al. Platelet-Derived Short-Chain Polyphosphates Enhance the Inactivation of Tissue Factor Pathway Inhibitor by Activated Coagulation Factor XI. *PLoS One*. 2016/10// 2016;11(10):e0165172. doi:10.1371/journal.pone.0165172

145. Puy C, Tucker EI, Matafonov A, et al. Activated factor XI increases the procoagulant activity of the extrinsic pathway by inactivating tissue factor pathway inhibitor. *Blood*. 2015;125(9):1488-1496. doi:10.1182/blood-2014-10-604587

146. Garland KS, Reitsma SE, Shirai T, et al. Removal of the C-Terminal Domains of ADAMTS13 by Activated Coagulation Factor XI induces Platelet Adhesion on Endothelial Cells under Flow Conditions. *Front Med (Lausanne)*. 2017/12// 2017;4:232. doi:10.3389/fmed.2017.00232

147. Lira AL, Kohs TCL, Moellmer SA, Shatzel JJ, McCarty OJT, Puy C. Substrates, Cofactors, and Cellular Targets of Coagulation Factor XIa. *Semin Thromb Hemost*. Mar 20 2023;doi:10.1055/s-0043-1764469

148. Cave BE, Shah SP. Turning Up to Eleven: Factor XI Inhibitors as Novel Agents to Maximize Safety and Maintain Efficacy in Thromboembolic Disease. *Curr Probl Cardiol*. Mar 2021;46(3):100696. doi:10.1016/j.cpcardiol.2020.100696

149. Nowotny B, Thomas D, Schwers S, Wiegmann S, Prange W, Yassen A, Boxnick S. First randomized evaluation of safety, pharmacodynamics, and pharmacokinetics of BAY 1831865, an antibody targeting coagulation factor XI and factor XIa, in healthy men. *J Thromb Haemost*. Jul 2022;20(7):1684-1695. doi:10.1111/jth.15744

150. Cichon S, Martin L, Hennies HC, et al. Increased activity of coagulation factor XII (Hageman factor) causes hereditary angioedema type III. *Am J Hum Genet*. Dec 2006;79(6):1098-104. doi:10.1086/509899

151. McCarty OJT, Conley RB, Shentu W, et al. Molecular Imaging of Activated von Willebrand Factor to Detect High-Risk Atherosclerotic Phenotype. *JACC: Cardiovascular Imaging*. 2010/09/01/ 2010;3(9):947-955. doi:doi:10.1016/j.jcmg.2010.06.013

152. McCarty OJ, Conley RB, Shentu W, et al. Molecular imaging of activated von Willebrand factor to detect high-risk atherosclerotic phenotype. *JACC Cardiovasc Imaging*. Sep 2010;3(9):947-55.

153. Latifi Y, Moccetti F, Wu M, et al. Thrombotic microangiopathy as a cause of cardiovascular toxicity from the BCR-ABL1 tyrosine kinase inhibitor ponatinib. *Blood*. Apr 4 2019;133(14):1597-1606. doi:10.1182/blood-2018-10-881557

154. Liu Y, Davidson BP, Yue Q, et al. Molecular imaging of inflammation and platelet adhesion in advanced atherosclerosis effects of antioxidant therapy with NADPH oxidase inhibition. *Circulation Cardiovascular imaging*. Jan 1 2013;6(1):74-82. doi:10.1161/CIRCIMAGING.112.975193

155. True C, Dean T, Takahashi D, Sullivan E, Kievit P. Maternal High-Fat Diet Effects on Adaptations to Metabolic Challenges in Male and Female Juvenile Nonhuman Primates. *Obesity (Silver Spring)*. Sep 2018;26(9):1430-1438. doi:10.1002/oby.22249

156. Havel PJ, Kievit P, Comuzzie AG, Bremer AA. Use and Importance of Nonhuman Primates in Metabolic Disease Research: Current State of the Field. *ILAR J*. Dec 1 2017;58(2):251-268. doi:10.1093/ilar/ilx031

157. Ngo ATP, Jordan KR, Mueller PA, et al. Pharmacological Targeting of Coagulation Factor XI Mitigates the Development of Experimental Atherosclerosis in Low-density Lipoprotein Receptor-deficient Mice. *Journal of Thrombosis and Hemostasis*. 2020;

158. Herrington W, Lacey B, Sherliker P, Armitage J, Lewington S. Epidemiology of Atherosclerosis and the Potential to Reduce the Global Burden of Atherothrombotic Disease. *Circ Res*. Feb 19 2016;118(4):535-46. doi:10.1161/CIRCRESAHA.115.307611

159. Ahmad FB, Anderson RN. The Leading Causes of Death in the US for 2020. *JAMA*. May 11 2021;325(18):1829-1830. doi:10.1001/jama.2021.5469

160. Libby P, Buring JE, Badimon L, et al. Atherosclerosis. *Nat Rev Dis Primers*. Aug 16 2019;5(1):56. doi:10.1038/s41572-019-0106-z

161. Habas K, Shang L. Alterations in intercellular adhesion molecule 1 (ICAM-1) and vascular cell adhesion molecule 1 (VCAM-1) in human endothelial cells. *Tissue Cell*. Oct 2018;54:139-143. doi:10.1016/j.tice.2018.09.002

162. Thayse K, Kindt N, Laurent S, Carlier S. VCAM-1 Target in Non-Invasive Imaging for the Detection of Atherosclerotic Plaques. *Biology (Basel)*. Oct 29 2020;9(11)doi:10.3390/biology9110368

163. Cenni B, Gutmann S, Gottar-Guillier M. BMX and its role in inflammation, cardiovascular disease, and cancer. *Int Rev Immunol*. Apr 2012;31(2):166-73. doi:10.3109/08830185.2012.663838

164. Neys SFH, Hendriks RW, Corneth OBJ. Targeting Bruton's Tyrosine Kinase in Inflammatory and Autoimmune Pathologies. *Front Cell Dev Biol*. 2021;9:668131. doi:10.3389/fcell.2021.668131

165. Ekman N, Lymboussaki A, Västrik I, Sarvas K, Kaipainen A, Alitalo K. Bmx tyrosine kinase is specifically expressed in the endocardium and the endothelium of large arteries. *Circulation*. Sep 16 1997;96(6):1729-32. doi:10.1161/01.cir.96.6.1729

166. Qiu L, Wang F, Liu S, Chen X-L. Current understanding of tyrosine kinase BMX in inflammation and its inhibitors. *Burns Trauma*. 2014;2(3):121-124. doi:10.4103/2321-3868.135483

167. Siveen KS, Prabhu KS, Achkar IW, et al. Role of Non Receptor Tyrosine Kinases in Hematological Malignances and its Targeting by Natural Products. *Molecular Cancer*. 2018/02/19 2018;17(1):31. doi:10.1186/s12943-018-0788-y

168. Atkinson BT, Ellmeier W, Watson SP. Tec regulates platelet activation by GPVI in the absence of Btk. *Blood*. Nov 15 2003;102(10):3592-9. doi:10.1182/blood-2003-04-1142

169. Byrd JC, Furman RR, Coutre SE, et al. Targeting BTK with ibrutinib in relapsed chronic lymphocytic leukemia. *N Engl J Med*. Jul 4 2013;369(1):32-42. doi:10.1056/NEJMoa1215637

170. Miklos D, Cutler CS, Arora M, et al. Ibrutinib for chronic graft-versus-host disease after failure of prior therapy. *Blood*. Nov 23 2017;130(21):2243-2250. doi:10.1182/blood-2017-07-793786

171. Ridker PM, Everett BM, Thuren T, et al. Antiinflammatory Therapy with Canakinumab for Atherosclerotic Disease. *N Engl J Med*. Sep 21 2017;377(12):1119-1131. doi:10.1056/NEJMoa1707914

172. Rajantie I, Ekman N, Iljin K, et al. Bmx tyrosine kinase has a redundant function downstream of angiopoietin and vascular endothelial growth factor receptors in arterial endothelium. *Mol Cell Biol*. Jul 2001;21(14):4647-55. doi:10.1128/MCB.21.14.4647-4655.2001

173. Zhang R, Xu Y, Ekman N, Wu Z, Wu J, Alitalo K, Min W. Etk/Bmx transactivates vascular endothelial growth factor 2 and recruits phosphatidylinositol 3-kinase to mediate the tumor necrosis factor-induced angiogenic pathway. *J Biol Chem*. Dec 19 2003;278(51):51267-76. doi:10.1074/jbc.M310678200

174. Parra-Izquierdo I, Melrose AR, Pang J, et al. Janus kinase inhibitors ruxolitinib and baricitinib impair glycoprotein-VI mediated platelet function. *Platelets*. Jun 7 2021:1-12. doi:10.1080/09537104.2021.1934665

175. Zheng TJ, Lofurno ER, Melrose AR, et al. Assessment of the effects of Syk and BTK inhibitors on GPVI-mediated platelet signaling and function. *Am J Physiol Cell Physiol*. May 1 2021;320(5):C902-C915. doi:10.1152/ajpcell.00296.2020

176. Marostica E, Sukbuntherng J, Loury D, et al. Population pharmacokinetic model of ibrutinib, a Bruton tyrosine kinase inhibitor, in patients with B cell malignancies. *Cancer Chemother Pharmacol*. Jan 2015;75(1):111-21. doi:10.1007/s00280-014-2617-3

177. Brown E, Ozawa K, Moccetti F, et al. Arterial Platelet Adhesion in Atherosclerosis-Prone Arteries of Obese, Insulin-Resistant Nonhuman Primates. *J Am Heart Assoc*. May 4 2021;10(9):e019413. doi:10.1161/JAHA.120.019413

178. Moccetti F, Brown E, Xie A, et al. Myocardial Infarction Produces Sustained Proinflammatory Endothelial Activation in Remote Arteries. *J Am Coll Cardiol*. Aug 28 2018;72(9):1015-1026. doi:10.1016/j.jacc.2018.06.044

179. Chadderdon SM, Belcik JT, Bader L, et al. Proinflammatory endothelial activation detected by molecular imaging in obese nonhuman primates coincides with onset of insulin resistance and progressively increases with duration of insulin resistance. *Circulation*. Jan 28 2014;129(4):471-8. doi:10.1161/CIRCULATIONAHA.113.003645

180. Holopainen T, Räsänen M, Anisimov A, et al. Endothelial Bmx tyrosine kinase activity is essential for myocardial hypertrophy and remodeling. *Proceedings of the National Academy of Sciences*. 2015;112(42):13063-13068. doi:10.1073/pnas.1517810112

181. Chen Q, Lv J, Yang W, et al. Targeted inhibition of STAT3 as a potential treatment strategy for atherosclerosis. *Theranostics*. 2019;9(22):6424-6442. doi:10.7150/thno.35528

182. Loren CP, Aslan JE, Rigg RA, et al. The BCR-ABL inhibitor ponatinib inhibits platelet immunoreceptor tyrosine-based activation motif (ITAM) signaling, platelet activation and aggregate formation under shear. *Thromb Res*. Jan 2015;135(1):155-60. doi:10.1016/j.thromres.2014.11.009

183. Rigg RA, Aslan JE, Healy LD, et al. Oral administration of Bruton's tyrosine kinase inhibitors impairs GPVI-mediated platelet function. *Am J Physiol Cell Physiol*. Mar 1 2016;310(5):C373-80. doi:10.1152/ajpcell.00325.2015

184. Wang ML, Rule S, Martin P, et al. Targeting BTK with Ibrutinib in Relapsed or Refractory Mantle-Cell Lymphoma. *New England Journal of Medicine*. 2013;369(6):507-516. doi:10.1056/NEJMoa1306220

185. Ramji DP, Davies TS. Cytokines in atherosclerosis: Key players in all stages of disease and promising therapeutic targets. *Cytokine Growth Factor Rev*. 2015;26(6):673-685. doi:10.1016/j.cytogfr.2015.04.003

186. Kim I, Moon SO, Kim SH, Kim HJ, Koh YS, Koh GY. Vascular endothelial growth factor expression of intercellular adhesion molecule 1 (ICAM-1), vascular cell adhesion molecule 1 (VCAM-1), and E-selectin through nuclear factor-kappa B activation in endothelial cells. *J Biol Chem*. Mar 9 2001;276(10):7614-20. doi:10.1074/jbc.M009705200

187. Binion DG, Heidemann J, Li MS, Nelson VM, Otterson MF, Rafiee P. Vascular cell adhesion molecule-1 expression in human intestinal microvascular endothelial cells is regulated by PI 3-kinase/Akt/MAPK/NF-kappaB: inhibitory role of curcumin. *Am J Physiol Gastrointest Liver Physiol*. Aug 2009;297(2):G259-68. doi:10.1152/ajpgi.00087.2009

188. Luo Y, Xu Z, Wan T, He Y, Jones D, Zhang H, Min W. Endothelial-Specific Transgenesis of TNFR2 Promotes Adaptive Arteriogenesis and Angiogenesis. *Arteriosclerosis, Thrombosis, and Vascular Biology*. 2010;30(7):1307-1314. doi:doi:10.1161/ATVBAHA.110.204222

189. Liu Y, Davidson BP, Yue Q, et al. Molecular Imaging of Inflammation and Platelet Adhesion in Advanced Atherosclerosis Effects of Antioxidant Therapy With NADPH Oxidase Inhibition. *Circulation: Cardiovascular Imaging*. 2013;6(1):74-82. doi:doi:10.1161/CIRCIMAGING.112.975193

190. Döring Y, Drechsler M, Soehnlein O, Weber C. Neutrophils in Atherosclerosis. *Arteriosclerosis, Thrombosis, and Vascular Biology*. 2015;35(2):288-295. doi:doi:10.1161/ATVBAHA.114.303564

191. Projahn D, Koenen RR. Platelets: key players in vascular inflammation. *J Leukoc Biol*. Dec 2012;92(6):1167-75. doi:10.1189/jlb.0312151

192. Posma JJ, Posthuma JJ, Spronk HM. Coagulation and non-coagulation effects of thrombin. *J Thromb Haemost*. Oct 2016;14(10):1908-1916. doi:10.1111/jth.13441

193. d'Alessandro E, Becker C, Bergmeier W, et al. Thrombo-Inflammation in Cardiovascular Disease: An Expert Consensus Document from the Third Maastricht Consensus Conference on Thrombosis. *Thromb Haemost*. Apr 2020;120(4):538-564. doi:10.1055/s-0040-1708035

194. Lorentz CU, Tucker EI, Verbout NG, et al. The contact activation inhibitor AB023 in heparin-free hemodialysis: results of a randomized phase 2 clinical trial. *Blood*. Dec 2 2021;138(22):2173-2184. doi:10.1182/blood.2021011725

195. Tucker EI, Marzec UM, White TC, et al. Prevention of vascular graft occlusion and thrombus-associated thrombin generation by inhibition of factor XI. *Blood*. Jan 22 2009;113(4):936-44. doi:10.1182/blood-2008-06-163675

196. Sanchez J, Elgue G, Riesenfeld J, Olsson P. Studies of adsorption, activation, and inhibition of factor XII on immobilized heparin. *Thromb Res*. Jan 1 1998;89(1):41-50. doi:10.1016/s0049-3848(97)00310-1

197. Keshari RS, Silasi R, Popescu NI, et al. Inhibition of complement C5 protects against organ failure and reduces mortality in a baboon model of Escherichia coli sepsis. *Proc Natl Acad Sci U S A*. Aug 1 2017;114(31):E6390-e6399. doi:10.1073/pnas.1706818114

198. Clemente L, Boeldt DS, Grummer MA, et al. Adenoviral transduction of EGFR into pregnancy-adapted uterine artery endothelial cells remaps growth factor induction of endothelial dysfunction. *Mol Cell Endocrinol*. Jan 1 2020;499:110590. doi:10.1016/j.mce.2019.110590

199. Kuhn M, Zhang Y, Favate J, et al. IMP1/IGF2BP1 in human colorectal cancer extracellular vesicles. *Am J Physiol Gastrointest Liver Physiol*. Oct 4 2022;doi:10.1152/ajpgi.00121.2022

200. Mitrugno A, Tassi Yunga S, Sylman JL, et al. The role of coagulation and platelets in colon cancer-associated thrombosis. *Am J Physiol Cell Physiol*. Feb 1 2019;316(2):C264-c273. doi:10.1152/ajpcell.00367.2018

201. Kohs TCL, Olson SR, Pang J, et al. Ibrutinib Inhibits BMX-Dependent Endothelial VCAM-1 Expression In Vitro and Pro-Atherosclerotic Endothelial Activation and Platelet Adhesion In Vivo. *Cell Mol Bioeng*. Jun 2022;15(3):231-243. doi:10.1007/s12195-022-00723-1

202. Kay JG, Grinstein S. Phosphatidylserine-mediated cellular signaling. *Adv Exp Med Biol*. 2013;991:177-93. doi:10.1007/978-94-007-6331-9_10

203. Vance JE, Steenbergen R. Metabolism and functions of phosphatidylserine. *Prog Lipid Res*. Jul 2005;44(4):207-34. doi:10.1016/j.plipres.2005.05.001

204. Zheng TJ, Kohs TCL, Mueller PA, et al. Effect of antiplatelet agents and tyrosine kinase inhibitors on oxLDL-mediated procoagulant platelet activity. *Blood Advances*. 2023;7(8):1366-1378. doi:10.1182/bloodadvances.2022007169

205. Ellulu MS, Patimah I, Khaza'ai H, Rahmat A, Abed Y. Obesity and inflammation: the linking mechanism and the complications. *Arch Med Sci*. Jun 2017;13(4):851-863. doi:10.5114/aoms.2016.58928

206. Hotamisligil GS. Inflammation and metabolic disorders. *Nature*. 2006/12/01 2006;444(7121):860-867. doi:10.1038/nature05485

207. Videm V, Albrigtsen M. Soluble ICAM-1 and VCAM-1 as markers of endothelial activation. *Scand J Immunol*. May 2008;67(5):523-31. doi:10.1111/j.1365-3083.2008.02029.x

208. Pfeffer MA, Vu H, Kohs TC, et al. Factor XI Inhibition for the Prevention of Catheter-Associated Thrombosis in Cancer Patients Undergoing Central Line Placement: A Phase 2 Clinical Trial. *Blood*. 2022;140(Supplement 1):1247-1249. doi:10.1182/blood-2022-170429

209. Molins B, Fuentes-Prior P, Adán A, Antón R, Arostegui JI, Yagüe J, Dick AD. Complement factor H binding of monomeric C-reactive protein downregulates proinflammatory activity and is impaired with at risk polymorphic CFH variants. *Scientific Reports*. 2016/03/10 2016;6(1):22889. doi:10.1038/srep22889

210. Prasad K. C-reactive protein (CRP)-lowering agents. *Cardiovasc Drug Rev*. Spring 2006;24(1):33-50. doi:10.1111/j.1527-3466.2006.00033.x

211. Zilberman-Rudenko J, Itakura A, Wiesenekker CP, et al. Coagulation Factor XI Promotes Distal Platelet Activation and Single Platelet Consumption in the Bloodstream Under Shear Flow. *Arteriosclerosis, thrombosis, and vascular biology*. 2016;36(3):510-517. doi:10.1161/ATVBAHA.115.307034

212. Cheng Q, Tucker EI, Pine MS, et al. A role for factor XIIa-mediated factor XI activation in thrombus formation in vivo. *Blood*. Nov 11 2010;116(19):3981-9. doi:10.1182/blood-2010-02-270918

213. Reitsma SE, Pang J, Raghunathan V, et al. Role of platelets in regulating activated coagulation factor XI activity. *Am J Physiol Cell Physiol*. Mar 1 2021;320(3):C365-C374. doi:10.1152/ajpcell.00056.2020

214. White-Adams TC, Berny MA, Tucker EI, et al. Identification of coagulation factor XI as a ligand for platelet apolipoprotein E receptor 2 (ApoER2). *Arterioscler Thromb Vasc Biol*. Oct 2009;29(10):1602-7. doi:10.1161/ATVBAHA.109.187393

215. Kaplanski G, Marin V, Fabrigoule M, et al. Thrombin-activated human endothelial cells support monocyte adhesion in vitro following expression of intercellular adhesion molecule-1 (ICAM-1; CD54) and vascular cell adhesion molecule-1 (VCAM-1; CD106). *Blood*. Aug 15 1998;92(4):1259-67.

216. Kossmann S, Lagrange J, Jackel S, et al. Platelet-localized FXI promotes a vascular coagulation-inflammatory circuit in arterial hypertension. *Sci Transl Med*. Feb 1 2017;9(375)doi:10.1126/scitranslmed.aah4923

217. Puy C, Ngo ATP, Pang J, et al. Endothelial PAI-1 (Plasminogen Activator Inhibitor-1) Blocks the Intrinsic Pathway of Coagulation, Inducing the Clearance and Degradation of FXIa (Activated Factor XI). *Arterioscler Thromb Vasc Biol*. Jul 2019;39(7):1390-1401. doi:10.1161/ATVBAHA.119.312619

218. Denic A, Johnson AJ, Bieber AJ, Warrington AE, Rodriguez M, Pirko I. The relevance of animal models in multiple sclerosis research. *Pathophysiology*. 2011;18(1):21-29. doi:10.1016/j.pathophys.2010.04.004

219. Göbel K, Kraft P, Pankratz S, et al. Prothrombin and factor X are elevated in multiple sclerosis patients. *Ann Neurol*. Dec 2016;80(6):946-951. doi:10.1002/ana.24807

220. Parsons ME, O'Connell K, Allen S, et al. Thrombin generation correlates with disease duration in multiple sclerosis (MS): Novel insights into the MS-associated prothrombotic state. *Mult Scler J Exp Transl Clin*. Oct-Dec 2017;3(4):2055217317747624. doi:10.1177/2055217317747624

221. Ahmed O, Geraldes R, DeLuca GC, Palace J. Multiple sclerosis and the risk of systemic venous thrombosis: A systematic review. *Mult Scler Relat Disord*. Jan 2019;27:424-430. doi:10.1016/j.msard.2018.10.008

222. Davalos D, Baeten KM, Whitney MA, et al. Early detection of thrombin activity in neuroinflammatory disease. *Ann Neurol*. Feb 2014;75(2):303-8. doi:10.1002/ana.24078

223. Peeters PJ, Bazelier MT, Uitdehaag BM, Leufkens HG, De Bruin ML, de Vries F. The risk of venous thromboembolism in patients with multiple sclerosis: the Clinical Practice Research Datalink. *J Thromb Haemost*. Apr 2014;12(4):444-51. doi:10.1111/jth.12523

224. Yoon H, Radulovic M, Drucker KL, Wu J, Scarisbrick IA. The thrombin receptor is a critical extracellular switch controlling myelination. *Glia*. 2015;63(5):846-859. doi:10.1002/glia.22788

225. Göbel K, Pankratz S, Asaridou CM, et al. Blood coagulation factor XII drives adaptive immunity during neuroinflammation via CD87-mediated modulation of dendritic cells. *Nat Commun*. May 18 2016;7:11626. doi:10.1038/ncomms11626

226. Gveric D, Herrera B, Petzold A, Lawrence DA, Cuzner ML. Impaired fibrinolysis in multiple sclerosis: a role for tissue plasminogen activator inhibitors. *Brain*. Jul 2003;126(Pt 7):1590-8. doi:10.1093/brain/awg167

227. Adams RA, Bauer J, Flick MJ, et al. The fibrin-derived γ377-395 peptide inhibits microglia activation and suppresses relapsing paralysis in central nervous system autoimmune disease. *Journal of Experimental Medicine*. 2007;204(3):571-582. doi:10.1084/jem.20061931

228. Han MH, Hwang S-I, Roy DB, et al. Proteomic analysis of active multiple sclerosis lesions reveals therapeutic targets. *Nature*. 2008;451(7182):1076-1081. doi:10.1038/nature06559

229. Ryu JK, Petersen MA, Murray SG, et al. Blood coagulation protein fibrinogen promotes autoimmunity and demyelination via chemokine release and antigen presentation. *Nature Communications*. 2015;6(1):8164-8164. doi:10.1038/ncomms9164

230. Langer HF, Choi EY, Zhou H, et al. Platelets contribute to the pathogenesis of experimental autoimmune encephalomyelitis. *Circ Res*. Apr 27 2012;110(9):1202-10. doi:10.1161/CIRCRESAHA.111.256370

231. Göbel K, Asaridou C-M, Merker M, et al. Plasma kallikrein modulates immune cell trafficking during neuroinflammation via PAR2 and bradykinin release. *Proceedings of the National Academy of Sciences*. 2019;116(1):271-276. doi:10.1073/pnas.1810020116

232. Merker M, Eichler S, Herrmann AM, Wiendl H, Kleinschnitz C, Göbel K, Meuth SG. Rivaroxaban ameliorates disease course in an animal model of multiple sclerosis. *Journal of Neuroimmunology*. 2017;313doi:10.1016/j.jneuroim.2017.08.013

233. Courville CB. The effects of heparin in acute exacerbations of multiple sclerosis. Observations and deductions. *Bull Los Angel Neuro Soc*. Dec 1959;24:187-96.

234. Maschmeyer J, Shearer R, Lonser E, Spindle DK. Heparin potassium in the treatment of chronic multiple sclerosis. *Bull Los Angel Neuro Soc*. Dec 1961;26:165-71.

235. Lider O, Baharav E, Mekori YA, Miller T, Naparstek Y, Vlodavsky I, Cohen IR. Suppression of experimental autoimmune diseases and prolongation of allograft survival by treatment of animals with low doses of heparins. *J Clin Invest*. Mar 1989;83(3):752-6. doi:10.1172/JCI113953

236. Stolz L, Derouiche A, Devraj K, Weber F, Brunkhorst R, Foerch C. Anticoagulation with warfarin and rivaroxaban ameliorates experimental autoimmune encephalomyelitis. *J Neuroinflammation*. Jul 28 2017;14(1):152. doi:10.1186/s12974-017-0926-2

237. Davalos D, Kyu Ryu J, Merlini M, et al. Fibrinogen-induced perivascular microglial clustering is required for the development of axonal damage in neuroinflammation. *Nature Communications*. 2012/11/27 2012;3(1):1227. doi:10.1038/ncomms2230

238. Gobel K, Pankratz S, Schneider-Hohendorf T, et al. Blockade of the kinin receptor B1 protects from autoimmune CNS disease by reducing leukocyte trafficking. *J Autoimmun*. Mar 2011;36(2):106-14. doi:10.1016/j.jaut.2010.11.004

239. Gruber A, Hanson SR. Factor XI-dependence of surface- and tissue factor-initiated thrombus propagation in primates. *Blood*. Aug 1 2003;102(3):953-5. doi:10.1182/blood-2003-01-0324

240. Rosen ED, Gailani D, Castellino FJ. FXI is essential for thrombus formation following FeCl3-induced injury of the carotid artery in the mouse. *Thromb Haemost*. Apr 2002;87(4):774-6.

241. Schumacher WA, Seiler SE, Steinbacher TE, et al. Antithrombotic and hemostatic effects of a small molecule factor XIa inhibitor in rats. *Eur J Pharmacol*. Sep 10 2007;570(1-3):167-74. doi:10.1016/j.ejphar.2007.05.043

242. Zhang H, Lowenberg EC, Crosby JR, et al. Inhibition of the intrinsic coagulation pathway factor XI by antisense oligonucleotides: a novel antithrombotic strategy with lowered bleeding risk. *Blood*. Nov 25 2010;116(22):4684-92. doi:10.1182/blood-2010-04-277798

243. Leung PY, Hurst S, Berny-Lang MA, et al. Inhibition of factor XII-mediated activation of factor XI provides protection against experimental acute ischemic stroke in mice. *Translational stroke research*. 2012;3(3):381-389.

244. Jordan KR, Wyatt CR, Fallon ME, et al. Pharmacological reduction of coagulation factor XI reduces macrophage accumulation and accelerates deep vein thrombosis resolution in a mouse model of venous thrombosis. *J Thromb Haemost*. Sep 2022;20(9):2035-2045. doi:10.1111/jth.15777

245. National Research Council Committee for the Update of the Guide for the C, Use of Laboratory A. The National Academies Collection: Reports funded by National Institutes of Health. *Guide for the Care and Use of Laboratory Animals*. National Academies Press (US)

246. Sinha S, Subramanian S, Emerson-Webber A, et al. Recombinant TCR ligand reverses clinical signs and CNS damage of EAE induced by recombinant human MOG. *J Neuroimmune Pharmacol*. Jun 2010;5(2):231-9. doi:10.1007/s11481-009-9175-1

247. Bebo BF, Jr., Vandenbark AA, Offner H. Male SJL mice do not relapse after induction of EAE with PLP 139-151. *J Neurosci Res*. Sep 15 1996;45(6):680-9. doi:10.1002/(sici)1097-4547(19960915)45:6<680::Aid-jnr4>3.0.Co;2-4

248. Dziennis S, Akiyoshi K, Subramanian S, Offner H, Hurn PD. Role of dihydrotestosterone in post-stroke peripheral immunosuppression after cerebral ischemia. *Brain Behav Immun*. May 2011;25(4):685-95. doi:10.1016/j.bbi.2011.01.009

249. Wang C, Gold BG, Kaler LJ, et al. Antigen-Specific Therapy Promotes Repair of Myelin and Axonal Damage in Established EAE. *Journal of Neurochemistry*. 2006;98(6):1817-1827. doi:https://doi.org/10.1111/j.1471-4159.2006.04081.x

250. Gelfand JM. Multiple sclerosis: diagnosis, differential diagnosis, and clinical presentation. *Handb Clin Neurol*. 2014;122:269-90. doi:10.1016/b978-0-444-52001-2.00011-x

251. Hulleck AA, Menoth Mohan D, Abdallah N, El Rich M, Khalaf K. Present and future of gait assessment in clinical practice: Towards the application of novel trends and technologies. *Front Med Technol*. 2022;4:901331. doi:10.3389/fmedt.2022.901331

252. Noseworthy JH. Clinical scoring methods for multiple sclerosis. *Ann Neurol*. 1994;36 Suppl:S80-5. doi:10.1002/ana.410360718

253. Miranda Acuña J, Hidalgo de la Cruz M, Ros AL, Tapia SP, Martínez Ginés ML, de Andrés Frutos CD. Elevated plasma fibrinogen levels in multiple sclerosis patients during relapse. *Mult Scler Relat Disord*. Nov 2017;18:157-160. doi:10.1016/j.msard.2017.09.033

254. Göbel K, Pankratz S, Asaridou CM, et al. Blood coagulation factor XII drives adaptive immunity during neuroinflammation via CD87-mediated modulation of dendritic cells. *Nature Communications*. 2016;7doi:10.1038/ncomms11626

255. Verbout NG, Yu X, Healy LD, et al. Thrombin mutant W215A/E217A treatment improves neurological outcome and attenuates central nervous system damage in experimental autoimmune encephalomyelitis. *Metabolic Brain Disease*. 2015;30(1):57-65. doi:10.1007/s11011-014-9558-8

256. Ryu JK, Rafalski VA, Meyer-Franke A, et al. Fibrin-targeting immunotherapy protects against neuroinflammation and neurodegeneration. *Nature Immunology*. 2018;19(11)doi:10.1038/s41590-018-0232-x

257. Davalos D, Akassoglou K. Fibrinogen as a key regulator of inflammation in disease. *Seminars in Immunopathology*. 2012;34(1):43-62. doi:10.1007/s00281-011-0290-8

258. Choi C-I, Yoon H, Drucker KL, Langley MR, Kleppe L, Scarisbrick IA. The Thrombin Receptor Restricts Subventricular Zone Neural Stem Cell Expansion and

Differentiation. *Scientific Reports*. 2018;8(1):9360-9360. doi:10.1038/s41598-018-27613-9

259. Brailoiu E, Shipsky MM, Yan G, Abood ME, Brailoiu GC. Mechanisms of modulation of brain microvascular endothelial cells function by thrombin. *Brain Research*. 2017;1657:167-175. doi:10.1016/j.brainres.2016.12.011

260. Colman RW, Schmaier AH. Contact system: a vascular biology modulator with anticoagulant, profibrinolytic, antiadhesive, and proinflammatory attributes. *Blood*. Nov 15 1997;90(10):3819-43.

261. Ivanov I, Matafonov A, Sun MF, et al. A mechanism for hereditary angioedema with normal C1 inhibitor: an inhibitory regulatory role for the factor XII heavy chain. *Blood*. Mar 7 2019;133(10):1152-1163. doi:10.1182/blood-2018-06-860270

262. Matafonov A, Leung PY, Gailani AE, et al. Factor XII inhibition reduces thrombus formation in a primate thrombosis model. *Blood*. Mar 13 2014;123(11):1739-46. doi:10.1182/blood-2013-04-499111

263. Schmaier AH. Coagulation Factor XIIa. *Handbook of Proteolytic Enzymes*. 2013;3:2881-2885. doi:10.1016/B978-0-12-382219-2.00637-2

264. Ponczek MB, Gailani D, Doolittle RF. Evolution of the contact phase of vertebrate blood coagulation. *J Thromb Haemost*. Nov 2008;6(11):1876-83. doi:10.1111/j.1538-7836.2008.03143.x

265. Renne T, Schmaier AH, Nickel KF, Blomback M, Maas C. In vivo roles of factor XII. *Blood*. Nov 22 2012;120(22):4296-303. doi:10.1182/blood-2012-07-292094

266. Juang LJ, Mazinani N, Novakowski SK, et al. Coagulation factor XII contributes to hemostasis when activated by soil in wounds. *Blood Adv*. Apr 28 2020;4(8):1737-1745. doi:10.1182/bloodadvances.2019000425

267. Revenko AS, Gao D, Crosby JR, et al. Selective depletion of plasma prekallikrein or coagulation factor XII inhibits thrombosis in mice without increased risk of bleeding. *Blood*. Nov 10 2011;118(19):5302-11. doi:10.1182/blood-2011-05-355248

268. Wallisch M, Lorentz CU, Lakshmanan HHS, et al. Antibody inhibition of contact factor XII reduces platelet deposition in a model of extracorporeal membrane oxygenator perfusion in nonhuman primates. *Res Pract Thromb Haemost*. Feb 2020;4(2):205-216. doi:10.1002/rth2.12309

269. Smith SA, Choi SH, Davis-Harrison R, Huyck J, Boettcher J, Rienstra CM, Morrissey JH. Polyphosphate exerts differential effects on blood clotting, depending on polymer size. *Blood*. Nov 18 2010;116(20):4353-9. doi:10.1182/blood-2010-01-266791

270. Crosby JR, Marzec U, Revenko AS, et al. Antithrombotic effect of antisense factor XI oligonucleotide treatment in primates. *Arterioscler Thromb Vasc Biol*. Jul 2013;33(7):1670-8. doi:10.1161/ATVBAHA.113.301282

271. Gruber A, Carlsson S, Kotze HF, Marzec U, Sarich TC, Hanson SR. Hemostatic effect of activated factor VII without promotion of thrombus growth in melagatran-anticoagulated primates. *Thromb Res*. 2007;119(1):121-7. doi:10.1016/j.thromres.2005.12.002

272. Hanson SR, Griffin JH, Harker LA, Kelly AB, Esmon CT, Gruber A. Antithrombotic effects of thrombin-induced activation of endogenous protein C in primates. *J Clin Invest*. Oct 1993;92(4):2003-12. doi:10.1172/JCI116795

273. Gruber A, Marzec UM, Bush L, et al. Relative antithrombotic and antihemostatic effects of protein C activator versus low-molecular-weight heparin in primates. *Blood*. May 1 2007;109(9):3733-40. doi:10.1182/blood-2006-07-035147

274. Harker LA, Marzec UM, Kelly AB, Chronos NR, Sundell IB, Hanson SR, Herbert JM. Clopidogrel inhibition of stent, graft, and vascular thrombogenesis with antithrombotic enhancement by aspirin in nonhuman primates. *Circulation*. Dec 1 1998;98(22):2461-9. doi:10.1161/01.cir.98.22.2461

275. White-Adams TC, Berny MA, Patel IA, Tucker EI, Gailani D, Gruber A, McCarty OJ. Laminin promotes coagulation and thrombus formation in a factor XII-dependent manner. *J Thromb Haemost*. Jun 2010;8(6):1295-301. doi:10.1111/j.1538-7836.2010.03850.x

276. Doyle AJ, Hunt BJ. Current Understanding of How Extracorporeal Membrane Oxygenators Activate Haemostasis and Other Blood Components. *Front Med (Lausanne)*. 2018;5:352. doi:10.3389/fmed.2018.00352

277. Sniderman J, Monagle P, Annich GM, G. M. Hematologic concerns in extracorporeal membrane oxygenation. *Research and Practice in Thrombosis and Haemostasis*. 2020;doi:10.1002/rth2.12346

278. Hastings SM, Ku DN, Wagoner S, Maher KO, Deshpande S. Sources of Circuit Thrombosis in Pediatric Extracorporeal Membrane Oxygenation. *ASAIO J*. Jan/Feb 2017;63(1):86-92. doi:10.1097/MAT.0000000000000444

279. Yaw HP, Van Den Helm S, MacLaren G, Linden M, Monagle P, Ignjatovic V. Platelet Phenotype and Function in the Setting of Pediatric Extracorporeal Membrane Oxygenation (ECMO): A Systematic Review. *Front Cardiovasc Med*. 2019;6:137. doi:10.3389/fcvm.2019.00137

280. Granja T, Hohenstein K, Schussel P, et al. Multi-Modal Characterization of the Coagulopathy Associated With Extracorporeal Membrane Oxygenation. *Crit Care Med*. May 2020;48(5):e400-e408. doi:10.1097/CCM.0000000000004286

281. Datzmann T, Trager K. Extracorporeal membrane oxygenation and cytokine adsorption. *J Thorac Dis*. Mar 2018;10(Suppl 5):S653-S660. doi:10.21037/jtd.2017.10.128

282. Risnes I, Wagner K, Ueland T, Mollnes T, Aukrust P, Svennevig J. Interleukin-6 may predict survival in extracorporeal membrane oxygenation treatment. *Perfusion*. May 2008;23(3):173-8. doi:10.1177/0267659108097882

283. Schopka S, Philipp A, Muller T, et al. The impact of interleukin serum levels on the prognosis of patients undergoing venoarterial extracorporeal membrane oxygenation. *Artif Organs*. Feb 11 2020;doi:10.1111/aor.13666

284. Clark CC, Hofman ZLM, Sanrattana W, den Braven L, de Maat S, Maas C. The Fibronectin Type II Domain of Factor XII Ensures Zymogen Quiescence. *Thromb Haemost*. Mar 2020;120(3):400-411. doi:10.1055/s-0039-3402760

285. Kato C, Oakes M, Kim M, Desai A, Olson SR, Raghunathan V, Shatzel JJ. Anticoagulation Strategies in Extracorporeal Circulatory Devices in Adult Populations. *European Journal of Haematology*. 2020;doi:10.1111/ejh.13520

286. Menaker J, Tabatabai A, Rector R, et al. Incidence of Cannula-Associated Deep Vein Thrombosis After Veno-Venous Extracorporeal Membrane Oxygenation. *ASAIO J*. Sep/Oct 2017;63(5):588-591. doi:10.1097/mat.0000000000000539

287. Jiritano F, Serraino GF, Ten Cate H, Fina D, Matteucci M, Mastroroberto P, Lorusso R. Platelets and extra-corporeal membrane oxygenation in adult patients: a systematic review and meta-analysis. *Intensive Care Med*. Jun 2020;46(6):1154-1169. doi:10.1007/s00134-020-06031-4

288. Schulman S, Kearon C. Definition of major bleeding in clinical investigations of antihemostatic medicinal products in non-surgical patients. *J Thromb Haemost*. Apr 2005;3(4):692-4. doi:10.1111/j.1538-7836.2005.01204.x

289. Schulman S, Kearon C, Subcommittee on Control of Anticoagulation of the S, Standardization Committee of the International Society on T, Haemostasis. Definition of major bleeding in clinical investigations of antihemostatic medicinal products in non-surgical patients. *J Thromb Haemost*. Apr 2005;3(4):692-4. doi:10.1111/j.1538-7836.2005.01204.x

290. Abrams D, Baldwin MR, Champion M, Agerstrand C, Eisenberger A, Bacchetta M, Brodie D. Thrombocytopenia and extracorporeal membrane oxygenation in adults with acute respiratory failure: a cohort study. *Intensive Care Med*. May 2016;42(5):844-852. doi:10.1007/s00134-016-4312-9

291. Greinacher A, Selleng S. How I evaluate and treat thrombocytopenia in the intensive care unit patient. *Blood*. Dec 29 2016;128(26):3032-3042. doi:10.1182/blood-2016-09-693655

292. Thiele T, Selleng K, Selleng S, Greinacher A, Bakchoul T. Thrombocytopenia in the intensive care unit-diagnostic approach and management. *Semin Hematol*. Jul 2013;50(3):239-50. doi:10.1053/j.seminhematol.2013.06.008

293. Zarychanski R, Houston DS. Assessing thrombocytopenia in the intensive care unit: the past, present, and future. *Hematology Am Soc Hematol Educ Program*. Dec 8 2017;2017(1):660-666. doi:10.1182/asheducation-2017.1.660

294. Thiagarajan RR, Barbaro RP, Rycus PT, et al. Extracorporeal Life Support Organization Registry International Report 2016. *ASAIO Journal*. 2017;63(1):60-67. doi:10.1097/mat.0000000000000475

295. Lukito P, Wong A, Jing J, et al. Mechanical circulatory support is associated with loss of platelet receptors glycoprotein Ibα and glycoprotein VI. *J Thromb Haemost*. Nov 2016;14(11):2253-2260. doi:10.1111/jth.13497

296. Strauss R, Wehler M, Mehler K, Kreutzer D, Koebnick C, Hahn EG. Thrombocytopenia in patients in the medical intensive care unit: bleeding prevalence, transfusion requirements, and outcome. *Crit Care Med*. Aug 2002;30(8):1765-71. doi:10.1097/00003246-200208000-00015

297. Kalbhenn J, Schlagenhauf A, Rosenfelder S, Schmutz A, Zieger B. Acquired von Willebrand syndrome and impaired platelet function during venovenous extracorporeal membrane oxygenation: Rapid onset and fast recovery. *J Heart Lung Transplant*. Aug 2018;37(8):985-991. doi:10.1016/j.healun.2018.03.013

298. Baharoglu MI, Cordonnier C, Al-Shahi Salman R, et al. Platelet transfusion versus standard care after acute stroke due to spontaneous cerebral haemorrhage associated with antiplatelet therapy (PATCH): a randomised, open-label, phase 3 trial. *Lancet*. Jun 25 2016;387(10038):2605-2613. doi:10.1016/s0140-6736(16)30392-0

299. Cashen K, Dalton H, Reeder RW, et al. Platelet Transfusion Practice and Related Outcomes in Pediatric Extracorporeal Membrane Oxygenation. *Pediatr Crit Care Med*. Feb 2020;21(2):178-185. doi:10.1097/PCC.0000000000002102

300. Kurihara C, Walter JM, Karim A, et al. Feasibility of Venovenous Extracorporeal Membrane Oxygenation Without Systemic Anticoagulation. *Ann Thorac Surg*. Mar 12 2020;doi:10.1016/j.athoracsur.2020.02.011

301. Olson SR, Murphree CR, Zonies D, Meyer AD, McCarty OJT, Deloughery TG, Shatzel JJ. Thrombosis and Bleeding in Extracorporeal Membrane Oxygenation (ECMO) Without Anticoagulation: A Systematic Review. *ASAIO J*. Jul 23 2020;doi:10.1097/MAT.0000000000001230

302. Combes A, Brodie D, Chen YS, et al. The ICM research agenda on extracorporeal life support. *Intensive Care Med*. Sep 2017;43(9):1306-1318. doi:10.1007/s00134-017-4803-3

303. Sy E, Sklar MC, Lequier L, Fan E, Kanji HD. Anticoagulation practices and the prevalence of major bleeding, thromboembolic events, and mortality in venoarterial extracorporeal membrane oxygenation: A systematic review and meta-analysis. *J Crit Care*. Jun 2017;39:87-96. doi:10.1016/j.jcrc.2017.02.014

304. Organization ELS. Extracorporeal Life Support Organization (ELSO) General Guidelines for All ECLS Cases. 2020. Updated August 2017. 2020. https://www.elso.org/Portals/0/ELSO%20Guidelines%20General%20All%20ECLS%20Version%201_4.pdf

305. Makdisi G, Wang IW. Extra Corporeal Membrane Oxygenation (ECMO) review of a lifesaving technology. *J Thorac Dis*. Jul 2015;7(7):E166-76. doi:10.3978/j.issn.2072-1439.2015.07.17

306. Organization ELS. *ECLS Registry Report International Summary 2022*. 2022. https://www.elso.org/registry/internationalsummaryandreports/internationalsummary.aspx

307. Abruzzo A, Gorantla V, Thomas SE. Venous thromboembolic events in the setting of extracorporeal membrane oxygenation support in adults: A systematic review. *Thrombosis Research*. 2022/04/01/ 2022;212:58-71. doi:https://doi.org/10.1016/j.thromres.2022.02.015

308. Olson SR, Murphree CR, Zonies D, Meyer AD, McCarty OJT, Deloughery TG, Shatzel JJ. Thrombosis and Bleeding in Extracorporeal Membrane Oxygenation (ECMO) Without Anticoagulation: A Systematic Review. *ASAIO J*. Mar 1 2021;67(3):290-296. doi:10.1097/mat.0000000000001230

309. Nunez JI, Gosling AF, O'Gara B, et al. Bleeding and thrombotic events in adults supported with venovenous extracorporeal membrane oxygenation: an ELSO registry analysis. *Intensive Care Med*. Feb 2022;48(2):213-224. doi:10.1007/s00134-021-06593-x

310. Treml B, Breitkopf R, Bukumirić Z, Bachler M, Boesch J, Rajsic S. ECMO Predictors of Mortality: A 10-Year Referral Centre Experience. *J Clin Med*. Feb 24 2022;11(5)doi:10.3390/jcm11051224

311. Kohs TCL, Liu P, Raghunathan V, et al. Severe thrombocytopenia in adults undergoing extracorporeal membrane oxygenation is predictive of thrombosis. *Platelets*. May 19 2022;33(4):570-576. doi:10.1080/09537104.2021.1961707

312. Wu Y. Contact pathway of coagulation and inflammation. *Thromb J*. 2015;13:17. doi:10.1186/s12959-015-0048-y

313. Sniderman J, Monagle P, Annich GM, MacLaren G. Hematologic concerns in extracorporeal membrane oxygenation. *Res Pract Thromb Haemost*. May 2020;4(4):455-468. doi:10.1002/rth2.12346

314. Levy JH, Staudinger T, Steiner ME. How to manage anticoagulation during extracorporeal membrane oxygenation. *Intensive Care Medicine*. 2022/08/01 2022;48(8):1076-1079. doi:10.1007/s00134-022-06723-z

315. Organization ELS. Codes for Extracorporeal Life Support (ECLS) Complications. 2023. https://www.elso.org/registry/supportdocuments/eclscomplicationscode.aspx

316. Organization ELS. *Extracorporeal Life Support Organization (ELSO) Registry Data Definitions*. 2022. https://www.elso.org/portals/0/files/pdf/elso%20registry%20data%20definitions%2005_17_22.pdf

317. Kirklin JK, Naftel DC, Pagani FD, et al. Pump thrombosis in the Thoratec HeartMate II device: An update analysis of the INTERMACS Registry. *The Journal of Heart and Lung Transplantation*. 2015/12/01/ 2015;34(12):1515-1526. doi:https://doi.org/10.1016/j.healun.2015.10.024

318. Boyle AJ, Jorde UP, Sun B, et al. Pre-Operative Risk Factors of Bleeding and Stroke During Left Ventricular Assist Device Support: An Analysis of More Than 900 HeartMate II Outpatients. *Journal of the American College of Cardiology*. 2014/03/11/ 2014;63(9):880-888. doi:https://doi.org/10.1016/j.jacc.2013.08.1656

319. Chung M, Cabezas FR, Nunez JI, et al. Hemocompatibility-Related Adverse Events and Survival on Venoarterial Extracorporeal Life Support: An ELSO Registry Analysis. *JACC: Heart Failure*. 2020/11/01/ 2020;8(11):892-902. doi:https://doi.org/10.1016/j.jchf.2020.09.004

320. Wiegers HMG, Middeldorp S. Contemporary best practice in the management of pulmonary embolism during pregnancy. *Ther Adv Respir Dis*. Jan-Dec 2020;14:1753466620914222. doi:10.1177/1753466620914222

321. Badheka A, Stucker SE, Turek JW, Raghavan ML. Efficacy of Flow Monitoring During ECMO. *Asaio j*. Jul/Aug 2017;63(4):496-500. doi:10.1097/mat.0000000000000538

322. Cushman M. Epidemiology and risk factors for venous thrombosis. *Semin Hematol*. Apr 2007;44(2):62-9. doi:10.1053/j.seminhematol.2007.02.004

323. Esmon CT. Basic mechanisms and pathogenesis of venous thrombosis. *Blood Rev*. Sep 2009;23(5):225-9. doi:10.1016/j.blre.2009.07.002

324. Ki KK, Passmore MR, Chan CHH, et al. Low flow rate alters haemostatic parameters in an ex-vivo extracorporeal membrane oxygenation circuit. *Intensive Care Med Exp*. Aug 20 2019;7(1):51. doi:10.1186/s40635-019-0264-z

325. Healy LD, Puy C, Fernandez JA, et al. Activated protein C inhibits neutrophil extracellular trap formation in vitro and activation in vivo. *J Biol Chem*. May 26 2017;292(21):8616-8629. doi:10.1074/jbc.M116.768309

326. Healy LD, Rigg RA, Griffin JH, McCarty OJT. Regulation of immune cell signaling by activated protein C. *J Leukoc Biol*. Mar 30 2018;103:1197-1203. doi:10.1002/JLB.3MIR0817-338R

327. Ji SR, Wu Y, Zhu L, Potempa LA, Sheng FL, Lu W, Zhao J. Cell membranes and liposomes dissociate C-reactive protein (CRP) to form a new, biologically active structural intermediate: mCRP(m). *Faseb j*. Jan 2007;21(1):284-94. doi:10.1096/fj.06-6722com

328. Kälsch AI, Csernok E, Münch D, et al. Use of highly sensitive C-reactive protein for followup of Wegener's granulomatosis. *J Rheumatol*. Nov 2010;37(11):2319-25. doi:10.3899/jrheum.100302

329. Molins B, Peña E, Vilahur G, Mendieta C, Slevin M, Badimon L. C-reactive protein isoforms differ in their effects on thrombus growth. *Arterioscler Thromb Vasc Biol*. Dec 2008;28(12):2239-46. doi:10.1161/atvbaha.108.174359

Biographical Sketch

Tia Kohs was born on November 15, 1996 in Wenzhou, Zhejiang, China.

Tia completed the International Baccalaureate Diploma Programme at Flathead High School in Kalispell, Montana. Following her graduation in 2015, she was selected for a National Foot Locker Scholarship and enrolled at Whitworth University (WU). There she was awarded the Presidential Scholarship and WU Diversity Scholarship from 2015-2019. She was named a Werner Rosenquist Scholar and was on the Provost's Honor Roll throughout her undergraduate studies. Tia became involved in research during her undergraduate studies in the laboratories of Drs. Frank Caccavo (Professor of Biology at WU), Kerry Breno (Associate Professor of Chemistry at WU), and Andrij Holian (Director of the Center for Environmental Health Sciences at the University of Montana). In May of 2019, she graduated magna cum laude with her Bachelor of Science in Biology and her Bachelor of Arts in Chemistry.

Tia continued her education at Oregon Health & Science University (OHSU), joining the laboratory of Dr. Owen McCarty in the Department of Biomedical Engineering in June of 2019. Tia's research has centered on elucidating the role of tyrosine kinase signaling and the contact activation pathway of coagulation in the setting of thromboinflammation. During her graduate studies at OHSU, her team won the Massachusetts Institute of Technology COVID-19 Challenge (2020) and she was selected for the School of Medicine's Paper of the Month (2021). Tia was also awarded two Early Career Awards from the International Society on Thrombosis and Haemostasis (2022, 2023), two Professional Development Scholarships from Women in Science Portland (2022), a Travel Award from the Center for Developmental Health at OHSU (2022), and a School of Medicine Graduate Student Organization Travel Award (2022). Tia has presented her research in peer-reviewed journals and at conferences throughout the United States and Europe. Upon completion of her doctorate at OHSU, Tia will be starting as an Associate at McKinsey & Company.

Tia's publications, presentations, and mentoring experiences are listed below:

Publications:

Peer-Reviewed

1. **Kohs TCL**, Fallon ME, Oseas EC, Healy LD, Lorentz CU, Tucker EI, McCarty OJT, Gailani D, Offner H, Verbout NG. Pharmacological targeting of coagulation factor XI attenuates experimental autoimmune encephalomyelitis in mice. *Metab Brain Dis* 2023: in Press.

2. Mao Y, Tan M, **Kohs TCL**, Sylman JL, Ngo ATP, Puy C, McCarty OJT, Walker TW. Transient Particle Tracking Microrheology of Plasma Coagulation via the Intrinsic Pathway. *Appl Rheol* 2023 Apr 1; 33(1): 20220129.

3. Zheng TJ, **Kohs TCL**, Pang J, Reitsma SE, Parra-Izquierdo I, Melrose AR, Larson MK, Williams CD, Hinds MT, McCarty OJT, Aslan JE. Effect of antiplatelet agents and tyrosine kinase inhibitors on oxLDL-mediated procoagulant platelet activity. *Blood Adv* 2022 Oct 11.

4. **Kohs TCL**, Olson SR, Pang J, Jordan KR, Zheng TJ, Xie A, Hodovan J, Muller M, McArthur C, Johnson J, Sousa B, Wallisch M, Kievit P, Aslan JE, Seixas JD, Bernardes GJ, Hinds MT, Lindner JR, McCarty OJT, Puy C, and Shatzel JJ. Ibrutinib inhibits BMX-dependent endothelial VCAM-1 expression *in vitro* and proatherosclerotic endothelial activation and platelet adhesion *in vivo*. *Cell Mol Bioeng* 2022 Apr 18;15(3):231-243. (Cover). PMC9124262.

5. Zheng TJ, Lofurno ER, Melrose AR, Lakshmanan HHS, Pang J, Phillips KG, Fallon ME, **Kohs TCL**, Ngo ATP, Shatzel JJ, Hinds MT, McCarty OJT, Aslan JE. Assessment of the effects of Syk and BTK inhibitors on GPVI-mediated platelet signaling and function. *Am J Physiol Cell Physiol* 2021 May 1;320(5):C902-C915. (Selected OHSU School of Medicine Paper of the Month). PMC8163578.

6. Silasi R,ϕ Keshari RS,ϕ Regmi G, Lupu C, Georgescu C, Simmons JH, Wallisch M, **Kohs TCL**, Shatzel JJ, Olson SR, Lorentz CU, Puy C, Tucker EI, Gailani D, Strickland S, Gruber A, McCarty OJT,* Lupu F.* Factor XII plays a pathogenic role in organ failure and death in baboons challenged with *Staphylococcus aureus*. *Blood* 2021 Jul 15;138(2):178-189. ϕequally contributing first authors; *co-senior authors. (Cover). PMC8288658.

7. **Kohs TCL**, Lorentz CU, Johnson J, Puy C, Olson SR, Shatzel JJ, Gailani D, Hinds MT, Tucker EI, Gruber A, McCarty OJT, Wallisch M. Development of coagulation factor XII antibodies for inhibiting vascular-device related thrombosis. *Cell Mol Bioeng* 2020 Oct 13;14(2):161-175. PMC8010086.

8. Lakshmanan HHS,ϕ Pore AA,ϕ **Kohs TCL**, Yazar F, Thompson RM, Jurney PL, Maddala J, Olson SR, Shatzel JJ, Vanapalli SA, McCarty OJT. Design of a microfluidic bleeding chip to evaluate antithrombotic agents for use in COVID-19 patients. *Cell Mol Bioeng* 2020 Aug 6;13(4):1-9. ϕco-first authors. PMC7408976.

<u>Systematic Review</u>

1. **Kohs TCL**, Liu P, Raghunathan V, Amirsoltani R, Oakes M, McCarty OJT, Olson SR, Masha L, Zonies D, Shatzel JJ. Severe thrombocytopenia in adults undergoing extracorporeal membrane oxygenation is predictive of thrombosis. *Platelets* 2022 May 19;33(4):570-576. PMC9089832.

2. Oakes M, Arastu A, Kato K, Somers J, Holly HD, Elstrott BK, Dy G, **Kohs TCL**, McCarty OJT, DeLoughery TG, Milano C, Raghunathan V, Shatzel JJ. Erythrocytosis and thromboembolic events in transgender individuals receiving gender-affirming testosterone. *Thromb Res* 2021 Sep 20;207:96-98. PMC9089832.

3. West M, Smith C, **Kohs T**, Amirsoltani R, Ribkoff J, Choung JL, Palumbo A, Shatzel J. CDK 4/6 inhibitors are associated with a high incidence of thrombotic events in women with breast cancer in real-world practice. *Eur J Haematol* 2021 May;106(5):634-642. PMC8087188.

4. Raghunathan V, Liu P, **Kohs TCL**, Amirsoltani R, Oakes M, McCarty OJT, Olson SR, Zonies D, Shatzel JJ. Heparin resistance is common in patients undergoing extracorporeal membrane oxygenation but is not associated with worse clinical outcomes. *ASAIO J* 2021 Aug 1;67(8):899-906. PMC9019066.

Review Articles and Editorials

1. **Kohs TCL**, Clarin SN, Carter RG, Mundorff K, Imoukhuede PI, Ramamurthi A, Bao G, King MR, McCarty OJT. Innovation and Entrepreneurship in Promotion and Tenure in Biomedical Engineering. *Cell Mol Bioeng* 2023 May 19;16(3):181-185. PMC10338410.

2. Lira AL, **Kohs TCL**, Moellmer SA, Shatzel JJ, McCarty OJT, Puy C. Substrates, cofactors, and cellular targets of coagulation FXIa. *Semin Thromb Hemost* 2023 Mar 20: in Press.

3. Johnson A, Reimer S, Childres R, Grace C, **Kohs TCL**, McCarty OJT, Kang YB. The Applications and Challenges of the Development of *In Vitro* Tumor Microenvironment Chips. *Cell Mol Bioeng* 2022 Dec 26;16(1):3-21. PMC9842840.

Under Review

1. Verbout NG, Su W, Pham P, Jordan KR, **Kohs TCL**, Tucker EI, McCarty OJT, Sherman LS. E-WE thrombin, a protein C activator, reduces disease severity and spinal cord inflammation in relapsing-remitting murine experimental autoimmune encephalomyelitis. Submitted to *Am J Physiol Cell Physiol* (August 2023).

2. Taskin B, **Kohs TCL**, Shatzel JJ, Puy C, McCarty OJT. Factor XI as a therapeutic target in neuroinflammatory disease. Submitted to *Current Opinion in Hematology* (July 2023).

3. **Kohs TCL**, Chobrutskiy B, McCarty OJT, Zonies D, Zakhary B, Shatzel JJ. Predictors of Thrombosis During VV ECMO: An Analysis of 9,809 patients from the ELSO Registry. Submitted to *J Thromb Thrombolysis* (June 2023).

4. Pfeffer MA, **Kohs TCL**, Vu HH, Jordan KR, Wang S, Lorentz CU, Tucker EI, Olson SR, DeLoughery TG, Hinds MT, McCarty OJT, Shatzel JJ. Factor XI Inhibition for the Prevention of Catheter-Associated Thrombosis in Cancer Patients Undergoing Central Line Placement: a Phase 2 Clinical Trial. Submitted to *Arterioscler Thromb Vasc Biol* (June 2023).

5. **Kohs TCL**, Parra-Izquierdo I, Vu HH, Jordan KR, Hinds MT, Shatzel JJ, Kievit P, Morgan TK, Tassi Yunga S, Ngo TM, Aslan JE, Wallisch M, Lorentz CU, Tucker EI, Puy C, Gailani D, Lindner JR, McCarty OJT. Pharmacological inhibition of coagulation factor XI reduces thromboinflammation in an obese nonhuman primate model of hyperlipidemia. Submitted to *Res Pract Thromb Haemost* (March 2023).

6. Bartlett T, **Kohs T**, Shatzel J, McCarty O, Masha L. Anti-FXa vs. aPTT: Which is the Superior Sentinel Lab in ECMO Patients. Submitted to *Crit Care Res Pract* (November 2022).

Research Conference Abstracts

1. **Kohs TCL**, Fallon ME, Oseas EC, Healy LD, Lorentz CU, Tucker EI, McCarty OJT, Gailani D, Offner H, Verbout NG. "Pharmacological targeting of coagulation factor XI attenuates experimental autoimmune encephalomyelitis in mice", *XXXI Congress of the International Society on Thrombosis and Haemostasis*, Montreal, Quebec (June 2023). Oral presentation. Selected for ISTH Congress Daily News.

2. **Kohs TCL**, Parra-Izquierdo I, Vu HH, Jordan KR, Hinds MT, Shatzel JJ, Kievit P, Morgan TK, Tassi Yunga S, Ngo TM, Aslan JE, Wallisch M, Lorentz CU, Tucker EI, Puy C, Gailani D, Lindner JR, McCarty OJT. "Pharmacological inhibition of coagulation factor XI reduces thromboinflammation in a nonhuman primate model of early atherosclerosis", *XXXI Congress of the International Society on Thrombosis and Haemostasis*, Montreal, Quebec (June 2023). Poster presentation.

3. **Kohs TCL**, Chobrutskiy B, McCarty OJT, Zonies D, Zakhary B, Shatzel JJ. "The impact of cannulation site on bleeding and thrombotic outcomes in venovenous ECMO", *XXXI Congress of the International Society on Thrombosis and Haemostasis*, Montreal, Quebec (June 2023). Poster presentation.

4. **Kohs TCL**, Parra-Izquierdo I, Vu H, Hinds MT, Shatzel JJ, Aslan JE, Wallisch M, Lorentz CU, Tucker EI, Puy C, Gailani D, McCarty OJT. "Antiplatelet effects of inhibiting coagulation factor XI in a diet-induced obesity model of early atherosclerosis", *64th American Society of Hematology Annual Meeting and Exposition*, New Orleans, LA (December 2022). Poster presentation.

5. Pfeffer MS, Vu H, **Kohs TCL**, Wang J, Lorentz CU, Tucker EI, Olson SR, Deloughery TG, Hinds MT, McCarty OJT, Shatzel JJ. "Factor XI Inhibition for the Prevention of Catheter-Associated Thrombosis in Cancer Patients Undergoing Central Line Placement: A Phase 2 Clinical Trial", *64th American Society of Hematology Annual Meeting and Exposition*, New Orleans, LA (December 2022). Oral presentation. Selected for Abstract Achievement Award.

6. **Kohs TCL**, Parra-Izquierdo I, Vu H, Hinds MT, Shatzel JJ, Aslan JE, Wallisch M, Lorentz CU, Tucker EI, Puy C, Gailani D, McCarty OJT. "Antiplatelet effects of inhibiting coagulation factor XI in a nonhuman primate model of atherosclerosis", *Biomedical Engineering Society Annual Meeting*, San Antonio, TX (October 2022). Poster presentation.

7. **Kohs TCL**, Parra-Izquierdo I, Vu H, Hinds MT, Shatzel JJ, Aslan JE, Wallisch M, Lorentz CU, Tucker EI, Puy C, Gailani D, McCarty OJT. "Antiplatelet effects of inhibiting coagulation factor XI in a nonhuman primate model of atherosclerosis", *4th Annual Oregon Bioengineering Symposium*, Corvallis, OR (October 2022). Oral presentation.

8. **Kohs TCL**, Olson SR, Pang J, Jordan KR, Zheng TJ, Xie A, Hodovan J, Muller M, McArthur C, Johnson J, Sousa B, Wallisch M, Kievit P, Aslan JE, Seixas JD, Bernardes GJ, Hinds MT, Lindner JR, McCarty OJ, Puy C, and Shatzel JJ. "Ibrutinib inhibits BMX-dependent endothelial VCAM-1 expression *in vitro* and proatherosclerotic endothelial activation and platelet adhesion *in vivo*", *XXX Congress of the International Society on Thrombosis and Haemostasis*, London, UK (July 2022). Oral presentation.

9. Vu H, **Kohs TCL**, Pang J, Jordan KR, Zheng TJ, Kievit P, Johnson J, Wallisch M, Hinds MT, Puy C, Lorentz CU, Tucker EI, Gailani D, Aslan JE, Shatzel JJ, McCarty OJT, Parra-Izquierdo I. "Antiplatelet effects of inhibiting coagulation factor XI in a nonhuman primate model of atherosclerosis", *XXX Congress of the International Society on Thrombosis and Haemostasis*, London, UK (July 2022). Oral presentation.

10. Reitsma S, Parra-Izquierdo I, Pang J, Melrose AR, **Kohs TCL**, Reddy A, Wilmarth P, David L, McCarty OJT, Aslan JE. "Quantitative Phosphoproteomics And Causal Analysis Reveal Distinct and Combinatorial Signaling Mechanisms In Protease-activated Receptor PAR1 And PAR4 Platelet Activation Programs", *XXX Congress of the International Society on Thrombosis and Haemostasis*, London, UK (July 2022). Oral presentation.

11. Zheng TJ, **Kohs TCL**, Pang J, Reitsma S, Parra-Izquierdo I, Melrose AR, Larson MK, Williams C, Hinds MT, McCarty OJT, Aslan JE. "P2Y receptor antagonists and tyrosine kinase inhibitors reduce oxLDL-mediated procoagulant platelet activity", *XXX Congress of the International Society on Thrombosis and Haemostasis*, London, UK (July 2022). Poster presentation.

12. **Kohs T**, Zheng T, Olson S, Xie A, Hodovan J, Muller M, McArthur C, Johnson J, Wallisch MW, Lorentz C, Verbout N, Kievit P, Larson M, Aslan J, Lindner J, McCarty O, Shatzel J. "The role of TEC family kinases in oxLDL-mediated platelet and endothelial activity in vitro and dysfunction *in vivo*", *XXIX Congress of the International Society on Thrombosis and Haemostasis*, Philadelphia, PA (July 2021). Poster presentation.

13. Zheng TJ, Lofurno ER, Melrose AR, Lakshmanan HHS, Pang J, Phillips KG, Fallon ME, **Kohs TCL**, Ngo ATP, Shatzel JJ, Hinds MT, McCarty OJT, Aslan JE. "Assessment of the effects of Syk and BTK inhibitors on GPVI-mediated platelet signaling and function", *XXIX Congress of the International Society on Thrombosis and Haemostasis*, Philadelphia, PA (July 2021). Poster presentation.

14. Oakes M, Aratsu A, Kato C, Somers J, Manning H, Dy G, **Kohs TCL**, McCarty OJT, Raghunathan V, Shatzel JJ. "Erythrocytosis and Thromboembolic Events in Transgender Individuals Undergoing Masculinizing Therapy with Testosterone", *XXIX Congress of the International Society on Thrombosis and Haemostasis*, Philadelphia, PA (July 2021). Poster presentation.

15. Zheng TJ, **Kohs TCL**, Pang J, Reitsma SE, Parra-Izquierdo I, Melrose AR, Larson MK, Williams CD, Hinds MT, McCarty OJT, Aslan JE. "Effect of antiplatelet agents and tyrosine kinase inhibitors on oxLDL-mediated procoagulant platelet activity", *Vascular Discovery: From Genes to Medicine Scientific Sessions 2022*, Seattle, WA (March 2022). Oral presentation.

16. West M, Smith C, **Kohs T**, Amirsoltani R, Ribkoff J, Choung JL, Palumbo A, Shatzel J. "CDK 4/6 inhibitors are associated with a high incidence of thrombotic events in real world practice", *San Antonio Breast Cancer Symposium*, San Antonio, TX (December 2020). Poster presentation.

17. **Kohs TCL**, Liu P, Raghunathan V, Amirsoltani R, Oakes M, McCarty O, Olson S, Zonies D, Shatzel J. "Severe Thrombocytopenia Is Common In Adults Undergoing Venoarterial Extracorporeal Membrane Oxygenation And Is Predictive Of Hemorrhage", *American Heart Association's Scientific Sessions 2020*, Dallas, TX (November 2020). Poster presentation.

18. Liu P, Raghunathan V, **Kohs T**, Amirsoltani R, Oakes M, McCarty O, Olson S, Zonies D, Shatzel J. "Heparin Resistance is Common in Patients Undergoing Extracorporeal Membrane Oxygenation but is not Associated with Worse Clinical Outcomes", *31st Annual Extracorporeal Life Support Organization Virtual Conference* (September 2020). Poster presentation.

19. **Kohs T**, Olson S, Xie A, Hodovan J, Muller M, McArthur C, Johnson J, Wallisch MW, Lorentz C, Verbout N, Kievit P, Aslan J, McCarty O, Lindner J, Shatzel J. "Effect of BTK Inhibition on Platelet-Mediated Inflammation in an Obese Rhesus Macaque Model of Early Atherosclerosis", *XXVIII Virtual Congress of the International Society of Thrombosis and Haemostasis* (July 2020). Poster presentation.

20. **Kohs T,** Sydor M, Ross A, Holian A, Anderson D. "Evaluation of the Behavior of Lanthanum Titanium Oxide in Nanoparticles in Macrophages", *Society of Toxicology 58th Annual Meeting and ToxExpo*, Baltimore, MD (March 2019). Poster presentation.

21. **Kohs T,** Sydor M, Ross A, Holian A, Anderson D. "Evaluation of the Behavior of Lanthanum Titanium Oxide in Nanoparticles in Macrophages", *Center for Environmental Health Sciences Undergraduate Research Program Final Presentation Symposium*, Missoula, MT (August 2018). Oral presentation.

22. **Kohs T**, Breno K. "Quantifying Alpha and Beta Acid in Hops", *Spokane Intercollegiate Research Conference*, Spokane, WA (April 2018). Poster presentation.

Professional Mentor

1. Karla Bonic (2020 – Present): Ph.D. Candidate in Biomedical Engineering at Oregon Health & Science University, Portland, OR

2. Mary McDonnell (2019 – Present): Ph.D. Candidate in Biomedical Engineering at Oregon Health & Science University, Portland, OR

3. Evelyn Calderon (2021 – 2022): Medical Assistant at Advanced Dermatology and Skin Surgery, Spokane Valley, WA

4. Ava Orr (2018 – 2020): Ph.D. Candidate in Toxicology at the University of Montana, Missoula, MT